

Improving the thermal tolerance of photosynthesis in wheat

Joanna Clare Scales

A thesis submitted for the degree of
Doctor of Philosophy

School of Biological Sciences

University of Essex

2015

Abstract

Wheat yields need to rise to meet growing demands due to population growth and changing diets. Additionally, the resilience of crop yields to climate change and rising temperatures needs to be improved.

Inhibition of photosynthesis under sub-optimal environmental conditions decreases carbon fixation, reducing crop yields. Heat stress inhibits photosynthesis, in part due to a decrease in the activation state of Rubisco. Rubisco activase (Rca) is required to restore and maintain the catalytic activity of Rubisco. Rca has a relatively low temperature optimum; improving its thermal tolerance would maintain Rubisco activity and enhance photosynthesis at higher temperatures, with predicted positive impacts on grain yields under moderate heat stress.

Two approaches were taken to improve the thermal tolerance of Rca in wheat. Firstly, natural variation in the thermal tolerance of Rca in wheat was investigated. Cultivars exhibiting differences in their photosynthetic performance were identified, but the complexity in breeding for increased thermal tolerance was highlighted, with both advantageous and disadvantageous characteristics being identified.

The second approach was to introduce the more thermally stable Rca from cotton into wheat in an attempt to broaden the range of temperatures at which photosynthesis operates. Transgenic plants were produced but the cotton Rca protein was undetectable in the wheat lines investigated.

Two genes encoding Rca in wheat were identified; one gene is alternatively spliced to produce α and β isoforms. Virus-Induced Gene Silencing of the Rca isoforms in wheat indicated that the Rca genes in wheat may be co-regulated. A non-radioactive activity assay was developed for use in Rubisco and Rca research, allowing high-throughput of samples and avoiding the difficulties some labs may have in completing radioactive assays. The information gained in this study will guide future approaches to optimise the thermal stability of Rca and generate temperature-resilient crops.

Acknowledgements

This project was funded by the BBSRC, their financial assistance is gratefully acknowledged.

First and foremost, I would like to thank my supervisors at Rothamsted, Martin Parry, John Andralojc, Elizabete Carmo-Silva and Pippa Madgwick for unconditional support and invaluable assistance and guidance. Gratitude must also go to my supervisory panel at Essex, Christine Raines and Tracy Lawson.

For their contributions to this project thanks must go to the Rothamsted Transformation Group for generating transgenic plants. Many thanks to Wing Sham Lee and Will Pelton for assistance with the VIGS experiments, to Alison Huttly, Peter Buchner and Alison Lovegrove for vital technical and lab assistance, and to Stephen Powers for excellent statistical advice and analysis. Thanks also to the glasshouse, controlled environment, farm and washing-up room staff for helping with experiments and strange requests. I was privileged to be able to work with Mike Salvucci and those at the U.S. Arid Land Agricultural Research Center in Arizona; thank you all for an incredible trip. I am grateful to the John Pickett Travel Fellowship for funding for this opportunity.

I would like to acknowledge all those who have helped me to achieve my research, and so much more, during my PhD. Thank you to the Photosynthesis Group at Rothamsted, for advice, laughter and Wednesday lunches, and to Sue Steele, Helen Jenkins and Donna Fellowes at Rothamsted, and Emma Revill at Essex, for help and support. I am grateful to Adélia de Paula for organising Rothamsted outreach events and to the Parliamentary Office of Science and Technology for a brilliant fellowship.

To all the Rothamsted PhD students, who throughout my PhD have always been around for morning coffee, lunch, afternoon coffee, and afternoon walks; thank you. Thank you also to my Rothamsted housemates (for vegetable planting, house dinners, and believing me that there really was a pheasant in the kitchen sink) and all the other friends who helped along the way, especially the Hoolies and the Sheffield Biologists. Thank you to my family for encouragement and support, and for managing to inspire yet another Biologist. Special thanks to my grandfather, Frank Round, and to my great uncle, Joe Reid, for academic inspiration, and to my parents, for always being willing to answer my endless questions.

Contents

1. Introduction	1-1
1.1 Global food demands	1-1
1.2 Global wheat production	1-3
1.3 Climate impacts on wheat yields.....	1-3
1.4 Improving wheat yields.....	1-4
1.5 Photosynthesis.....	1-6
1.5.1 Photosynthesis and temperature.....	1-8
1.5.1 Other abiotic limitations on photosynthesis	1-9
1.6 Rubisco as a route to overcoming photosynthetic limitations.....	1-10
1.6.1 Limitations and improvement of Rubisco	1-12
1.6.2 Specificity	1-12
1.6.3 Amount.....	1-15
1.6.4 Inhibitors	1-15
1.6.5 Regulation in response to environmental conditions	1-15
1.7 Rubisco activase.....	1-17
1.7.1 Interaction of Rubisco and Rubisco activase	1-17
1.7.2 Rubisco activase isoforms	1-17
1.7.3 Rubisco activase regulation.....	1-18
1.8 Rubisco activase and heat stress.....	1-21
1.8.1 Acclimation to heat stress	1-23
1.9 Improving Rubisco activase	1-24
1.9.1 Exploiting natural variation.....	1-25
1.9.2 Generating new Rubisco activase variants	1-26
1.9.3 Alternative routes to improving Rubisco activase thermal tolerance.....	1-26
1.9.4 Potential problems with altering Rubisco activity	1-26
1.10 Improvement of wheat Rubisco activation.....	1-27
1.11 Thesis Aims and Objectives.....	1-28
2. Searching for variation between the photosynthetic response of elite wheat cultivars to high temperatures	2-29
2.1 Introduction.....	2-29
2.2 Materials and methods	2-31
2.2.1 Plant material and growth conditions.....	2-31

2.2.2	Meteorological conditions.....	2-33
2.2.3	Cultivar yield grouping and lineage.....	2-36
2.2.4	Plant development and biomass measurements.....	2-37
2.2.5	Photosynthetic response to elevated temperature treatment.....	2-39
2.2.6	Rubisco activation state response to elevated temperature treatment.....	2-42
2.2.7	Data analysis.....	2-43
2.3	Results.....	2-44
2.3.1	Wheat cultivar development and biomass measurements.....	2-44
2.3.2	Response of wheat cultivars to elevated temperature treatment.....	2-50
2.4	Discussion.....	2-59
3.	Genetic transformation to improve the thermal tolerance of photosynthesis in wheat.....	3-66
3.1	Introduction.....	3-66
3.2	Materials and methods.....	3-68
3.2.1	Plant material and growth conditions.....	3-68
3.2.2	Activation of wheat Rubisco with cotton Rubisco activase <i>in vitro</i>	3-68
3.2.3	Design and development of constructs for expression of cotton Rubisco activase in wheat.....	3-70
3.2.4	Biolistic transformation of wheat.....	3-72
3.2.5	Gene presence and expression in transgenic wheat plants.....	3-73
3.2.6	Cotton Rubisco activase in transgenic wheat plants.....	3-76
3.2.6.1	Western blot analysis of cotton and wheat Rubisco activase.....	3-76
3.2.6.2	Western blot analysis of Rubisco activase in transgenic wheat plants.....	3-78
3.2.6.3	Isoelectric focusing of Rubisco activase in transgenic wheat plants.....	3-79
3.2.7	Photosynthetic analysis of transgenic plants.....	3-81
3.2.7.1	Temperature response of photosynthesis in wheat.....	3-81
3.2.7.2	Effect of high temperature on photosynthesis of transgenic wheat plants.....	3-82
3.3	Results.....	3-85
3.3.1	Engineering cotton Rubisco activase into wheat.....	3-85
3.3.2	Protein expression analysis of transgenic wheat plants.....	3-93
3.3.3	Photosynthetic analysis of transgenic wheat plants.....	3-98
3.4	Discussion.....	3-102
4.	Characterisation and regulation of Rubisco activase in wheat.....	4-109
4.1	Introduction.....	4-109
4.2	Materials and methods.....	4-111
4.2.1	Plant material and growth conditions.....	4-111

4.2.2	Characterising wheat Rubisco activase genes	4-111
4.2.3	Diurnal Rubisco activase protein cycle	4-112
4.2.4	Virus-induced gene silencing of Rubisco activase in wheat	4-113
4.3	Results	4-117
4.3.1	Wheat Rubisco activase gene structure	4-117
4.3.2	Diurnal Rubisco activase protein amount	4-121
4.3.3	Virus-induced gene silencing of Rubisco activase in wheat	4-121
4.4	Discussion	4-125
5.	Non-radioactive assay for measuring Rubisco and Rubisco activase activity.....	5-129
5.1	Introduction	5-129
5.2	Materials and methods	5-130
5.2.1	Materials.....	5-130
5.2.2	Plant material and growth conditions.....	5-131
5.2.3	Isolation and expression of cDNAs and protein for dPGM and PEP carboxylase.....	5-131
5.2.4	Measurement of Rubisco activase activity using purified proteins.....	5-132
5.2.5	Measurement of Rubisco activation state.....	5-133
5.2.6	Two-stage assay for Rubisco activity using purified proteins.....	5-133
5.2.7	Data analysis	5-134
5.2.8	Miscellaneous.....	5-134
5.3	Results	5-135
5.3.1	Considerations in developing the assay.....	5-135
5.3.2	Validation of the assay	5-137
5.3.3	Modification of the standard assay for measuring Rubisco activity and activation state.....	5-142
5.3.4	Adapting assay to a two-stage method for high-throughput analysis.....	5-144
5.4	Discussion	5-145
5.4.1	The interaction of Rubisco and Rubisco activase	5-145
5.4.2	Significance of measuring Rubisco activase activity at variable ADP: ATP.....	5-145
5.4.3	Measuring Rubisco activity and Rubisco activation state.....	5-146
5.4.4	Summary	5-147
6.	General Discussion	6-148
7.	Conclusions	7-156
8.	References	8-158

Figures and Tables

Figure 1.1. Global projections for yield (tons ha ⁻¹) for maize, rice, wheat and soybean.....	1-2
Figure 1.2. Increase (%) in world production per decade of the three major cereal grains.....	1-2
Figure 1.3. The Calvin- Benson Cycle reproduced from Raines (2011).....	1-6
Figure 1.4. CO ₂ assimilation rates in relation to leaf temperature.	1-9
Figure 1.5. Carbon assimilation of sweet potato (<i>Ipomoea batatas</i>) in response to CO ₂ and temperature..	1-10
Figure 1.6. Diagram of Rubisco and Rca interactions.....	1-12
Figure 1.7. The change in the <i>in vitro</i> activity of Rubisco and Rca with increasing temperature.....	1-21
Figure 2.1. Location of field experiments in 2011-2012 and 2012-2013.....	2-32
Figure 2.2. Randomised field plot layouts for ERYCC panel experiments.	2-33
Figure 2.3. Daily maximum and minimum air temperature (°C; red) and daily precipitation (mm; blue) at Rothamsted Research, over the 2011- 2012 (A) and the 2012- 2013 (B) growing seasons.....	2-35
Figure 2.4. Zadoks growth stage scale for wheat development.	2-38
Figure 2.5. Photographs from field work in 2012 and 2013.	2-40
Figure 2.6. Mean Zadoks growth stage across the three replicated plots (value are means of three plots) of each cultivar at each measurement date over the growing period in 2012 (A) and 2013 (B).	2-44
Figure 2.7. Accumulated thermal time across wheat development in 2011- 2012 (red) and 2012- 2013 (black).	2-46
Figure 2.8. Mean plant height (cm) over the growing season for each cultivar in 2012 (A) and 2013 (B). Values are the mean of nine plants at each time point for each cultivar.	2-47
Figure 2.9. Mean chlorophyll content (SPAD) for each cultivar throughout plant development in 2012 (A) and 2013 (B). Values are the mean of nine plants at each time point for each cultivar.	2-48
Figure 2.10. Grain yield (t ha ⁻¹), above ground dry matter (t ha ⁻¹ ; AGDM) and harvest index (HI) for each cultivar in 2012 and 2013. Values are the mean of three plots of each cultivar, ± SEM.	2-49
Figure 2.11. A-Ci curves (µmol CO ₂ mol air ⁻¹ ; µmol mol ⁻¹) for selected cultivars (n=3) pre-anthesis (Zadoks growth stage 4.3- 4.5) in 2012 (A) and 2013 (B) and post-anthesis (7 days after Zadoks growth stage 6.5; B) in 2013 (C).	2-50
Figure 2.12. Initial screen of photosynthetic response to elevated temperature (% decrease in photosynthesis between 25 and 35°C) of the 64 ERYCC panel wheat cultivars in 2012.	2-51
Figure 2.13. Initial screen of Rubisco activation state at 35°C in the 64 ERYCC panel cultivars in 2012..	2-52
Figure 2.14. The relationship in 2012 between the photosynthetic rate (µmol m ⁻² s ⁻¹) and the initial Rubisco activity (µmol CO ₂ m ⁻² s ⁻¹) for the selected wheat cultivars at 25°C (white) and 35°C (grey).	2-53
Figure 2.15. Graphs of the photosynthetic parameters for each cultivar at each of the temperature treatments (20°C and 35°C) in 2013.	2-55
Figure 2.16. The photosynthetic rate (µmol m ⁻² s ⁻¹) for the grouping of the higher and lower yielding cultivars at 20°C (black) and 35°C (grey).....	2-56
Figure 2.17. Rubisco activation state in 2013 for each wheat cultivar (A) and for the higher and lower yielding cultivar groups (B).	2-57
Figure 2.18. The average Rubisco amount (mgR mL ⁻¹) and photosynthetic rate (µmol m ⁻² s ⁻¹) in 2013, for each cultivar at 20°C and 35°C in 2013.	2-57
Figure 3.1. The effect of temperature on light activation of Rubisco.	3-67
Figure 3.2. Temperature response of Rca activity in cool (<i>Camelina sativa</i> ; Camelina) and warm (<i>Gossypium hirsutum</i> ; Cotton) season species.	3-67
Figure 3.3. Diagram of the construct components for the expression of <i>GhRca-α</i> and <i>GhRca-β</i>	3-72

Figure 3.4. Photographs of the plant regeneration stages during biolistic wheat transformation.	3-73
Figure 3.5. Randomised layout of transgenic plants for photosynthesis measurements following an elevated temperature treatment in the glasshouse.	3-85
Figure 3.6. Wheat Rubisco activity following incubation of the inhibited enzyme with cotton Rca.	3-86
Figure 3.7. Representative sample of GUS stained leaf tissue at five different time points from Rice <i>actin-1</i> -GUS (top) and Maize <i>ubiquitin-1</i> -GUS plants (bottom).	3-86
Figure 3.8. Nucleotide sequence for cotton α (<i>GhRca-α</i>) and β (<i>GhRca-β</i>) Rca isoforms.	3-89
Figure 3.9. Amino acid sequence for cotton α (<i>GhRca-α</i>) and β (<i>GhRca-β</i>) Rca isoforms.	3-89
Figure 3.10. Nucleotide (A) and amino acid (B) sequence for the wheat Rubisco small subunit transit peptide (WtRSSU-TP) and amino acid sequence.	3-89
Figure 3.11. Comparison of amino acid sequence for the mature Rca α and β peptides from wheat and cotton.	3-91
Figure 3.12. SDS-Page gel showing the Rubisco large subunit and Rca western blot of wheat and cotton leaf extracts.	3-92
Figure 3.13. Gene expression analysis (Relative NRQ) of plants from lines of pAHC17GhRcaA/B (black bars) and p302AcGhRcaA/B (white bars).	3-93
Figure 3.14. Representative example of an Rca western blot of p302AcGhRcaA/B plants using 48-well Criterion gels.	3-94
Figure 3.15. Total Rca amount (mean western blot band intensity) in p302AcGhRcaA/B transformed lines (black bars) and negative line (white bar) from Criterion 48-well gel western blots.	3-94
Figure 3.16. Representative example of western blot analysis of pAHC17GhRcaA/B plant samples on 11% gels.	3-94
Figure 3.17. Amount (Western blot band density) of Rca α (white bars) and β (black bars) isoforms in p302AcGhRcaA/B lines (A), and pAHC17GhRcaA/B lines (B) on 11% gels.	3-95
Figure 3.18. Native IEF criterion gels and Rca western blot of wheat leaf protein samples.	3-95
Figure 3.19. Denatured cotton and wheat leaf protein samples run on a native IEF gel.	3-96
Figure 3.20. Denatured cotton and wheat leaf protein samples run on a denaturing IEF gel.	3-96
Figure 3.21. Coomassie stained second dimension gels of wheat leaf total protein (A; 200 μ g) and cotton total protein (B; 50 μ g).	3-97
Figure 3.22. Western blot of the 2 nd dimension gel of 100 μ g of wheat (A), 100 μ g of cotton (B), and a mixture of 100 μ g total wheat and cotton (C).	3-98
Figure 3.23. False colour overlay of second dimension western blots of wheat and cotton α and β Rca proteins.	3-98
Figure 3.24. Rate of wheat photosynthesis predicted from ACi Curve measurements taken at a range of temperatures.	3-99
Figure 3.25. Photosynthetic rates (μ mol m ⁻² s ⁻¹) of transgenic lines for each construct compared to DNA negative plants, cadenza and negative transformation controls.	3-100
Figure 3.26. Mean grain weight (g per plant) of transgenic lines from each construct and for the equivalent DNA negative plants.	3-101
Figure 4.1. A representative schematic of the <i>TaRca</i> isoform gene sequences (<i>TaRca1</i> and <i>TaRca2</i>), and the splice variants of <i>TaRca2</i>	4-118
Figure 4.2. Predicted amino acid sequence and the structural protein regions of <i>TaRca1</i> and <i>TaRca2</i>	4-119
Figure 4.3. The relative amounts of Rca protein in wheat (cv. Cadenza) leaves collected at regular intervals during the light-dark diurnal cycle.	4-121
Figure 4.4. Sequence of <i>TaRca</i> genes with the five BSMV:Rca construct sequences indicated by coloured lines.	4-123

Figure 4.5. The relative gene expression levels (NRQ) of the three <i>TaRca</i> isoforms in wheat leaf tissue samples inoculated with BSMV:Rca silencing constructs.	4-124
Figure 4.6. The relative protein amounts of Rca (A) and Rubisco (B) in wheat leaves of plants inoculated with Rca silencing constructs compared to the control (BSMV:asGFP).	4-125
Figure 5.1. Reaction schemes for measuring the activities of Rca and Rubisco in continuous assays.	5-136
Figure 5.2. Continuous measurement of Rubisco activity demonstrating the conversion of Rubisco from the inactive ER to the active ECM form by Rca.	5-138
Figure 5.3. Effect of Rca concentration on Rca activity.	5-138
Figure 5.4. Effect of Rubisco concentration on Rca activity.	5-139
Figure 5.5. Effect of ADP:ATP ratio on the activity of Rca.	5-140
Figure 5.6. Activation of wild-type (black) and His-tagged modified Rubisco (grey) by Rca.	5-141
Table 1.1. <i>Rca</i> gene and Rca isoform number in different plant species.	1-19
Table 2.1. Monthly average rainfall (mm) at Rothamsted Research for the growing seasons of 2012 and 2013.	2-34
Table 2.2. Monthly average air temperature (daily minimum and maximum; °C) and sunshine (hours) at Rothamsted Research, for the growing seasons of 2012 and 2013.	2-35
Table 2.3. Collated yield data (t ha ⁻¹) for selected ERYCC panel cultivars.	2-36
Table 2.4. Detailed information on the wheat cultivars being investigated.	2-37
Table 2.5. The mean number of days after sowing at which 50% of each cultivar plot was recorded as having 50% of ears at anthesis (Zadoks growth stage 6.5).	2-45
Table 2.6. Key correlations, coefficients and p values for photosynthetic, yield and Rubisco traits in 2012 and 2013.	2-58
Table 3.1. Primers used to amplify the <i>GhRca</i> genes from the pENTR constructs to introduce appropriate restriction sites for ligation into p302AcNos.	3-71
Table 3.2. Primer sequences for PCR DNA testing of transgenic plants.	3-74
Table 3.3. Primers for qRT-PCR of the cotton Rca transgenes and control genes (<i>TIP</i> and <i>eIF4E</i>) in transgenic p302AcGhRcaA/B and pAHC17GhRcaA/B plants.	3-76
Table 3.4. Transgenic lines from p302AcGhRcaA/B and pAHC17GhRcaA/B grown for measurement of photosynthetic performance following an elevated temperature treatment.	3-84
Table 3.5. Cleavage sites between the transit peptides and mature protein sequence for p302AcGhRcaA/B and pAHC17GhRcaA/B.	3-90
Table 3.6. Comparison of cotton and wheat Rca isoform nucleotide and amino acid sequence lengths.	3-90
Table 4.1. Primers used to amplify <i>TaRca</i> genes for sequencing.	4-112
Table 4.2. Sample collection times for measuring diurnal Rca protein amounts.	4-113
Table 4.3. Primers used for amplification of <i>TaRca</i> gene fragments for VIGS construct preparation.	4-114
Table 4.4. qRT-PCR primer pairs for measuring <i>TaRca</i> gene expression in wheat plants inoculated with VIGS constructs.	4-116
Table 4.5. Comparison of the mature coding sequence of <i>TaRca</i> genes and resulting proteins.	4-120
Table 5.1. Differences in the sensitivity of β -isoform Rca to inhibition by ADP.	5-140
Table 5.2. Effect of irradiance on the activation state of Rubisco in wild-type Arabidopsis and the transgenic line, rwt43.	5-143
Table 5.3. Effect of temperature on the activation state of Rubisco in camelina.	5-143
Table 5.4. Effect of Rca on the activation of Rubisco, measured in a two-stage assay.	5-144

Abbreviations

A-Ci	Rate of net CO ₂ assimilation (Photosynthesis) /Intercellular CO ₂ concentration
ADP	Adenosine diphosphate
AGDM	Above Ground Dry Matter
A _j	Electron transport-limited rate of CO ₂ assimilation
AS	Alternatively Spliced (referring to genes)
ATP	Adenosine triphosphate
2,3-bisPGA	2,3-Bisphosphoglycerate
bp	Base Pairs
BSMV	Barley Stripe Mosaic Virus
CA1P	2-carboxy-D-arabinitol-1-phosphate
cDNA	Complementary DNA
dPGM	2,3-Bisphosphate-dependent phosphoglycerate mutase
dPGM-ST	2,3-Bisphosphate-dependent phosphoglycerate mutase with a S-Tag
ECM	Rubisco carbamylated and stabilised by Mg ²⁺ (active)
EDTA	Ethylenediaminetetraacetic acid
eIF4E	Eukaryotic Translation Initiation Factor
ER	Rubisco enzyme uncarbamylated and bound to RuBP (inhibited)
ERYCC	Earliness & resilience for Yield in a Changed Climate
Fv'/Fm'	Maximum quantum efficiency of PSII photochemistry (Ratio of variable to maximum fluorescence)
GFP	Green Fluorescent Protein
gs	Stomatal Conductance
GUS	β-glucuronidase
IEF	Isoelectric Focusing
HI	Harvest Index
LSD	Least Significant Difference
mRNA	messenger RNA

NADH / NAD ⁺	Nicotinamide adenine dinucleotide (reduced/oxidised form)
NADPH	Nicotinamide adenine dinucleotide phosphate
NRQ	Normalised Relative Quantity
Nos	nopaline synthase terminator from <i>Agrobacterium tumefaciens</i>
PEP	Phosphoenolpyruvic acid/ phosphoenolpyruvate
PEG	Polyethylene glycol
PEPC	Phosphoenolpyruvate carboxylase
Pi	Inorganic Phosphate group
φPSII	Effective quantum yield of photochemical energy conversion in Photosystem II
3-PGA	3-Phosphoglyceric acid
2-PGA	2-Phosphoglyceric acid
3-PGA kinase	3-phosphoglycerate kinase
PSII	Photosystem II
PVP	Polyvinylpyrrolidone
Rca	Rubisco activase
RNAi	interfering RNA
RuBP	Ribulose-1,5-bisphosphate
Rubisco	Ribulose-1,5-bisphosphate carboxylase/oxygenase
WtRSSU-TP	Rubisco Small Subunit transit peptide
S-Tag	Strep-tactin-binding peptide
Taq	DNA polymerase from <i>Thermus aquaticus</i>
qRT-PCR	quantitative Real Time Polymerase Chain Reaction
QTL	Quantitative Trait Loci
SEM	Standard error of the mean
TIP	Tonoplast Intrinsic Protein
TP	Transit Peptide
TSP	Total Soluble Protein
VIGS	Virus-induced gene silencing

1. Introduction

1.1 Global food demands

Global crop production needs to increase by 70% to meet the projected demands in 2050 (Figure 1.1) from increasing global populations, dietary change, and increasing consumption of biofuels (Ray *et al.*, 2013, Tilman *et al.*, 2011). Predictions indicate that global populations will reach over 9 billion by 2050 (Gerland *et al.*, 2014). Additionally, increased meat and dairy consumption due to increasing affluence, will amplify demand for food (WHO, 2003). Current energy intake ranges from 2681 kcal per capita per day in developing countries to 3380 kcal per capita per day in industrialised countries. The impacts of this discrepancy in calorific intake, with ~870 million people globally considered to be chronically undernourished, and over-consumption in the developing world, must also be considered.

It is estimated that crop yields are no longer rising in 24- 39% of the world's most important cropland area (Ray *et al.*, 2012). For the key global crops including maize, rice, wheat, and soybean (which currently produce nearly two-thirds of global agricultural calories) yields are not increasing at the same rate as previously (Figure 1.2; Long and Ort (2010)). In Europe over the last two decades a decline in this growth trend, even to the point of stagnation, is being seen for both wheat and barley (Brisson *et al.*, 2010). Climate change is also putting crop production at risk. Climate change models (IPCC, 2013) predict that: global temperatures will rise by 2- 4°C in the next century, precipitation will decrease in the subtropics, and increase at higher latitudes, and that the frequency of extreme climatic events will increase, with greater temperature extremes being seen and increased risk of drought. We therefore need to increase food production to meet growing demands, whilst also ensuring the resilience of crop yields to unpredictable climatic conditions.

There are three main potential routes to increase crop production: expanding the land area used for agriculture (leading to arguments regarding changes in land use, and associated environmental and biodiversity impacts); increasing the frequency at which land is cropped (which may result in increased intensification and greater use of fertilisers and irrigation); or increasing the yield obtained from crops per

unit area (may be through improving the crop itself, increasing agricultural inputs or adapting agricultural methods).

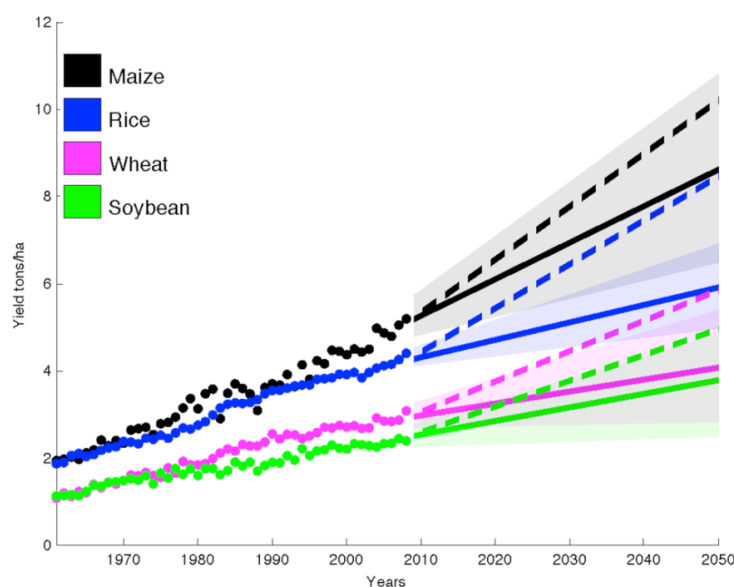


Figure 1.1. Global projections for yield (tons ha^{-1}) for maize, rice, wheat and soybean. The observed area-weighted global yield for 1961–2008 (closed circles) and projections to 2050 (solid lines) are shown. Shading shows the 90% confidence region derived from 99 bootstrapped samples. Also shown is the trend (dashed line) of the $\sim 2.4\%$ yield improvement required each year to double production in these crops by 2050 without bringing additional land under cultivation, starting in the base year of 2008. Reproduced from Ray *et al.* (2013).

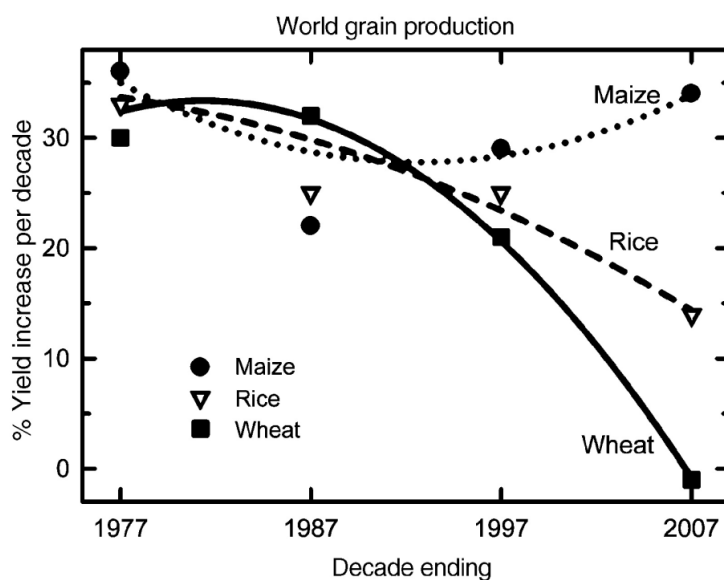


Figure 1.2. Increase (%) in world production per decade of the three major cereal grains. Based on UN Food and Agriculture Organization records, with 2007 as the last year for which complete data were available. Reproduced from Long and Ort (2010)

1.2 Global wheat production

Wheat currently provides one-fifth of the total calories consumed by the world's population (Reynolds *et al.*, 2011) and it is grown globally on over 220 Mha of land (FAO, 2015). Wheat is best adapted to temperate regions (Gill *et al.*, 2004) however, it is also grown in semi-arid regions, where the less favourable climate (temperature and rainfall pattern) results in lower yields.

The global demand for wheat is increasing and predictions suggest that grain production must increase annually by 2.4% to meet human needs in 2050 (Ray *et al.*, 2013). However, current increases in global wheat productivity are only 0.9% per year, which makes it necessary to increase wheat production, if agricultural land area is not to be significantly increased, alongside ensuring yields are resilient to the changing climate.

1.3 Climate impacts on wheat yields

The annual grain yield loss of wheat due to biotic and abiotic factors (including heat and drought; Gill *et al.* (2004)) is approximately 25%, but losses will rise due to the greater stresses associated with changes in climate (Lobell & Field, 2007). Wheat is affected by heat stress; this reduces both yield quality and quantity. Heat stress can result in increased investment in the shoot compared to root, and leaves with a lower leaf mass per unit leaf area (Poorter *et al.*, 2009). Reductions in yield are associated with both long-term high temperatures, as well as heat shocks, particularly where higher than average temperatures occur during mid or late reproductive wheat stages, including grain filling; Wardlaw and Wrigley (1994). Heat stress during anthesis increases floret abortion therefore reducing yield. Vara Prasad and Djanaguiraman (2014), found two times during reproductive development (8- 6 days before anthesis and 2- 0 days before anthesis) were the most sensitive to short episodes (2 or 5 days) of high temperature stress, and caused the greatest decrease in floret fertility. Additionally, heat stress speeds up development of the spike, reducing spikelet number and therefore the number of grains per spike (Porter & Gawith, 1999). Drought and increased temperature before the end of grain filling shortens the grain filling period and lowers grain yield, mean grain weight and specific weight (Ferris *et al.*, 1998, Gooding *et al.*, 2003). Therefore, both grain number and weight are sensitive to elevated temperature.

Global wheat production is estimated to fall by 6% for each °C of further temperature increase, and to become more variable over space and time (Asseng *et al.*, 2014). The predicted mean rate of warming in current wheat growing areas is approximately 0.5°C per decade, which indicates that a decrease in yields of about 2% per decade may be experienced. The most significant impacts of rising temperatures on wheat yields will be observed at low latitudes, where approximately 100 million ha of wheat are cultivated, producing approximately 280 million tons of grain (Cossani & Reynolds, 2012). In contrast, some benefits at high latitudes are expected. In Europe, heat stress is predicted to be the main climatic cause of future wheat yield losses (Semenov & Shewry, 2011). There is the suggestion that with higher temperatures wheat may mature faster so avoiding drought later in the season, but will still be affected by high temperature stress (a shorter life cycle may also decrease productivity due to a shorter reproductive stage; Ainsworth & Ort (2010)). Lobell and Field (2007) demonstrated that growing season temperature and precipitation can explain ~30% (or more) of yearly variation in global average yields for the six most widely grown crops globally. For wheat, maize and barley, there is clearly a negative response of global yields to increased temperatures, for which they estimate that (as of 2002) warming since 1981 has caused annual combined losses of these three crops representing roughly 40 Mt or \$5 billion per year.

1.4 Improving wheat yields

Since the Green Revolution of the 1960's increases in crop yield have been attributed to modern varieties, improved farming practises and agricultural machinery, and increased fertiliser (and pesticide) use (Evenson & Gollin, 2003). There is limited potential to improve crop yields further using similar methods and so novel routes must be considered. The factors determining crop yield potential, the yield of a cultivar when grown in environments to which it is adapted with nutrients and water being non-limiting, and with pests, diseases, weeds, lodging and other stresses effectively controlled; can be summarised (as below) in an equation following the principles of Monteith and Moss (1977).

$$P_n = S_t \cdot \varepsilon_i \cdot \varepsilon_c / k \quad \text{Equation 1}$$

$$Y_p = \eta \cdot P_n \quad \text{Equation 2}$$

Equation 1: Where P_n is the primary productivity at a given location (i.e. the total plant biomass produced over the growing season); S_t is the total photosynthetically active solar radiation across the growing season (MJ m^{-2}); ε_i is the light interception efficiency (determined by the speed of canopy development and closure, canopy longevity, size and architecture); ε_c is the conversion efficiency (determined by the combined photosynthetic rate of all leaves within the canopy, less crop respiratory losses); k is the energy content of the plant mass (MJ m^{-2})

Equation 2: Where Y_p is the potential crop yield at a given location (kg m^{-2}); η is the energy content of the harvested component (J kg^{-1}); P_n is the primary productivity (from Equation 1; Long *et al.* (2006b).

This equation can be used to identify what the future focus should be to increase crop yield potential.

Conventional breeding has to a large extent optimised the light interception by the canopy, although improvements in light distribution within the canopy may still give significant gains. In most cereals, harvest index (HI) has been optimised through breeding and is now at or close to its theoretical maximum, i.e. ~0.62 for wheat (Austin *et al.*, 1980, Foulkes *et al.*, 2007, Shearman *et al.*, 2005). When 12 CIMMYT spring wheat cultivars, developed in irrigated, high-potential environments between 1966-2009 (since the introduction of semi-dwarfing genes), were compared it was found that yield increases over time have been associated with increased harvest biomass production whilst maintaining HI (Aisawi *et al.*, 2015). The increase in biomass appears to have contributed to increases in grain yield through heavier grains rather than more grains per square meter. As a result, the general consensus is that increasing the canopy conversion efficiency, which depends on the efficiency at which the absorbed light energy can be transduced into biomass (the efficiency of photosynthesis, corrected for respiratory losses), is likely to result in increased crop yields in the future (Long *et al.*, 2006b).

Photosynthesis, specifically carbon reduction in the Calvin-Benson cycle, is the key pathway involved in the fixation of carbon by plants and therefore is the primary determinant of plant biomass (reviewed by Parry *et al.* (2011)). It has been found that increasing whole plant photosynthesis increases crop yield as long as other factors do not become limiting (Ainsworth & Long, 2004). Free-air CO_2 enrichment studies provide evidence that increased photosynthesis does translate into increased crop yields, although these increases due to elevated CO_2 , were smaller than was predicted (Long *et al.*, 2006a). Investigating the rate limiting steps of photosynthesis, in plants under different climatic conditions, may indicate potential points at which optimisation could increase photosynthetic rate and crop yield.

1.5 Photosynthesis

In photosynthesis products from the light reactions (ATP and NADPH) are used in the Calvin-Benson cycle to fix atmospheric carbon dioxide (CO_2) into organic compounds, which are used to biosynthesise starch and sucrose for use in plant growth and development (Raines, 2010). The Calvin-Benson cycle is initiated by the enzyme ribulose-1, 5-bisphosphate carboxylase/oxygenase (Rubisco; EC 4.1.1.39).

Rubisco catalyses the carboxylation of ribulose-1, 5-bisphosphate (RuBP), forming two molecules of 3-phosphoglycerate (3-PGA), these are then used to form triose phosphates using ATP and NADPH. The cycle is then completed when these triose phosphates are regenerated into RuBP (reviewed by Raines (2003)). The majority of 3-PGA is used to regenerate RuBP but in the steady-state some will exit the cycle, and be used for the production of starch and sucrose. Rubisco can also carry out the competing process of RuBP oxygenation, initiating photorespiration. Oxygen competes with CO_2 for reaction with RuBP at the active site of Rubisco. The process of photorespiration, by which the toxic product 2-phosphoglycolate is salvaged, results in the loss of fixed carbon, nitrogen and energy (See Figure 1.3).

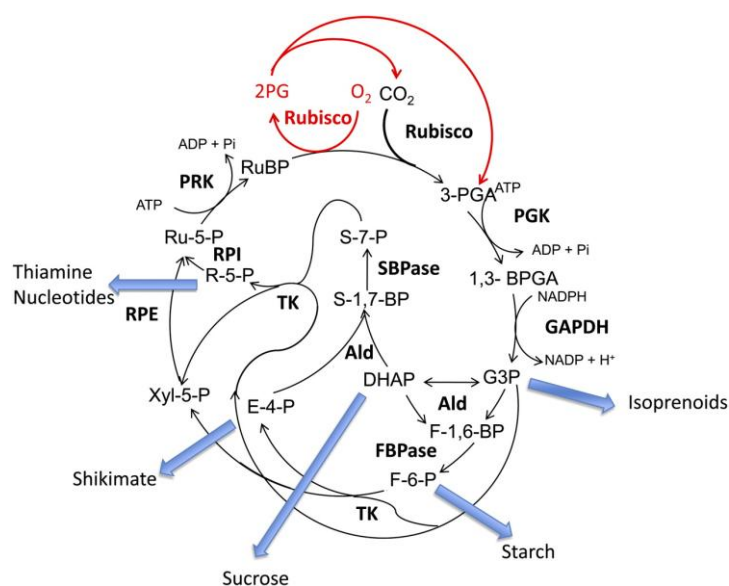


Figure 1.3. The Calvin- Benson Cycle reproduced from Raines (2011).

Rubisco catalyses the carboxylation of RuBP forming 3-PGA. Reactions catalysed by 3-PGA kinase (PGK) and GAPDH, produce G-3-P from 3-PGA, consuming ATP and NADPH. The G-3-P is used to ultimately regenerate RuBP. Catalysed by aldolase (Ald) and either FBPase or SBPase, Fru-6-P (F-6-P) and sedoheptulose-7-P (S-7-P) are produced. Fru-6-P and sedoheptulose-7-P are then utilised in reactions catalysed by Transketolase (TK), R-5-P isomerase (RPI), and ribulose-5-P (Ru-5-P) epimerase (RPE), producing Ru-5-P. In a final step Ru-5-P is converted to RuBP, catalysed by PRK. The oxygenation reaction of Rubisco fixes O_2 into the acceptor molecule RuBP, forming PGA and 2-phosphoglycolate (2PG), and the process of photorespiration (shown in red) releases CO_2 and PGA. The five export points from the pathway are shown with blue arrows.

Many factors limit photosynthesis (reviewed by Sage *et al.* (2008), and these have been investigated with use of knowledge based models. Attempts to model the biochemical processes underlying gas exchange in leaves, and therefore photosynthetic carbon assimilation in C₃ plants, were originally made by Farquhar *et al.* (1980), with many subsequent refinements i.e. Cen *et al.* (2005). These studies indicated ‘bottlenecks’ at which the rate of photosynthesis was likely to be rate limiting; photosynthesis is considered to be limited by diffusion barriers and metabolic processes.

The diffusion of CO₂ from the atmosphere to the site of reaction with RuBP in the chloroplast may be restricted due to: boundary layer effects close to the leaf surface, stomatal aperture, the arrangement of intercellular spaces surrounding photosynthetic cells and the collective effects of the cell wall, the cytosol and the chloroplast envelope on the passage of CO₂ (Sage *et al.*, 2008). These factors are collectively referred to as ‘diffusion limitations’ on photosynthesis. Whilst many components within the leaf affecting CO₂ diffusion are largely fixed, the stomata regulate this process in response to temperature, light and water availability.

Three major hypotheses for the limitation of photosynthesis by biochemical processes can be highlighted. Firstly, the regeneration of RuBP (Cen & Sage, 2005) which depends upon the action of Calvin-Benson cycle enzymes (i.e. Rubisco, SBPase, transketolase, FBPase, reviewed by Raines (2003)), a supply of ATP and NADPH from the light reactions (electron transport) and the supply of phosphoglycerate from Rubisco. Secondly, the capacity of starch and sucrose synthesis to consume triose phosphates and regenerate inorganic phosphate (Pi) for photophosphorylation (Pi regeneration-limited photosynthesis or triose phosphate use-limited photosynthesis) can be limiting. Finally, the catalytic capacity of Rubisco to carry out carboxylation; if the activity of this enzyme is reduced the capacity of the plant to fix carbon is often also limited (Portis & Parry, 2007, Spreitzer & Salvucci, 2002).

1.5.1 Photosynthesis and temperature

Temperature is one of the most important limiting factors controlling the geographical distribution of plant species and their growth and development (Berry & Bjorkman, 1980). The thermal optimum of C₃ photosynthesis is typically between 20- 35°C and with increased temperature the rate of photosynthesis decreases, as shown in Figure 1.4 (Sage *et al.*, 2008). The cumulative rate of photosynthesis over the entire growing season determines crop biomass and therefore it is important to understand both the short-term (minutes to hours) and long-term effects of exposure to temperatures above the thermal optimum for photosynthesis.

Figure 1.4 shows that Rubisco activity is seen to be the primary limiting factor at elevated temperature, while electron transport capacity/ RuBP regeneration under the same conditions were found to be in excess (Weis, 1981). Investigation by Feller *et al.* (1998) found that increasing temperatures resulted in inhibition of Rubisco, with different temperature thresholds in different plant species: 35°C for cotton and 30°C for wheat. Electron transport (as measured by chlorophyll fluorescence) was not greatly altered (in either species) until over 40°C, and so appeared to be more stable than Rubisco activation state under moderate heat stress. Rubisco inhibition was found to be reversible at temperatures below 40°C. Pi limitation is commonly associated with photosynthesis at low temperatures (Sage *et al.*, 2008). However, Pi regeneration is quick to acclimate to low temperatures and so these effects may only be present in the short-term.

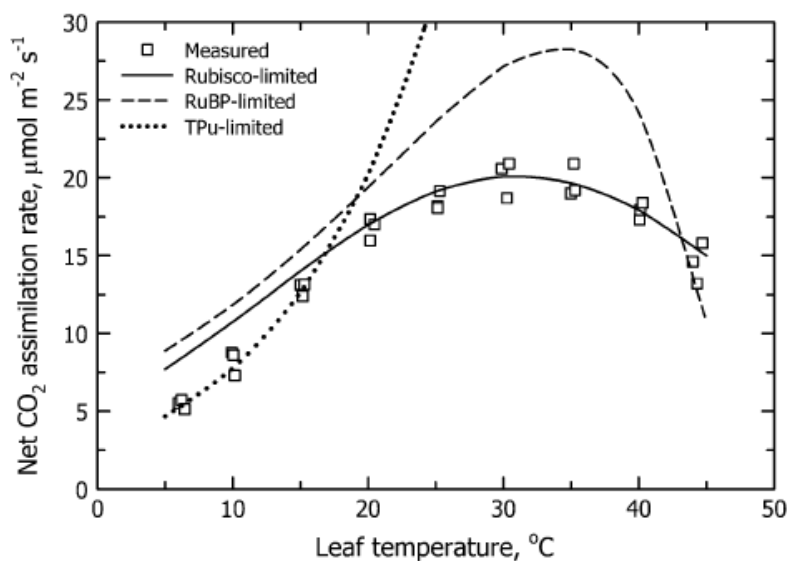


Figure 1.4. CO₂ assimilation rates in relation to leaf temperature. Modelled assimilation in tobacco with Rubisco limitation (solid line), RuBP limitation (dashed line) and triose phosphate use limitation (dotted line). Rubisco limitation shows the lowest carbon assimilation rate and a lower peak than RuBP limitation. Reproduced from Sage *et al.* (2008).

1.5.1 Other abiotic limitations on photosynthesis

Water limits plant productivity in many regions of the world (reviewed by Chaves *et al.* (2009)). Drought can be seen to cause a reduction in photosynthesis due to direct changes in plant biochemistry or due to a trade-off between stomatal closure to reduce water loss and the need for stomata to remain open to supply the leaf with CO₂ (Chaves *et al.*, 2002, Parry *et al.*, 2006). However, increasing the external CO₂ concentration does not reverse the negative impact on carbon assimilation, suggesting that severe drought stress also impacts upon metabolism directly (Chaves *et al.*, 2009). Early biochemical effects of drought involve alterations in photophosphorylation with a decrease in the amount of ATP leading to a decreased regeneration of RuBP (Lawlor, 2002).

The global atmospheric CO₂ concentration is predicted to increase to over 550 ppm by the middle of this century (Le Quere *et al.*, 2009). The impacts of this increase are complex with the stimulation of photosynthesis due to a reduction in photorespiration being possible. With this increase in CO₂ the factors limiting to photosynthesis may shift away from Rubisco towards RuBP regeneration or the ability of starch and sucrose synthesis to regenerate Pi. The temperature optimum of photosynthesis also varies with

CO₂ concentration (as shown in Figure 1.5; Sage & Kubien (2007)); at low CO₂ levels the curve has a shallow peak, usually centred in the 20°C range. Increasing CO₂ levels results in a shift in the optimum to higher temperatures, and the peak sharpens, meaning that at high CO₂, photosynthesis exhibits a sharp peak, centred around 30- 35°C in most species. If the CO₂ concentration should fall below ambient, for example, in response to stomatal closure, then CO₂ assimilation has been shown to become increasingly limited by the catalytic capacity of Rubisco.

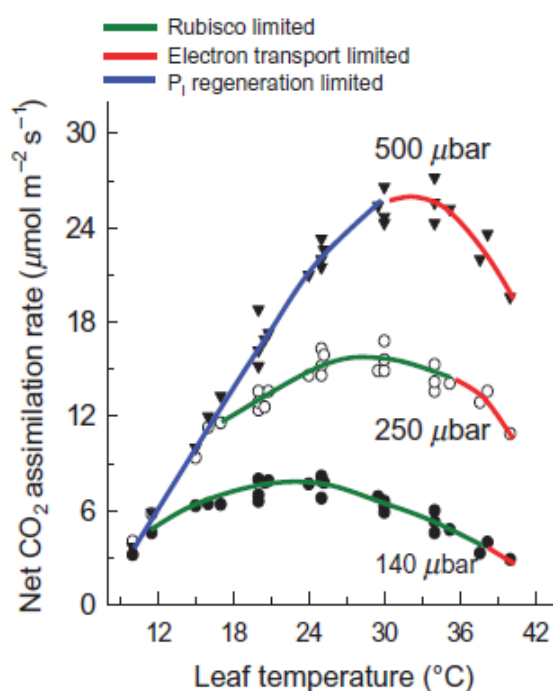


Figure 1.5. Carbon assimilation of sweet potato (*Ipomoea batatas*) in response to CO₂ and temperature. The biochemical limitation dominating under the different intercellular CO₂ partial pressures (μbar) is indicated; Rubisco-limited (green); electron transport-limited (red); Pi regeneration-limited (blue). Determined using empirical estimates of V_{cmax} , J_{max} and Pi regeneration capacity and the model of Farquhar *et al.* (1980), as described by Cen & Sage (2005). Reproduced from Sage and Kubien (2007).

1.6 Rubisco as a route to overcoming photosynthetic limitations

Rubisco is the most abundant protein found on earth (Ellis, 1979, Raven, 2013) and comprises up to 50% of all soluble protein in leaves (Spreitzer & Salvucci, 2002). As mentioned previously, it catalyses both carboxylation and oxygenation. Rubisco has a low turnover number and so large amounts are required to

match the capacity of the other Calvin-Benson cycle enzymes and so to sustain sufficient photosynthetic rates.

Rubisco is found in different forms in photosynthetic organisms: Form II Rubisco is found in bacteria and some dinoflagellates. The more common Form I type is found in bacteria, algae and higher plants. The Form I class is further divided into the 'green' subclass, found in bacteria and cyanobacteria (Form IA and Form IB) and green algae and higher plants (Form IB), and the 'red' subclass, found in bacteria (Form IC) and non-green algae (Form ID; Pearce (2006)).

In higher plants (Form I) Rubisco is seen to have a molecular mass of 560 kDa (reviewed by Spreitzer & Salvucci (2002)). The structure of Rubisco is hexadecameric comprising of eight large chloroplast-encoded sub-units arranged as four dimers and eight small nuclear-encoded subunits (Parry *et al.*, 2008). Each large subunit has two main structural domains; an N-terminal and a C-terminal domain. The C-terminal is an alpha/beta barrel. The active sites of the enzyme are contributed by loops at the mouth of the alpha/beta barrel with the remaining residues being supplied by two loop regions in the N-terminal domain of the second large subunit within a dimer.

Rubisco activity (see Figure 1.6) is regulated by carbamylation of an essential lysine residue found at the catalytic site (Eckardt & Portis, 1997, Mate *et al.*, 1993, Portis, 2003, Portis *et al.*, 1986, Spreitzer & Salvucci, 2002). The resulting carbamate is then stabilised by an Mg^{2+} ion which results in a catalytically active complex with an open conformation (ECM form of Rubisco). The tight binding of low molecular weight inhibitors, such as sugar-phosphates, either before (e.g. RuBP), or after, carbamylation (e.g. 2-carboxy-D-arabinitol-1-phosphate; CA1P), acts as a regulatory mechanism. These block the active site resulting in a closed form of the enzyme and either prevent the substrate from binding or prevent carbamylation. The enzyme, Rubisco activase (Rca), is required to activate Rubisco through the removal of tightly bound sugar-phosphates from the catalytic sites of both carbamylated and decarbamylated Rubisco.

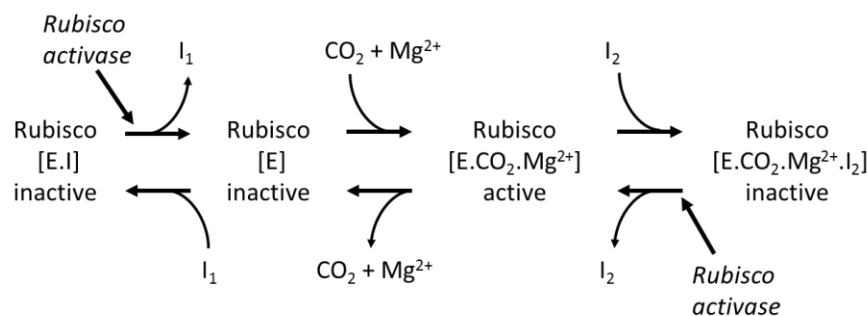


Figure 1.6. Diagram of Rubisco and Rca interactions.

Reversible carbamylation and inhibitor binding to carbamylated or non carbamylated Rubisco.

[E], unmodified enzyme ('decarbamylated' Rubisco); [E.I], decarbamylated enzyme with substrate (RuBP) or misfire product (XuBP) bound at active sites—in this context both compounds are inhibitors (I); [E.CO₂.Mg²⁺], ternary complex with catalytically competent active site geometry; [E.CO₂.Mg²⁺.I], carbamylated enzyme with catalytic site occupied by tight binding inhibitor. I₁=RuBP; I₂ includes CA1P and Pentadiulose 1,5-bisphosphate (PDBP). Based upon Parry *et al.* (2007)

1.6.1 Limitations and improvement of Rubisco

The major limitations of Rubisco which impact upon carbon assimilation are its relative specificity for CO₂ and O₂, its concentration in leaf tissue, the presence of specific inhibitors and changes in its catalytic rate due to environmental conditions (reviewed by Parry *et al.* (2013)). Additionally, Rubisco is a slow enzyme, necessitating uncharacteristically large amounts to support photosynthesis.

1.6.2 Specificity

The specificity of Rubisco refers to the relative capacity of the enzyme to catalyse carboxylation and oxygenation of RuBP. Specificity determines the relative rates of carbon fixation and photorespiration under different environmental conditions (Cousins *et al.*, 2010). The affinity of wheat Rubisco for CO₂ (Km 9.7 μM) and O₂ (Km 244 μM) is equivalent to the concentrations of the gases in air-saturated water (CO₂ ~11 μM and O₂ ~280 μM at 25°C; Ku *et al.* (1978)), meaning that carboxylation and oxygenation both proceed at significant rates in leaves. However, photorespiration increases as temperature increases, as with increasing temperature the concentration of CO₂ in solution declines more severely than the concentration of oxygen. Additionally, the reaction between the 2,3-enediol intermediate of Rubisco and O₂ has a higher free energy of activation than its reaction with CO₂ and so elevated temperatures also favour the oxygenase activity (Chen & Spreitzer, 1992). If low water availability accompanies high

temperatures, the consequent stomatal closure may cause a greater fall in intercellular CO₂ than O₂, due to the vastly greater abundance of the latter. The rates of photorespiration are about 20% of the rate of net CO₂ assimilation in C₃ plants under ambient CO₂ concentrations at 25°C. Any improvement in the ability of Rubisco to discriminate in favour of CO₂ would reduce photorespiration (Raines, 2006). Doubling the specificity of Rubisco for CO₂ in wheat could theoretically increase A (max) by ~20% (Reynolds *et al.*, 2000b).

Differences in the specificity of Rubisco from different species have been found (Galmes *et al.*, 2005). The exploitation of this natural variation by engineering crops to contain Rubisco with higher catalytic rates and specificity could improve crop yields. Galmes *et al.* (2005) investigated Rubisco from 24 C₃ species finding that specificity is closely related to the selection pressures imposed by the environment in which they grow. Plants from drier environments and those which were evergreen showed higher specificity factors. It was predicted that replacing wheat Rubisco with that from the drought tolerant Mediterranean species, *Limonium gibertii*, which has Rubisco with a significantly higher specificity factor, would increase net assimilation by 12%.

Research has attempted to introduce Rubisco with superior characteristics from algae into tobacco (Whitney *et al.*, 2001). Initially, problems with incorrect folding and assembly of the proteins were found and overall reductions in rate were seen but further research has enabled functional assembly of the large and small Rubisco subunits (Whitney *et al.*, 2009). Although the replacement of native Rubisco with that from other species holds great promise, it remains a challenging objective, requiring context-specific expression, assembly, post-translational modification, and activity regulation. The requirement for chaperones to ensure the correct folding of Rubisco (investigated with cyanobacteria form 1 Rubisco by Liu *et al.* (2010)) indicates the complexities required in engineering an improved Rubisco. Continued work to understand the folding and assembly of red-type Rubisco in proteobacterium may facilitate the engineering of crop plants with improved Rubisco (Joshi *et al.*, 2015). Another barrier to the introduction of Rubisco from other species is that the large subunit of Rubisco is chloroplast encoded and so modification of this requires chloroplast transformation, a technique which has only been developed for a few plant species (Verma & Daniell, 2007). Even within wheat, differences in the properties of Rubisco

have been noted, including wheat, and this natural diversity might also be exploited through targeted breeding. Evans and Austin (1986) measured the specific activity of Rubisco in crude extracts of leaves from euploid, amphiploid and alloplasmic lines of wheat and found that *in vitro* the activities fell into high or low categories.

One problem with increasing the specificity of Rubisco is the apparent inverse correlation between Rubisco specificity and catalytic rate (Zhu *et al.*, 2004). One explanation for this is that the higher the specificity, the tighter the binding of the carboxylase catalytic intermediate, resulting in slower product release and lower turnover rates (Tcherkez, 2006). Such a relationship will inevitably limit the extent to which both higher specificity and higher catalytic capacity (rate) can be realised. However, it is thought that increasing the catalytic rate may in itself be enough to increase photosynthesis under certain conditions. Furthermore, notable exceptions to this inverse correlation (between rate and specificity) have been identified in form II Rubisco from a number of different photosynthetic organisms (Savir *et al.*, 2010). One approach would be to express such Rubisco variants in crop plants.

Alternatively, the genetic manipulation of Rubisco, through the identification and alteration of amino acid residues which are involved in the catalytic mechanism of the enzyme may also be successful in improving the properties of this enzyme (Whitney *et al.*, 2011). To date, no mutagenesis approach has produced an enzyme with superior properties when compared to those in existing crops (reviewed in Parry *et al.* (2003) and Zhu *et al.*(2004)). Systems have been developed to direct the evolution of Rubisco in bacteria, enabling the selection of Rubisco mutations which confer superior properties from populations containing thousands of random genetic mutations. Thus, with use of *E. coli*, Rubisco mutants with increased activity have been developed (Parikh *et al.*, 2006). Ultimately, it may be possible to introduce these modifications into crop plants; this approach has not yet successfully modified higher plant Rubisco (Mueller-Cajar & Whitney, 2008).

1.6.3 Amount

The amount of Rubisco has also been found to have impacts upon the overall photosynthetic rate of the plant. Antisense *rbcS* genes have successfully decreased the amount of Rubisco in plants (Hudson *et al.*, 1992). Over-expression of the gene has often resulted in a decrease in the amount of Rubisco due to co-suppression. The amount has been seen to increase due to transformations of other genes but as other photosynthetic elements may also have been altered it is difficult to determine clear cause-effect relationships. Increasing the abundance of Rubisco, which already accounts for a significant proportion of leaf protein, may also be problematic due to the resultant increased nitrogen requirements of the plant (Parry *et al.*, 2011).

Nitrogen is stored in many crop species during vegetative growth as increased photosynthetic capacity in leaves, with there being a proportionally greater increase in Rubisco content. Therefore, increasing photosynthetic capacity under high nitrogen supply to maximise storage, and decreasing it under low nitrogen supply may maximize nitrogen use efficiency (Carmo-Silva *et al.*, 2014).

1.6.4 Inhibitors

Investigating the synthesis and degradation of Rubisco inhibitors may enable better regulation of Rubisco. CA1P is the best characterised inhibitor of Rubisco. It is found in the chloroplast and binds tightly to the active site of carbamylated Rubisco, in certain plant species (Andralojc *et al.*, 2006, Andralojc *et al.*, 2012, Gutteridge *et al.*, 1986). Diurnal variation has been seen in the activity of Rubisco with CA1P being removed from the active site by Rca and dephosphorylated by a CA1P phosphatase, both of which are activated by light (Heo & Holbrook, 1999). When light levels fall re-phosphorylation can then occur, meaning that CA1P can accumulate overnight.

1.6.5 Regulation in response to environmental conditions

Rubisco activity can be seen to be a major limiting factor to photosynthesis under heat stress. A reduction in the activation state of Rubisco occurs above the optimum temperature for carbon assimilation, resulting in reduced photosynthetic capacity. However, this drop in photosynthetic capacity is not due to Rubisco

itself, which is in fact relatively thermostable and able to withstand temperatures of up to 50°C with negligible loss of activity (Crafts-Brandner & Salvucci, 2000). *In vitro*, as temperature increases Rubisco becomes more flexible and so sugar phosphates bind less tightly and spontaneous dissociation is faster, so in fact (to a point) Rubisco activity is not seen to decline (Schrader *et al.*, 2006). Photosynthetic capacity falls due to a decline in Rca activity which results in the deactivation of Rubisco at high temperatures (Salvucci & Crafts-Brandner, 2004b). Rca is thermally labile and has a relatively low temperature optimum for reactivating Rubisco. Therefore, improving the thermal properties of Rca could improve the thermal tolerance of photosynthesis (as discussed in more detail in the following sections). A decline in the availability of Mg²⁺ has also been suggested to cause inactivation of Rubisco at high temperatures (Kim & Portis, 2006).

During drought stress a decrease in the amount of Rubisco small subunit transcripts potentially indicates decreased Rubisco synthesis (Vu *et al.*, 1999). Drought causes a decrease in Rubisco activity. For example, Majumdar *et al.* (1991) found a rapid loss of Rubisco activity in soybean (*Glycine max* L. cv. Jackson) accompanied drought. It has been proposed that a decrease in Rubisco activity is due to tight binding inhibitors accumulating in Rubisco active sites. Rubisco may not be the cause of reduced photosynthesis during water stress but it may still play an important role as it could be involved in rapid recovery of photosynthesis after re-watering (Ennahli & Earl, 2005).

A correlation was found in Mediterranean species between stomatal conductance and Rubisco activity, with Rubisco being deactivated due to low CO₂ concentrations resulting from water stress (Galmes *et al.*, 2011). Species with lower stomatal conductance (under well-watered conditions) better maintain Rubisco activity under drought conditions. Photosynthesis in Mediterranean species may be constrained by lower Rubisco activation as a consequence of the need to keep stomata largely closed in a water-scarce environment.

1.7 Rubisco activase

Rca plays an important role in the modulation of the activity of Rubisco. Rca is a nuclear-encoded, cytosol-synthesised protein, described first by Salvucci *et al.* (1985), following experiments with a mutant of *Arabidopsis thaliana* (*Arabidopsis*) capable of activating Rubisco. This molecular chaperone is a member of the AAA+ family of ATPases (reviewed by Spreitzer & Salvucci (2002)). The crystal structure of the Rca-Rubisco recognition domain has been described (Henderson *et al.*, 2011), with research being completed in creosote bush (*Larrea tridentata*). Without Rca *Arabidopsis* cannot grow successfully in ambient CO₂ concentrations as the active site of Rubisco does not become fully carbamylated (Salvucci *et al.*, 1985). Plants with reduced Rca expression show reductions in growth (Eckardt *et al.*, 1997, He *et al.*, 1997, Jiang *et al.*, 1994, Mate *et al.*, 1996).

1.7.1 Interaction of Rubisco and Rubisco activase

The mechanism of the interaction between Rca and Rubisco, which leads to the removal of sugar-phosphate inhibitors from the Rubisco active sites, is unknown. It is thought that electrostatic and other forces at amino acid regions on both proteins are involved. Rca catalyses both Rubisco activation and ATP hydrolysis; in fact, Rubisco activation requires ATPase activity. When Rubisco and Rca are interacting ATP hydrolysis promotes movement of the C-terminal sensor-2 domain of Rca (Henderson *et al.*, 2011, Parry *et al.*, 2008). This domain contains an arginine residue which interacts with the bound nucleotide. This would provide an explanation for the coupling of ATP hydrolysis with the movement of the sensor-2 region on Rca, and therefore the movement of the N-terminal domain of Rubisco. Movement in the N-terminal domain of Rubisco could break the interaction between Glu-60, Lys-334 in loop 6, and the bound sugar-phosphate. Loop 6 would then be able to move out of the way of the active site, allowing the sugar-phosphate within the catalytic site to be released.

1.7.2 Rubisco activase isoforms

In some plants two isoforms of Rca can be found; a long (α) isoform of 43- 47 kDa, and a short (β) isoform of 41- 42 kDa (Salvucci *et al.*, 1987). The difference between them is that the α isoform has an extended C-terminus (of an additional 27- 36 amino acids) containing redox-sensitive Cysteine residues

(reviewed by Portis *et al.* (2008)). *In vitro* experiments have shown that the long and short isoforms of Rca from spinach (*Spinacia oleracea*) are both capable of promoting Rubisco activation but that they differ in their sensitivity to ATP and ADP (Shen *et al.*, 1991). The number of Rca encoding genes can vary between species and in some species the Rca transcript undergoes alternative splicing to result in the different isoforms of Rca; for a comprehensive species list see Table 1.1; Carmo-Silva, Scales *et al.* (2014).

1.7.3 Rubisco activase regulation

Rca expression is tissue specific; occurring only in green parts of the plant and it is developmentally regulated by leaf age and light (Liu *et al.*, 1996, Watillon *et al.*, 1993). Circadian oscillations of Rca have been detected in some plant species (i.e. apple; Watillon *et al.* (1993)). These changes in mRNA level may be from transcriptional or post-transcriptional regulation.

Rca is regulated by light via the stromal ADP/ATP ratio (Robinson & Portis, 1989a). Changes in ADP/ATP do not fully explain light-modulation of Rubisco activity (Brooks *et al.*, 1988), implying that other mechanism of Rca regulation (the redox status of the chloroplast stroma) must also be involved *in vivo* (Zhang & Portis, 1999). As the light level decreases, the ratio of ADP/ATP increases, the activity of Rca becomes increasingly inhibited and inhibitory sugar-phosphates accumulate at the Rubisco catalytic sites, thereby modulating CO₂ assimilation. Zhang and Portis (1999) showed that both the ATPase and the Rubisco activation activities of the α isoform of Rca are sensitive to the ADP/ATP ratio and this sensitivity depends on the redox status.

For example, in Arabidopsis the α isoform, but not the β isoform of Rca, is regulated by redox-modulation via thioredoxin-f (Zhang & Portis, 1999). When oxidized to the disulphide form, the affinity for ATP decreases and sensitivity to inhibition by ADP increases. Physiological ratios of ADP/ATP inhibit the α Rca when oxidized, but this inhibition is less pronounced when the isoform has been reduced by thioredoxin-f. The β Rca is not redox-regulated and is less sensitive to ADP inhibition. The α isoform of Arabidopsis Rca seems to regulate the β isoform allosterically. In tobacco and maize, only the β

isoform is present, although Rubisco activity is still regulated by the irradiance level (Salvucci & Anderson, 1987).

Table 1.1. *Rca* gene and *Rca* isoform number in different plant species.

Key references and sequence accession numbers are shown with the corresponding isoform names where possible. Number of isoforms refers to number visible on western blot. Where clearly identified in the relevant reference alternative splicing of genes is noted (AS).

Plant Name	Number of genes and isoforms	Key Gene Accession numbers	Key References
Wheat <i>Triticum aestivum</i>	2 genes (<i>rca1</i> , <i>rca2</i> (AS)) 2 isoforms (<i>RcaB1</i> , <i>RcaA2</i> , <i>RcaB2</i>)	LM992844 (<i>TaRca1-β</i>) LM992845 (<i>TaRca2-β</i>) LM992846 (<i>TaRca2-α</i>)	Carmo-Silva, Scales <i>et al.</i> (2014)
Spinach <i>Spinacia oleracea</i>	1 gene (AS) 2 isoforms	J03610.1 S45033.1 (AS)	Werneke <i>et al.</i> (1989), Werneke <i>et al.</i> (1988)
Arabidopsis <i>Arabidopsis thaliana</i>	1 gene (AS) 2 isoforms	X14212.1	Werneke <i>et al.</i> (1988), Werneke <i>et al.</i> (1989), Salvucci <i>et al.</i> (1985)
Cotton <i>Gossypium hirsutum</i>	3 genes (AS), 2 isoforms (<i>GhRCAα1</i> , <i>GhRCAα2</i> , <i>GhRCAβ</i>)	AF329935.1 (<i>RCA2</i>) AF329934.1 (<i>RCA1</i>) DQ233255.1 (<i>GhRCAα2</i>)	Deridder and Salvucci (2007), Salvucci <i>et al.</i> (2003), Feller <i>et al.</i> (1998)
Creosote bush <i>Larrea tridentate</i>	2 isoforms (<i>RCA1α</i> , <i>RCA2β</i>)	AY312575 (<i>RCA1α</i>) AY312576 (<i>RCA2β</i>)	Salvucci and Crafts-Brandner (2004a)
Antarctic hairgrass <i>Deschampsia antarctica</i>	1 gene? 2 isoforms (<i>RCA1α</i> , <i>RCA2β</i>)	AY312573 (<i>RCA1α</i>) AY312574 (<i>RCA2β</i>)	Salvucci and Crafts-Brandner (2004a)
Tobacco <i>Nicotiana tabacum</i>	3- 5 genes β isoform only	U35111.1 Z14979.1 Z14980.1 Z14981.1	Qian and Rodermel (1993), Wang <i>et al.</i> (1992)
Barley <i>Hordeum vulgare</i>	2 genes (AS) 2 isoforms (<i>RcaA1</i> , <i>RcaA2</i> , <i>RcaB</i>)	M55446.1 (<i>RcaA1</i>) M55447.1 (<i>RcaA2</i>) M55448.1 (<i>RcaB</i>)	Rundle and Zielinski (1991)
Rice <i>Oryza sativa</i>	1 gene (AS) 2 isoforms, (<i>RCAI</i> , <i>RCAII</i>)	U74321.1 AB034748.1 (Small A2) AB034698.1 (Large A1) KC140121 (Small) HQ324826 (Small) AB110180.1 (Large)	To <i>et al.</i> (1999)
Maize <i>Zea Mays</i>	2 genes β isoform only, unless in stress conditions.	AF305876.3 (<i>Zmrca2</i>) AF084478.3 (<i>Zmrca1</i>) JX863889.1 (<i>Zmrca3</i>)	Vargas-Suarez (2004), Crafts-Brandner and Salvucci (2002), Ayala-Ochoa <i>et al.</i> (2004), Yin <i>et al.</i> (2014)
Soybean <i>Glycine Max</i>	2 genes (three other genes identified with potential roles) 2 isoforms (<i>GmRCAα</i> , <i>GmRCAβ</i>).	GQ917180 (<i>GmRcaα</i>) GQ917184 (<i>GmRcaβ</i>)	Yin <i>et al.</i> (2010)

Plant Name	Number of genes and isoforms	Key Gene Accession numbers	Key References
Red maple <i>Acer rubrum</i>	1 gene (AS) 2 isoforms (RCA1, RCA2)	DQ915973 DQ915974 DQ915975 DQ915976	Weston <i>et al.</i> (2007)
Sweet potato <i>Ipomoea batatas</i>	2 genes 2 isoforms (Ib-RCA1, Ib-RCA2)	EU287993.1 JQ923423—JQ9234231	Xu <i>et al.</i> (2010) Jiang <i>et al.</i> (2013)
Apple <i>Malus domestica</i>	1 gene (AS) 2 isoforms	Z21794.1	Watillon <i>et al.</i> (1993)
Grass-leaved Arrowhead <i>Sagittaria graminea</i>	1 gene (AS) 2 isoforms (Sgrca1, Sgrca2)	KC678993.1 (rca1) KC678994.1 (rca2) KC553979.1 (rca)	Wang <i>et al.</i> (2014)
French bean <i>Phaseolus vulgaris</i>	2 isoforms	AF041068 (Rca1) KF569537 (Rca) KF378790 (Rca1)	Ryan <i>et al.</i> (1998)
Coastal plains yellowtop <i>Flaveria bidentis</i>	2 isoforms	EU202926.1 (small)	Hendrickson <i>et al.</i> (2008), von Caemmerer <i>et al.</i> (2005)
Other species with two isoforms	Large crabgrass <i>Digitaria sanguinalis</i> Sorghum <i>Sorghum bicolor</i> Celery <i>Apium graveolens</i> Pea <i>Pisum sativum</i>	Oat <i>Avena sativa</i> Smooth pigweed <i>Amaranthus hybridus</i> Common Purslane <i>Portulaca oleracea</i> Common Dandelion <i>Taraxacum officinale</i>	Salvucci <i>et al.</i> (1987)

1.8 Rubisco activase and heat stress

Under heat stress a reduction in the activity and amount of Rca available to maintain the activation state of Rubisco leads to decreased photosynthesis (Salvucci *et al.*, 2006). Rca is more heat labile than Rubisco and at high temperatures it is irreversibly inactivated (Figure 1.7 provides an example of the temperature response of a warm season species, namely tobacco) due to loss of the structural integrity of the protein as high temperatures disrupt the forces that normally stabilize protein folding (Salvucci *et al.*, 2001). Hence, as temperatures increase Rca becomes less effective at reactivating Rubisco and cannot keep up with the increased rates of Rubisco deactivation seen at higher temperatures (Crafts-Brandner & Salvucci, 2000). When considered in terms of the individual thermal tolerance of Rubisco and Rca it is clear that reductions in assimilation at high temperature can be associated with a decline in Rca activity (Carmo-Silva *et al.*, 2012).

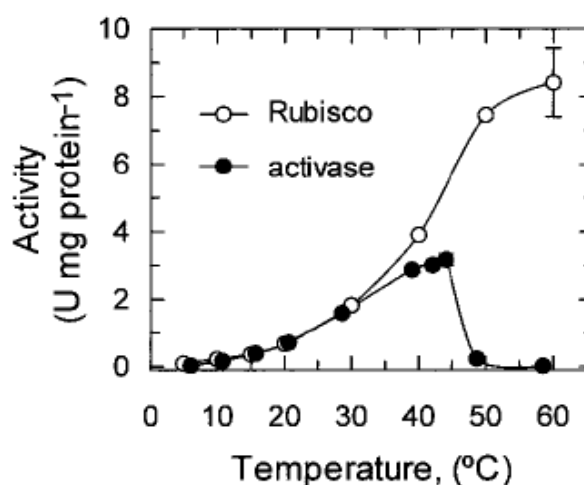


Figure 1.7. The change in the *in vitro* activity of Rubisco and Rca with increasing temperature. Experiments completed with tobacco (*Nicotiana rustica* cv. Pulmila) Rubisco and Rca. Reproduced from Salvucci *et al.* (2001).

At moderately high temperatures, Rubisco deactivation is proposed to occur because the production of inhibitory compounds (e.g. D-xylulose-1,5-bisphosphate (XuBP) and D-glycero-2,3-pentodiulose-1,5-bisphosphate (PDBP); reviewed by Carmo-Silva *et al.* (2014)) exceeds the capacity of Rca to remove them from the catalytic sites of Rubisco (Salvucci & Crafts-Brandner, 2004b). Above a species-specific temperature, Rca itself may denature, forming insoluble aggregates that are incapable of removing

inhibitors and promoting Rubisco activation (Feller *et al.*, 1998, Salvucci *et al.*, 2001). Consequently, a high activation state of Rubisco cannot be maintained. It has been suggested that the accumulation of insoluble Rca during heat stress involves binding to the thylakoid membrane (Rokka *et al.*, 2001) and that this could play a role in the regulation of chloroplast proteins. Although, it may be that in the experimental set up used to investigate this the denatured Rca was just co-precipitating with the heaviest fraction from the thylakoid membrane, the polysomes (Salvucci, 2008).

It was originally hypothesised that changes in the oxidation state of the stroma under moderate heat stress (Schrader *et al.*, 2004) impacted upon Rca activity and therefore Rubisco activation state. This was supported by Kim and Portis (2005) using transgenic Arabidopsis plants expressing only the redox-regulated α isoform of Rca in which photosynthesis was more sensitive to inhibition by moderate, temporary, heat stress. This was when compared to photosynthesis in wild-type plants, or in plants expressing only the non-redox-regulated β isoform or a modified α isoform incapable of redox regulation. However, differences in the amount rather than the form of Rca might explain the difference in thermotolerance between transgenic lines that expressed the different forms of Rca.

Salvucci *et al.* (2006) studied transgenic Arabidopsis lines, expressing lower amounts of the α isoform or of the non-redox-regulated β isoform of Rca. The temperature response results are inconsistent with an involvement of stromal oxidation in the loss of Rubisco activation under moderate heat stress. While the redox-sensitive disulphide of the α isoform of Rca could be adversely affected by increased stromal oxidation, the results with transgenic Arabidopsis lines expressing suboptimal levels of either the 43 kDa (β suboptimal amounts, $\Delta 43$) or 46 kDa (α suboptimal amounts, *rwt46*) Rca isoform showed that photosynthesis in both lines was sensitive to inhibition by moderate heat stress. However, Rubisco activation was slightly more sensitive to moderate heat stress in the α suboptimal plants, compared with the β suboptimal plants. This is consistent with the finding that the α isoform is more heavily regulated than the β isoform (Zhang *et al.*, 2002, Zhang & Portis, 1999) and could reflect a slightly greater sensitivity of this form of Rca to changes in redox, ATP/ADP ratio, or other conditions in the chloroplast. The results are consistent with thermal denaturation of Rca under moderate heat stress, the effects of which on Rubisco activation would be enhanced when Rca levels became suboptimal for photosynthesis.

Kurek *et al.* (2007) observed a significant heat sensitivity of Arabidopsis lines expressing the β isoform, but lacking the α isoform ($\Delta rcaRCA1$) compared with wild-type plants (expressing both α and β isoforms) when exposed to extended heat stress. This heat sensitivity could be partially compensated at 26°C by a more thermostable gene shuffled β isoform. Thermostable Rca gene variants were produced by gene shuffling and introduced into Arabidopsis Rca deletion lines. In gene shuffling libraries of sequences are generated containing the information from a family of related genes, the genes are fragmented and reassembled, and the novel sequences are screened for a desired function. Thermostable variants were identified among the transgenic plants, showing higher photosynthetic rates and improved growth and developmental characteristics, compared to the wild-type controls. It was suggested that the α isoform may act as a molecular chaperone during prolonged exposure to heat stress.

1.8.1 Acclimation to heat stress

Rca inactivation may have a protective role when a plant is heat stressed, with reversible decarbamylation of Rubisco possibly ensuring that the plant does not experience more serious damage to Rubisco and other photosynthetic enzymes (Sharkey *et al.*, 2001). The two polypeptides of Rca (often arising from alternative splicing of pre-mRNA) have been seen to have different thermal stability (Salvucci *et al.*, 2001). In spinach (*Spinacia oleracea* L.) it was found that the optimum temperature for ATP hydrolysis of the 45 kDa (α) form was 13°C higher than that for the 41 kDa (β) form (Crafts-Brandner *et al.*, 1997). However, when the forms were mixed the hybrid enzyme showed a temperature optimum similar to that of the 45 kDa form. The 45 kDa form was more thermostable alone and increases the stability of the 41 kDa form. A loss of interaction between these subunits appears to be the initial cause of deactivation of Rca.

Several studies have found that environmental stress may induce new isoforms of Rca or modulate expression. In maize (*Zea mays* L.) a 41 kDa Rca polypeptide is present which is regulated by limited proteolysis of the 43 kDa Rca at its amino-terminal region, the ratio is impacted by stress conditions (Vargas-Suarez, 2004). In cotton (*Gossypium hirsutum* L.) expression of a 46 kDa form was induced with heat stress; upon returning the plants to control conditions after an hour this increased expression had

ceased (Law *et al.*, 2001). In wheat (Law & Crafts-Brandner, 2001) temperatures of 38°C reduced total Rca mRNA levels. However, immunoblot analysis found that heat stress in fact increased the accumulation of the 42 kDa form of Rca and induced a 41 kDa form. A positive correlation in wheat was seen between expression of 45- 46 kDa Rca and productivity under heat stress, suggesting that endogenous levels of Rca may also have an important role in plant productivity (Ristic *et al.*, 2009).

It has been suggested that in rice (*Oryza sativa* L.) the large form of Rca may play a role in acclimation to heat stress, and may be induced during heat stress (Wang *et al.*, 2010). Conversely, the small isoform is important in maintaining Rubisco activity in normal temperatures. DeRidder and Salvucci (2007) suggest a mechanism in cotton for the post-transcriptional regulation of Rca which results in the accumulation of thermally stable transcripts. This is through the production of mRNA transcripts which contain alternative polyadenylation sites which alter their stability. Increasing stability may result in the maintenance of enough Rca mRNA to allow the synthesis of new proteins during heat stress as opposed to the increase in transcripts being due to increased synthesis.

Alternatively, it may be the total amount of Rca which impacts upon thermal sensitivity, rather than the form. Salvucci *et al.* (2006) showed that transgenic Arabidopsis expressing suboptimal amounts of either the redox-regulated 46 kDa isoform or the non-redox-regulated 43 kDa isoform of Rca showed inhibition at moderately high temperatures. In support of this, a greater amount of Rca has been found in high yielding populations of maize (*Zea mays*; Martinez- Barajas *et al.* (1997)). Twenty agronomic selection cycles for grain yield improvement was completed in maize and when the original population and the improved population were compared, the Rubisco activity of the higher yielding plants was greater, although the amount of Rubisco protein was similar.

1.9 Improving Rubisco activase

Improving Rca is a target to maintain Rubisco activation state and to increase photosynthetic rates, in particular under high temperature and variable stress conditions; however different approaches could be taken to achieve these goals.

1.9.1 Exploiting natural variation

Rca enzymes from heat tolerant plants have been characterised (Salvucci & Crafts-Brandner, 2004b) and differences between them have been found. Creosote bush (*Larrea tridentata*) is a desert plant which can be exposed to temperatures over 45.8°C. In comparison, Antarctic hairgrass (*Deschampsia antarctica*) experiences daytime temperatures of 0- 6°C and is rarely exposed to temperatures over 20°C. Comparison between Creosote bush and Antarctic hairgrass showed that the optimum for Rubisco activation was 10°C higher in Creosote bush than in Antarctic hairgrass.

Differences in the thermal tolerance of Rca have led to suggestions that thermally tolerant forms may be used to increase thermal tolerance of photosynthesis in crop species. However, Rca exhibits species specificity (Wang *et al.*, 1992) which may complicate this type of genetic engineering. Some success accompanied the creation of chimeric Rca; Kumar *et al.* (2009) showed that Arabidopsis plants which expressed a thermally stable chimeric Rca showed increased growth and photosynthetic rates at elevated temperatures. A chimeric Rca was created with the Rca from tobacco (*Nicotiana tabacum*) but containing an Arabidopsis Rubisco recognition domain, to ensure functional activity and protein interaction of the gene product in transgenic Arabidopsis.

Rca has been investigated in algae (*Chlamydomonas reinhardtii* (Roesler & Ogren, 1990) and *Chlorococcum littorale* (Beuf *et al.*, 1999)) with the hope that novel characteristics may be found which could improve crop plants. As of yet, Rca from such species has been found to be quite similar to that in higher plants. The protein CbbX was identified as an Rca of red-type Rubisco in the bacteria *Rhodobacter sphaeroides*, despite being a protein that exhibits little obvious sequence homology to Rca (Mueller-Cajar *et al.*, 2011). In some cyanobacteria, such as *Anabaena* sp. strain CA (Li *et al.*, 1993), unusual properties have been found, with the central ATP-binding sites being conserved but the N and C terminals being considerably different. As the amino terminus is required for interaction with Rubisco in higher plants, this suggests that its interaction may be different (Portis, 2003).

1.9.2 Generating new Rubisco activase variants

Kurek *et al.* (2007) used gene shuffling technology to generate Arabidopsis Rca variants with improved thermal stability. This genetic manipulation of Rca indicates another possible route to engineer crop plants with increased productivity at higher temperatures.

Heat stress affects alternative splicing of certain plant genes (Lazar & Goodman, 2000). This could also be the case with Rca, resulting in unique products from this gene. This has potential for increasing the thermal stability of the enzyme by altering the sequence composition (Crafts-Brandner *et al.*, 1997, DeRidder *et al.*, 2012). It is hypothesised that Rubisco and Rca have co-evolved such that amino acid changes occurring in one of the proteins through mutation or selection pressure resulted in complementary changes in the other (Wang *et al.*, 1992). In terms of engineering more thermo-tolerant forms of Rca, the parallel preservation of the complex interactions between these two enzymes is likely to be critical.

1.9.3 Alternative routes to improving Rubisco activase thermal tolerance

Altering other aspects of plant physiology which may impact upon Rca may also facilitate the generation of plants with improved traits. For example, Cpn60 β may also play a role in the acclimation of photosynthesis to heat stress by protecting Rca from denaturation (Salvucci, 2008). This protein associates with Rca in a high molecular mass complex, its association with Rca increased with the duration and intensity of heat stress. The protective proteins Cpn60 β , Hsp90, and Hsp70 all increased in both abundance and gene expression in heat tolerant rice after 24 hours of heat exposure (Scafaro *et al.*, 2010). Rca was also strongly up-regulated, with the large isoform having the largest relative increase in protein abundance together with a significant parallel increase in gene expression.

1.9.4 Potential problems with altering Rubisco activity

The loss of Rubisco functionality during heat stress may be beneficial. This loss of activity may play a role in protecting the plant (and its Rubisco) from damage. Rubisco deactivation may also prevent very high levels of photorespiration at high temperatures and so may prevent energy losses within the plant

(Sharkey, 2005). Photorespiration also produces metabolites used in other processes by the plant and so may in fact play a positive role in C₃ plants (Wingler *et al.*, 2000). Inhibitors may increase the stability of Rubisco under heat stress. CAIP has been seen to protect Rubisco against proteolytic degradation and the consequent irreversible loss of catalytic activity (Khan *et al.*, 1999). Therefore, when looking at altering Rubisco activity the potential negative impacts of the changes to the plant, including the plants nitrogen balance, must also be considered.

1.10 Improvement of wheat Rubisco activation

Research into Rubisco and Rca indicates that these enzymes play an important role in plant thermal tolerance. Theoretical estimations indicate that wheat yield potential could be increased by up to 50% through the genetic improvement of radiation use efficiency (Reynolds *et al.*, 2011); the improvement of Rca is one route to achieving this.

There is strong evidence for the existence of variation in the genes involved in photosynthetic capacity and efficiency indicating the potential for use of this genetic potential in the engineering of improved wheat cultivars (Reynolds *et al.*, 2011). Comprehensive screening to determine the extent of such genetic variation is required. Plant breeding continues to improve wheat production but is limited by the gene pool (Bhalla, 2006). However, the engineering of crops with improved traits taken from other species is also possible (Kumar *et al.*, 2009), with the use of genes taken from different species having been shown to be successful.

1.11 Thesis Aims and Objectives

The overall project aim was to consider routes to improving the thermal tolerance of Rca, and therefore photosynthesis under heat stress conditions, in wheat. This includes:

- Investigating the natural diversity of Rca in wheat by studying the differences in the thermal tolerance of Rca in 64 historical and current wheat cultivars (Chapter 2)
- Improving the thermal tolerance of Rca in wheat through the expression of the more thermally tolerant Rca from cotton. It is hypothesised that this will allow wheat to exhibit a broader range of thermal tolerance (Chapter 3)
- Characterisation of wheat Rca (Chapter 4)
- Development of a non-radioactive assay to measure Rubisco and Rca activity in purified proteins and leaf extracts (Chapter 5)

2. Searching for variation between the photosynthetic response of elite wheat cultivars to high temperatures

2.1 Introduction

Projections of climate change indicate that decreases in wheat production will occur in the future, with an estimated 6% yield decrease for each °C of further temperature increase (Asseng *et al.*, 2014). Therefore, the resilience of wheat to climate change, and in particular to heat stress, needs improving. Efforts have been made to improve heat and drought stress resistance in wheat, but differences in heat tolerance between wheat genotypes can be associated with multiple processes and mechanisms, involving heat shock proteins, transcription factors, and other stress related genes (Kumar *et al.*, 2013). As a result, the genetic basis of heat adaptation is complex and the genetic information is incomplete. Due to this, identification of the physiological traits associated with heat tolerance, and of the corresponding combinations of favourable alleles, may provide the best route to genetic improvement of crops.

The proposed routes to improving thermal tolerance in wheat can be divided into those associated with light interception, partitioning of assimilates and radiation use efficiency (Cossani & Reynolds, 2012). Improving light interception may include achieving rapid ground cover and canopy establishment, for which genetic diversity has been exploited in Mediterranean type environments to reduce soil evaporation (Mullan & Reynolds, 2010). Stay green is recognised as an adaptive physiological trait for stress conditions, and has a role to play in improving light interception, although the optimal pattern of senescence/pigment loss in terms of improving grain yield under heat stress has not been identified.

Optimising plant and leaf architecture may also improve light interception. Quantitative trait loci (QTL) for light interception have been identified in wheat mapping populations or cultivars (Kumar *et al.*, 2010, Ristic *et al.*, 2007, Vijayalakshmi *et al.*, 2010). The efficiency of light interception by wheat canopies has been improved by breeding to the extent that it is unlikely to be improved much more, although focusing on specific heat tolerant characteristics could yet lead to improvements (reviewed by Zhu *et al.* (2010)).

With regard to partitioning of assimilates, the adaptation of reproductive growth to heat stress is critical to determining grain sink strength. The ability to synthesize, store, and remobilize starch at high temperature will determine final kernel weight (Cossani & Reynolds, 2012).

Net radiation use efficiency, is the result of gross carbon assimilation, minus losses associated with growth, maintenance and repair (collectively referred to as dark respiration), metabolic inefficiencies (i.e. photorespiration), and a range of photo-protective strategies. Variation in photosynthetic parameters has been identified in C3 plants (Wullschleger, 1993), and between wheat cultivars (Blum, 1990, Chytky *et al.*, 2011, Driever *et al.*, 2014, Fischer *et al.*, 1981, Reynolds *et al.*, 2000a, Sadras *et al.*, 2012, Watanabe *et al.*, 1994). The efficiency of energy conversion into biomass is only about one-third of the theoretical maximum for most crop species, regardless of environmental stress (Zhu *et al.*, 2008b). Together, this evidence suggests that there is potential to improve wheat yield productivity and resilience through increasing photosynthesis, provided that other constraints do not become limiting.

The reduction in Rubisco activation state, and therefore carbon assimilation, with increased temperature has been associated with inactivation of Rubisco activase (Rca; Carmo-Silva *et al.* (2012)). There is variation in Rca thermal tolerance between species (Salvucci & Crafts-Brandner, 2004c). Therefore, investigating wheat cultivars for variation in the thermal tolerance of a protein (Rca), which is known to be impacted upon by temperature (Salvucci & Crafts-Brandner, 2004a), and to impact upon plant CO₂ assimilation, is an appealing strategy to address the complex challenge of improving wheat thermal tolerance.

Natural variation in the thermal stability of Rca in field grown wheat was investigated in the current work through assessment of the photosynthetic performance and Rubisco activity at elevated temperatures in 64 wheat cultivars. The wheat cultivars investigated belong to the 'ERYCC panel' (selected for their Earliness & Resilience for Yield in a Changed Climate), which is composed of three groups: 16 historical cultivars released between 1953 and 1996; 26 modern cultivars and 22 cultivars with phenological traits of interest. Cultivars were selected for early maturation and the ability to cope with environmental stress.

Each group contains cultivars for both bread making and feed, with many of the cultivars having represented a significant proportion of UK wheat crop.

Data was collected during two field seasons, 2011- 2012 (described as 2012) and 2012- 2013 (described as 2013). In the 2012 field season a wide screen of all of the 64 cultivars was completed to look for variation between them. Following this, later in 2012, and then in 2013, ten cultivars were investigated in greater depth. The screen assessed photosynthetic performance and Rubisco activation state of the different cultivars following exposure to elevated temperatures. The aim of the screen was to identify differences in the thermal tolerance of Rca that could be used by breeders to increase the thermal tolerance of wheat. Breeding programmes require an expansion of the available knowledge regarding the variation in the wheat gene pool to improve heat tolerance and to allow targeted programmes to be established.

2.2 Materials and methods

2.2.1 Plant material and growth conditions

The ERYCC panel of 64 wheat cultivars (*Triticum aestivum* L.), was cultivated in 2011- 2012 and 2012- 2013. The 2012 experiment was planted on 5th October 2011 in Great Field 1/2 (at coordinates 51.806239, -0.362698), at Rothamsted Research, and harvested on the 17th August 2012. The 2013 experiment was planted on the 12th December 2012 on the Rothamsted farm in Redbourn (Black Horse Field, at coordinates 51.802715, -0.393874), and harvested on the 28th August 2013 (Figure 2.1). Each year three plots of each cultivar were grown in the field in a random three block design (Figure 2.2), each block contained eight rows, with eight plots per row, totalling 192 plots. In 2012 (field trial WW/1218) plots were 2 x 1 m and in 2013 (field trial WW/1315) plots were 3 x 1 m. 1 m was left between rows and 0.5 m between adjacent plots. GenStat (2014, 17th Edition, VSN International Ltd, Hemel Hempstead, UK) randomisation was used for the field plot layout. For the 2012 experiment the preceding season's crop (in 2010- 11) was oilseed rape. For the 2013 experiment the previous crop (in 2011- 2012) was oats.

The soil in both fields is composed of a moderately well-drained flinty clay loam containing flints and/or chalk. Ground preparation and crop treatment was essentially the same in both years. The ground was

treated with application of systemic herbicide, followed three weeks later by ploughing, with cultipressing and power harrowing at intervals of one week thereafter, to produce a suitable seed bed. Wheat grain was drilled at a rate of 350 grains m⁻², and the plots rolled. The plots were treated periodically, pre and post emergence, with herbicides, insecticides, and fungicides to encourage weed and disease-free development. Nitrogen and sulphur (Doubletop: GrowHow UK) and nitrogen alone (F34 Nitram: GrowHow UK) were applied in mid March and mid May, respectively (185 kg ha⁻¹ on each occasion). The tall cultivars (including Cappelle Desprez) were staked to reduce lodging in 2012. Harvest took place once all the cultivars had reached physiological maturity and the kernels were hard (Zadoks growth stage 9.1–9.2; Zadoks *et al.* (1974)).

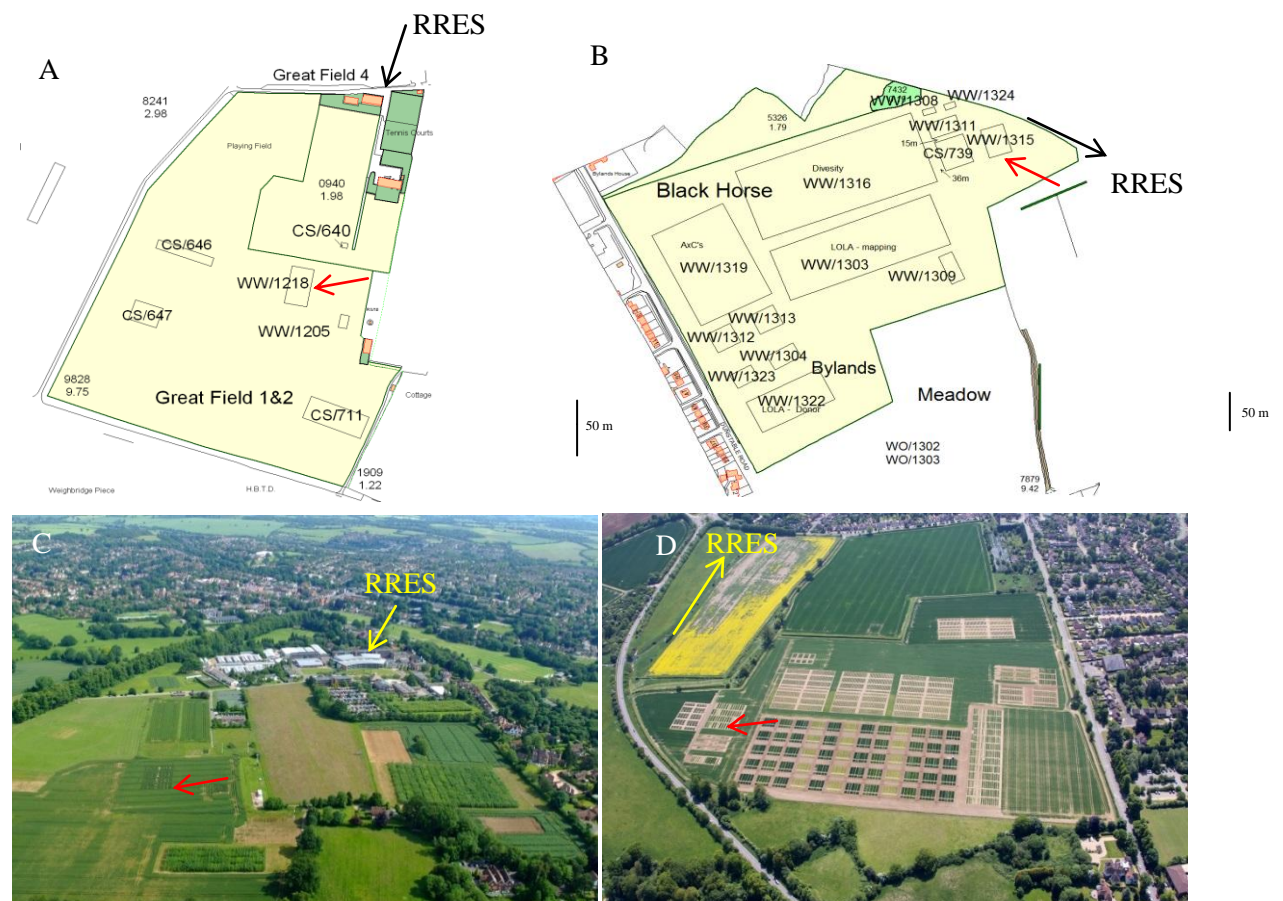


Figure 2.1. Location of field experiments in 2011-2012 and 2012-2013. Maps are shown for experiments in 2011- 2012 (WW/1218; A, C) and 2012- 2013 (WW/1315; B, D). Arrows indicate location (A, C) or direction (B, D) to Rothamsted Research (RRES). Red arrows indicate experimental field plots.

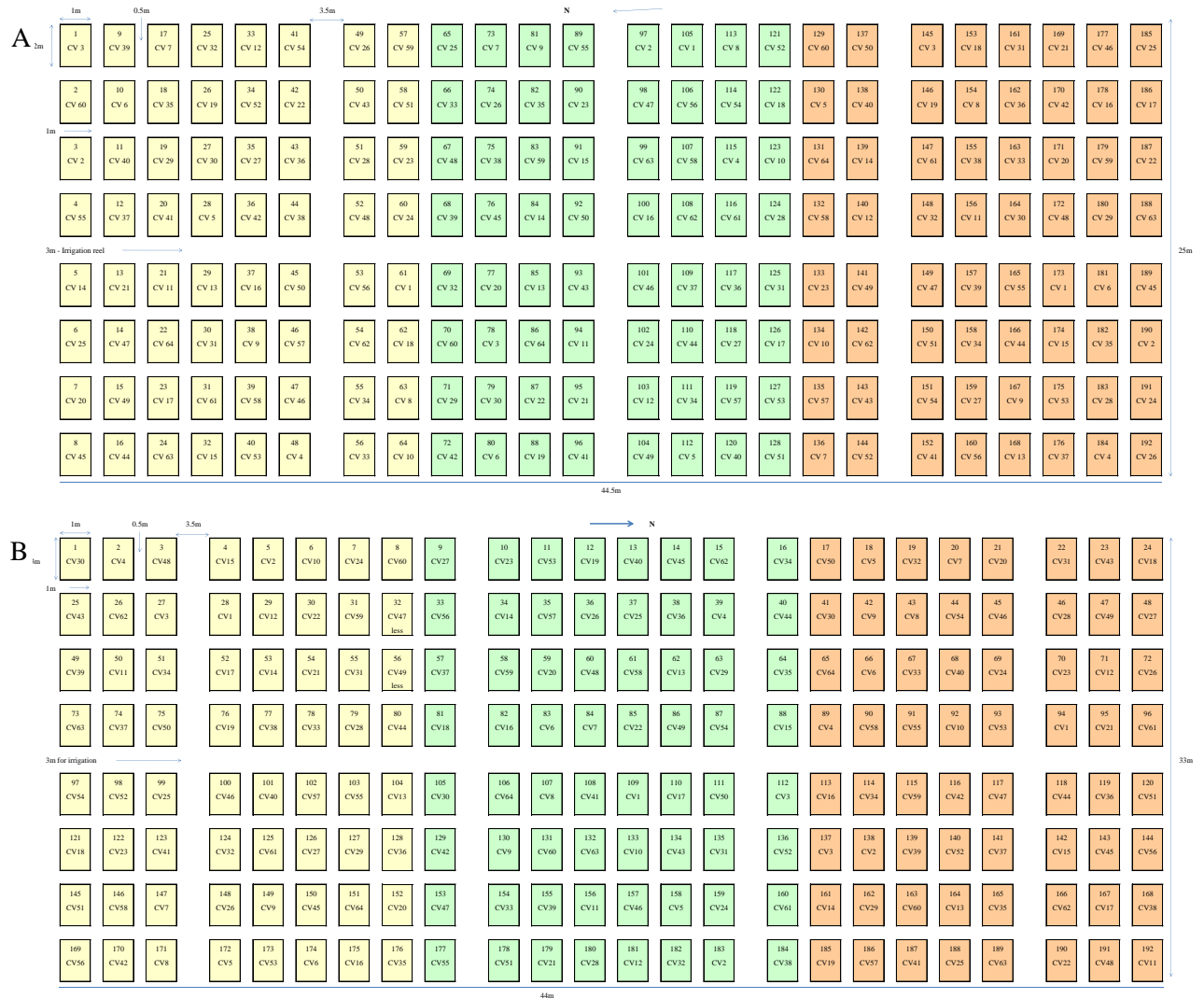


Figure 2.2. Randomised field plot layouts for ERYCC panel experiments. Maps are shown for experiments in 2011- 2012 (A) and 2012- 2013 (B).The key cultivars investigated and associated CV numbers are: Bacanora (64), Battalion (37), Cadenza (58), Cappelle Desprez (47), Gatsby (32), Maris Huntsman (51), Rialto (13), Robigus (3), Roysac (11), Savannah (50), and Xi19 (26)

2.2.2 Meteorological conditions

Rothamsted Met station (accessible via the electronic Rothamsted Archive) collects meteorological data each day and this is included here for comparison of the 2011- 2012 and 2012- 2013 field seasons.

Deviations from the 30 year (1981- 2010) average for each month have been calculated. Rainfall (Table 2.1) from April to July in 2012 was considerably higher than in the same period in 2013. In 2012 the winter and spring maximum and minimum temperatures (Table 2.2) were above the 30 year average for the UK. This was in contrast to winter and spring 2013 where temperatures were 1- 4°C lower than either

the 30 year average or 2012 conditions. In July and August 2012 temperatures were 1- 2°C cooler than in 2013 and also when compared to the 30 year average. Accumulated thermal time was calculated from the mean of the daily minimum and maximum temperatures, taking °C days above 0°C, across the wheat growth season. The winter months of 2012 had almost double the number of hours of sunshine than 2013. In 2012 from April through to July the number of hours of sunshine was low compared to the 30 year average, but in summer 2013 the number of hours of sunshine was relatively high and close to the UK 30 year average. The daily rainfall and minimum and maximum temperatures throughout the growing season from the day of sowing is illustrated in Figure 2.3.

Table 2.1. Monthly average rainfall (mm) at Rothamsted Research for the growing seasons of 2012 and 2013. Measured with a tipping bucket. The difference from the 30 year average (1981- 2010) is shown alongside (\pm), and the total rainfall in each year. Data was sourced from the Rothamsted Met Station.

Field Year	Rainfall (mm)			
	2012		2013	
	Total mm	30 yr	Total mm	30 yr
Jan	58.0	-12.0	31.0	-23.5
Feb	24.7	-25.4	45.2	+3.0
Mar	34.7	-16.1	60.2	+14.3
Apr	168.6	+113.6	26.8	-25.4
May	52.6	-2.1	74.6	+21.3
Jun	166.5	+113.2	27.2	-22.9
Jul	128.4	+78.6	37.2	-12.7
Aug	54.9	-8.8	43.8	-14.0
Sep	40.4	-17.3	50.4	-6.7
Oct	115.8	+34.1	104.4	+33.5
Nov	100.4	+23.8	56.8	-5.7
Dec	114.2	+44.7	74.6	+18.8
Year Total	1059.2		632.2	

Table 2.2. Monthly average air temperature (daily minimum and maximum; °C) and sunshine (hours) at Rothamsted Research, for the growing seasons of 2012 and 2013. The difference from the 30 year average (1981- 2010) is shown alongside (\pm). Data was sourced from the Rothamsted Met Station.

Field Year	Sunshine (hours)				Mean temperatures (°C)							
	2012		2013		2012		2013		2012		2013	
	Hr	30 yr	Hr	30 yr	°C	30 yr	°C	30 yr	°C	30 yr	°C	30 yr
Jan	82.2	+20.2	43.7	-16.3	8.5	+1.8	5.4	-1.6	2.5	+1.3	0.4	-0.8
Feb	109.3	+29.0	76.7	+1.7	6.4	-0.5	5.6	-1.8	0.1	-0.8	-0.1	-1.0
Mar	193.5	+78.6	80.7	-32.8	12.8	+2.9	5.6	-4.7	3.1	+0.4	-0.8	-3.5
Apr	150.1	-11.1	197.6	+46.7	11.5	-1.1	13.1	+0.1	3.3	-0.7	2.9	-0.8
May	175.6	-19.1	179.8	-7.4	16.1	+0.1	15.5	-1.1	7.9	+1.0	5.4	-1.1
Jun	144.9	-53.3	184.0	-3.9	17.6	-1.5	18.6	-1.0	10.0	+0.3	9.2	-0.3
Jul	172.3	-32.9	255.3	+58.2	19.8	-2.0	24.7	+2.6	11.6	-0.2	12.3	+0.7
Aug	176.5	-19.8	178.1	-10.8	21.7	+0.2	22.7	+0.8	12.8	+0.9	12.3	+0.7
Sep	179.6	+36.2	133.0	-4.1	18.3	+0.0	21.6	+2.9	8.4	-1.5	10.5	+0.9
Oct	86.0	-25.7	89.3	-22.5	12.7	-1.4	16.9	+2.4	6.7	-0.5	10.1	+3.2
Nov	76.9	+6.1	64.8	-1.5	9.4	-0.3	9.2	-0.7	3.6	-0.2	3.2	-0.6
Dec	68.2	+14.4	63.8	+18.2	7.5	+0.6	9.7	+2.5	1.4	-0.2	2.9	+1.4
Year Total	1615.1		1546.8									

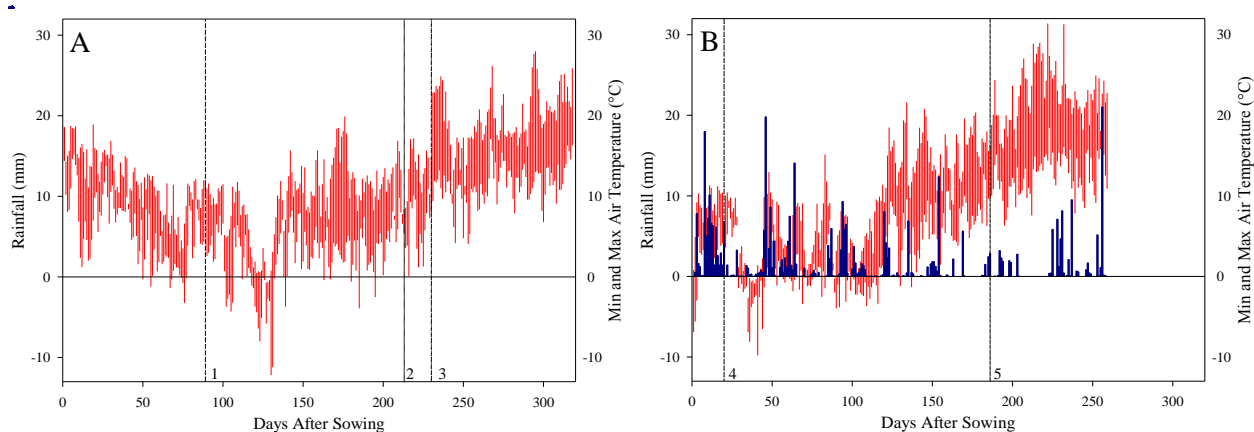


Figure 2.3. Daily maximum and minimum air temperature (°C; red) and daily precipitation (mm; blue) at Rothamsted Research, over the 2011- 2012 (A) and the 2012- 2013 (B) growing seasons. Data was sourced from the Rothamsted Met Station. The days are represented as the number of days after the experiment was sown; the 2011- 2012 experiment was planted on 5th October 2011 and harvested on the 17th August 2012. The 2012- 2013 experiment was planted on the 12th December 2012 and harvested on the 28th August 2013. Key dates are highlighted: Julian Day 1 2012 (1), Initial Screen 2012 (2), Elevated temperature experiment 2012 (3), Julian Day 1 2013 (4), Elevated temperature experiment 2013 (5).

2.2.3 Cultivar yield grouping and lineage

To allow the cultivars to be grouped for analysis the data from previous trials regarding grain yield was collated (Table 2.3). The data used to identify yield differences between cultivars is based on reliable average yield data (Clarke *et al.*, 2012, Ober *et al.*, 2014) for the season of 2008 (obtained at nine different locations in the UK) and 2009 (obtained by Eric Ober under irrigated and rain sheltered conditions). This data was used to split the cultivars into two groups of higher and lower yielding cultivars for the 2013 field season analysis. The average of all the yield data (including the 2009 ‘dry’ data) indicates the same five lower yielding and higher yielding cultivars. The geographical origins, seasonal planting habit (which impacts upon the requirements for vernalisation prior to flowering) and parentage of each cultivar were also collated (Table 2.4).

Table 2.3. Collated yield data (t ha⁻¹) for selected ERYCC panel cultivars. Data was used to group the wheat cultivars being studied into 5 higher and 5 lower yielding cultivars. Data is sourced from Ober *et al.* (2014) and Clarke *et al.* (2012). ‘Dry’ and ‘wet’ refer to yield under an irrigated or rain sheltered experimental set up.

Cultivar	2008	2009 wet	2009 dry	Average wet	Average all
Bacanora	8.0	8.5	6.4	8.2	7.6
Maris Huntsman	11.9	11.8	6.9	11.9	10.2
Roysac	11.4	13.5	8.1	12.5	11.0
Cadenza	13.2	13.0	8.0	13.1	11.4
Robigus	14.0	12.4	7.1	13.2	11.2
Rialto	13.7	13.3	7.9	13.5	11.6
Savannah	13.7	13.6	8.4	13.6	11.9
Xi19	14.0	13.4	8.2	13.7	11.9
Gatsby	14.1	13.4	6.6	13.8	11.4
Battalion	14.3	13.8	8.1	14.1	12.1

Table 2.4. Detailed information on the wheat cultivars being investigated.

Data includes the release date, origin, habit, and parentage of wheat cultivars. Data is sourced from the Genetic Resources Information System for Wheat and Triticale (CIMMYT): <http://wheatpedigree.net/>; and The Scottish Wheat Variety Database: http://wheat.agricrops.org/varietyindex.php?page_no=1.

ERYCC Cultivar	ERYCC Code (CV)	Release Date	Origin	Habit	UK Market	ERYCC Group	Parentage
Bacanora	64	1988	Mexico	Spring		Phenology	(Jupateco-73 X (Sib)Bluejay) X Ures-81
Battalion	37	2006	UK	Winter		Modern	98-St-08 X Aardvark
Cadenza	58	1992	France	Spring		Phenology	Tonic X Axona; Tonic X Axona
Cappelle Desprez	47	1946	France	Winter	Feed	Historical	Vilmorin-27 X Hybride-Du-Joncquois
Gatsby	32	2007	UK	Winter		Phenology	Nelson X Wasmo
Maris Huntsman	51	1971	UK	Winter	Feed	Historical	[(C1.12633 X Cappelle-Desprez) X Hybrid-46] X Professeur-Marchal
Rialto	13	1993	UK	Winter	Bread	Historical	Haven(Sib) X (Sib)Fresco
Robigus	3	2005	UK	Winter	Feed	Modern	Z-836 X 1366; Z-836 X Putch
Roysac	11	2003	France	Winter		Phenology	N/A
Savannah	50	1998	UK	Winter		Historical	Riband X Brigadier
Xi19	26	2002	UK	Winter		Modern	(Cadenza X Rialto) X Cadenza

2.2.4 Plant development and biomass measurements

Developmental and physiological measurements were taken regularly over the wheat growing season.

Leaves or plants selected for measurement were taken from the central sector of the plot to avoid any impact of edge effects. Measurements were taken on healthy leaves with no evidence of damage.

Height

The height of three individual plants were measured with a ruler from soil level to the highest point of the plant, either a leaf or ear tip. The mean plot and cultivar height was calculated.

Zadoks growth stage

Developmental growth over time was assessed for three plants of each plot. A figure was determined based upon the Zadoks growth stage scale (Figure 2.4; Zadoks *et al.* (1974)). The most advanced decimal code was used to determine the mean for each plot.

Leaf chlorophyll measurements

The chlorophyll content was measured in the centre of three leaves per plot using a chlorophyll meter (SPAD-502; Konica Minolta, Inc., Tokyo, Japan).

Grain yield and straw biomass measurements

Grain yields were obtained with a Haldrup plot combine, the straw being weighed on the back of the combine by means of a supplementary load cell. HI was calculated from these measurements. The moisture content was determined, and data is expressed as weight at 85% (grain yield) or 100% (biomass) dry matter.

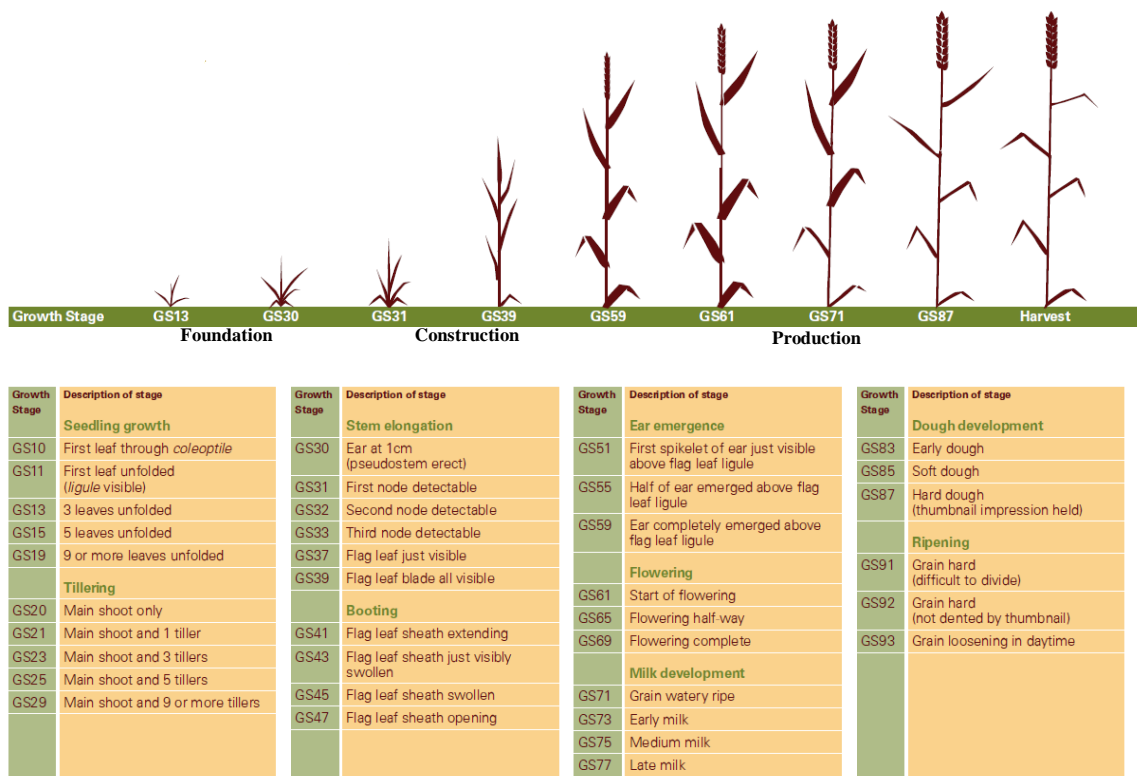


Figure 2.4. Zadoks growth stage scale for wheat development. Reproduced from HGCA (2008).

2.2.5 Photosynthetic response to elevated temperature treatment

Net CO₂ assimilation under various CO₂ concentrations (A-Ci curves) was measured for each of the ERYCC panel cultivars by the Photosynthesis group at Rothamsted Research and The University of Essex. Details for the methodology used to determine the A-Ci curves on field grown material can be found in Driever *et al.* (2014). A-Ci curves were measured using a 2 cm² leaf chamber with an integral blue-red LED light source (LI-6400-40; LI-COR, Lincoln, USA) for each of the 64 cultivars.

Measurements of photosynthesis were all taken at 1500 $\mu\text{mol photons m}^{-2} \text{ s}^{-1}$, $20 \pm 1^\circ\text{C}$ leaf temperature, and a vapour pressure deficit of 0.9 kPa. Measurements were completed in succession at 400, 300, 200, 100, 75, 400, 550, 700, 1000 and 1200 $\mu\text{L L}^{-1}$ reference CO₂. In 2012 triplicate A-Ci curves for each cultivar were completed at Zadoks growth stage 4.3- 4.5. In 2013 triplicate A-Ci curves were completed for each cultivar pre (at booting; Zadoks growth stage 4.3- 4.5) and post-anthesis (7 days after Zadoks growth stage 6.5).

An initial screen was completed to investigate the thermal tolerance across all 64 ERYCC panel cultivars. This screen was not replicated and used one leaf from one plot of each cultivar (Figure 2.5).

Measurements were taken on the 4th, 8th and 9th May 2012 (days 125, 129 and 130 of the Julian calendar) at which point plants were at Zadoks growth stage ~3.7. A representative shoot of each cultivar was taken from the field at dusk. Shoots were cut at the base of the plant and then were immediately cut again, under water, to ensure that air did not penetrate the vascular system and kept overnight in a small growth chamber (15°C, 90% RH) in the dark in water in 15 mL falcon tubes. The following day, one by one, the fully expanded leaf was cut 2 cm from its point of attachment to the stem (while this section of the leaf was submerged), the cut end was placed in a small tube of water and the leaf transferred to a high-light controlled environment room (60% RH, 25°C, 600 $\mu\text{mol photons m}^{-2} \text{ s}^{-1}$, provided by 400W HQI lamps) for light induction to take place. After 30- 90 min, leaf photosynthesis was measured using an infra-red gas analyser (as above) at the conditions listed below.

Measurements were taken for each leaf at two CO₂ concentrations before increasing the leaf temperature:

- 1- Leaf temperature 25°C, 450 μL L⁻¹ CO₂, 2000 μmol photons m⁻² s⁻¹
- 2- Leaf temperature 25°C, 300 μL L⁻¹ CO₂, 2000 μmol photons m⁻² s⁻¹
- 3- Leaf temperature 35°C, 400 μL L⁻¹ CO₂, 2000 μmol photons m⁻² s⁻¹
- 4- Leaf temperature 35°C, 400 μL L⁻¹ CO₂, 2000 μmol photons m⁻² s⁻¹ (same as in 3, but after the leaf had been kept for 5 min under these conditions in the LI-COR chamber, immediately prior to the tissue being freeze clamped)

The relationship between photosynthesis and the intercellular CO₂ concentration was plotted from the data taken at 25°C. From this, the value for photosynthesis at 400 μL L⁻¹ CO₂ at 25°C could be calculated, based upon the C_i at 400 μL L⁻¹ CO₂ at 35°C, allowing direct comparisons between the measurements at the different temperatures to be made. The percentage difference between photosynthetic rates at 25°C and 35°C could then be calculated. During the gas exchange measurements, the width of the leaf on either side of the leaf chamber was measured, to allow an accurate estimate of the area of the leaf within the chamber. After these measurements, freeze clamping tongs (Figure 2.5) were used to rapidly sample and freeze a 3.14 cm² section of the leaf tissue that had been within the LI-COR chamber for Rubisco activity assays (see below for details).



Figure 2.5. Photographs from field work in 2012 and 2013. Experimental field plots in 2012 (A), LI-COR for photosynthesis measurements (B) and freeze clamping samples for Rubisco activation state measurements (C).

The cultivars were ranked on the Rubisco activation state (ratio of Rubisco initial/ total activity) at 35°C (see below for assay methodology) from the initial screen, and the ten cultivars with the most extreme responses (the five highest and five lowest performers with the elevated temperature treatment) were investigated further in replicated experiments. Measurements were taken on the 21st and 22nd May 2012 (days 142 and 143 of the Julian calendar) at which point plants were at Zadoks growth stage ~3.9. For photosynthesis measurements six shoots of each cultivar were taken (two from each of the three replicate plots) at dusk, as before. Photosynthetic measurements as described previously (1- 4) were made on one leaf from each plot; these leaves were sampled (as before) for subsequent Rubisco activity assays after exposure at 35°C. The other shoots, i.e., one leaf from each plot, were measured and sampled at 25°C for Rubisco activity assays:

5- Leaf temperature 25°C, 400 $\mu\text{L L}^{-1}$ CO₂, 2000 $\mu\text{mol photons m}^{-2} \text{ s}^{-1}$

In 2013 the same cultivars as in 2012 were investigated, except that Cappelle Desprez was excluded (due to it being very badly affected by mildew), and was replaced with Rialto. Measurements were taken on the 16th June 2013 (control temperature) and 17th June 2013 (high temperature), these were days 167 and 168 of the Julian calendar at which point the plants were at an average Zadoks growth stage of 4.7. Three representative shoots of each cultivar were cut (as before), pre-dawn (~3 am), from each replicated field plot. As above, plants were kept in darkness in a cool CE chamber (15°C 90% RH), measurements were started once the natural light period had begun. Therefore, photosynthetic measurements were begun about 4 hours after sample collection. Prior to measurement the leaves were light-induced in the illuminated controlled environment room for an hour (see below for CE room conditions). Leaf photosynthesis was measured using the infra-red gas analysers described above, and the conditions listed below. Photosynthetic rate was recorded twice in succession on each leaf to ensure that the leaf had reached a stable state and the mean of these readings was taken. The illuminated controlled environment room conditions were adjusted to allow photosynthesis to be measured at control (20°C) and elevated (35°C) temperatures, on two consecutive days, meaning that leaves were exposed to the temperature treatment during the one hour of light adaptation prior to measurement. In total, nine different leaves of each cultivar were measured at each of two temperatures; 20 and 35°C.

1- Control temperature treatment-

CE room conditions- 20°C, 700 $\mu\text{mol photons m}^{-2} \text{ s}^{-1}$, 60% Relative Humidity

LI-COR chamber conditions- Block temperature 20°C, 550 $\mu\text{L L}^{-1} \text{ CO}_2$, 700 $\mu\text{mol photons m}^{-2} \text{ s}^{-1}$,

11- 11.5 Reference Chamber Water content

2- Elevated temperature treatment-

CE room conditions- 35°C, 700 $\mu\text{mol photons m}^{-2} \text{ s}^{-1}$, 90% Relative Humidity

LI-COR chamber conditions- Block temperature 35°C, 550 $\mu\text{L L}^{-1} \text{ CO}_2$, 700 $\mu\text{mol photons m}^{-2} \text{ s}^{-1}$,

11- 11.5 Reference Chamber Water content

After photosynthesis was measured, freeze clamping tongs were used to rapidly sample a 3.14 cm^2 section of leaf tissue from just above where the LI-COR chamber had been clamped, for Rubisco activity assays.

2.2.6 Rubisco activation state response to elevated temperature treatment

Rubisco activity assays using $^{14}\text{CO}_2$ were used to measure Rubisco activation state in leaf samples freeze clamped immediately after measuring photosynthesis. Rubisco was extracted from the frozen leaf samples and its activity was determined by measuring the amount of ^{14}C incorporated into acid-stable products through the carboxylation of RuBP. Frozen leaf tissue was extracted in extraction 500 μL or 750 μL of extraction buffer (50 mM Bicine-NaOH, pH 8.2, 20 mM MgCl_2 , 1 mM Ethylenediaminetetraacetic acid (EDTA), 2 mM benzamidine, 5 mM ϵ -aminocaproic acid, 50 mM 2-mercaptoethanol, 10 mM DTT, Sigma plant protease inhibitor cocktail (P9599; used at a 100-fold dilution) and 1 mM Phenylmethanesulfonyl fluoride (PMSF)), with 150 mg / gFW insoluble Polyvinylpyrrolidone (PVP-40) and 10 mg of acid washed sand, using a pestle and mortar. After extraction the sample was clarified by centrifugation for 3 min at 14, 000 $\times g$ at 4 °C.

Assays were completed in a total volume of 500 μL , with 25 μL of leaf extract supernatant. Initial Rubisco activity was determined at room temperature immediately after extraction in assay buffer (containing 100 mM Bicine-NaOH, pH 8.2, 20 mM MgCl_2 , 10 mM $\text{NaH}^{14}\text{C}\text{CO}_3$ (0.5 $\mu\text{Ci } \mu\text{mol}^{-1}$) and

0.4 mM RuBP). Assays were allowed to proceed for 30 s before being quenched with 100 μ L 10 M Formic acid. Total Rubisco activity was determined after incubation of the extract in assay buffer (minus RuBP) for 3 min to fully carbamylate the enzyme prior to initiating the reaction with the addition of RuBP. Samples were dried at 100°C until a crystalline residue appeared, then cooled and rehydrated with 400 μ L of water, followed by 3.6 mL of liquid scintillation cocktail (Ultima Gold, Perkin-Elmer, Seer-Green, UK), prior to measuring the acid-stable ^{14}C content.

The amount of Rubisco present in each sample was determined using a [^{14}C]CABP binding assay (Parry *et al.*, 1997) to enable the activity measured in each individual sample to be expressed relative to the corresponding Rubisco content of that sample. To this end a volume of 150 μ L of the leaf extract supernatant was added to 150 μ L [^{14}C]CABP binding solution (containing 200 mM Na_2SO_4 , 400 mM Bicine-NaOH, pH 8.0, 80 mM MgCl_2 , 40 mM NaHCO_3 , 200 mM β -mercaptoethanol and 0.1mM neutralised ([^{14}C]CABP (1 μCi / μmol)) and mixed thoroughly. The sample was incubated for 20 min on ice after which 25% (w/v) PEG-4000 was added with thorough mixing. The samples were incubated for a further 30 min on ice during which time precipitation of Rubisco occurred. Samples were centrifuged for 10 min at 14,000 $\times g$ at 4°C. The supernatant was discarded and the pellet was overlaid with 300 μ L of 20% PEG Buffer (50 mM Bicine-NaOH, pH 8.2, 20 mM MgCl_2 , 1 mM EDTA, 2 mM benzamidine, 5 mM ϵ -aminocaproic acid, 50 mM 2-mercaptoethanol and 20% (w/v) PEG-4000), this was left on ice for 15 min, with occasional vortexing and then centrifuged for 10 min at 14,000 $\times g$ at 4°C. The pellet was resuspended in 300 μ L of 20% PEG Buffer, as above, and centrifuged again before the pellet was finally resuspended in 500 μ L of 1% (v/v) Triton X100. Radioactivity was determined in 450 μ L of the solution after mixing with 3.6 mL liquid scintillation cocktail (as above).

2.2.7 Data analysis

Photosynthetic data was analysed with use of Residual Maximal Likelihood in Genstat to fit a linear mixed model to the data. Rubisco activity data was analysed with use of ANOVA. Pearson correlation coefficients were calculated between all pairs of yield and photosynthetic variables to consider

associations between them. These were tested using the F-Test. Significant ($p < 0.05$, F-Test) correlations (larger than 0.5 and either positive or negative) were considered as being indicative of an association.

2.3 Results

2.3.1 Wheat cultivar development and biomass measurements

Zadoks growth stage was measured for each cultivar throughout the growing season. Due to the cold temperatures early in the 2013 growing season little difference was seen in the initial developmental rate of the cultivars, whereas, in 2012 a greater difference was noted earlier in the season (Figure 2.6). The date of anthesis was determined for each cultivar in 2013 (Table 2.5). The mean anthesis date in 2013 of the higher yielding cultivars was later than for the lower yielding cultivars. The date of anthesis in 2012 was earlier than in 2013 for all cultivars. Bacanora reached anthesis significantly earlier than the grouped mean and Gatsby significantly later. Owing to the very wet weather Zadoks growth stage measurements were taken on fewer occasions in 2012 than in 2013. Even so, anthesis dates could be estimated from the recorded data; and showed that the cultivars reaching anthesis relatively early or late were the same in each year.

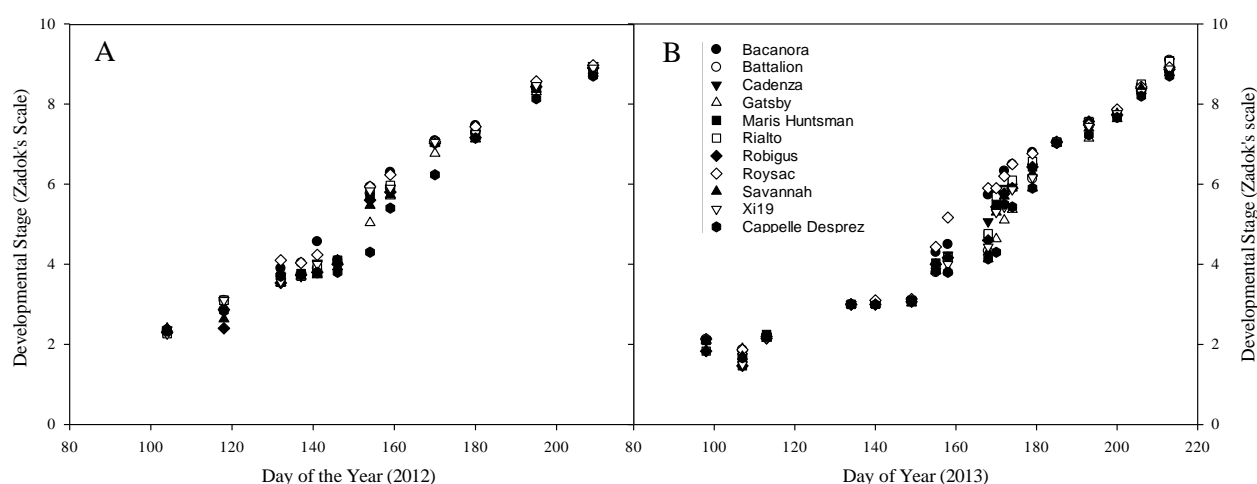


Figure 2.6. Mean Zadoks growth stage across the three replicated plots (value are means of three plots) of each cultivar at each measurement date over the growing period in 2012 (A) and 2013 (B). Bacanora (Closed circles), Battalion (Open circles), Cadenza (Inverted closed triangle), Gatsby (Open triangle), Maris Huntsman (Closed square), Rialto (Open square), Robigus (Closed diamond), Roysac (Open diamond), Savannah (Closed triangle), Xi19 (Open inverted triangle), Cappelle Desprez (Closed hexagon).

Table 2.5. The mean number of days after sowing at which 50% of each cultivar plot was recorded as having 50% of ears at anthesis (Zadoks growth stage 6.5).

In 2012 day 162 was the 10th June and in 2013 day 174 was the 23rd June.

Cultivar	Mean number of Days After Sowing to reach Zadoks 6.5	Equivalent Julian Day	Mean number of Days After Sowing to reach Zadoks 6.5	Equivalent Julian day
	2012	2012	2013	2013
Bacanora	250	162	193	174
Roysac	251	163	193	174
Rialto	253	165	197	178
Cadenza	253	165	198	179
Maris Huntsman	253	165	199	180
Robigus	254	166	199	180
Savannah	254	166	199	180
Xi19	253	165	201	182
Battalion	253	165	202	183
Gatsby	255	167	202	183
Cappelle Desprez	261	173	203	184

The thermal time accumulated by the field grown wheat was calculated and compared for the years 2012 and 2013 (Figure 2.7). The 2012 field trial was planted far earlier in the year than the 2013 trial (5th Oct 2011 compared to the 12th December 2012) and the temperature earlier in the growing season was higher in 2012 than 2013. The wheat developmental rate was compressed in 2013, with the cultivars reaching maturity despite not having reached the indicated number of degree days.

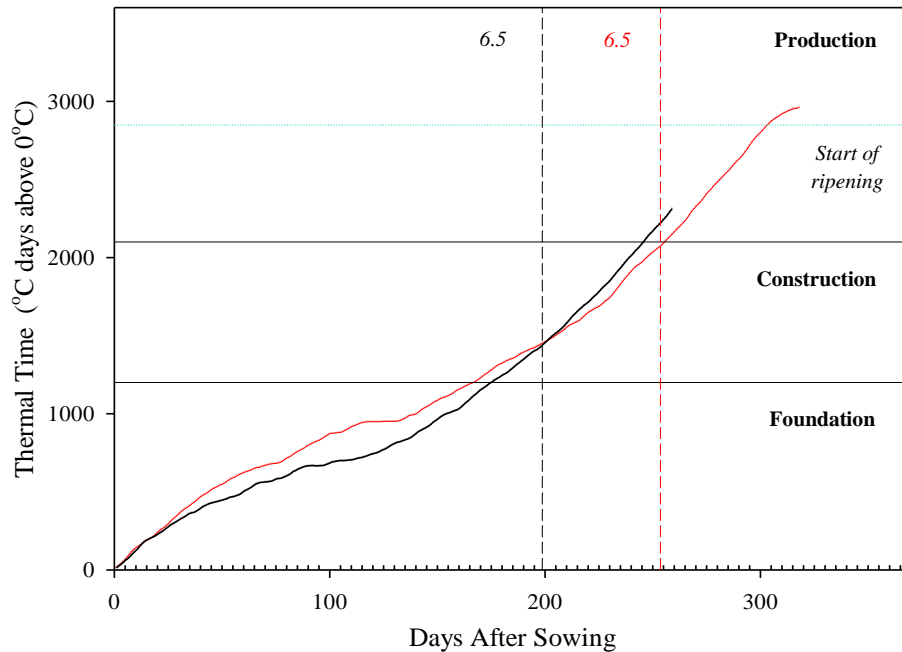


Figure 2.7. Accumulated thermal time across wheat development in 2011- 2012 (red) and 2012- 2013 (black). The accumulated thermal time is shown calculated from the minimum and maximum daily temperatures from Rothamsted met station data using 0°C as a baseline temperature. Key developmental stages are highlighted at which it is predicted that the switch from foundation to construction (1200), from construction to production (2100) and then the start of grain ripening (dashed line; 2850) should occur. The mean day that the ten selected cultivars reached Zadoks growth stage 6.5 in each year is shown.

The height of each cultivar was measured through the growing season (Figure 2.8). The rate of growth differed between cultivars, with initial growth being rapid in some (i.e. Roysac, which grew rapidly early in the growth season of 2013 but obtained the lowest overall height in both years), and others having increased growth later on in the season (i.e. Maris Huntsman). Cappelle Desprez was far taller than any of the other cultivars, followed by Maris Huntsman. The mean height of all 64 cultivars of the ERYCC panel on the final date of measurement in 2012 was 85.6cm on Julian day 170 (18th June 2012), by which date the ears had fully emerged and the flag leaves were fully expanded, and so height was maximal, whereas in 2013 average of all cultivars was day Julian day 185 was 62.5 cm (4th June 2013).

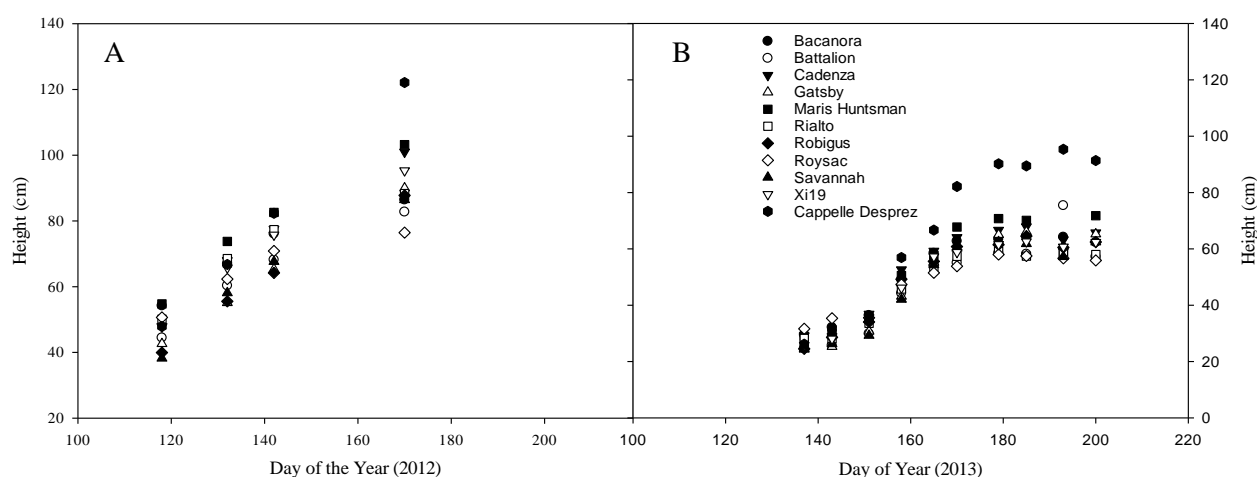


Figure 2.8. Mean plant height (cm) over the growing season for each cultivar in 2012 (A) and 2013 (B). Values are the mean of nine plants at each time point for each cultivar. Bacanora (Closed circles), Battalion (Open circles), Cadenza (Inverted closed triangle), Gatsby (Open triangle), Maris Huntsman (Closed square), Rialto (Open square), Robigus (Closed diamond), Roysac (Open diamond), Savannah (Closed triangle), Xi19 (Open inverted triangle), Cappelle Desprez (Closed hexagon).

The chlorophyll content of each cultivar was assessed (Figure 2.9); with a steady increase being seen through development in 2013, peaking just prior to anthesis (~Julian day 180 in 2013). Data was collected until senescence began at which point the chlorophyll measurements were discontinued. The variation between measurement days for each cultivar is large making it hard to draw solid conclusions on the identity of cultivars which had the highest chlorophyll content or stayed green the longest. However, Cappelle Desprez and Maris Huntsman had comparatively lower chlorophyll content. Cadenza and Xi19

consistently showed relatively high chlorophyll content. The variation between the cultivars, and therefore in comparison to the calibration, may compound difficulties in comparing between cultivars.

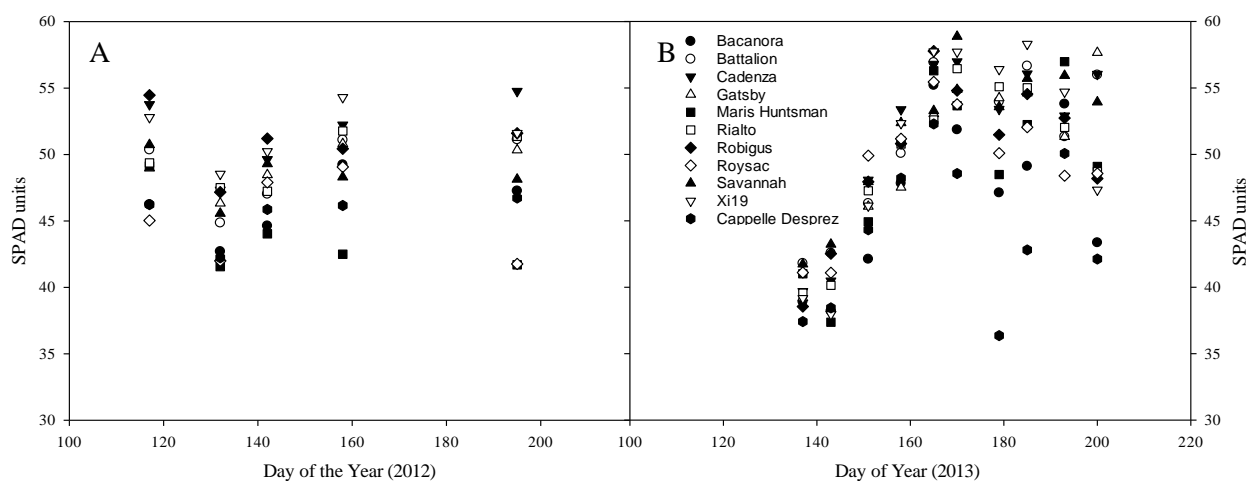


Figure 2.9. Mean chlorophyll content (SPAD) for each cultivar throughout plant development in 2012 (A) and 2013 (B). Values are the mean of nine plants at each time point for each cultivar. Bacanora (Closed circles), Battalion (Open circles), Cadenza (Inverted closed triangle), Gatsby (Open triangle), Maris Huntsman (Closed square), Rialto (Open square), Robigus (Closed diamond), Roysac (Open diamond), Savannah (Closed triangle), Xi19 (Open inverted triangle), Cappelle Desprez (Closed hexagon).

Yield of both grain and above ground dry matter (AGDM) was compared between cultivars (Figure 2.10A and B). Grain yields were on average 40% lower in 2013 than 2012. In 2012 there was a 32% difference in grain yield between the highest (Gatsby) and lowest (Bacanora) yielding cultivars in 2012, and in 2013 there was a 29.9% difference between the highest (Savannah) and lowest (Cadenza) yielding cultivars. In 2012 Gatsby was also highest yielding in terms of its AGDM and Roysac (low grain yield) had the lowest AGDM yield. In 2013 Cappelle Desprez had the greatest (14.4 t ha^{-1}) AGDM yield and Roysac the lowest (11.6 t ha^{-1}).

A positive trend can be seen in 2012 with increased grain yield being associated with increased AGDM yield. Cappelle Desprez is an anomaly to this, having a low grain yield and but among the highest AGDM yield. Whereas, Savannah yielded lower than expected AGDB compared to its grain yield in 2012. HI integrates grain yield and AGDM (Figure 2.10C) and in both 2012 and 2013 Savannah had the highest HI (along with the highest yield in 2013). Roysac and Battalion also had high HI in both years; however Battalion had relatively high grain yield and Roysac relatively low. Cappelle Desprez had the lowest HI

in 2012 (0.4) but in 2013 this was Cadenza (0.38). There was a 0.19 difference in HI between the highest and lowest cultivars in 2012 and 0.17 in 2013.

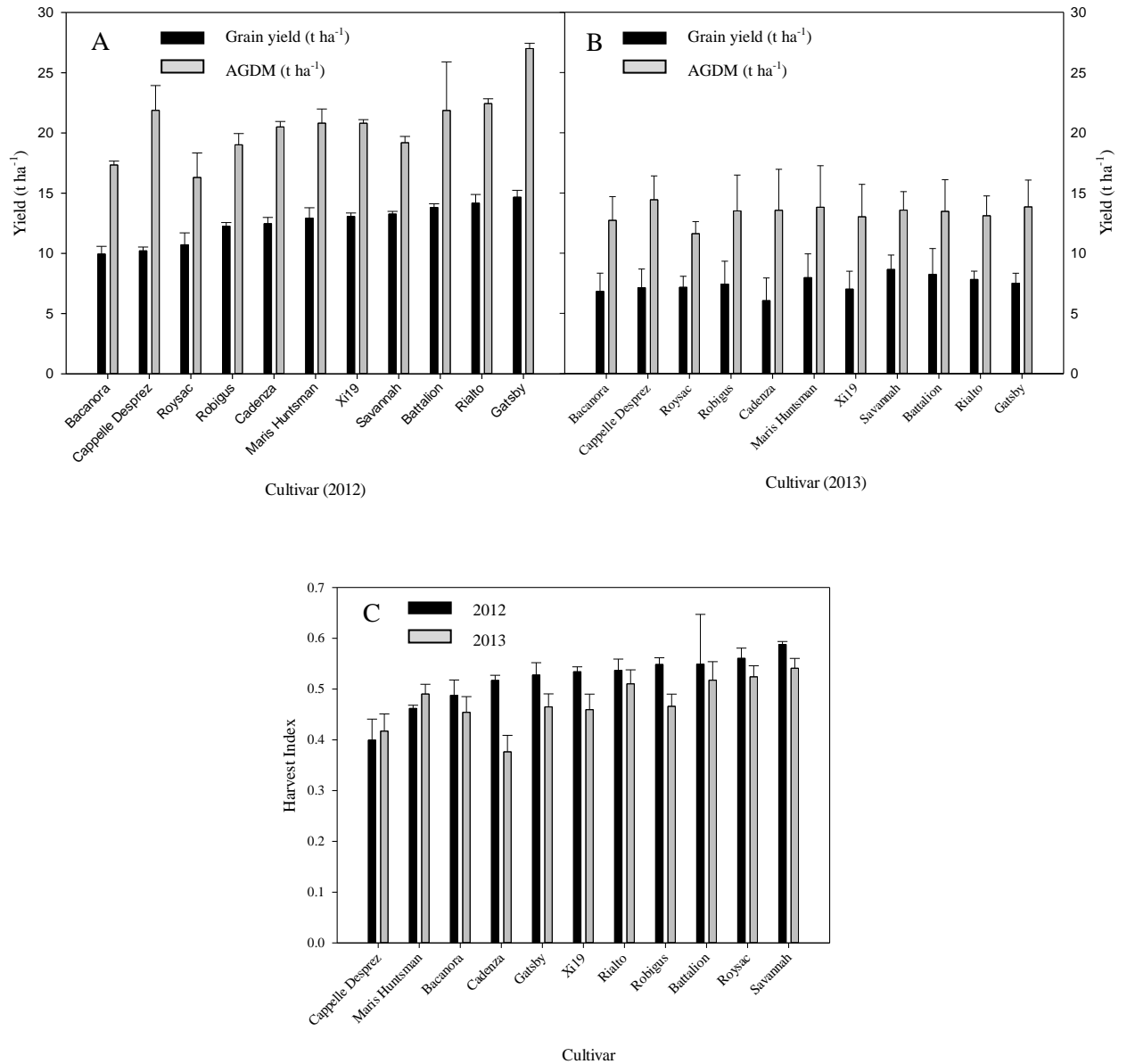


Figure 2.10. Grain yield (t ha⁻¹), above ground dry matter (t ha⁻¹; AGDM) and harvest index (HI) for each cultivar in 2012 and 2013. Values are the mean of three plots of each cultivar, ± SEM. Grain yield (t ha⁻¹) at 85% dry matter (black) and AGDM yield (t ha⁻¹) at 100% dry matter (grey) are shown for 2012 (A) and 2013 (B) for each cultivar. Cultivars are ordered by their grain yield for each year. HI (D) for each cultivar in 2012 (black) and 2013 (grey).

2.3.2 Response of wheat cultivars to elevated temperature treatment

A-Ci curves showed that, in 2012 (Figure 2.11A) Cadenza demonstrated the highest photosynthetic rates at ambient Ci values (~210 at ambient CO₂ of 400 μmol CO₂ mol air⁻¹), at which CO₂ assimilation was largely limited by the activity of Rubisco, whereas Maris Huntsman the lowest. In 2013 (Figure 2.11B), pre-anthesis, the cultivar with the highest photosynthetic rates at ambient CO₂ was Bacanora and Robigus was the lowest. The photosynthetic rates of all the cultivars decreased post-anthesis (Figure 2.11C); however, Rialto maintained the highest photosynthetic rates, and Gatsby decreased to the lowest rates. Cadenza maintained high photosynthetic rates at both developmental stages.

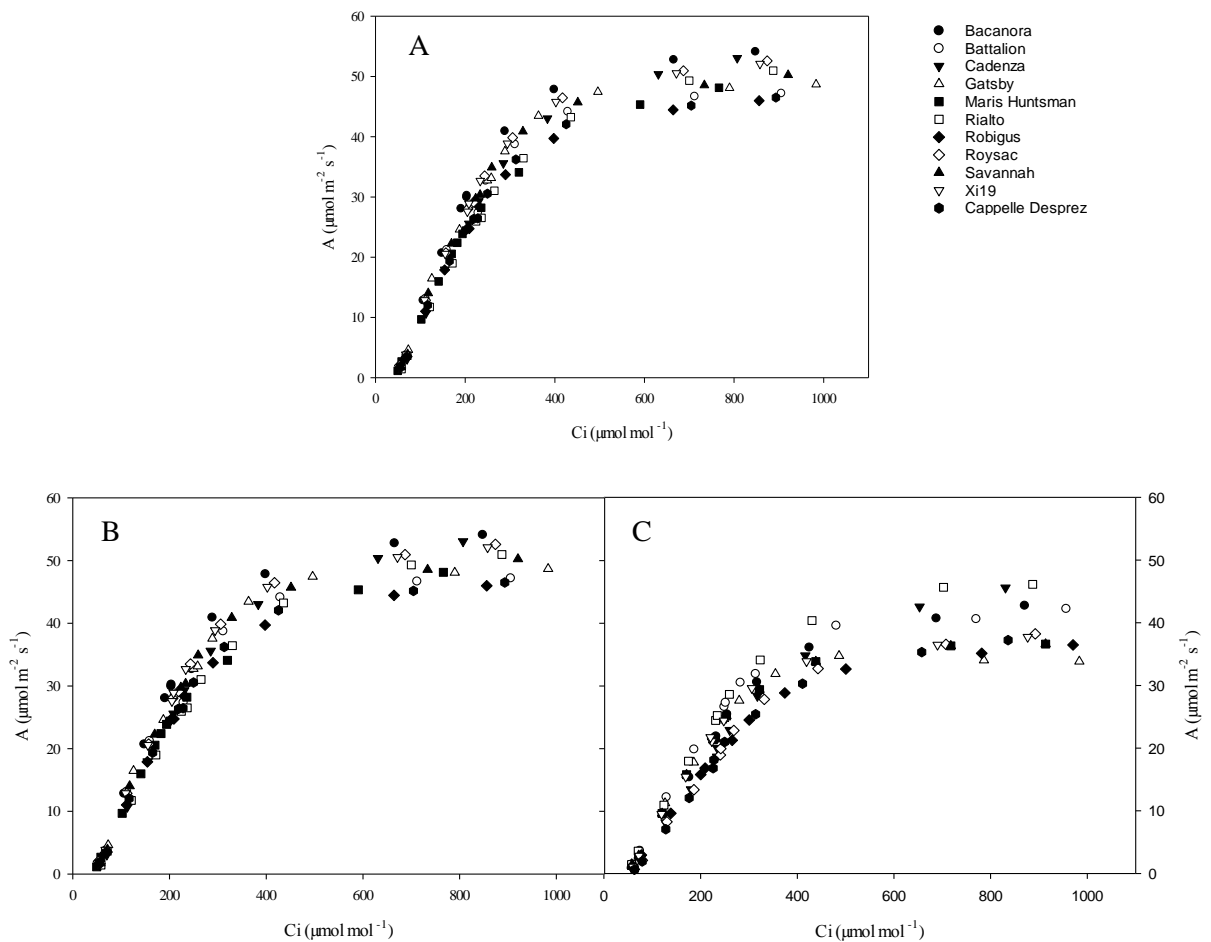


Figure 2.11. A-Ci curves ($\mu\text{mol CO}_2 \text{ mol air}^{-1}$; $\mu\text{mol mol}^{-1}$) for selected cultivars ($n=3$) pre-anthesis (Zadoks growth stage 4.3- 4.5) in 2012 (A) and 2013 (B) and post-anthesis (7 days after Zadoks growth stage 6.5; B) in 2013 (C).

Values are the mean of three leaves for each cultivar. Bacanora (Closed circles), Battalion (Open circles), Cadenza (Inverted closed triangle), Gatsby (Open triangle), Maris Huntsman (Closed square), Rialto (Open square), Robigus (Closed diamond), Roysac (Open diamond), Savannah (Closed triangle), Xi19 (Open inverted triangle), Cappelle Desprez (Closed hexagon).

The response of the 64 ERYCC panel cultivars to elevated temperatures was determined in 2012 in an initial screen to identify differences in their ability to cope with moderate heat stress. Photosynthesis was lower at 35°C compared to 25°C for all cultivars. There was an 86% difference in the extent of the decrease in photosynthesis due to increased temperature across the 64 cultivars with a high decrease representing highest sensitivity to the warmer temperature (Figure 2.12). With regard to Rubisco activity, cultivars with lower values for the ratio of initial/total activity are those less negatively affected by the high temperature than those with a higher value (Figure 2.13). The five highest and the five lowest cultivars (heat tolerant or susceptible), in terms of Rubisco activation state, were chosen for a more detailed and replicated analysis. The selected cultivars when ranked were evenly distributed throughout the panel in terms of their photosynthetic response to the elevated temperature treatment (Figure 2.12).

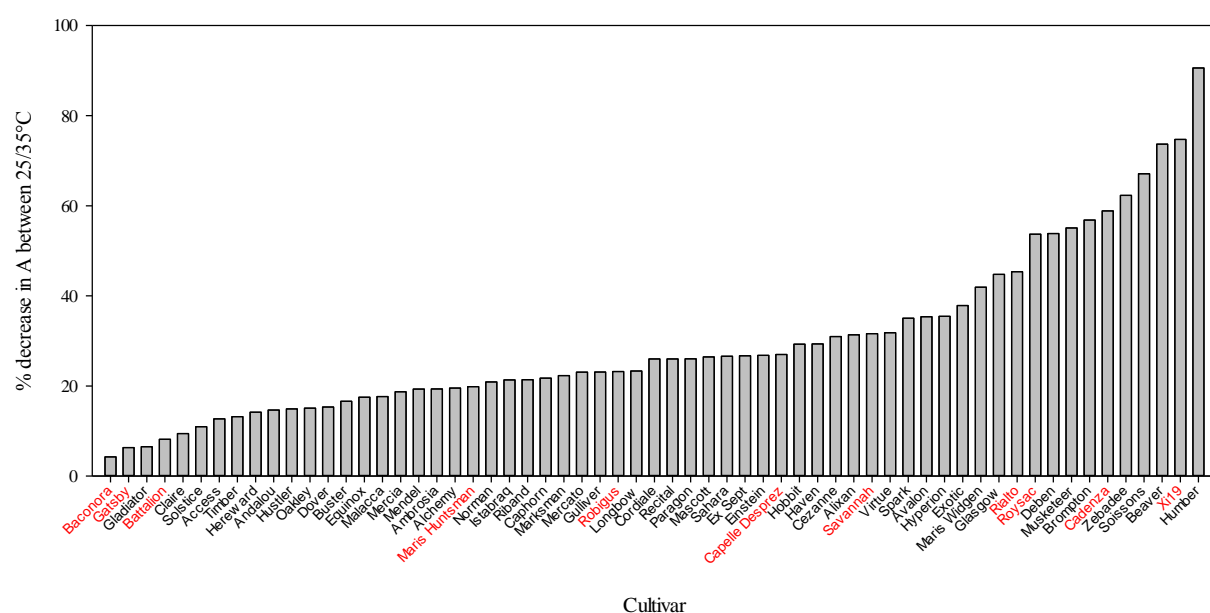


Figure 2.12. Initial screen of photosynthetic response to elevated temperature (% decrease in photosynthesis between 25 and 35°C) of the 64 ERYCC panel wheat cultivars in 2012. Value are for one leaf of each cultivar. The % decrease in photosynthesis (A) at 400 $\mu\text{L L}^{-1}$ CO_2 , between measurements at 25 and 35°C, was calculated for each cultivar. Each value corresponds to one sample. Cultivars highlighted in red are those for which further research was conducted.

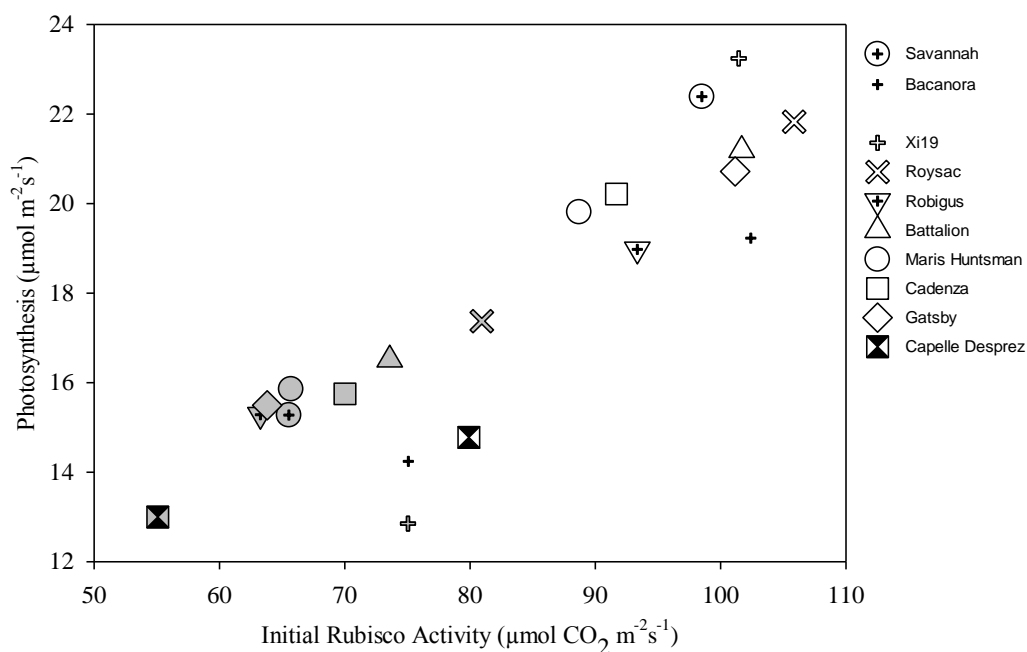


Figure 2.14. The relationship in 2012 between the photosynthetic rate ($\mu\text{mol m}^{-2} \text{s}^{-1}$) and the initial Rubisco activity ($\mu\text{mol CO}_2 \text{m}^{-2} \text{s}^{-1}$) for the selected wheat cultivars at 25°C (white) and 35°C (grey). Values are the mean of three leaves from each cultivar. Savannah (Dotted circle), Bacanora (Small crosshair), Xi19 (Large plus), Roysac (Large X), Robigus (Inverted triangle), Battalion (Triangle), Maris Huntsman (Circle), Cadenza (Square), Gatsby (Diamond), Cappelle Desprez (Square with hourglass).

Measurements similar to those in 2012 were conducted in 2013 to investigate further the cultivar specific temperature responses. The elevated temperature treatment (Figure 2.15A), resulted in a decrease in photosynthesis when all cultivars were considered together ($p=0.001$, F-Test). Overall, the effect of cultivar was also significant ($p=0.025$, F-Test) indicating there were differences between the responses of different cultivars. However, the interaction between cultivar and temperature was less strong ($p=0.055$, F-Test). Bacanora had the greatest decrease in photosynthetic rate, with a decrease of $7.02 \mu\text{mol m}^{-2} \text{s}^{-1}$ (26.9%), between 20 and 35°C ($p<0.05$, LSD). Other cultivars with significantly different photosynthetic rates at the two temperatures were Cadenza, Savannah and Robigus. Gatsby had the smallest decrease in photosynthetic rate, $3.2 \mu\text{mol m}^{-2} \text{s}^{-1}$ ($p>0.05$, LSD), and among the highest photosynthetic rates (and stomatal conductance) at both temperatures.

Stomatal conductance to water vapour (g_s ; Figure 2.15C) was not significantly different between temperatures over all the cultivars ($p=0.565$, F-Test); however there was a strong effect of cultivar ($p<0.001$, F-Test). There was also an interaction between cultivar and temperature ($p=0.055$, F-Test).

However, it is indicated that the decrease in photosynthesis cannot be primarily attributed to the plants closing their stomata at the higher temperature, as g_s was not significantly different for a cultivar at the two temperatures, indicating that the leaves were not water stressed. The intercellular carbon dioxide concentration (C_i ; Figure 2.15B) was not significantly different between cultivars ($p=0.160$, F-Test), although there was a significant interaction of temperature ($p<0.001$, F-Test), with C_i being greater (or the same) at the higher temperature. Therefore, a decrease in C_i or g_s cannot be considered as the cause of the reduced photosynthesis at the higher temperature. There was no significant difference in leaf temperature between the cultivars at the two different temperature treatments ($p=0.071$, F-Test; Figure 2.15D), cultivars all attained the same elevated leaf temperature.

The maximum quantum efficiency of photosystem II in light-adapted leaves (F_v'/F_m' , Figure 2.15E) was significantly decreased by the elevated temperature treatment in all cultivars ($p<0.001$, F-Test) with Bacanora having the greatest difference and Gatsby the least. A smaller difference in F_v'/F_m' was measured in the higher yielding cultivars between the two temperatures (a mean difference of 0.035), than in the lower yielding (a mean difference of 0.072).

When considering the association between photosynthetic parameters and final yield (Figure 2.16), the temperature treatment had a significant impact on both yield groups ($p=0.034$, F-Test). At both 20 and 35°C the high and low yielding groups were significantly different from each other, with photosynthesis in the lower yielding cultivars being significantly lower than that of the higher yielding cultivars. The lower yielding cultivars demonstrated a larger decrease in photosynthesis at the higher temperature ($p<0.05$, LSD) than the higher yielding counterparts.

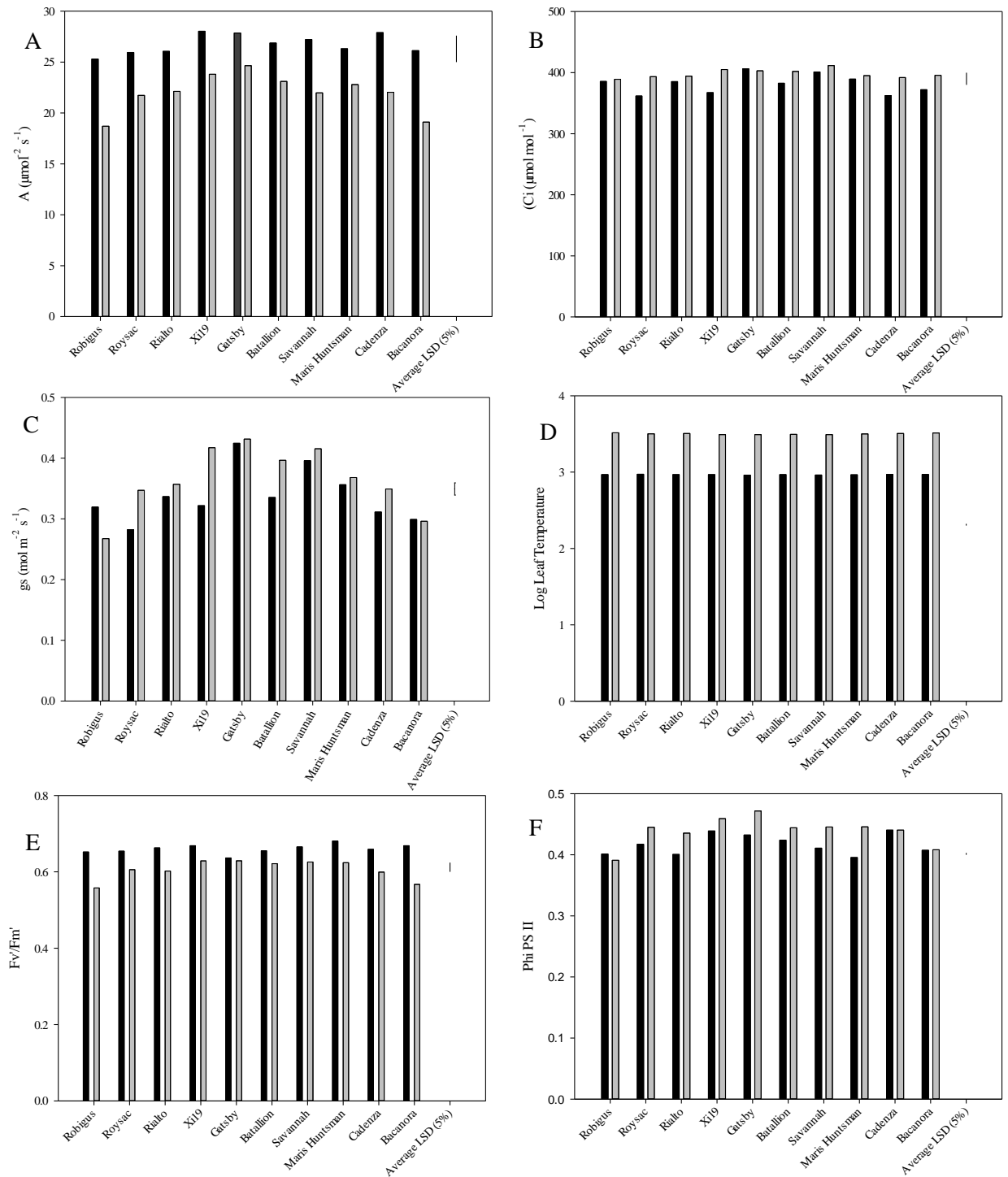


Figure 2.15. Graphs of the photosynthetic parameters for each cultivar at each of the temperature treatments (20°C and 35°C) in 2013.

Values are the mean of nine leaves of each cultivar. Photosynthetic carbon assimilation ($\mu\text{mol}^2 \text{s}^{-1}$; A), Intercellular CO_2 ($\mu\text{mol CO}_2 \text{ mol air}^{-1}$; B), Conductance ($\text{mol m}^{-2} \text{s}^{-1}$; C), Leaf temperature (log leaf temperature; D), F_v/F_m' (E), Φ_{PSII} (F). Graphs are plotted from the predicted means from the ANOVA statistical analysis, with average LSD being calculated with this. Measurements were taken at either 20°C (black) or 35°C (grey).

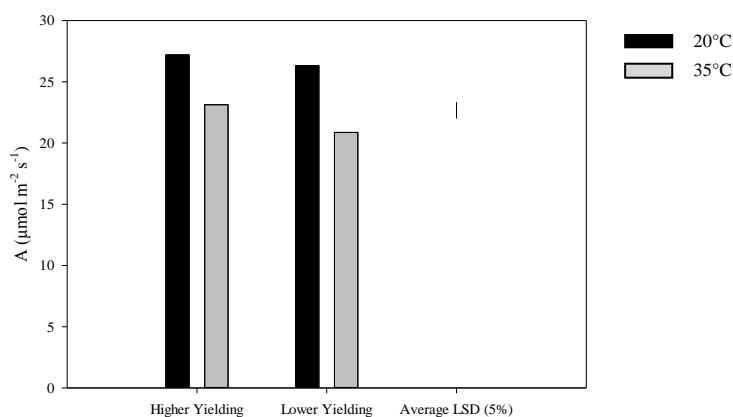


Figure 2.16. The photosynthetic rate ($\mu\text{mol m}^{-2} \text{s}^{-1}$) for the grouping of the higher and lower yielding cultivars at 20°C (black) and 35°C (grey).

The activation state of Rubisco relates directly to the function of Rca (i.e. ability of Rca to maintain the activity of Rubisco). All cultivars measured had a decreased Rubisco activation state (Figure 2.17A) at 35°C compared to 20°C ($p < 0.001$, F-Test). For Rubisco activation state there was also evidence of an interaction between cultivars and temperature ($p = 0.042$, F-Test), with different cultivars having different responses to the high temperature treatment. The cultivars with the greatest reduction in activity between 20 and 35°C were Xi19 and Cadenza, 37.6% and 35.8%, respectively. Bacanora had the greatest activity at both temperatures, but this was not significantly different from Robigus, for which the smallest change between the two temperatures was measured; with a 26.0% decrease in activity between 20 and 35°C. Total Rubisco activity was not significantly different between cultivars ($p = 0.336$, F-Test). When grouped according to yield, Rubisco activation state (Figure 2.17B) was significantly different (0.004, F-Test) with the lower yielding groups having a lower activation state at both temperatures.

The amount of Rubisco (Figure 2.18) was significantly different between cultivars ($p < 0.001$). Xi19 and Savannah had the greatest amount of Rubisco, with Xi19 being significantly different from all the other cultivars ($p < 0.05$, LSD), apart from Savannah. Robigus had the least amount of Rubisco. Gatsby was intriguing since it had high photosynthetic rates but relatively little Rubisco, for a member of the high yielding group. Even so, the high yielding group had more Rubisco on average (1.22 mg mL^{-1}) than the lower yielding group (1.13 mg mL^{-1}).

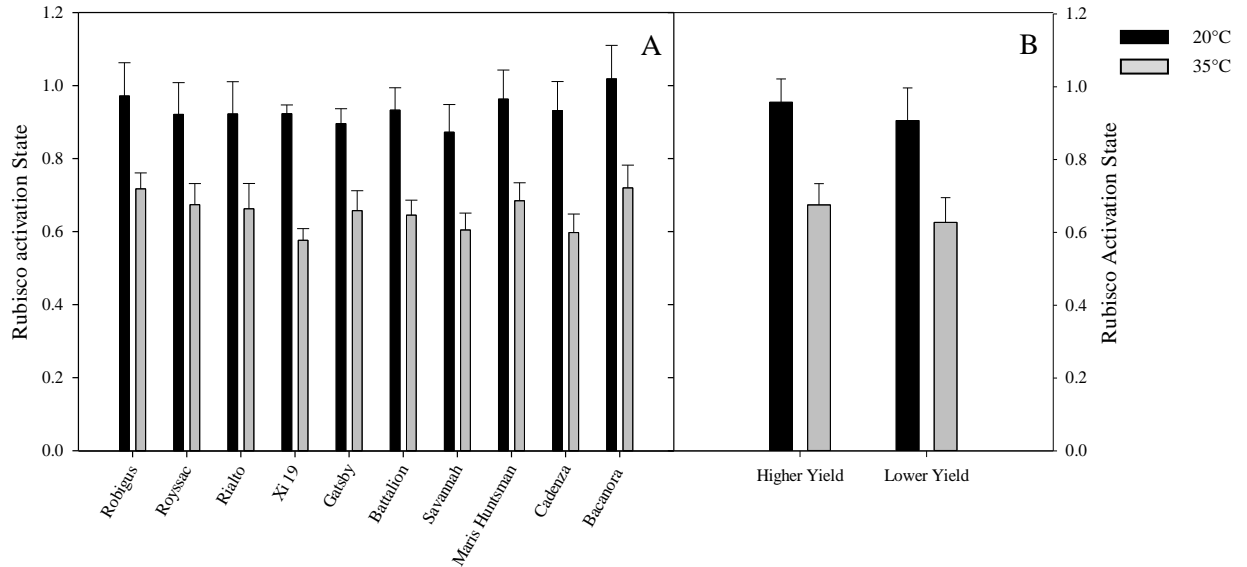


Figure 2.17. Rubisco activation state in 2013 for each wheat cultivar (A) and for the higher and lower yielding cultivar groups (B). Measurements taken at 20°C (black) and 35°C (grey). Data was log transformed prior to analysis (to comply with assumptions of ANOVA) therefore SD is shown not the LSD to allow true values to be illustrated.

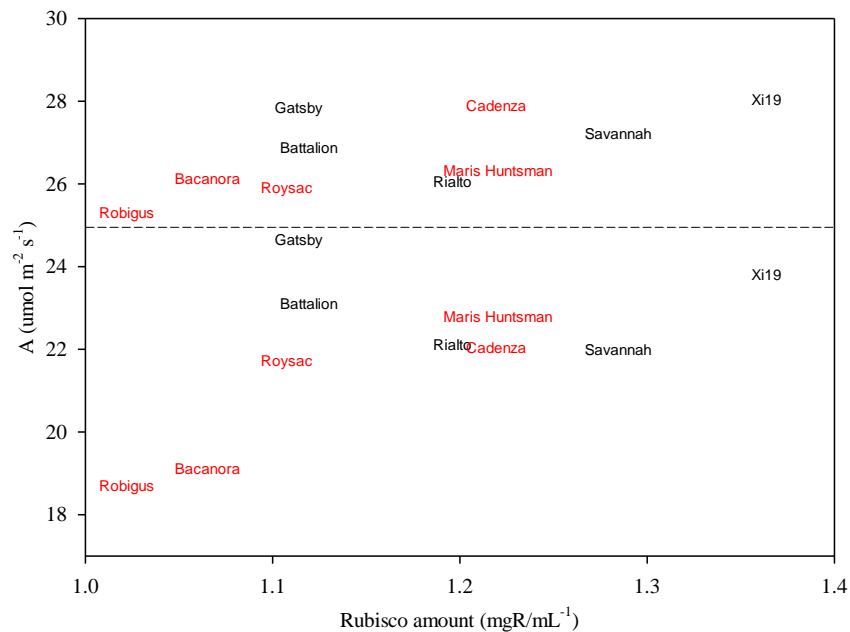


Figure 2.18. The average Rubisco amount (mgR mL⁻¹) and photosynthetic rate ($\mu\text{mol m}^{-2} \text{s}^{-1}$) in 2013, for each cultivar at 20°C and 35°C in 2013. Points below the line are measurements at 35°C and those above are at 20°C. Cultivars in red are lower yielding and those in black higher yielding. Photosynthesis for each cultivar is taken from the predicted means from the ANOVA analysis.

All parameters measured were correlated, the relevant correlations are shown below. Photosynthetic rates measured at control temperatures for the ten wheat cultivars correlated positively with HI in 2012, but not 2013 (Table 2.6). A positive correlation was found between photosynthesis and Rubisco amount in both years. Rubisco activation state and Rubisco initial activity at the control temperature both correlated negatively with Rubisco amount in 2012 and 2013.

Photosynthetic rates at control temperatures correlated positively with rates measured at 35°C in 2012 and weakly in 2013 (p=0.064). The difference between photosynthesis at control and elevated temperatures correlated positively with photosynthesis measured at control temperatures, suggesting that the higher the start rate at control temperatures, the larger the decrease at the higher temperature. Conversely, the difference between rates measured at the two temperatures correlated negatively with rates at 35°C, as cultivars having higher rates at the higher temperature were less susceptible to heat, thus had a lower decrease in photosynthesis with the temperature increase.

Table 2.6. Key correlations, coefficients and p values for photosynthetic, yield and Rubisco traits in 2012 and 2013.

Traits		Correlation coefficient 2012	p value 2012	Correlation coefficient 2013	p value 2013
Photosynthesis	Harvest index	0.48	0.01	-0.32	0.09
Photosynthesis	Rubisco amount	0.43	0.02	0.40	0.03
Rubisco activation state	Rubisco amount	-0.35	0.06	-0.36	0.05
Rubisco initial activity	Rubisco amount	-0.46	0.01	-0.66	0.00
Photosynthesis control temperature	Photosynthesis elevated temperature	0.41	0.03	0.34	0.06
% difference photosynthesis control and elevated temperature	Photosynthesis control temperature	0.49	0.01	0.12	0.53
% difference photosynthesis control and elevated temperature	Photosynthesis elevated temperature	-0.58	0.00	-0.89	0.00

2.4 Discussion

The cumulative carbon assimilation through the growth season is the primary determinant of crop biomass and therefore it is predicted that improving photosynthetic capacity in wheat could raise the baseline for yield potential by 50% or more (Reynolds *et al.*, 2011). A positive correlation was observed between photosynthetic rate and yield parameters in the data from 2012, but not 2013 (Table 2.6). However, when the cultivars were grouped depending on their grain yield over multiple growing seasons, the higher yielding cultivars did demonstrate higher photosynthetic rates in 2013. The results of this correlation analysis contrast to those obtained from experiments looking at the 64 cultivars of the ERYCC panel in the same years. Driever *et al.* (2014) in 2012 found no consistent correlation between photosynthetic capacity and grain yield and Carmo-Silva *et al.* (2015) in 2013 saw a positive correlation. The differences between this study and the above studies on the whole panel is indicative of the variation between the cultivars in the panel. The cultivars investigated in this study represent some of the greatest extremes in the panel, in particular regarding development and biomass production. For example, Bacanora (Clarke *et al.*, 2012) has previously been among the lowest yielding cultivars in the ERYCC panel and also has very rapid development, often being the first to reach each growth stage. In contrast, Gatsby has previously been among the highest cultivars for crop biomass; having the highest number of grains per m², yet a below average number of grains per ear.

The difference between the data from 2012 and 2013 for cultivar grain yield, above ground biomass, height and photosynthetic capacity, must be considered in relation to the dramatically different meteorological conditions and planting times of the two years (the 2013 experiment was planted very late in the season). 2012 was a much wetter and cooler year during the critical months for wheat development, while 2013 was a hotter, drier year (particularly during grain filling); highlighting the difficulty in breeding cultivars resilient enough to withstand seasonal climatic variation. Yields were much lower in 2013 than in 2012, that the difference in growing conditions may have impacted upon Rubisco activity must also be considered. High wheat yields are strongly associated with low average minimum temperatures (Lobell *et al.*, 2005), and high radiation levels for a period of 30 days (20 days prior to anthesis and 10 days post-anthesis), however it is clear that the response of individual cultivars to

environmental conditions can be very diverse (Ortiz *et al.*, 2008). Research is required to ensure that, alongside increasing grain yields, breeding efforts also optimise thermal tolerance in the context of environmental variability in current and future climates. The higher yielding cultivars investigated here also had lower decreases in photosynthesis and Rubisco activation state when exposed to the elevated temperature treatment; this may be of benefit in breeding for improved thermal tolerance. Battalion, Gatsby and Rialto (all UK winter wheat cultivars, classed as higher yielding) all showed relatively small changes in Rubisco activation state and no significant decrease in photosynthesis due to the elevated temperature treatment (in 2013). This may suggest that these cultivars have relatively thermally tolerant Rca. Additionally, there was no significant difference between the Rubisco content of these cultivars.

In more detail, Battalion (a UK winter wheat) showed no significant decrease in photosynthesis with the temperature treatment in 2013, and in 2012 it was the cultivar which demonstrated the smallest change in photosynthetic rate. Battalion is a high yielding cultivar with high HI, showing average to low rates of photosynthesis in the A-Ci curve assessment. However, it reached anthesis late in the season (Julian day 183 in 2013, with the last cultivar reaching anthesis on Julian day 184), and so the timing of heat stress in relation to grain development would have to be carefully considered, in terms of a future changing climate and subsequent yield impacts in this cultivar. Indeed, early heading cultivars have been associated with increased thermal tolerance (Semenov *et al.*, 2014).

Roysac (a French origin winter wheat), classed as a low yielding cultivar here, showed high photosynthetic rates at both temperatures in 2012, no decrease with the high temperature treatment in 2013, and only a small decrease in Rubisco activation state. In the A-Ci curves from 2013 it showed relatively high photosynthetic potential at booting but did not maintain this post-anthesis. Roysac had among the higher HI in 2012; however this resulted from it having the lowest AGBM as well as low grain yield. This illustrates the range of traits, which may not be in ideal combination, that one cultivar can exhibit. The Rca thermal tolerance of Roysac could be of benefit to breeders if included in breeding programmes associated with high grain yielding traits. Robigus (a UK winter wheat), is also a lower yielding cultivar, and had the lowest amount of Rubisco in 2013. This is interesting as Robigus was also

the cultivar least affected by high temperature, in terms of its change in Rubisco activation state, however it showed a significant decrease in photosynthesis at 35°C.

The most efficient use of resources would be high photosynthetic rates and a minimal decrease with elevated temperature associated with low Rubisco amounts maintaining high activity, as seen in a cultivar such as Gatsby (Figure 2.18). Rubisco is a large nitrogen sink for the plant, and as this is a limited and expensive nutrient to apply to crop systems, reducing the nitrogen requirements of the plant (and ensuring that what is applied is utilised efficiently) would be of benefit to the farmer (Parry *et al.*, 2011). Studies of plants with reduced amounts of Rubisco suggest that this enzyme may actually be in excess under most climatic conditions and that a modest decrease could be beneficial, especially as atmospheric CO₂ levels rise (Lauerer *et al.*, 1993, Parry *et al.*, 2003).

The origin of the cultivars investigated here differ, and this may have impacted upon their thermal tolerance due to disparate adaptations to different environments. For example, Gatsby, a UK winter wheat, had the highest yield in 2012 but a lower yield in the hotter and drier year of 2013 (Figure 2.10). Cultivars of more recent origins have also been seen to have increased photosynthetic performance as well as improved grain yields (Watanabe *et al.*, 1994). Across the whole ERYCC panel it was seen that grain yield and HI increased with year of introduction, which was achieved through grain number and number of ears per m², not changes to thousand grain weight (Clarke *et al.*, 2012). It is interesting to see similarities in the performance of cultivars in both 2012 and 2013 (i.e. Battalion showed little decrease in photosynthesis with the temperature treatment in 2013 or in 2012), regardless of the difference in the weather conditions; this yield stability is of merit.

Developmental rate is accelerated by increasing temperatures and it is predicted that a consequence of this may be that the biggest threat to wheat yields will be that of heat stress not drought, since accelerated development can be beneficial, resulting in crops escaping low water availability later in the season (Semenov & Shewry, 2011). Therefore, maintaining high yields whilst ensuring rapid but efficient development may be critical to ensuring stable grain yields under elevated temperatures. Early heading cultivars perform better at elevated temperatures than later heading cultivars as they produce fewer leaves

per tiller, retain more green leaves, have longer grain filling periods and complete grain filling earlier in the season when air temperatures are lower (Tewolde *et al.*, 2006). Bacanora (Mexican origin), Roysac and Cadenza (French origin) are all non UK cultivars which had the fastest developmental rates of the cultivars studied. A correlation was seen between speed of development and yield parameters, as these modern cultivars were also all classified as being higher yielding.

Stay green characteristics may increase thermal tolerance (Reynolds *et al.*, 2001, Xu *et al.*, 2000), however, this trait may be a disadvantage as it is associated with the tendency to retain the stem and leaf reserves (Blum, 1998). Higher leaf chlorophyll content cultivars also tend to be more heat tolerant (Hede *et al.*, 1999), and have higher stomatal conductance (Rees *et al.*, 1993). However, this trend was not seen strongly here, with the cultivars showing highest chlorophyll measurements not being those indicated as being thermally tolerant as far as Rca is concerned.

A study in wheat by Lu *et al.* (2000) showed that at moderately high temperatures (30- 37.5°C) the decrease in the quantum yield of PSII electron transport and the efficiency of excitation energy capture by open PSII reaction centres was reversible. In severely elevated temperatures (higher than 37.5°C), the further decrease in the quantum yield of PSII electron transport and F_v'/F_m' was irreversible. Light energy absorbed by chlorophyll molecules can be used to drive photosynthesis (photochemistry), or excess energy can be dissipated as heat or it can be re-emitted as light (chlorophyll fluorescence). Any increase in the efficiency of one of these processes will result in a decrease in the other two; therefore measurement of chlorophyll fluorescence can provide information about changes in the efficiency of photochemistry and heat dissipation. The flow of electrons through PSII is indicative of the overall rate of photosynthesis. Therefore it can be used to estimate photosynthetic performance. PSII is accepted to be the most vulnerable part of the photosynthetic apparatus to light-induced damage (Maxwell & Johnson, 2000). F_v'/F_m' can be used to assess the relative contribution of PSII to photochemical capacity and thermal decay processes to the overall efficiency of PSII photochemistry in the light (Liu *et al.*, 2012). ϕ_{PSII} is the effective quantum yield of photochemical energy conversion in PSII (measures the efficiency of PSII photochemistry). Cultivars such as Gatsby, showing greater efficiency of PSII at the elevated

temperature treatment may be of benefit in breeding programmes to improve the thermal tolerance of photosynthesis.

Various other characteristics, which were not investigated here have also been identified as resulting in increased thermal tolerance and greater yield in wheat, for example, membrane stability (Saadalla *et al.*, 1990, Shanahan *et al.*, 1990), canopy temperature depression (Amani *et al.*, 1996) and mobilisation of stem reserves at grain filling in stress conditions (Blum, 1998). Cultivars which maintain grain weight during heat stress at grain filling can also be a useful indicator for improved heat tolerance (Dias & Lidon, 2009).

Recent modelling efforts have indicated strategies, and supported existing evidence, regarding how to adapt crop phenology to future weather patterns (Semenov *et al.*, 2014, Stratonovitch & Semenov, 2015). One aspect highlighted in these studies is that extending the duration of grain filling is important if future wheat yields are to be improved in southern and central Europe. Maintenance of green leaf area until the end of grain filling was also of benefit. A shift of anthesis date to earlier in the year to avoid heat stress during flowering and grain fill is also predicted to be of benefit in Southern Europe (e.g Spain).

The results here indicate that cultivar differences can be found when looking at the response of photosynthesis to an elevated temperature of 35°C. Whilst the lack of replication in the initial screen enabled all the lines in the ERYCC panel to be considered it also meant that that further research would be necessary to confirm the results obtained. The aim of this high-throughput screen was to identify diversity and it enabled investigation of diverse cultivars, with a focus on identifying the outliers.

However, as anticipated there were some discrepancies between the results in the initial screen and the subsequent replicated experiments. Whilst this may be due to the lack of replication in the initial screen, the difference between the sampling time of the initial screen and that of replicated experiment (18 days, start to finish) may also have had an effect on the ability of the plant to cope with increased temperatures; the leaves were significantly older on the replicated experiment and a period of warm weather was experienced between the two sampling time points.

Rubisco activation state was considered to be the best indicator of changes in Rca function amongst the cultivars. The initial activity is the activity of Rubisco in the sample at the instant it was frozen and therefore reflects activity *in vivo*. The total activity shows the Rubisco activity obtained after Rubisco was incubated with CO₂ and Mg²⁺, to ensure that all the available catalytic sites were carbamylated and active, and indicates the carboxylation potential of the sample (Parry *et al.*, 2002). Therefore, the total activity usually exceeds the initial activity. The activation state reflects the proportion of the total sites that are in the active form, which in turn depends on the function of Rca. This measurement provides a valid estimate of the activity of Rca in the leaf because the activation state of Rubisco in the light is a direct consequence of the activity of Rca (Andrews *et al.*, 1995, Eckardt & Portis, 1997, Portis *et al.*, 1986, Salvucci *et al.*, 1985).

Short-term exposure to high temperature has been shown elsewhere to impact upon Rubisco activation state in wheat. For example, Feller *et al.* (1998) used a five minute exposure for cotton or wheat leaf discs to a high temperature treatment, after which a reversible decrease in activation state was seen. When looking for a more heat tolerant Rca this can be considered a viable strategy, as the instantaneous heat stress, and therefore reduction in Rubisco activation state, will reflect the response of Rca. However, the impact of prolonged heat stress on overall grain yield and photosynthesis was not captured here as plants were grown under field conditions.

Studies have shown that endogenous amounts of Rca are important for plant photosynthesis under both optimal and supraoptimal temperatures. In tobacco (*Nicotiana tabacum* L.), Rca deficient plants had reduced rates of CO₂ fixation at 25°C, despite having increased Rubisco amounts (Mate *et al.*, 1993), and the heat sensitivity of photosynthesis increased compared to plants with normal levels of Rca (Sharkey *et al.*, 2001). Martinez- Barajas *et al.* (1997) examined grain yield and amounts of Rca in two genetically related populations of the same maize cultivar under field conditions. They observed that the high yielding population had higher levels of Rca than the low yielding population. Differences in the amount of Rca between wheat cultivars have also been seen (Ristic *et al.*, 2009). Related to this, the turnover rate of Rca may differ between cultivars, which may impact upon their thermal tolerance.

In wheat there are both longer and shorter (α and β) isoforms of Rca, both isoforms can activate Rubisco but they are differentially regulated in the plant. The individual Rca isoforms present and their ratios could also be important in understanding the difference in Rca thermal tolerance in wheat. Under heat stress Qin *et al.* (2008) found that the Rca β gene was induced more in a heat tolerant cultivar (TAM107) than in a heat susceptible cultivar (Chinese Spring). Investigating whether there are different amounts of the Rca isoforms in a wider panel of cultivars than those investigated here, or over expressing Rca in wheat, may improve heat tolerance.

Knowledge about the specifics of Rca thermal tolerance, and any correlation between the other factors which have a role to play in thermal tolerance, may inform an integrated breeding strategy which may ultimately result in the ability to maintain yield stability under heat stress. Maximum photosynthetic potential is rarely achieved in the field (reviewed by Murchie *et al.* (2009)), and as yield is the result of many integrated processes field based research is critical, despite the problems of attempting to breed crops in current climates, for future climates Close consideration of the impacts that developmental rate, phenology and resource allocation play on final yield, and the link between these traits and photosynthesis is critical.

3. Genetic transformation to improve the thermal tolerance of photosynthesis in wheat

3.1 Introduction

Rubisco activase (Rca) is sensitive to elevated temperatures and has been shown to limit photosynthesis in some species under relatively moderate heat stress conditions (Crafts-Brandner & Salvucci, 2000, Sage *et al.*, 2008, Salvucci & Crafts-Brandner, 2004b). Studies with *Arabidopsis* have demonstrated that increasing the thermal stability of Rca improves both photosynthesis and plant growth under moderate heat stress (Kumar *et al.*, 2009, Kurek *et al.*, 2007). In a wild relative of Rice (*Oryza meridionalis*) higher Rubisco activation state was also associated with improved photosynthetic thermotolerance (Scafaro *et al.*, 2012). The Rca from species native to warm environments is less thermally sensitive than the Rca from species native to cool environments (Carmo-Silva & Salvucci, 2011, Carmo-Silva & Salvucci, 2012, Crafts-Brandner & Law, 2000). In this work, wheat (*Triticum aestivum* L.) was genetically engineered to express cotton (*Gossypium hirsutum*) Rca to test the hypothesis that expression of the more thermally stable isoforms of Rca from cotton, in combination with the native less thermally stable forms of Rca from wheat, would broaden the temperature range of wheat Rubisco activation and photosynthesis.

The activity of Rubisco in response to temperature was compared between cotton and wheat by Feller *et al.* (1998). In Figure 3.1 wheat and cotton leaf discs were exposed to an elevated temperature treatment, which was either followed by a recovery (lower temperature) treatment or not, Rubisco activity of the discs was then measured. At any given temperature the inhibition of Rubisco activity due to the elevated temperature treatment (compared to the control treatment), was greater in wheat than in cotton. However, Rubisco itself was not directly affected by the moderately high temperatures and its activity could be restored. This indicates that it was Rca being affected by the temperature treatment and that the wheat Rca was much more susceptible to structural damage than cotton Rca. Feller *et al.* (1998) hypothesised that differences in the amino acid sequence of Rca, or the presence of different Rca polypeptide isoforms

accounted for the greater thermal sensitivity of Rubisco activity in wheat compared with cotton. The difference in the thermal stability of Rca activity in cool and warm season species was further confirmed by Carmo-Silva *et al.* (2011), since Rca from Camelina (*Camelina sativa*), a cool season species (like wheat) showed a decline in activity after exposure to less extreme temperatures than were required to cause a similar decline in cotton Rca (Figure 3.2).

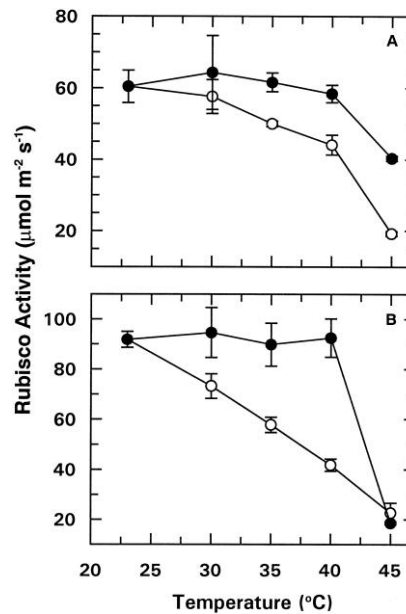


Figure 3.1. The effect of temperature on light activation of Rubisco. Intact cotton (A) and wheat (B) leaf tissue was irradiated with $1800 \text{ mol photons m}^{-2} \text{ s}^{-1}$ PAR either for 15 min at 22.5°C followed by an additional 5 min at the indicated temperature (white circles), or for 5 min at the indicated temperature followed by a 15 min incubation at 22.5°C (black circles). After the 20 min irradiation period, leaf tissue was immediately homogenized to determine Rubisco activity. Each point represents the mean SE of two replications. Figure reproduced from Feller *et al.* (1998).

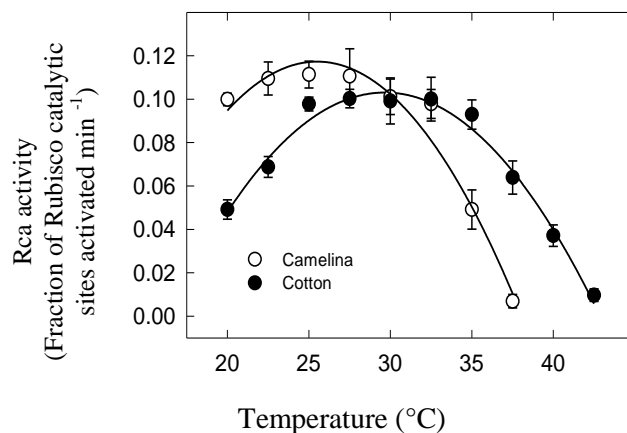


Figure 3.2. Temperature response of Rca activity in cool (*Camelina sativa*; Camelina) and warm (*Gossypium hirsutum*; Cotton) season species. Figure modified from Carmo-Silva & Salvucci (2011).

In this chapter genetic transformation was used with the aim of improving the thermal tolerance of photosynthesis in wheat. Two separate transformation constructs were created to independently express the α and β isoforms of cotton Rca (Salvucci *et al.*, 2003) in wheat. Constructs were made to express *GhRca- α* and *GhRca- β* with either the wheat Rubisco small subunit transit peptide (*WtRSSU-TP*) or the cotton Rca transit peptide (*GhRca-TP*). Following biolistic transformation the resultant wheat plants were assessed for presence of cotton Rca protein, and photosynthetic performance at elevated temperature was measured.

3.2 Materials and methods

3.2.1 Plant material and growth conditions

Wheat plants (*Triticum aestivum* L. cv. Cadenza and transgenic Cadenza lines) were grown in the glasshouse (16 hr day, 20°C day/16°C night, with natural light supplemented by banks of Son T 400W sodium lamps (Osram Ltd., Langley, UK) giving 400–1,000 $\mu\text{mol m}^{-2} \text{s}^{-1}$ at plant height due to variation in the light entering the glasshouse). Seeds were first planted in either vermiculite or Levington compost (Levington F2+S, Seed & Modular Compost, plus sand). After four weeks of growth plants were transplanted into 10 x 10 cm pots with Rothamsted Prescription Mix compost. Rothamsted Prescription Mix compost contained: 75% (w/w) medium grade peat, 12% (w/w) screened sterilised loam, 3% (w/w) medium grade vermiculite, 10% (w/w) grit (5 mm screened, lime free), 3.5 kg m^{-3} Osmocote Exact, 0.5 kg m^{-3} PG mix fertiliser, lime to pH 5.5- 6.0 and 200 mL m^{-3} and Vitax Ultrawet wetting agent. Cotton (*Gossypium hirsutum* cv. Vicky) leaf samples for western blot and isoelectric focusing (IEF) trials were obtained from Liz Isgar at Rothamsted Research.

3.2.2 Activation of wheat Rubisco with cotton Rubisco activase *in vitro*

To test whether cotton Rca was able to activate wheat Rubisco, assays were performed using radioactively labelled sodium bicarbonate ($\text{NaH}^{14}\text{CO}_3$). Cotton Rca activity was measured as the ability to restore activity to the inactive wheat Rubisco-RuBP (ER) complex (Barta *et al.*, 2011b, Salvucci *et al.*,

1985). Cotton Rca was purified (according to Barta *et al.* (2011a)) by Mike Salvucci, and assays were completed by our collaborators at the USDA, Elizabete Carmo-Silva and Mike Salvucci.

Wheat Rubisco was purified at Rothamsted Research. Two week old leaf tissue (100 g in total) was blended in 300 mL extraction buffer (20 mM Tris-base, 10 mM MgCl₂, 10 mM NaHCO₃, 2 mM dithiothreitol (DTT), 1 mM EDTA, 1 mM Na₂HPO₄·12H₂O, 1 mM benzamidine, 5 mM ε-aminocaproic acid, 50 mM 2-mercaptoethanol, 1% (w/v) insoluble PVP-40 and 1 mM PMSF). This material was filtered through muslin and the filtrate was brought to 35% saturation by the addition of freshly made saturated (100%) ammonium sulphate. The filtrate was centrifuged at 17, 664 x g for 25 min at 4°C to sediment the precipitate. The supernatant was then taken to 55% ammonium sulphate saturation. After further centrifugation (17, 664 x g for 25 min at 4°C) the pellet was re-suspended in 45 mL Q-Sepharose Column Buffer (10 mM Tris-Base, pH 8.0, 10 mM MgCl₂, 10 mM NaHCO₃, 2 mM DTT, 1 mM EDTA and 1 mM Na₂HPO₄·12H₂O).

This solution was then pipetted onto the surface of a series of sucrose gradients (0.3- 1.2 M sucrose) and centrifuged at 43, 4094 x g at 4°C for 2.5 hr. The contents of each tube were divided into fractions of 2 mL by means of a peristaltic pump, running at 1 mL min⁻¹. Equivalent fractions from each sucrose gradient were pooled. Samples showing the highest Rubisco activity (determined with the radioactive bicarbonate assay) were loaded onto a prewashed Q Sepharose column (with a volume of 142 mL). A NaCl gradient (0- 0.6 M) was used elute the protein from the column. The fraction (12 mL fractions collected at 1.5 mL min⁻¹) containing the peak of protein was determined with use of the Bradford reagent (Bradford, 1976). The fractions containing Rubisco were then desalted on a G-25 Sephadex column at 2 mL min⁻¹, using a buffer containing 5mM Bicine, and 10 mL fractions were collected. Those fractions containing Rubisco (identified with use of Bradford reagent) were pooled and stored at -80°C, Rubisco activity was subsequently determined by radiometric assay.

3.2.3 Design and development of constructs for expression of cotton Rubisco activase in wheat

The two constitutive promoters which were used to express the *GhRca* genes in wheat were trialled to demonstrate that expression could be identified in leaf tissue throughout wheat development. Expression of the β -glucuronidase (*gus*) gene was compared under the control of either the Rice *actin-1* or Maize *ubiquitin-1* promoters. Transgenic wheat plants expressing the *gus* gene under the control of either promoter were received from the Rothamsted Transformation Group and grown in the glasshouse as above. Four transformed wheat lines were studied, two with the Rice *actin-1* promoter and two with the Maize *ubiquitin-1* promoter. Between four and six plants showing GUS expression in each line were assessed.

Leaf samples were taken 2 hr after the beginning of the photoperiod, at each of five sampling time points throughout the development of the plants. The developmental stage of the plants was recorded at each sampling time point using Zadoks growth stages (Zadoks *et al.*, 1974). A 2 cm long leaf sample was taken, 2 cm down from the tip of the youngest fully expanded leaf of a secondary tiller. The leaf sample was cut into smaller pieces and these were put into the wells of a 24-well cell culture plate. A maximum of 10 min between sample collection and assaying was allowed to ensure leaf samples did not degrade. To assay GUS activity, 450 μ L of X-Gluc (5-Bromo, 4-chloro, 3-indolyl β -D glucuronide) mix and 10 μ L of 1% (v/v) Triton X-100 was added to each well. The X-Gluc mix contained: 25 mg X-Gluc in 0.5 mL Methyl cellosolve, mixed with 10 mL 0.5M NaHPO₄, pH 7.0 and 0.5 mL 50 mM potassium ferrocyanide, the solution was brought to volume (50 mL) with distilled water.

The plate was briefly put into a vacuum chamber to ensure the assay solution infiltrated the leaf samples. The samples were incubated overnight at 37°C before being transferred into 70% (v/v) ethanol. Following another overnight incubation the samples were transferred into 100% ethanol for storage prior to photographing.

GhRca- α and *GhRca- β* genes (with the associated cotton Rca transit peptide) were supplied in pENTR constructs by Mike Salvucci (USDA). Flanking primers (Table 3.1) were used to amplify the genes and

their transit peptides with Phusion proofreading Taq (New England BioLabs Inc., Hitchin, UK). PCR conditions were 98°C for 30 s followed by 40 cycles of, 98°C for 10 s, 46°C for 20 s and 72°C for 20 s, and a final extension step at 72°C for 5 min.

Table 3.1. Primers used to amplify the *GhRca* genes from the pENTR constructs to introduce appropriate restriction sites for ligation into p302AcNos.

	Primer sequences
p302AcGhRcaA	
F- FCottonRca_A	CAG ACG TCC CAT GGC GGC TGC C
R- RCottonRca_A	CTG ATA TCA GAT CTT TAA AAT TGG TAA GTG C
p302AcGhRcaB	
F- FCottonRca_B	CAG ACG TCC CAT GGC GGC TGC CGT C
R- RCottonRca_B	CGC AGC TGA GAT CTT TAG AAA GCT CCT CTC

The amplified *GhRca* genes and transit peptides were first cloned into pGEM-T Easy vectors according to the manufacturer's protocol (Promega, Southampton, UK), allowing the genes to be easily sequenced and moved between vectors. The *GhRca* genes were then cloned into p302AcNos (vector containing the Rice *actin-1* promoter and Nos (nopaline synthase terminator from *Agrobacterium tumefaciens*) terminator, received from Peter Buchner, Rothamsted Research). The genes were cloned into p302AcNos at the *Sma*I site, with the *Zra*I and *Eco*RV restriction enzymes being used for cloning *GhRca- α* , and *Zra*I and *Pvu*II for *GhRca- β* .

The cotton Rca transit peptide could be ineffective at targeting the protein to the wheat chloroplast, therefore, a second pair of constructs containing the wheat Rubisco small subunit transit peptide (*WtRSSU-TP*) were produced (see Primavesi *et al.* (2008) for transit peptide details). ChloroP was used as predictive software for transit peptide cleavage sites (Emanuelsson *et al.*, 1999). The *GhRca* genes and *WtRSSU-TP* sequence were synthesised and codon optimised for *Triticum aestivum* L. (GenScript USA Inc., Piscataway, NJ, USA) and then cloned, using *Eco*RI and *Bam*HI restriction sites, into pAHC17 (vector containing the Maize *ubiquitin-1* promoter and the Nos terminator, received from Caroline Sparks, Rothamsted Research).

In both construct pairs, antibiotic resistance (ampicillin) was used for selection in cloning. For a summary of the four constructs produced see Figure 3.3.

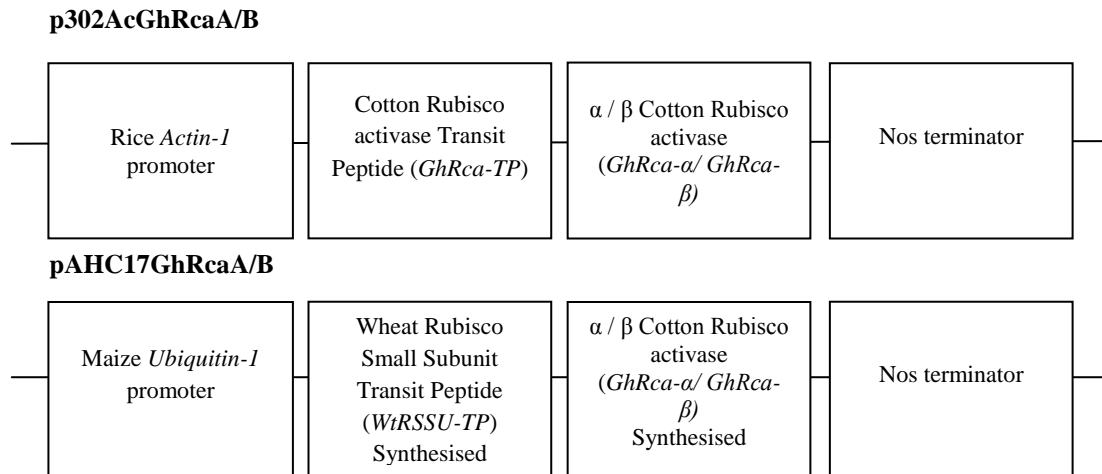


Figure 3.3. Diagram of the construct components for the expression of *GhRca- α* and *GhRca- β* . Two constructs were made to express each of the *GhRca- α* and *GhRca- β* genes in wheat. p302AcGhRcaA/B constructs contain the Rice *actin-1* promoter, and the Cotton Rca transit peptide (*GhRca-TP*). pAHC17GhRcaA/B constructs contain the Maize *ubiquitin-1* promoter, and the Wheat Rubisco small subunit transit peptide (*WtRSSU-TP*).

3.2.4 Biolistic transformation of wheat

Biolistic transformation was used to introduce the constructs described in Figure 3.3 into wheat (*Triticum aestivum* L. cv. Cadenza). The transformation was carried out by the Transformation Group at Rothamsted Research using a standard protocol (Sparks & Jones, 2009). The protocol involved using submicron gold particles coated with plasmid DNA which were bombarded into regenerative wheat tissue by means of an acceleration device under a partial vacuum (Sanford *et al.*, 1993). The regenerative tissue used here was embryogenic callus from immature wheat scutella. Co-bombardment with a plasmid (pAHC20) providing herbicide resistance (the Basta herbicide resistance (*bar*) gene) was performed, to allow selection in the tissue regeneration stages. Embryos were regenerated on plates containing media supplemented with growth hormones. Plantlets (with both roots and shoot) were transferred into culture boxes and finally into Rothamsted Prescription Mix compost in the glasshouse as before (Figure 3.4). Transgenic lines are named with a bombardment number, a replicate number and a plant number.

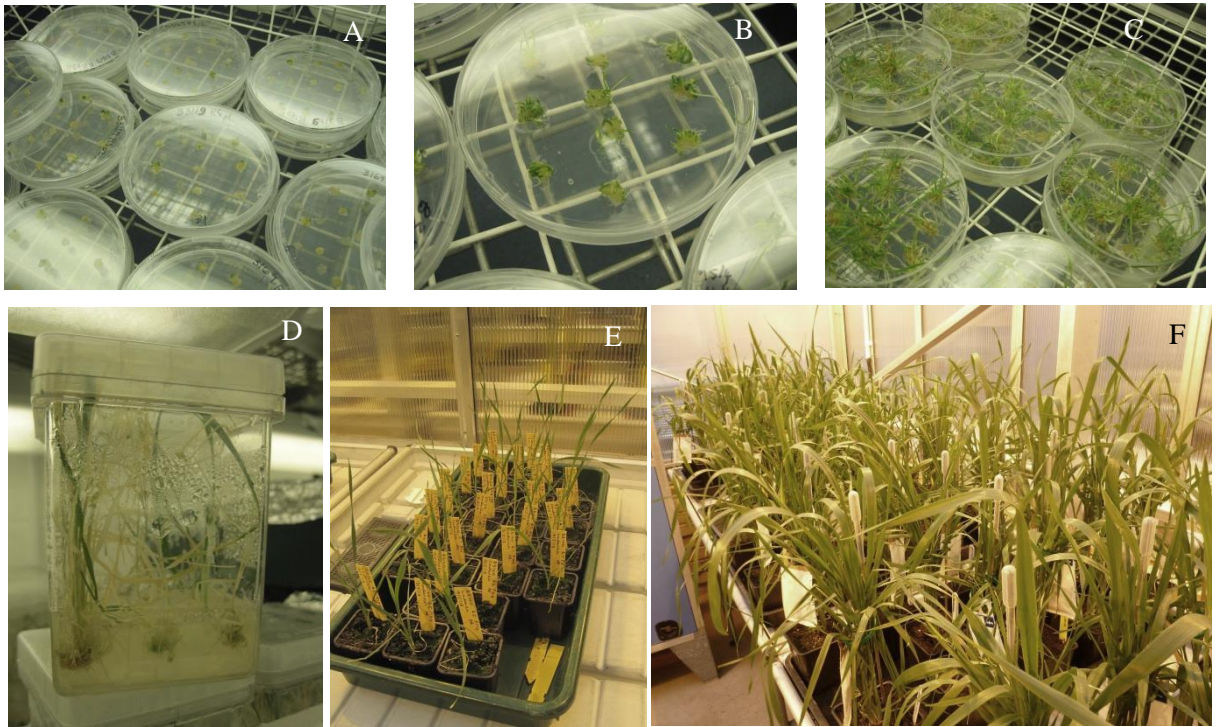


Figure 3.4. Photographs of the plant regeneration stages during biolistic wheat transformation. Photographs show wheat embryonic tissue prior to bombardment (A), regeneration, greening and root/shoot development (B- D), and regenerated wheat plants (E- F).

3.2.5 Gene presence and expression in transgenic wheat plants

Positive and negative transformants were screened by DNA extraction and PCR. A 96-well plate based system was used for high-throughput DNA extraction (based upon a protocol from Van Deynze *et al.* (2006)). Leaf tissue samples 5 cm long were taken from young leaves of three to four week old plants, placed directly into deep well blocks (Life Technologies, Paisley, UK) and freeze dried for two days. Two 5 mm ball bearings were added to each well and the leaf material was ground using a TissueLyser (Retsch MM200, TissueLyser, Qiagen, Manchester, UK) for two 30 s intervals. Extraction buffer (100 mM Tris-KOH, pH 9.5, 1 M KCl, 10 mM EDTA, 7.5 g L⁻¹ PVP-40 and 3.6 g L⁻¹ NaHSO₃) was added to each well (600 µL) using a multidropper (Multidrop DW, Thermo Fisher Scientific Inc., Hemel Hempstead, UK) and the plate was inverted to mix. The plates were incubated at 65°C for 1 hr in a heated shaker (Titramax 1000, Heidolph, Saffron Walden, UK) and then spun at 50 x g for 1 min to remove material from the lid.

200 μ L of KAc (5 M potassium acetate, pH 5.8, 11.5% glacial (v/v) acetic acid) was added to each well and the plate was inverted by hand before being centrifuged at 100 x *g* for 10 min.

300 μ L of the supernatant containing DNA was transferred into blocks containing 165 μ L of chilled isopropanol (-20°C) and left at room temperature for 10 min. DNA was pelleted by centrifugation at 100 x *g* for 10 min. The supernatant was poured off, 500 μ L of 70% ethanol was added to each well, and the plate was inverted by hand. The plates were centrifuged at 100 x *g* for 5 min and the supernatant discarded. DNA pellets were dried at 40°C for 30 min before being resuspended in 200 μ L TER (10 mM Tris, 0.1 mM EDTA, with 0.05 mg mL⁻¹ pancreatic RNase), and incubated at 50°C for 1 hr.

PCR to check for the presence of the *GhRca* genes was completed (Table 3.2). PCR was also completed using primers for the Rubisco Small Subunit (*RSSU*) gene, as a control to indicate that the DNA was intact. PCR was completed in 20 μ L reactions (as per manufacturer's instructions; GoTaq DNA Polymerase, Promega, Southampton, UK), with 4 μ L of DNA. PCR conditions for Rca primers were 95°C for 2 min followed by 40 cycles of 95°C for 30 s, 60°C for 70 s and 72°C for 1 min, with a final extension step at 72°C for 1 min. The PCR conditions for the SSU primers were 95°C for 2 min followed by 40 cycles of 95°C for 10 s, 64°C for 10 s and 72°C for 1 min, with a final extension step at 72°C for 1 min.

Table 3.2. Primer sequences for PCR DNA testing of transgenic plants.

	Primer sequences
p302AcGhRcaA/B	
F- p302Gh_F	TTT CTG CTG CTT CGT CAG GCT
R- p302Gh_R	CCA TAC GAC CGT CAC GGA TGA
pAHC17GhRcaA/B	
F- JS_activase	AAG CTC ATC AGG CAA CGC TAC C
R-nos R3	CCT GTT GCC GGT CTT GCG ATG ATT
SSU primers	
F- SSUpro_1F7500	CGG CTC TGT TTG GAT GTG TCC T
R- SSUpro1_R8650	CCT GCC CAT CGT GAC CAG CC

To evaluate the expression of *GhRca* in the wheat transgenic plants, 10 cm long sections of the youngest fully expanded leaf were collected from 9 week old plants, 4 hr after the start of the light period. Samples were placed in 1.5 mL Eppendorf tubes and stored at -80°C prior to RNA extraction. RNA extractions for

qRT-PCR were completed using a modified hot phenol method (Shinmachi *et al.*, 2010, Verwoerd *et al.*, 1989). In the first extraction, 1 mL of hot (80°C) 1:1 Phenol/ Extraction buffer (0.1 M Tris-HCl, pH 8.0, 0.1 M LiCl, 1% (w/v) SDS and 10 mM EDTA) and 0.5 mL Chloroform/Isoamylalcohol (IAA; 24:1) was added to leaf samples which had been ground in liquid nitrogen. Samples were centrifuged for 5 min at 13, 000 x g at 4°C, the aqueous phase was collected and an equal volume of Chloroform/IAA was added and centrifuged as before. One volume of 4 M LiCl was added to precipitate the RNA with overnight incubation at 4°C. Samples were centrifuged for 30 min at 13,000 x g at 4°C, the supernatant was removed and the pellet was washed with 70% (v/v) ethanol in a 5 min centrifugation at 13, 000 x g. The pellet was dried and then DNase treated with RQ1 RNase-Free DNase, as per the manufacturer's instructions (Promega, Southampton, UK). Two phenol/chloroform/IAA (25:2:1, Tris-HCl, pH 8.0, 1 mM EDTA) extractions were completed, samples were centrifuged for 5 min as before and the aqueous phase was collected. 3 M NaOAc (one-tenth of the volume of the aqueous phase) and 100% ethanol (2.5 times the volume of the aqueous phase) were added to precipitate the RNA and the samples were left overnight at -20°C. Samples were then centrifuged for 5 min as previously, the supernatant was discarded, and the pellet washed with 70% (v/v) ethanol (as above), prior to being dried and dissolved in DEPC treated water (Sigma-Aldrich Company Ltd., Gillingham, UK).

The RNA concentration was determined with a Nanodrop spectrometer (Nanodrop 2000c, Thermo Fisher Scientific Inc., Hemel Hempstead, UK) and run on a 1% (w/v) agarose gel to check for quality. A sub-sample of 1 µg of RNA was used for cDNA synthesis, using Superscript III as per the manufacturer's instructions (Life Technologies Ltd. Paisley, UK).

For qRT-PCR a 1: 10 dilution of cDNA was used with SYBRGreen (Platinum® SYBR® Green qPCR SuperMix-UDG w/ROX, Life Technologies, Paisley, UK), in 15 µL reactions, as per the manufacturer's instructions. Primer pairs specific to the *GhRca* transgene of each plant were used for qRT-PCR (Table 3.3), qRT-PCR conditions were: 50°C for 2 min, 95°C for 10 min, followed by 40 cycles of 95°C for 15 s and 60°C for 1 min. Melt curves were also completed: 95°C for 15 s, 60°C for 1 min and 95°C for 15 s (7500 Real Time PCR machine, Applied Biosystems, Life Technologies, Paisley, UK).

Primer efficiency was analysed (based upon a cDNA dilution series) and primer pairs with efficiencies between 85 and 115% were used. The mean primer efficiency was estimated using the linear phase of all individual reaction amplification curves (Ramakers *et al.*, 2003) and calculated using the LinRegPCR package (Tuomi *et al.*, 2010). The Tonoplast Intrinsic Protein (*TIP*) and Eukaryotic Translation Initiation Factor (*eIF4E*) genes were used for the normalized relative quantification of expression. The normalized relative quantity (NRQ) of expression was calculated in relation to the cycle threshold (CT) values and the primer efficiency (E) of the target gene (X) and the normalizing reference gene (N), based on (Rieu & Powers, 2009): $NRQ = (E_X)^{-CT, X} / (E_N)^{-CT, N}$

Five transgenic wheat lines of each construct pair were investigated for expression levels. A minimum of three DNA positive plants was tested for each line.

Table 3.3. Primers for qRT-PCR of the cotton Rca transgenes and control genes (*TIP* and *eIF4E*) in transgenic p302AcGhRcaA/B and pAHC17GhRcaA/B plants.

	Primer sequences
TIP	
F- prTYW399_TIP41L_L_359	TGC AGC AAA ATG GAA ATT CA
R- prTYW400_TIP41L_R_475	TGC GTA GCA TCT TGG TTC AG
eIF4E	
F- eIF4E-1F	TGG CAA GCA GTG GAA GGA GT
R- eIF4E-1R	TCA CGG GAT CAA ACG GTG TAG
p302AcGhRcaA	
F- P302qRT AF	TAT GGC AAA GCA GCA CAA CAA GTT GGG
R- P302qRT AR	AGT GCA AGT TCC ATC ATC ACT TCT AGC C
p302AcGhRcaB	
F- P302qRT BF	ATG GAT CGG AGA GGT AGG AGT CAA TAG
R- P302qRT BR	CTC CAA CAG CTT CTC AAT GGT CAT CGT A
pAHC17GhRcaA	
F- pAHCqRT A F	CAA GTG GGC GTC CCT GTT CCT G
R- pAHCqRT A R	CAG AAT TGG TAC GTG CAG GTG CCA T
pAHC17GhRcaB	
F- pAHCqRT B F	TCA ATC GAT TTC TTC GGG GCT CTC AGA
R- pAHCqRT B R	AGT TAA CCA GCT TCT TGC CGA CAG AGT

3.2.6 Cotton Rubisco activase in transgenic wheat plants

3.2.6.1 Western blot analysis of cotton and wheat Rubisco activase

To determine if the wheat and cotton Rca isoforms could be distinguished by western blot analysis, samples of 5 cm of wheat and cotton leaf tissue were ground in a mortar and pestle in 0.5 mL ice cold protein extraction buffer (50 mM Tricine-NaOH, pH 8.0, 10 mM EDTA, 1% (w/v) PVP-40, 20 mM 2-

mercaptoethanol, 1 mM PMSF and 10 μ M leupeptin) with 10 mg sand. Samples were centrifuged for 3 min at 14,000 $\times g$ at 4°C. A sub-sample of 50 μ L of supernatant was added to 50 μ L of 2x SDS-loading buffer (5% (w/v) SDS, 30% (w/v) sucrose, 0.1% (w/v) bromophenol blue and 0.25 M DTT) and incubated at 95°C for 4-5 min to denature proteins.

Total soluble protein concentration (TSP) was determined in the supernatant using Bradford reagent (Bradford, 1976). Samples were diluted to 1 mg mL⁻¹ TSP with 1:1 extraction buffer and SDS loading buffer. Samples were run on 8-16% and 10% SDS-polyacrylamide gels (Precise Protein gels, Thermo Scientific, Hemel Hempstead, UK) together with a standard protein molecular weight marker (Precision Plus Protein™ Dual Color Standards, Bio-Rad, Hercules, USA). Polypeptides were electrophoretically transferred to PVDF membrane using an iBlot Gel Transfer Device (Thermo Fisher Scientific Inc., Hemel Hempstead, UK). The membrane was then blocked with 4% Blotto (4% (w/v) skimmed milk powder in TBS (50 mM Tris, pH 7.5, 150 mM NaCl)) and then incubated with the Primary Antibody overnight (Anti-Rca protein, produced in rabbit against cotton Rca, (Salvucci, 2008), 1:10000 in 0.5% (w/v) Blotto). After six 15 min washes in TBST (0.05% (v/v) Tween-20 in TBS), the membrane was then incubated with Secondary Antibody (Anti-rabbit IgG Alkaline Phosphatase antibody, produced in goat, 1:3000 in 0.5% (w/v) Blotto) for 2 hr and washed four times in TBST, for 15 min per wash. For detection, the membrane was rinsed in alkaline phosphatase reaction buffer (0.1 M Tris-HCl, pH 9.5, 0.1 M NaCl and 5.0 mM MgCl₂) and immersed in detection solution (Nitro blue tetrazolium (NBT), 5-bromo-4-chloro-3-indolyl-phosphate (BCIP) stock solution, Roche, Welwyn Garden City, UK; 175 μ L in 10 mL of alkaline phosphatase reaction buffer).

For Coomassie staining, after electrophoresis, the gel was rinsed in water and then immersed in Bradford reagent (Bradford, 1976) until the protein bands became visible. The Bradford reagent was replaced with water and rinsed several times until the background colour was clear.

The membranes and gels were photographed using a G:BOX system (Syngene, Cambridge, UK) and images were analysed using Image Studio Lite (LI-COR, Lincoln, USA) and SigmaPlot 12.5 software (Systat Software Inc., San Jose, USA).

3.2.6.2 Western blot analysis of Rubisco activase in transgenic wheat plants

The Rca amount in transgenic wheat plants was determined by western blotting using E-Page gels (Novex, 48-well 8% E-Page gels, Life Technologies, Paisley, UK) to allow high-throughput of samples. Wheat leaf tissue samples from p302AcGhRcaA/B transgenic lines were ground with a mortar and pestle in 0.8 mL ice-cold protein extraction buffer (described above). Samples were centrifuged for 3 min at 14,000 $\times g$ at 4°C. A sub-sample of 52 μL of supernatant was added to 20 μL E-Page Loading Buffer 1 (10 mM Tris-HCl, pH 7.5, 1 mM EDTA, 0.005% Bromophenol blue, 0.005% Xylene cyanol FF) and 8 μL Novex Reducing Agent (500 mM DTT, Novex, NuPAGE). Samples were incubated at 95°C for 4 min to denature proteins.

TSP concentration was determined in the supernatant by the Bradford method (Bradford, 1976), using BSA as a standard. Samples were diluted to 1 mg mL⁻¹ and 2 μg TSP of sample was loaded in each lane. Samples were run on 48-well precast gels, on an E-Base platform (E-Base™ Integrated Device & E-Holder™ Platform, Life Technologies, Paisley, UK). Gels were western blotted and visualised as above. Five 48-well gels were used to allow a minimum of nine plants from each line to be tested in triplicate. Western blots were visualised and analysed as above but with the inclusion of a dilution series from a wild-type leaf extract providing a standard curve for quantification of the relative amounts of protein in each sample.

Although enabling higher throughput, the E-Page gels did not enable the two wheat Rca isoforms to be distinguished. To achieve this, leaf extracts prepared, as above, in SDS-loading buffer were run on hand-cast 11%, acrylamide gel (10 x 7.5 cm). Gels were cast (based upon Laemmli (1970)) with 1 mm spacers and run in a Mini Trans Blot cell (Bio-Rad, Hercules, USA). Gels consisted of a resolving gel to ~1.5 cm from the top of the glass plate (11% (v/v) Acrylamide, 0.2% (v/v) Bisacrylamide, 0.4 M Tris, 0.03 M HCl, 1% (v/v) SDS, 0.1% (v/v) TEMED and 0.6% (v/v) Ammonium persulfate) and a stacking gel (5% (v/v) Acrylamide, 0.2% (v/v) Bisacrylamide, 0.05 M Tris, 0.03 M H₂SO₄, 1% (v/v) SDS, 0.1% vTEMED and 1.2% (v/v) Ammonium persulfate) in which the comb was placed. The resolving gel layer was overlaid with isobutanol whilst setting to ensure the gel had a level surface. Gels were run at 100 V until the dye front reached the base of the gel (~1 h) using running buffer containing 0.04 M Tris, 0.04 M

borate and 2% (w/v) SDS. Western Blots were completed and analysed as above, with the difference between the Rca amount between DNA positive and true negative samples being calculated. Five transgenic lines from each construct were investigated for protein expression with a minimum of nine DNA positive plants tested per line.

3.2.6.3 Isoelectric focusing of Rubisco activase in transgenic wheat plants

IEF was used in an attempt to resolve cotton and wheat Rca in samples from the transgenic wheat plants. Transgenic wheat leaf protein samples prepared as above in SDS-loading buffer were diluted to $2 \mu\text{g } \mu\text{L}^{-1}$ TSP and combined 1:1 with 50% (v/v) glycerol. Volumes corresponding to 5, 10 and 15 μg of total soluble protein were loaded per well. Samples were run on native Criterion Precast IEF gels (pH 5- 8, 1 mm thick, 18-well gels; Bio-Rad, Hercules, USA), using the Criterion Cell running system. Gels were run at 100 V for 60 min, 250 V for 60 min and then 500 V for 30 min.

The same system was trialled with denatured samples of wild-type wheat and cotton. Tissue was ground in protein extraction buffer as above, centrifuged for 3 min at 4°C at 14, 000 x g and diluted in rehydration buffer (7 M Urea, 2 M thiourea, 2% (w/v) CHAPS, 40 mM DTT, 0.5% (v/v) IPG ampholytes and a few grains bromophenol blue) to $1.6 \mu\text{g } \mu\text{L}^{-1}$ TSP, before adding glycerol to a concentration of 10% (v/v).

The first dimension Criterion gel was divided into sections. A section of the gel was western blotted directly using the iBlot system described above. A second section of the gel was fixed before staining by immersion in 20% (v/v) trichloroacetic acid (TCA). The gel was then washed with 10 mL of a solution containing 10% (v/v) acetic acid and 30% (v/v) methanol, before staining with Bradford Reagent. For running a second dimension gel, the relevant lanes were cut out of the first dimension gel and soaked in equilibration buffer (0.0541 M Tris, 0.0267 M H₂SO₄, 2.3% (v/v) SDS and 5% (v/v) 2-mercaptoethanol) for 15 min. The lane of the first dimension gel was inserted between the glass plates at the surface of the second dimension gel (11% resolving gel, without the stacking gel). Agarose (0.5% (w/v) containing bromophenol blue) was used to seal the gel strip to the second dimension gel. Gels were run at 100 V until the dye front reached the bottom of the gel (~2 h) and then stained or western blotted as above.

As an alternative method, denaturing IEF gels (1 mm thick, 10-well, 10 x 7.5 cm) were hand-cast as in Ploegh (1995). Gels contained: 9.1 M urea, 2% (v/v) Triton X-100, 2% (v/v) pH 4-7 ampholytes (GE Healthcare, Little Chalfont, UK), 30% (v/v) acrylamide, 1.6% (v/v) bisacrylamide, 0.2% (v/v) ammonium persulfate and 0.1% (v/v) TEMED. Samples were extracted (50mM Tris-HCl, pH 8.0, 1% (w/v) PVP-40, 10 μ M leupeptin and 1 mM PMSF) and diluted in IEF solubilisation buffer (9.5 M urea, 2% (v/v) Triton X-100, 2% (v/v) pH 4-7 ampholytes and 5% (v/v) 2-mercaptoethanol). The Mini Trans Blot (Bio-Rad, Hercules, USA) casting and running system was used. Gels were run at 100 V for 1 hr, 200 V for 1 hr and 455 V for 30 min. Gel sections were directly western blotted or fixed and stained as above.

Following attempts with denaturing gels denaturing IEF gel strips were used to enable better separation of Rca in the transgenic samples. To run leaf protein samples on denaturing IEF gel strips, leaf material (2 mL Eppendorf tubes two-thirds full) was ground in liquid nitrogen, was extracted in 1 mL of Solution I (10% (w/v) TCA and 0.07% (w/v) DTT in acetone). This was vortexed at maximum speed for 2 min and precipitated at -20°C for at least 1 hr. Samples were centrifuged at 15,000 x g for 10 min at 4°C and the supernatant was discarded. The pellet was re-suspended in 1 mL of solution II (0.07% (w/v) DTT in acetone), by vortexing, and centrifuged at 15,000 x g for 10 min at 4°C . The supernatant was discarded and the pellet was washed twice more before being dried in the fume hood under a stream of nitrogen gas. The pellet was re-suspended in 500 μ L of rehydration buffer (7 M urea, 2 M thiourea, 2% (w/v) CHAPS, 40 mM DTT and 0.5% (v/v) IPG ampholytes, pH 4-7). The sample was vortexed for 5 min and centrifuged at 13,000 x g at room temperature for 5 min. The protein concentration of the samples was determined with Bradford reagent, using BSA as a standard. Aliquots were flash frozen in liquid nitrogen and stored at -80°C until use.

Samples were diluted with rehydration buffer as needed; to 50 or 100 μ g TSP per IEF strip (Immoblino Dry Strip, pH 4-7, 13 cm, GE Healthcare, Little Chalfont, UK) in a total volume of 250 μ L. The gel strip was covered with DryStrip cover oil and the gel strips were rehydrated for 13.5 hr in the IPGphor (Pharmacia Biotech, Amersham; GE Healthcare, Little Chalfont, UK). Strips were run until they had reached 16000-20000 Vhr, i.e. 500 V for 1 hr (500 Vhr), 1000 V for 1 hr (1000 Vhr) and 8000 V for 2 hr (16000 Vhr).

Gel strips were frozen at -80°C for future use. Prior to being run in a second dimension gel the frozen gel strips were equilibrated for 15 min on rocking platform with equilibration buffer (50 mM Tris-HCl, pH 8.8, 6 M urea, 2% (w/v) SDS, 30% (v/v) glycerol and a few grains of Bromophenol blue) containing 1% (w/v) DTT, and then for a further 15 min in equilibration buffer containing 4% (w/v) iodoacetamide. A resolving gel of 18 x 16 cm was used with 1.5 mm spacers (11% (v/v) Acrylamide, 0.2% (v/v) Bisacrylamide, 0.4 M Tris, 0.03 M HCl, 1% (v/v) SDS, 0.1% (v/v) TEMED and 0.6% (v/v) Ammonium persulfate). Gel strips were placed onto the surface of the resolving gel with the positive end of the strip was on the left hand side of the gel, and 10 μL of marker (Precision Plus Protein™ Dual Color Standards, Bio-Rad, Hercules, USA) was applied to small piece of filter paper and inserted between the glass plates so that it touched the gel surface at the left hand side of the gel. Gels were run (25 mM Tris, 192 mM glycine and 0.1% (v/v) SDS) at 30 mA for 4 hr or until the dye front had reached the bottom of the gel (SE600 series, Standard Dual Cooled Vertical Unit; Hoefer, Holliston, MA, USA). Western blots were completed using the equivalent equipment (Hoefer, Holliston, MA, USA) and transfer buffer containing 50mM Tris and 50mM Boric acid. Protein transfer was completed at 72 V for 1 hr 40 min at 4°C ; western blots were completed and detected as before.

3.2.7 Photosynthetic analysis of transgenic plants

3.2.7.1 Temperature response of photosynthesis in wheat

Net CO_2 assimilation was determined at a range of temperatures in glasshouse grown 4- 5 week old plants of Cadenza wheat using a LI-6400XT photosynthesis system with leaf chamber fluorometer 6400-40 (LI-COR, Lincoln, USA). Three plants were measured at each of eight temperatures. Photosynthesis measurements were made on the penultimate leaf (immediately below the flag leaf). The room temperature was set at 25°C day and 20°C night. For temperatures up to 35°C , the room temperature was kept at 25°C , but for 37.5°C and 40°C , the room air conditioning was turned off to enable the LI-COR block temperature to increase. A-Ci curves were measured on three plants simultaneously using three LI-COR 6400XT, at: 400, 300, 200, 100, 400, 500, 700, 1000 and 1200 $\mu\text{L L}^{-1}$ reference CO_2 . A-Ci data for each leaf was modelled using A-Ci Curvefitting_10.1 (<http://landflux.org/Tools.php>). Mean values of A_j (the electron transport-limited rate of CO_2 assimilation) from three leaves at each temperature were

derived using this curve fitting program for a CO₂ concentration of values taken from the model output at 210 µL L⁻¹ CO₂.

3.2.7.2 Effect of high temperature on photosynthesis of transgenic wheat plants

The temperature response of glasshouse grown transgenic wheat plants, together with their respective control lines (plants which had gone through the transformation process but which were negative for the transgene), were compared. Plants of each transgenic line were screened four weeks after germination for the presence of the transgene and all positive plants, and a maximum of three negatives, were kept as a control for each individual line. Each plant was numbered and each line assigned an identifying letter (Table 3.4). A Genstat randomisation prepared by a statistician (Stephen Powers, Rothamsted Research) was used to arrange plants and lines across the glasshouse benches with a 25 cm gap between pots (Figure 3.5). After four weeks of growth (16 hr days, 25°C day/ 20°C night), the temperature was increased (to 35°C day/ 30°C night) for a week before measuring photosynthesis, to allow plants to acclimate to the increased temperature. The supplemental lighting was turned off when the temperature was increased to prevent the plants from being scorched. Plants were well watered throughout.

Photosynthesis was measured on the youngest fully expanded leaf of each plant. All plants were at Zadoks growth stage 4- 5, while the flag leaf sheath was extending. Measurements were accomplished with the LI-6400XT fluorometer (LI-COR, Lincoln, USA) at the room temperature of 35°C.

Measurements were started 4 hr after the beginning of the photoperiod and were concluded within 7 hr. The plants were well-watered throughout. The humidity of the room was elevated by ensuring the floor and benches were wetted regularly. LI-COR measurements were taken at a block temperature of 35°C, 400 µL L⁻¹ CO₂, 1500 µmol photons m⁻² s⁻¹ and 50- 70% relative humidity.

The leaves were allowed to acclimate in the chamber for 10 min prior to the measurements being taken. LI-COR IRGAs were always matched immediately before taking every single measurement, and three consecutive readings were taken to provide a mean value for each data point. The leaf width at either end of the LI-COR chamber was measured for accurate area calculation, as in most cases the leaf was not

wide enough to completely fill the chamber. Photosynthetic measurements were completed on two consecutive days with three LI-CORs being operated simultaneously to ensure all the plants of each construct pair were completed in the same day. Plants were measured at random through the day to avoid any diurnal bias when comparing lines.

Grain weight, ear number and straw biomass were measured after the plants had matured. Weight and photosynthesis data was analysed with use of Residual Maximum Likelihood in GenStat, as there were different numbers of DNA negative and positive plants per line, which precluded the application of ANOVA. A linear mixed model was fitted to the data, to test for the main effect of Cadenza compared to the transgenic lines overall, the effect of the negative control line, and then main effects and interaction of line and type (Null vs Positive) for the lines with both types present. All these are fixed terms in the linear mixed model. The use of three different LI-CORs was accounted for by including this as a random term in the linear mixed model.

Table 3.4. Transgenic lines from p302AcGhRcaA/B and pAHC17GhRcaA/B grown for measurement of photosynthetic performance following an elevated temperature treatment. Letters were assigned to each different line (lines are numbered as bombardment, replicate and plant) for illustration in the randomised pot layout of Figure 3.5, and the numbers of positive and negative plants of each line tested, are shown.

	DNA positive (+) /null (-)	Bombardment	Rep	Plant	Number of Plants
p302AcGhRcaA					
A	Parent (Cadenza)				4
B	Negative	3123	1	1	2
C	+	3123	3	2	2
C'	-				2
D	+	3123	6	1	3
D'	-				3
E	+	3137	3	1	5
E'	-				3
p302AcGhRcaB					
F	Negative	3130	1	1	4
G	+	3130	4	3	6
G'	-				3
H	+	3130	4	4	9
H'	-				1
I	+	3130	4	5b	9
I'	-				1
J	+	3136	2	3	6
J'	-				3
K	+	3136	2	4	7
K'	-				2
pAHC17GhRcaA					
L	Parent (Cadenza)				5
M	Negative	3147	2	1	6
N	+	3147	3	1	6
N'	-				2
O	+	3147	5	1	7
O'	-				3
P	+	3147	6	2	6
P'	-				3
Q	+	3147	7	1	6
Q'	-				3
R	+	3168	6	2	7
R'	-				2
pAHC17GhRcaB					
S	Negative	3148	1	1	6
T	+	3148	3	1	3
T'	-				2
U	+	3148	5	1a	4
U'	-				2
V	+	3148	9	5a	4
V'	-				3
W	+	3169	6	2a	5
W'	-				3

A

	1			2		3		4		5		6		7					
	56 I			33 G		38 H		39 H		12 D		60 J		51 I					
8		9	10		11	12		13	14		15	16		17	18	19	20		21
7 C		31 G	23 E'		3 A	67 K		46 H	29 G		26 F	8 C		50 I	16 D'		65 J'	34 G	66 J'
	22			23			24		25			26		27			28		
	10 C'			70 K			27 F		43 H			2 A		64 J'			62 J		
29		30	31		32	33		34	35		36	37		38	39	40	41		42
72 K		6 B	5 B		47 H'	24 E'		48 I	21 E		14 D'	17 E		58 J	13 D	20 E	15 D'		4 A
	43			44		45		46		47		48		49					
	22 E'			35 G'		57 I'		30 G		52 I		63 J		45 H					
50		51	52		53	54		55	56		57	58		59	60	61	62		63
73 K		18 E	54 I		59 J	32 G		1 A	42 H		44 H	28 F		74 K'	37 G'	49 I	68 K		55 I
	64			65		66		67		68		69		70					
	40 H			75 K'		71 K		9 C'						19 E					36 G'
71		72	73		74	75													
41 H		61 J	53 I		11 D	25 F													

B

	1			2		3		4		5		6		7		8						
	39 Q			33 P		37 P'		82 W		23 O		80 V'		57 S		49 R						
9		10		11	12	13	14		15	16		17	18	19	20	21	22		23			
46 Q'		59 S		84 W	32 P	30 P	54 R		6 M	43 Q		51 R	71 U		8 M	77 V	16 N	45 Q'	81 W			
	24			25		26		27		28		29		30		31						
	18 N'			61 S		47 Q'		65 T		13 N		66 T'		36 P'		15 N						
32		33	34		35	36		37	38		39	40		41	42	43	44	45	46	47		
78 V'		70 U	31 P		60 S	2 L		21 O	17 N		52 R	9 M		76 V	83 W		85 W	3 L	44 Q	28 O'	34 P	
	48			49		50		51		52		53		54		55						
	7 M			35 P		75 V		88 W'		67 T'		11 M		68 U		25 O						
56		57	58		59	60		61	62		63	64		65	66		67	68		69	70	71
55 R'		12 N	53 R		5 L	40 Q		10 M	24 O		62 S	48 R		63 T	58 S		79 V'	1 L		29 O'	64 T	72 U'
	72			73		74		75		76		77		78		79						
	73 U'			22 O		56 R'		27 O'		69 U		26 O		14 N								50 R
80		81	82		83	84		85	86		87	88										
87 W'		74 V	41 Q		86 W'	4 L		20 O	19 N'		42 Q	38 P'										

Figure 3.5. Randomised layout of transgenic plants for photosynthesis measurements following an elevated temperature treatment in the glasshouse. Layout of p302AcGhRcaA/B plants (A); layout of pAHC17GhRcaA/B plants (B). Pot numbers are shown in the top right of each position. The plant number and the letter assigned to each transgenic line are shown at the bottom left of each position.

3.3 Results

3.3.1 Engineering cotton Rubisco activase into wheat

It was critical to test whether cotton Rca would successfully activate wheat Rubisco prior to transformation being attempted. This was found to be the case *in vitro*, indicating that the foreign Rca would perform its expected activity *in planta* in wheat (Figure 3.6). The activity of Rubisco in its ER (uncarbamylated Rubisco, 'E', to which RuBP, 'R' is bound) and ECM forms (carbamylated Rubisco, 'C' stabilised by Mg^{2+} , 'M') was also measured through the course of the assay for comparison. The residues (K311 and V314) indicated by Li *et al.* (2005) as conferring substrate recognition in Rca are both conserved in cotton and wheat (Figure 3.11).

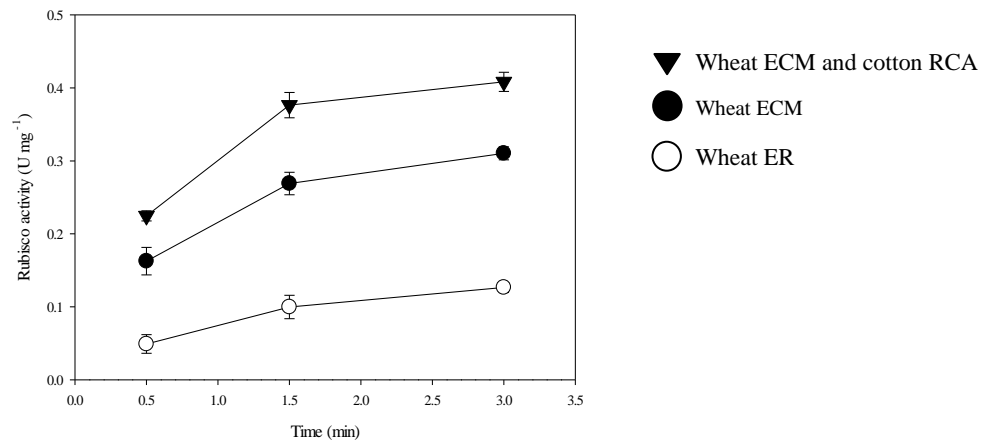


Figure 3.6. Wheat Rubisco activity following incubation of the inhibited enzyme with cotton Rca. ER activity (white circles), ECM activity without RuBP but with Rca (black circles), with cotton Rca (inverted black triangles), relative to the Rubisco amount.

To demonstrate the activity of the two promoters being used to express *GhRca* in wheat (*Rice actin-1* and maize *ubiquitin-1*) blue colouration in the GUS assay was monitored. Colouration was seen at each stage of plant development tested up to flowering (Figure 3.7). Colour intensity decreased over developmental time (possibly due to reduced infiltration of the assay mix into the leaf tissue), but no difference was noted between the promoters, with both still showing expression.

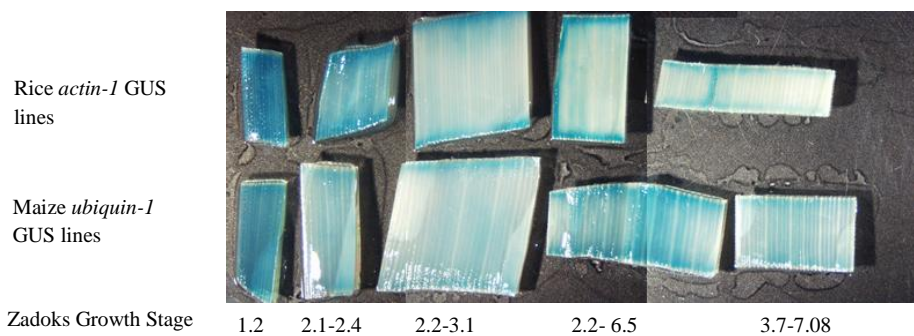


Figure 3.7. Representative sample of GUS stained leaf tissue at five different time points from *Rice actin-1*-GUS (top) and *Maize ubiquitin-1*-GUS plants (bottom).

Samples shown for each promoter are from the same plant over time, the range of Zadoks growth stages of the plants at each sampling time point are indicated. Leaf pieces are not representative of actual leaf width as leaves were cut up to fit into micro plate wells.

The cotton Rca α and β nucleotide and amino acid sequences (Salvucci *et al.*, 2003) in the p302AcGhRcaA/B constructs (using the cotton Rca transit peptide) are shown in Figures 3.8 and 3.9. There are three separate genes encoding Rca in cotton, two encode α isoforms and one the β isoform.

There are nine amino acid differences between the two α isoforms; the gene and sequence used here is that which was expressed and characterised in relation to ATPase activity and temperature response in Salvucci *et al.* (2003).

For development of the pAHC17GhRcaA/B constructs for expression of the cotton Rca with the WtRSSU-TP whether or not to include the amino acids 'RMQ' found at the end of the transit peptide was considered. Alignment of *WtRSSU* genes from Sasanuma (2001) show *WtRSSU-TP* sequences of differing lengths but all show the same end to the first exon of the gene. The *WtRSSU-TP* ligated to *GhRca- α* is shown in Figure 3.10. Salvucci *et al.* (2003) purified cotton Rca protein and determined the amino acid sequence by Edman degradation analysis, showing AEEKE (in *GhRca- α*) to be at the start of the mature polypeptide. Hence, although ChloroP predicts AAEKE to be the start AEEKE was used as the start of the mature peptide in these constructs (Table 3.5). ChloroP predicted cleavage of the WtRSSU-TP codon optimised sequence in the pAHC17GhRcaA/B constructs before the 'RMQ' amino acids.

For the pAHC17GhRcaA/B constructs, the Kozak (translation initiation) sequence (ACCATGG; Kozak (1984)) was also added at the start of the genes and the nucleotide sequences were codon optimised for expression in wheat. The nucleotide changes to use codons more commonly found in wheat left the amino acid sequences unchanged: in the *GhRca- β* mature peptide sequence 237 of 1140 bases were altered, in the *GhRca- α* mature peptide sequence 276 of 1260 bases were altered.

When compared, the cotton and wheat α and β nucleotide and amino acid sequences showed small differences in length (Table 3.6), mostly due to differences at either end of the mature peptide sequence. The pairwise identity when considering the amino acid sequence from cotton, with that from all three wheat genomes, is 87.7% for TaRca2- α , 94.1% for TaRca1- β and 91.9% for TaRca2- β .

Kurek *et al.* (2007) indicated that one amino acid substitution alone (T274R) was sufficient to improve thermal tolerance of Rca in *Arabidopsis* and a further two pairs of three amino acid substitutions (F168L, V257I, K310N and M131V, V257I, K310N) resulted in a 10°C increase in stability. Some of these same residues differ between the two wheat genes and between wheat and cotton, whereas other residues considered to alter thermal tolerance in *Arabidopsis* are the same in wheat and cotton (Figure 3.11).

GhRca-α AGCCCGTCCCATGGCGGCTGCCGTCTCCACCATCGGTGCTGTCAACCGAGCACCGTTGAGT 61
GhRca-β AGCCCGTCCCATGGCGGCTGCCGTCTCCACCATCGGTGCTGTCAACCGAGCACCGTTGAGT 61

GhRca-α TTGA-TGGATCAGGTGCCGGAGCTTCTGCTCCAAGCTCAGCTTTCATGGGGAACAGCTTGA 122
GhRca-β TTGAATGGATCAGGTGCCGGAGCTTCTGCTCCAAGCTCAGCTTTCATGGGGAACAGCTTGA 122

GhRca-α AGAAAGTGAGCGCTAGGTTCAACAACACCAGGCAGGTTCCCTTCGGGAAGTTTTAAGGTGAT 183
GhRca-β AGAAAGTGAGCGCTAGGTTCAACAAC-ACGGCAAGGCTCCAGTGGGAAGTTTTAAGGTGAT 183

GhRca-α GGCGGCGGAAAAAGAGATAGACGAAGAGACACAGACCGAAAAGGACCGATGGAAGGGTGTG 244
GhRca-β GGCGGCGG---AAGAAATCGACGAAGACACACAGACCGACCAGGACCGATGGAAGGGTCTT 244

GhRca-α GCTTACGATATTTTCGGACGACCAACAAGACATTACTCGAGGGAAAGGGATGGTGGATTCCCT 305
GhRca-β GCTTATGATATCTCCGATGACCAACAAGACATTACCAGAGGGAAAGGTATGGTGCAGTCCAT 305

GhRca-α TGTCCAAGCTCCCATGAATGATGGAAGTCACTATGCTGTCATGAGTTCCTATGAATACCT 366
GhRca-β TGTCCAAGCTCCCATGAACGATGGTACTCACTATGCTGTCATGAGTTCCTATGAGTACAT 366

GhRca-α GCACCAAGGCTTTAAAACGTACAATTTGGACAACAACATGGATGGTTCCTACATTGCTCCT 427
GhRca-β TAGCCAAGGCCTTCGCACATACGACTTGGACAACAACATGGATGGATTCTACATTGCCCA 427

GhRca-α GCATTCATGGACAAGCTTGTGTTCACATCACCAAGAAGTTCATGTCCTCCCTAACATTA 488
GhRca-β GCTTTCATGGACAAGCTTGTGTTCACATCACCAAGAAGTTCATGACCTTCCTAACATTA 488

GhRca-α AGGTTCTCTAATCTTGGGTATTTGGGGAGGCAAAGGTCAAGGAAAATCTTCCAATGTGA 549
GhRca-β AGGTTCTCTTATCTTGGGTATTTGGGGAGGCAAAGGTCAAGGAAAATCTTCCAATGTGA 549

GhRca-α GCTTGTGTTTGCCAAGATGGGTATCAACCCCATCATGATGAGTGCCGGAGAAGTGGAAAGT 610
GhRca-β GCTTGTCTTTTGCCAAGATGGGAATCAACCCCATTATGATGAGTGCCGGAGAATTGGAAAGT 610

GhRca-α GGAAACGCCGGTGAACAGCCAAGTTGATCAGGCAAAGGTACCGTGAAGCTGCCGACATAA 671
GhRca-β GGGAAACGCCGGAGAACCAGCCAAGTTGATCAGGCAAAGGTACCGTGAAGGCCGCCGACATTA 671

GhRca-α TCAAAAAGGGCAAAATGTGCGCCCTCTTCATTAACGATCTCGATGCTGGTGCCGGTCGTAT 732
GhRca-β TCAAGAAAAGGGCAAAATGTGTTGCCCTCTTATCAACGATCTCGACGCTGGAGCCGGTCGTAT 732

GhRca-α GGGAGGAACCACCAATACACCGTCAACAACCAGATGGTTAATGCTACCCTCATGAACATC 793
GhRca-β GGGAGGAACCACACAATACACAGTGAACAACCAATGGTGAACGCCACACTCATGAACATC 793

GhRca-α GCCGATAACCCACCAACGTTCCAGCTCCCCGGTATGTACAACAAGGAAGGAACCCCGTAG 854
GhRca-β GCTGATAACCCACCAACGTTCCAGCTCCCCGGTATGTACAACAAGGAAGAGAACCCCTCGTG 854

GhRca-α TCCCCATTATCGTCACTGGTAACGATTTCTCCACACTGTATGCTCCTCTCATCCGTGACGG 915
GhRca-β TTCCGATCATTGTCACCGGTAACGATTTCTCCGACGCTGTACGCGCCGCTCATCCGTGACGG 915

GhRca-α TCGTATGGAGAAAATTTTACTGGGCACCAACTAGGGACGACCGTGTGGTGTGTTGCAAAGGT 976
GhRca-β TCGTATGGAGAAATTTTACTGGGCACCCACCAGGGAAGATAGGATCGGTGTTTGCACAGGT 976

GhRca-α ATTTTCAGGACCGACGGCATCCCAGATGAAGACATTGTTAAGCTCGTGCACACCTTCCCCG 1037
GhRca-β ATTTTCAGGACCGACAATGTTCCCGTTGATGACATTGTTAAGCTTGTGACACCTTCCCCG 1037

GhRca-α GCCAATCCATCGATTCTTCGGTGCCTTGAGGGCTCGGGTTTACGATGACGAAGTGAGGAA 1098
GhRca-β GCCAATCCATTGACTTTTTCGGTGCCTTGAGGGCCAGAGTTTACGATGACGAAGTGAGGAA 1098

GhRca-α ATGGATCAGTGATGTCGGAGTTGCAGGCGTAGGGAAGAAGTTAGTGAACCTCAAGGGACGGA 1159
GhRca-β ATGGATCGGAGAGGTTAGGAGTCAATAGTGTGGGAAAAGCTCGTGAACCTCAAGGGAAAGG 1159

GhRca-α CCTCCAACATTTGAGCAACCGAAAATGACCATTGAAAAGCTATTGGAATATGGAACATGC 1220
GhRca-β CCACCATCTTTCGAGCAACCTACGATGACCATTGAGAAGCTGTTGGAGTATGGAACATGC 1220

GhRca-α TTGTTGCTGAGCAAGAGAATGTTAAGAGAGTCCAATTGGCTGACAAATACTTGAGTGAAGC 1281

GhRca-β TTGTTGCTGAA CAAGAGAAC GTGAAGAGG GTTCAATTGGCTGACAAATATTTGAGTGAAGC 1281
GhRca-α TGCCCTTGGTGAAGCTAATGAAGATTCTATCAACAGAGGAACTTTCTATGGCAAAGCAGCA 1342
GhRca-β TGCCCTTGGAAATGCTAATGACGATGCTATCAAGAGAGGAGCTTTCTAA 1342
GhRca-α CAACAAGTTGGGGTTCCAGTTCCCGAAGGATGCACTGATCCAAATGCTGATAACTTTGATC 1403
GhRca-α CAACGGCTAGAAGTGATGATGGAACCTGCACTTACCAATTTTAAAGATCTGATGGGGG--- 1464

Figure 3.8. Nucleotide sequence for cotton α (*GhRca-α*) and β (*GhRca-β*) Rca isoforms. α isoform is based upon the sequence with accession number DQ233255. Nucleotide differences at each position between the *GhRca-α* and *GhRca-β* sequence are highlighted (grey). The start of the transit peptide (pink), start codon of the mature peptide (green) and the stop codon (blue) are indicated.

GhRcaα MAAAVSTIGAVNRAPLSLNGSGAGASAPSSAFMGNSLKKVSARFNNTRQVPVSGSFKVMAA 60
GhRcaβ MAAAVSTIGAVNRAPLSLNGSGAGASAPSSAFMGNSLKKVSARFNNNGKAPVGSFKIVA 60
GhRcaα EKEIDEETQTEKDRWKGLAYDISDDQQDITRKGKGVDSLFQAPMNDGTHYAVMSSYEYLS 120
GhRcaβ -KEIDEDTQTDQDRWKGLAYDISDDQQDITRKGKGVDSLFQAPMNDGTHYAVMSSYEYIS 120
GhRcaα QGLKTYNLDNNMDGFYIAPAFMDKLVVHITKNFMSLPNIKVPLIILGIWGGKQGKSFQCE 180
GhRcaβ QGLRITYDLNNDMDGFYIAPAFMDKLVVHITKNYMTLPNIKVPLIILGIWGGKQGKSFQCE 180
GhRcaα LVFAKMGINPIMMSAGELESGNAGEPAKLIRQRYREAADI IKKGKMCALFINDL DAGAGR 240
GhRcaβ LVFAKMGINPIMMSAGELESGNAGEPAKLIRQRYREAADI IKKGKMCCLFINDL DAGAGR 240
GhRcaα MGGTTQYTVNNQMVNATLMNIADNPTNVQLPGMYNKEENPRVPI IVTGNDFSTLYAPLIR 300
GhRcaβ MGGTTQYTVNNQMVNATLMNIADNPTNVQLPGMYNKEENPRVPI IVTGNDFSTLYAPLIR 300
GhRcaα DGRMEKIFYWAPTRDDRVGVCKGIFRTDGIPEDEIVKLVDTFPGQSIDFFGALRARVYDDE 360
GhRcaβ DGRMEKIFYWAPTREDRIGVCTGIFRTDNVVDIVKLVDTFPGQSIDFFGALRARVYDDE 360
GhRcaα VRKWI SDVGVAGVGGKLVNSRDGPPTFEQPKMTIEKLLEYGNMLVAEQENVKRVQLADKY 420
GhRcaβ VRKWI GEVGVNSVGGKLVNSREGPPTSFEQPTMTIEKLLEYGNMLVAEQENVKRVQLADKY 420
GhRcaα L-SEAAALGEANEDSINRGTFYGKAAQQVGPVPEGCTDPNADNFDPTARSDDGTCTYQF* 480
GhRcaβ LASEAALGNANDDAIKRGAF*----- 480

Figure 3.9. Amino acid sequence for cotton α (*GhRca-α*) and β (*GhRca-β*) Rca isoforms. Sequences from (Salvucci *et al.*, 2003). Amino acid differences at each position are highlighted (grey) and the start of the mature peptide (green) shading.

WtRSSU-TP-GhRcaα GGATCCACCATGGCCCCCGCCGTGATGGCCTCGTCGGCCACCTCCGTCGCTCCTTT
WtRSSU-TP-GhRcaα CCAGGGGCTCAAGTCCACCGCCGCGCCTCCCGTCAGCCGCGCTCCAACGGCGCTA
WtRSSU-TP-GhRcaα GCCTCGGCAGCGTCAGCAACGGTGGAAGGATCAGGCGCATGCAGGCCGAGAAGGAG
WtRSSU-TP-GhRcaα ATCGACGAGGAGACCCAGACGGAG
WtRSSU-TP-GhRcaα GSTMAPAVMASSATSVAPFQGLKSTAGLPVSRRSNGASLGSVSNNGRIRRM
WtRSSU-TP-GhRcaα QA EKEIDEETQTE

Figure 3.10. Nucleotide (A) and amino acid (B) sequence for the wheat Rubisco small subunit transit peptide (*WtRSSU-TP*) and amino acid sequence.

This leads onto the Cotton Rca α (*GhRca-α*) gene sequence.

Indicated are the first amino acid of the mature cotton peptide (green), *WtRSSU-TP* sequence (grey), the kozak sequence (underlined) and the 'RMQ' sequence from the *WtRSSU-TP* (blue).

Table 3.5. Cleavage sites between the transit peptides and mature protein sequence for p302AcGhRcaA/B and pAHC17GhRcaA/B.

The start of the mature peptide in cotton as found in Salvucci *et al.* (2003) is stated and the equivalent predictions using ChloroP. The red letter indicates the first amino acid of the mature peptide.

Sequence tested with ChloroP	Cleavage site
Cotton TP and Cotton <i>Rca α</i> (p302AcGhRcaA) Mature protein as in Salvucci <i>et al.</i> (2003)	AAEKEID
Cotton TP and Cotton <i>Rca β</i> (p302AcGhRcaB) Mature protein as in Salvucci <i>et al.</i> (2003)	AA-KEID
Cotton TP and Cotton <i>Rca α</i> (p302AcGhRcaA) ChloroP prediction	AAEKEID
Cotton TP and Cotton <i>Rca β</i> (p302AcGhRcaB) ChloroP prediction	AA-KEID
Wheat TP and Cotton <i>Rca α</i> optimised (pAHC17GhRcaA) ChloroP prediction	GRIRRMQAE
Wheat TP and Cotton <i>Rca β</i> optimised (pAHC17GhRcaB) ChloroP prediction	GRIRRMQAK
Wheat TP and Cotton <i>Rca α</i> (Minus RMQ; Not cloned) ChloroP prediction	GRIRRAE
Wheat TP and Cotton <i>Rca β</i> (Minus RMQ; Not cloned) ChloroP prediction	GRIRRAK

Table 3.6. Comparison of cotton and wheat *Rca* isoform nucleotide and amino acid sequence lengths. The sequence for the cotton α and β proteins (*GhRca-α* and *GhRca-β*) were compared to the α and β wheat sequences for the two genes (*TaRca1* and *TaRca2*) and three genomes (A, B and D).

	<i>GhRca-α</i>	<i>GhRca-β</i>	<i>TaRca1-β</i>	<i>TaRca2-β</i>	<i>TaRca1-α</i>
Total number of nucleotides (minus TP)	1260	1140	1155	1143	1254
Protein	GhRca-α	GhRca-β	TaRca1-β	TaRca2-β	TaRca1-α
Total number of amino acids (minus TP)	419	379	384	380	417

TaRca1 β	AAKKE ⁵ LDEGKQ ¹⁰ TNADRWKGLAYDISDDQ ¹⁵ QDITSGKGI ²⁰ VDSL ²⁵ FQAPMGDGT 50
TaRca2 β / α	AAEN ⁵ -LDEK ¹⁰ RNT--DKWKGLAYDISDDQ ¹⁵ QDITRGKGI ²⁰ VDSL ²⁵ FQAPTGDGT 50
GhRca β	A-KE ⁵ IDE ¹⁰ DTQ ¹⁵ T ²⁰ Q ²⁵ Q--DRWKGLAYDISDDQ ³⁰ QDITRGKGMV ³⁵ DLS ⁴⁰ FQAPMNDGT 50
GhRca α	AEKE ⁵ IDE ¹⁰ ETQ ¹⁵ TEK--DRWKGLAYDISDDQ ²⁰ QDITRGKGMV ²⁵ DLS ³⁰ FQAPMNDGT 50
<hr/>	
TaRca1 β	HEATLSS ⁵ YEY ¹⁰ TSQGLRKYDFDNTMDGLYIAPAFMDKLI ¹⁵ VH ²⁰ LAKNFM ²⁵ TLPN 100
TaRca2 β / α	HEAVLSS ⁵ YEY ¹⁰ VSQGLKKYDFDNTMGGFYIAPAFMDKLI ¹⁵ VH ²⁰ LSKNFM ²⁵ TLPN 100
GhRca β	HYAVMSS ⁵ YEY ¹⁰ TSQGLR ¹⁵ TYDL ²⁰ DN ²⁵ NMDGFYIAPAFMDKLI ³⁰ VH ³⁵ LTKNYM ⁴⁰ TLPN 100
GhRca α	HYAVMSS ⁵ YEY ¹⁰ TSQGLK ¹⁵ TYN ²⁰ LD ²⁵ NNMDGFYIAPAFMDKLI ³⁰ VH ³⁵ LTKN ⁴⁰ FMSLPN 100
<hr/>	
TaRca1 β	IKVPLILGIWGGKQ ⁵ GKSFQ ¹⁰ CELVFAKMGINPIMMSAGELES ¹⁵ GNAGEPAK 150
TaRca2 β / α	IKVPLILGIWGGKQ ⁵ GKSFQ ¹⁰ CELVFAKMGINPIMMSAGELES ¹⁵ GNAGEPAK 150
GhRca β	IKVPLILGIWGGKQ ⁵ GKSFQ ¹⁰ CELVFAKMGINPIMMSAGELES ¹⁵ GNAGEPAK 150
GhRca α	IKVPLILGIWGGKQ ⁵ GKSFQ ¹⁰ CELVFAKMGINPIMMSAGELES ¹⁵ GNAGEPAK 150
<hr/>	
TaRca1 β	LIRQRYREAAD ⁵ TI ¹⁰ INKGKMC ¹⁵ CLFINDLDAGAGRMGGT ²⁰ TQYTVNNQ ²⁵ MVNATL 200
TaRca2 β / α	LIRQRYREAAD ⁵ MI ¹⁰ IKKGKMC ¹⁵ CLFINDLDAGAGRMGGT ²⁰ TQYTVNNQ ²⁵ MVNATL 200
GhRca β	LIRQRYREAAD ⁵ TI ¹⁰ IKKGKMC ¹⁵ CLFINDLDAGAGRMGGT ²⁰ TQYTVNNQ ²⁵ MVNATL 200
GhRca α	LIRQRYREAAD ⁵ TI ¹⁰ IKKGKMC ¹⁵ CLFINDLDAGAGRMGGT ²⁰ TQYTVNNQ ²⁵ MVNATL 200
<hr/>	
TaRca1 β	MNIADAP ⁵ TNVQLPGMYNKEENPRVPI ¹⁰ IVTGNDFSTLYAPLIRDGRMEK ¹⁵ FY 250
TaRca2 β / α	MNIADAP ⁵ TNVQLPGMYNKEENPRVPI ¹⁰ IVTGNDFSTLYAPLIRDGRMEK ¹⁵ FY 250
GhRca β	MNIADNPTNVQLPGMYNKEENPRVPI ¹⁰ IVTGNDFSTLYAPLIRDGRMEK ¹⁵ FY 250
GhRca α	MNIADNPTNVQLPGMYNKEENPRVPI ¹⁰ IVTGNDFSTLYAPLIRDGRMEK ¹⁵ FY v
<hr/>	
TaRca1 β	WAPTR ⁵ EDRIGVCKGIFR ¹⁰ TDNVPDEAVVRLVDTFPGQSIDFFGALRARVYD 300
TaRca2 β / α	WAPTR ⁵ DDRIGVCKGIFR ¹⁰ TDNVSD ¹⁵ SVVKLVDTFPGQSIDFFGALRARVYD 300
GhRca β	WAPTR ⁵ EDRIGVCTGIFR ¹⁰ TDNVPD ¹⁵ IVKLVDTFPGQSIDFFGALRARVYD 300
GhRca α	WAPTR ⁵ DDRVGVCKGIFR ¹⁰ TDGP ¹⁵ DEIVKLVDTFPGQSIDFFGALRARVYD 300
<hr/>	
TaRca1 β	DEV ⁵ RK ¹⁰ WVGEI ¹⁵ GVENIS ²⁰ KRI ²⁵ VNSREG ³⁰ PP ³⁵ TFD ⁴⁰ QPKMT ⁴⁵ IEK ⁵⁰ LMEYGHMLVQ ⁵⁵ EQ 350
TaRca2 β / α	DEV ⁵ RK ¹⁰ WV ¹⁵ STG ²⁰ TE ²⁵ NI ³⁰ GKRI ³⁵ VNSR ⁴⁰ DGP ⁴⁵ VTFE ⁵⁰ QPKMT ⁵⁵ VEK ⁶⁰ LMEYGHMLVQ ⁶⁵ EQ 350
GhRca β	DEV ⁵ RK ¹⁰ WV ¹⁵ GEV ²⁰ GVNS ²⁵ VGK ³⁰ KI ³⁵ VNSR ⁴⁰ EG ⁴⁵ PP ⁵⁰ SFE ⁵⁵ QPTMT ⁶⁰ IEK ⁶⁵ LMEYGNMLV ⁷⁰ AEQ 350
GhRca α	DEV ⁵ RK ¹⁰ WV ¹⁵ SL ²⁰ GV ²⁵ AV ³⁰ GVG ³⁵ KI ⁴⁰ VNSR ⁴⁵ GP ⁵⁰ PTFE ⁵⁵ QPKMT ⁶⁰ IEK ⁶⁵ LMEYGNMLV ⁷⁰ AEQ 350
<hr/>	
TaRca1 β	ENVKRVQLADKYLSEAA ⁵ LGQANDDAMKTGA-FY ¹⁰ GK----- 400
TaRca2 β	DNVKRVQLADTYMSQAALGDANQDAMKTGS-FY ¹⁰ G----- 400
TaRca2 α	DNVKRVQLADTYMSQAALGDANQDAMKTGS-FY ¹⁰ GKGAQQGTL ¹⁵ PVPAGCTD 400
GhRca β	ENVKRVQLADKYLASEAA ⁵ LG ¹⁰ NANDDAIK ¹⁵ RGA ²⁰ F----- 400
GhRca α	ENVKRVQLADKYL-SEAA ⁵ LG ¹⁰ EA ¹⁵ NEDS ²⁰ INR ²⁵ GT ³⁰ FY ³⁵ GKAAQ ⁴⁰ VG ⁴⁵ VPV ⁵⁰ PE ⁵⁵ GCTD 400
<hr/>	
TaRca1 β	----- ⁴¹⁹ ----- 419
TaRca2 β	----- ⁴¹⁹ ----- 419
TaRca2 α	QTAKNFDPTARSDDGSCLYTF 419
GhRca β	----- ⁴¹⁹ ----- 419
GhRca α	PNADNFDPTARSDDGTCTYQF 419

Figure 3.11. Comparison of amino acid sequence for the mature Rca α and β peptides from wheat and cotton. Differences between the amino acids in cotton and wheat (grey, magenta and green shading are used where multiple different amino acids can be found at the same position). The coloured lines above the sequence correspond to the wheat protein regions N (green), AAA+ (yellow), Rubisco binding domain (blue), C-terminus (red) and C-terminal extension for α isoforms (orange). Boxes (black) indicate the residues involved in Rubisco/ Rca interaction in the sensor 2 domain (Li et al 2005). Due to the difference in the numbering of bases in the paper (269, 302/202, 308, 311 and 314) and here in wheat, the base number in wheat equals the base number in the paper plus five. Boxes (red) indicate residues highlighted as increasing thermal tolerance by Kurek et al (2007). Due to the difference in the numbering of bases in the paper (131, 168, 257, 274 and 310) and here in wheat, the base number in wheat equals the base number in the paper plus three.

In order to test whether it was possible to distinguish cotton and wheat Rca in western blots, trials were run with cotton and wheat leaf protein extracts. The Rubisco large subunit (SDS-Page gel, Figure 3.12A) can be distinguished between cotton and wheat leaf extracts. In wheat the TaRca- α isoform is present in very low amounts compared to the TaRca- β isoform (Western blot, Figure 3.12B), whereas in cotton both the GhRca- α and GhRca- β isoforms are present in similar amounts. From these results it appears that the TaRca- α Rca isoform of wheat may be slightly smaller than the GhRca- α , and as there is significantly less of the α isoform in wheat, it may be possible to distinguish the two proteins in the transgenic plants. On the other hand, the β isoforms of cotton and wheat Rca are too similar in size and cannot be distinguished by this method.

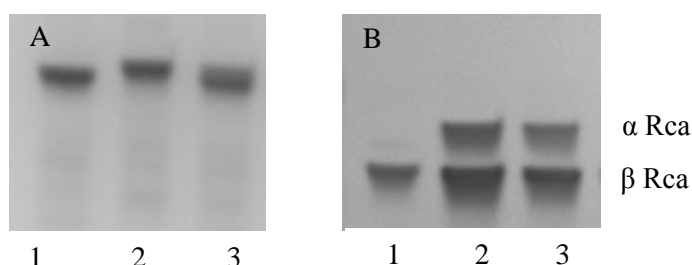


Figure 3.12. SDS-Page gel showing the Rubisco large subunit and Rca western blot of wheat and cotton leaf extracts.

Lanes contain wheat (1), cotton (2) and wheat and cotton leaf extracts mixed in equal proportions (3). Samples were run on 8-16% gels (A). In the western (B), the top band of each pair corresponds to the α isoform and the bottom band to the β isoform.

Biolistic transformation was used to generate 25 independent transgenic lines of pAHC17GhRcaA, 25 of pAHC17GhRca B, 16 of p302AcGhRcaA and 26 of p302AcGhRcaB. Transformants were selected by their ability to grow in the presence of the herbicide Basta. PCR confirmed that these lines contained the selectable marker, the *bar* gene, and additional PCR identified plants with *GhRca* genes. Segregation at the T1 generation predicts that 75% of the plants should be DNA positive, and this was seen in the majority of the transgenic lines in which DNA positive plants were found.

In the T1 generation, qRT-PCR was used to investigate the expression of *GhRca- α* and *GhRca- β* in different transgenic wheat lines of each construct (Figure 3.13). The negative lines showed no expression as expected. Several lines were identified as showing expression of the transgene and production of mRNA. The expression level varied between lines but also between plants of the same line.

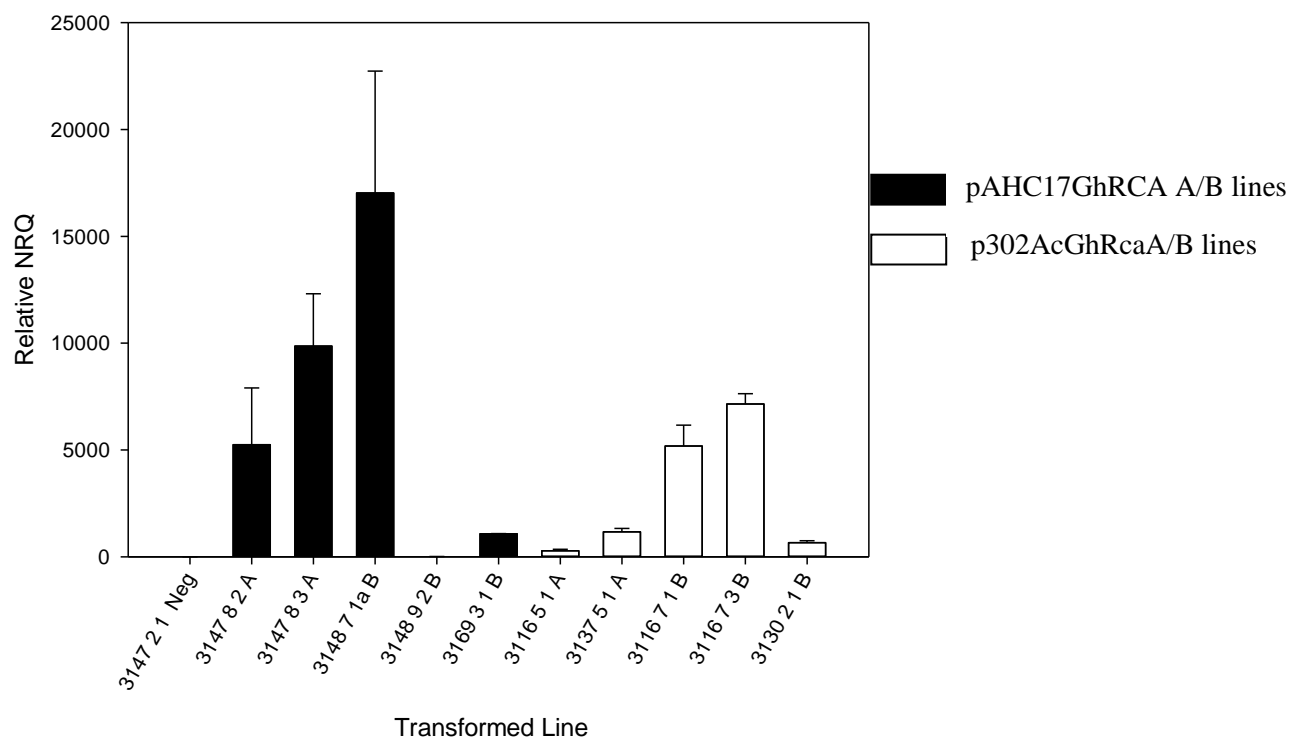


Figure 3.13. Gene expression analysis (Relative NRQ) of plants from lines of pAHC17GhRcaA/B (black bars) and p302AcGhRcaA/B (white bars). Values are means of a minimum 3 plants per line \pm SEM.

3.3.2 Protein expression analysis of transgenic wheat plants

Western blots were completed in an attempt to identify cotton Rca protein in the transgenic plants.

Initially, the total Rca amount in the p302AcGhRcaA/B transgenic lines was compared to control plants by using a high-throughput system that does not allow separation of the α and β isoforms of Rca (Figure 3.14). No difference in total Rca amount was seen between p302AcGhRcaA/B lines and their controls (Figure 3.15).

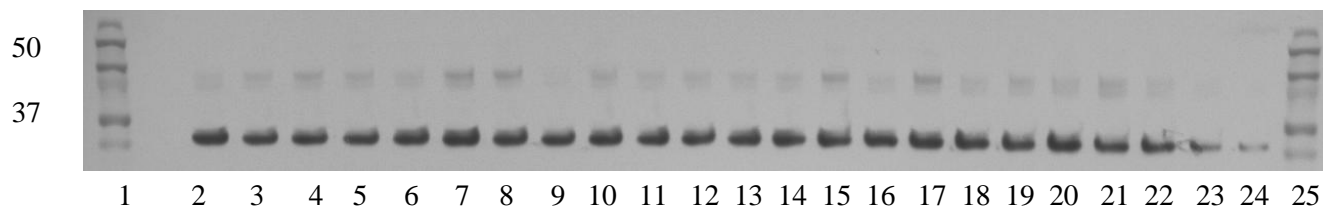


Figure 3.14. Representative example of an Rca western blot of p302AcGhRcaA/B plants using 48-well Criterion gels.

Triplicate samples of p302AcGhRcaA/B lines were randomised through a series of gels, for which 2 µg TSP of sample was used. Wells 2-19 are samples from DNA positive plants with wells 3, 8 and 13 being from plants which tested negative for the transgene DNA. A standard curve using 2, 1.5, 1, 0.5, 0.25 µg mL⁻¹ TSP, can be seen in wells 20-24.

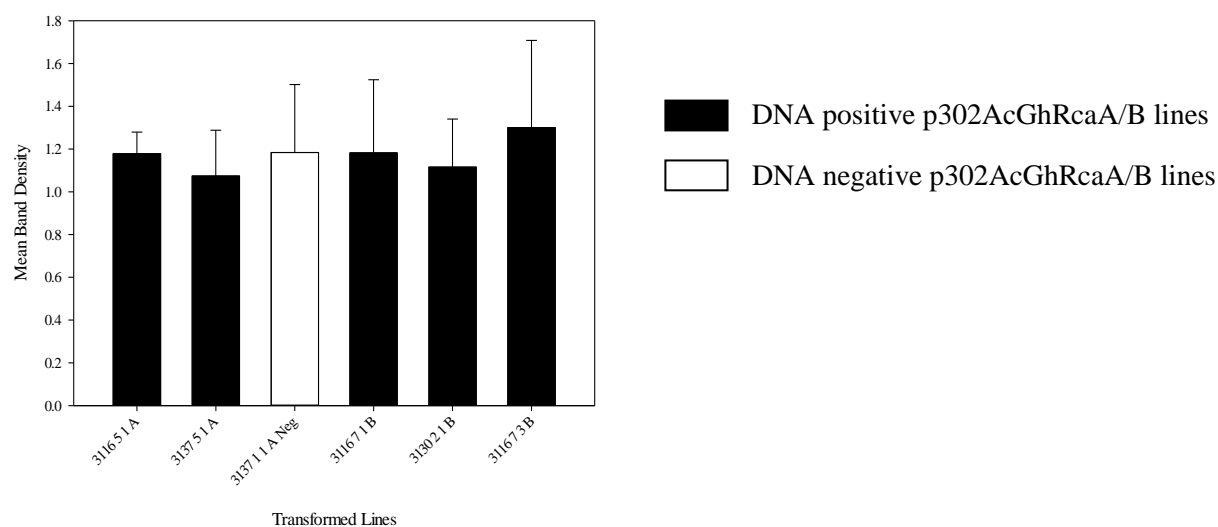


Figure 3.15. Total Rca amount (mean western blot band intensity) in p302AcGhRcaA/B transformed lines (black bars) and negative line (white bar) from Criterion 48-well gel western blots.

Values are mean (\pm SEM) of a minimum of 6 plants per line.

Western blots were then performed using 11% mini gels (Figure 3.16) which allow separation of the α and β Rca isoforms. The amount of each Rca isoform was calculated and compared to DNA negative samples. No difference in the Rca amount was identified in any construct, or in any transgenic line, for either isoform (Figure 3.17).

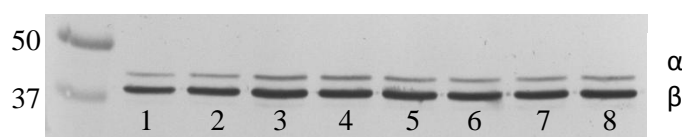


Figure 3.16. Representative example of western blot analysis of pAHC17GhRcaA/B plant samples on 11% gels. Standard curve of 0.1 µg (1), 1 µg (2) and 2 µg (3) TSP 3147-8-2-11 (4) 3147-2-1-1 neg line (5) 3147-8-3-10 (6) 3147-9-2-6 (7) 3148-7-1a-9 (8). 1µg of TSP run per sample.

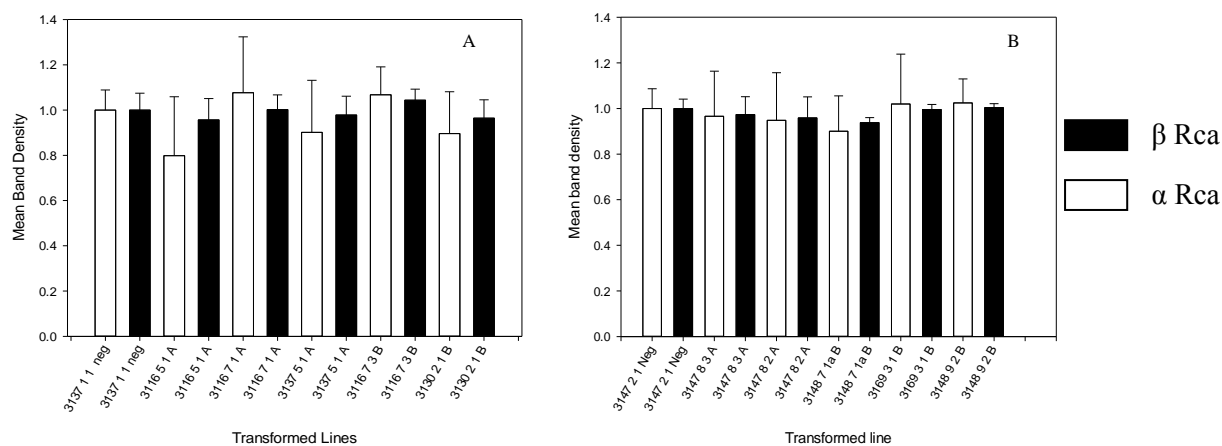


Figure 3.17. Amount (Western blot band density) of Rca α (white bars) and β (black bars) isoforms in p302AcGhRcaA/B lines (A), and pAHC17GhRcaA/B lines (B) on 11% gels. Values are an average of a minimum of three plants per line, \pm SEM, with DNA negative plants as controls.

The predicted difference in isoelectric point (pI) from the sequence of the wheat and cotton β isoforms is 0.2. The isoelectric point for cotton was estimated with the ExPasy calculator (Gasteiger *et al.*, 2005) to be 5.07, and for wheat 5.29, therefore it should be possible to separate the two cotton and wheat Rca β proteins by IEF.

Problems were encountered in effectively separating the Rca isoforms by IEF. Wheat leaf protein samples were separated using native Criterion gels. Gels were stained with Coomassie blue (Figure 3.18A), western blotted directly (Figure 3.18B) or run on a second dimension gel before western blotting (Figure 3.18C). Rca can be identified along the length of the lanes in the western blot in Figure 3.18B. In Figure 3.18C Rca is identifiable between the 37 and 50kDA marker bands. This is present as a smear indicating that the first dimension did not separate the protein by isoelectric point into a single spot.

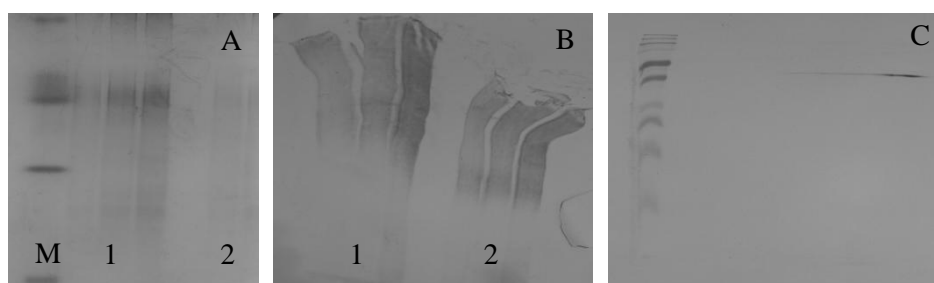


Figure 3.18. Native IEF criterion gels and Rca western blot of wheat leaf protein samples. Stained IEF gel (A) and corresponding Rca western blot (B) of wheat leaf samples: two sets (1, 2) of 5, 10, and 15 μ g TSP were loaded in consecutive lanes. Western blot of second dimension gel IEF (C) of wheat leaf sample containing 15 μ g TSP.

Denaturing the proteins in wheat and cotton leaf extracts prior to running on native Criterion gels (Figure 3.19A) showed that Rca could again be detected throughout the lanes (Figure 3.19B). Rca isoforms could be distinguished in western blots of the second dimension gels (Figures 3.19C- E), in wheat TaRca- α is clearly less abundant than TaRca- β , whereas both isoforms are similarly abundant in cotton.

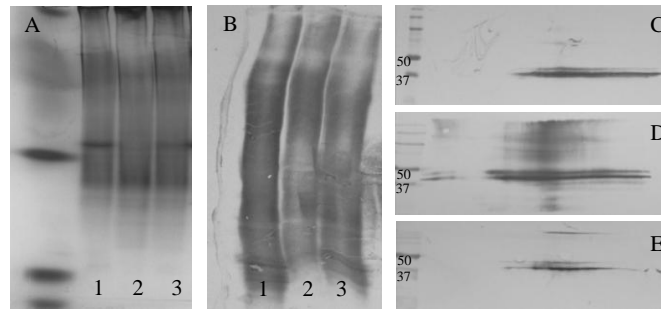


Figure 3.19. Denatured cotton and wheat leaf protein samples run on a native IEF gel. Coomassie stained IEF gel (A) and corresponding western blot of IEF gel (B), lanes contain: wheat leaf protein (1), cotton leaf protein (2), mixed wheat and cotton leaf protein (3). Western blots of the second dimension IEF gel, with 43.2 μ g TSP of: wheat leaf protein (C) cotton leaf protein (D) and wheat and cotton leaf protein mixed (E)

Denatured samples of wheat and cotton were run on a denaturing IEF gel with greater success. Clear separation of different proteins by their isoelectric point can be seen in the IEF gel (Figure 3.20A), with the band pattern being clearly different for cotton and wheat. The different Rca isoforms can be identified in the subsequent western blot, but the difference between cotton and wheat Rca cannot be clearly identified due to the curvature of the lanes due to heating of the gel during running (Figure 3.20B).

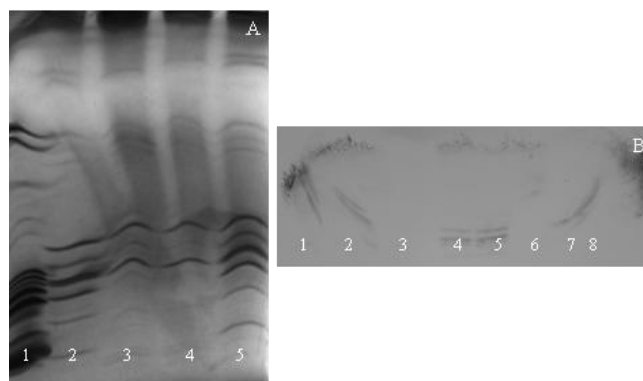


Figure 3.20. Denatured cotton and wheat leaf protein samples run on a denaturing IEF gel. IEF denaturing gel (A) with: Marker (1), Cotton (2), Wheat (3), Wheat (4), Cotton (5). Western blot of denaturing IEF gel (B) of wheat and cotton leaf protein samples of: Cotton (1), Cotton (2), Blank (3), Wheat (4), Wheat (5), Blank (6), Cotton (7), Cotton (8).

To attempt to more reliably separate cotton and wheat Rca, denatured samples were run on IEF gel strips and then run on large agarose gels (Figure 3.21). For wheat, Rubisco large and small subunits could clearly be identified at 50 and 12 kDa. For cotton, far fewer spots were visible. This was replicated with the same results being seen. The wheat samples run on the strips were from transgenic plants showing high levels of expression of cotton Rca. Figure 3.22 shows the western blots of second dimension gels for wheat (Figure 3.22A), cotton (Figure 3.22B) and a mix of wheat and cotton (Figure 3.22C). The spots corresponding to wheat and cotton could be distinguished in the mixed blot. In each species the α and β Rca isoforms were separated by molecular weight and appeared to be present as several spots, indicating Rca proteins with different isoelectric points. These patterns of spots were species specific, with the same pattern being seen in multiple samples. A false colour overlay of western blots for a mixed sample of cotton and wheat was used to facilitate identification of wheat and cotton specific Rca spots (Figure 3.23). A representative overlay of a transgenic wheat sample, with high Rca expression, with the mixed cotton and wheat sample showed that the Rca protein present in the transgenic sample was only that of wheat.

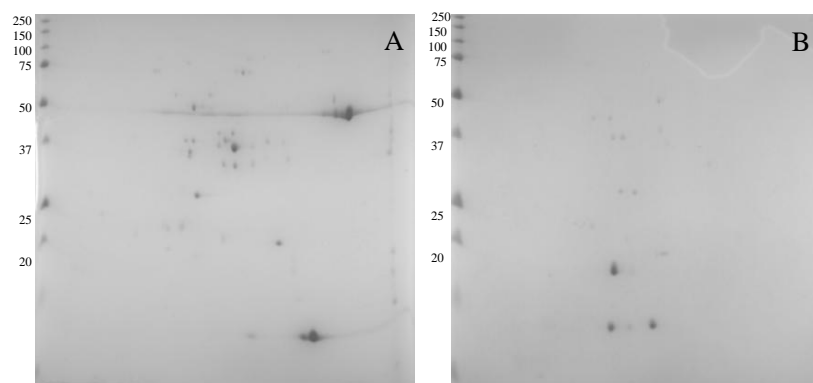


Figure 3.21. Coomassie stained second dimension gels of wheat leaf total protein (A; 200 µg) and cotton total protein (B; 50 µg).

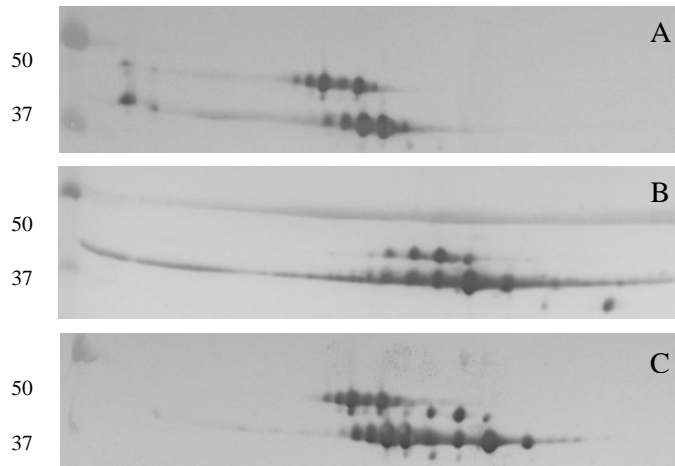


Figure 3.22. Western blot of the 2nd dimension gel of 100µg of wheat (A), 100µg of cotton (B), and a mixture of 100 µg total wheat and cotton (C).

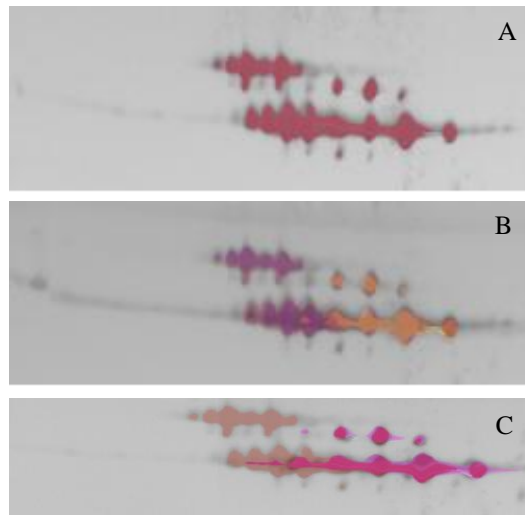


Figure 3.23. False colour overlay of second dimension western blots of wheat and cotton α and β Rca proteins. Mixed blot of wheat and cotton (red) (A). Altered colour image with overlay of individual cotton and wheat blots indicating wheat (purple) and cotton (orange) Rca (B). Example of a computer overlay of a western blot from a DNA positive plant (pAHC17GhRcaB), and a mixed blot of cotton (pink) and wheat (pale orange).

3.3.3 Photosynthetic analysis of transgenic wheat plants

The temperature response of photosynthesis was measured in young leaves of wheat (cv. Cadenza) grown at daytime temperatures of 25°C, to determine a baseline for the temperature response of photosynthesis in glasshouse grown wheat. The rate of photosynthesis increased up to a leaf temperature of around 28°C and then declined as leaf temperature further increased (Figure 3.24).

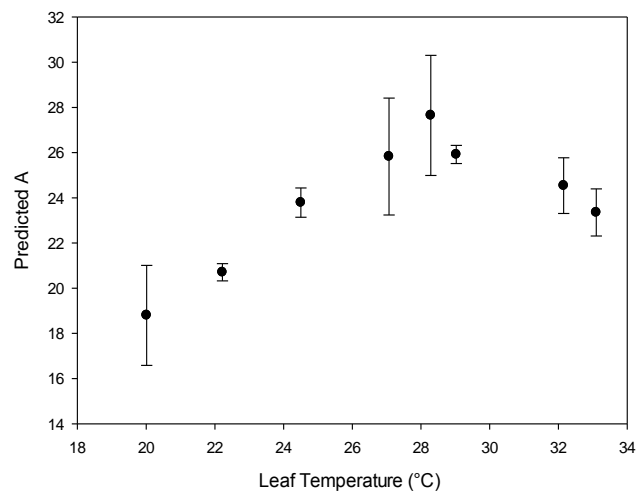


Figure 3.24. Rate of wheat photosynthesis predicted from ACi Curve measurements taken at a range of temperatures. .

Predicted photosynthetic rate at $210 \mu\text{L L}^{-1} \text{CO}_2$ from ACi curves of three leaves at each of eight temperatures (\pm SEM).

Photosynthesis was measured at 35°C in plants of the transgenic wheat lines and respective controls after exposure to this elevated temperature, to investigate whether any difference could be identified due to transformation with *GhRca* genes. There was no significant difference in photosynthesis at 35°C between null transformants and DNA positive plants for any of the four constructs (Figure 3.25; p302AcGhRcaA, $p=0.073$, F-Test, p302AcGhRcaB, $p=0.118$, F-Test, pAHC17GhRcaA $p=0.446$, F-Test, pAHC17GhRcaB, $p=0.247$, F-Test). Critically, there was no significant difference in the leaf temperatures; ensuring measurement of different leaves was equivalent.

When productivity parameters were considered, there was also no significant effect of the transgene on straw biomass, grain weight, ear number, grains per ear or HI in p302AcGhRcaA or pAHC17GhRcaB (Figure 3.26). In p302AcGhRcaB straw biomass was significantly different when positive and respective negative controls were considered ($p=0.012$, F-test), but not when the interaction with lines was included ($p=0.182$, F-Test). In pAHC17GhRcaA, straw biomass was just significant for the interaction of DNA positive and negative with lines ($p=0.048$, F-Test). The same was true for grain weight ($p=0.026$, F-Test) and HI ($p=0.006$, F-Test), mostly as a consequence of lines 3147-3-1 and 3147-6-2 which had opposite responses compared to their nulls. However, these lines responded in opposite directions, with 3147-3-1 showing greater productivity in the null plants, and 3147-6-2 greater productivity in positive plants. There

were six positive and only two or three null plants for each line respectively, and variation between individual plants was very high. The positive plants were not significantly different ($p < 0.05$, LSD) from the cadenza control.

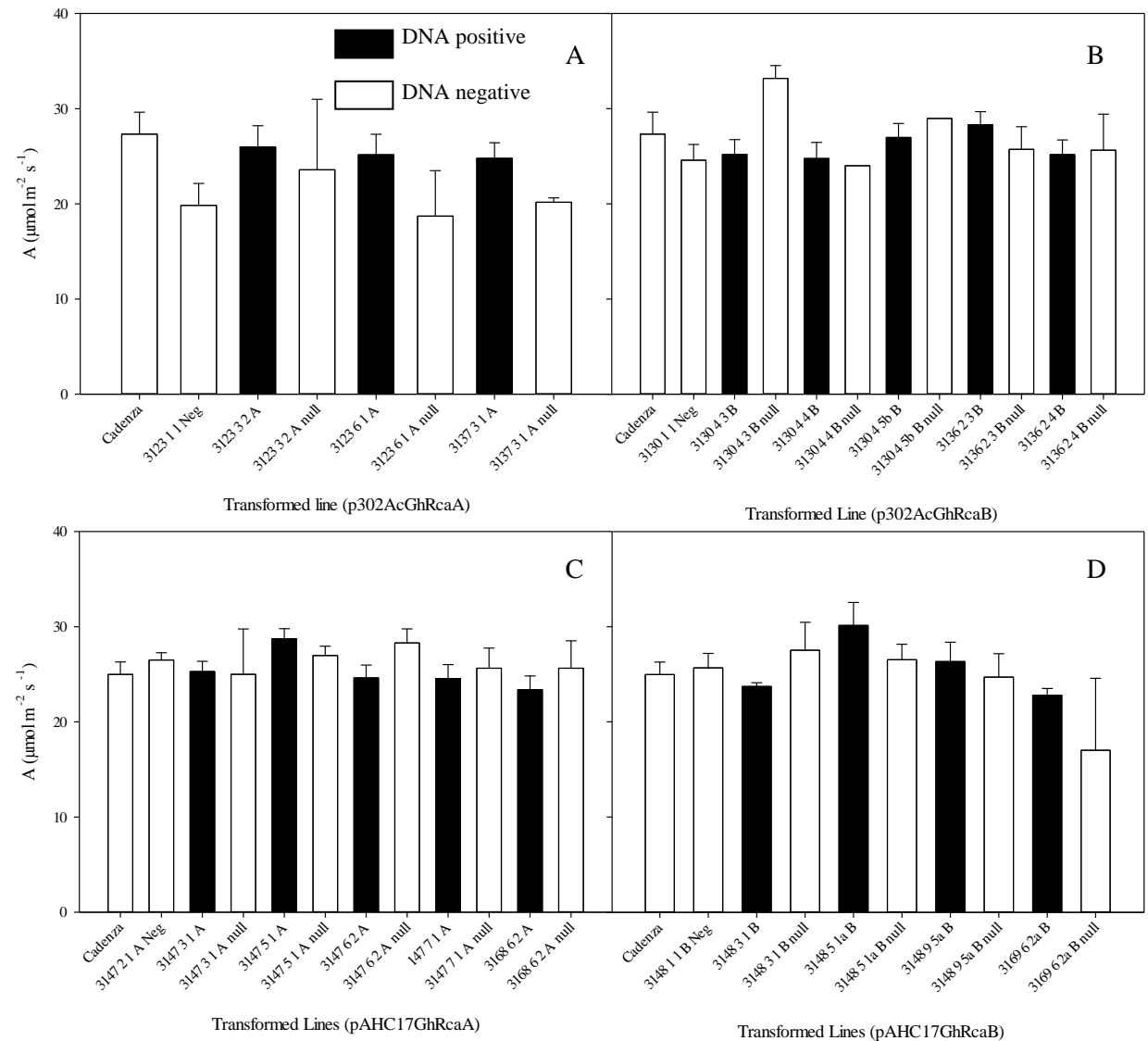


Figure 3.25. Photosynthetic rates ($\mu\text{mol m}^{-2} \text{s}^{-1}$) of transgenic lines for each construct compared to DNA negative plants, cadenza and negative transformation controls.

p302AcGhRcaA/B plants are shown in graphs A and B and pAHC17GhRcaA/B plants in C and D. White bars indicate controls, representing either WT cadenza, negative lines or null (DNA negative plants) for a specific line. Black bars indicate DNA positive plants. Values are means of at least three plants \pm SEM.

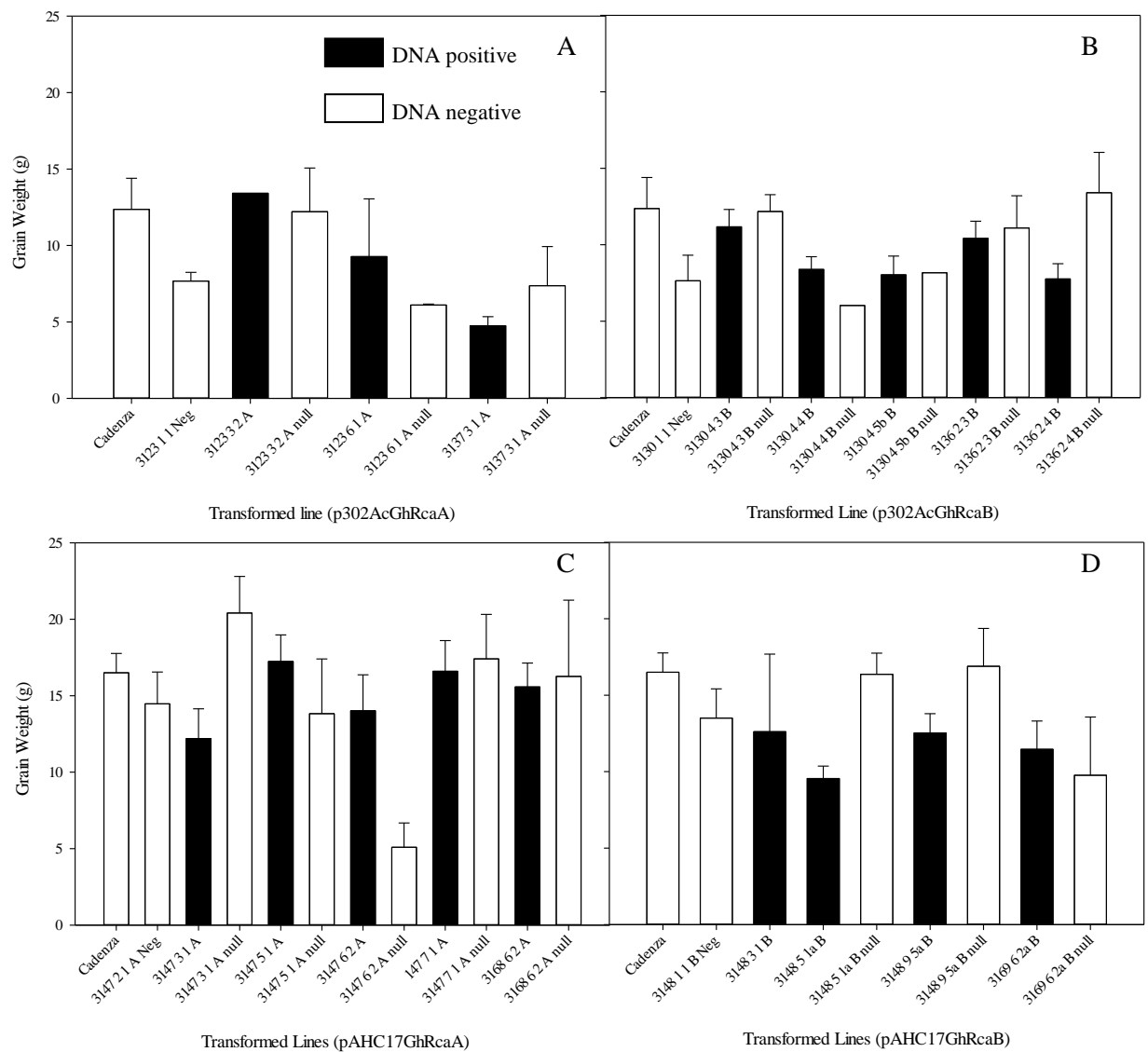


Figure 3.26. Mean grain weight (g per plant) of transgenic lines from each construct and for the equivalent DNA negative plants. p302AcGhRcaA/B plants are shown in graphs A and B and pAHC17GhRcaA/B plants in C and D. White bars indicate controls, either WT cadenza, negative lines or null (DNA negative plants), for a specific transgenic line. Black bars indicate DNA positive plants. Values are means of at least three plants \pm SEM.

3.4 Discussion

The aim of this chapter was to genetically engineer wheat so that it would be able to maintain photosynthesis at high temperatures and to test the hypothesis that this could be achieved by the introduction of a thermally stable Rca from cotton. Transgenic plants containing the *GhRca* genes were successfully obtained and transcript was identified, but no GhRca protein was detected in the transgenic lines tested to date. Possible reasons for this and future work required to further investigate this strategy of improving thermal tolerance are discussed below.

Since the TaRca- α isoform represents only ~12.5% of total Rca in wheat (Law & Crafts-Brandner, 2001) it should be feasible to identify the corresponding GhRca- α isoform in the transgenic wheat lines.

However, no difference could be detected in the amount of either isoform when the transgenic lines were compared to control lines by western blots. Therefore, alternate methods were identified which could be used to identify cotton Rca protein in the transgenic lines if the expression level was very low or if the regulation of the native Rca isoforms was altered by expression of the transgene (IEF and measuring the photosynthetic rates of transgenic plants). IEF was successfully used to distinguish between Rca from wheat and cotton. However, there was no evidence of cotton Rca protein within the transgenic samples tested. The inefficiency of the gel strip IEF system makes it inappropriate for wide-scale screens, such as those required for testing many transgenic lines; a cheaper and more convenient method is required.

Further development may improve the quality of the results from the denaturing IEF gels, such as the use of temperature controlled gel tanks and lower voltages to ensure these gels run more evenly, but the solution is likely to involve a separate methodology. Despite the lack of evidence for cotton Rca protein in the wheat transgenic plants, expression of the *GhRca* genes was confirmed in a few lines.

The inability to identify the GhRca protein in these plants could be due to a number of factors, including post-translational modification of the protein or rapid proteolysis. The close regulation of the wheat *Rca* isoforms may also impact upon Rca protein production in the transgenic lines, and also make it difficult to detect changes in the amount of Rca in the transgenic plants (see Chapter 4, for evidence of how regulation of different genes and isoform amounts, is potentially linked). These results, and the difficulty

in achieving high-throughput IEF screening of transgenic plants, led to an alternative approach represented by the heat stress experiment to investigate the thermal tolerance of photosynthesis in the transgenic wheat plants.

There was no difference in the photosynthetic rates or grain weight of wheat transgenic lines compared to control plants after a high temperature (35°C) treatment. Had the *GhRca* gene been functional and an *Rca* with greater thermal stability been present in the wheat transgenics, then photosynthesis by the transformed plants at high temperature should have been higher than in the controls. In *Arabidopsis* engineered to express *Rca* with improved thermal tolerance, the transgenic lines had higher photosynthesis, biomass and seed yield compared with wild-type plants, following exposure to extended periods of moderately elevated temperature (Kumar *et al.*, 2009). In this experiment the transgenic wheat plants were exposed to heat treatment at a relatively early developmental stage to avoid potentially negative impacts on grain production that could compromise the next generation of plants. The temperature response of wheat indicated a drop in photosynthesis at leaf temperatures above 28°C, indicating that the heat treatment of 35°C should negatively impact wild-type wheat photosynthetic rates, making it an appropriate heat stress treatment.

Biolytic gene delivery can result in complex transgene integration patterns which can cause problems for analysis (Jones, 2005). Genetic transformation is a two-stage process in which DNA is transferred into the cell, followed by its integration into the genome. Integration into the genome is random, but the sites of integration have been associated with naturally occurring chromosome breaks or transcriptionally active regions of the genome, particularly the sub-terminal regions of the chromosomes, possibly because the DNA is more accessible in these areas (Kohli *et al.*, 2006). The integration of DNA is largely dependent on host proteins involved in DNA replication, repair and recombination. Cases of non-expressed intact transgenes have been attributed to many different causes and plant mechanisms (Meza *et al.*, 2001). For example, rearrangement of the transgene DNA may occur, including truncations, internal deletions, interspersions of genomic DNA and inversions.

The transgene may insert multiple times and this has been associated with silencing (reviewed by (Kooter *et al.*, 1999, Matzke & Matzke, 1998), however, there are conflicting examples that demonstrate that multi-copy transgenic plants can show stable but higher expression of the gene when compared to plants with single copies (for example in wheat; Stoger *et al.* (1998)). Two routes to homology-dependent gene silencing have been studied; transcriptional transgene silencing and post-transcriptional transgene silencing. Transcriptional transgene silencing is characterized by inactivated promoters, where the promoter sequence is methylated. Post-transcriptional transgene silencing on the other hand, involves formation of aberrant RNA molecules and induces silencing of any genes producing RNA similar to the transgenic sequence, methylation may also be associated with this (reviewed by (Fire, 1999). Post translational modification may also have occurred (Jensen, 2006), with modification of the protein or rapid proteolysis resulting in difficulties identifying it in the transgenic plants. Further investigation is required to determine precisely which events result in an inability to identify the GhRca protein in these transgenic plants.

The design of the expression constructs could be responsible for the absence of cotton Rca in the transgenic wheat plants. In the p302AcGhRcaA/B constructs there is a non-functional bar gene, which although considered unlikely to influence the transgenic plants produced, is not ideal. The majority of proteins in chloroplasts, including Rca, are encoded by the nuclear genome and synthesized as precursors with N-terminal targeting signals called transit peptides (Li & Chiu, 2010). Despite their apparent specificity, what constitutes a transit peptide is poorly understood, with the length of known transit peptides varying from 13 to 146 amino acids. It is known that transit peptides from monocots are successfully recognised by other monocots, and the same is seen between dicots (Primavesi *et al.*, 2008), but there is no evidence that the cotton Rca transit peptide (from a dicot) will correctly target proteins to the wheat chloroplast (a monocot). Therefore, both the cotton Rca transit peptide and the wheat Rubisco small subunit transit peptide were used in separate constructs. In the second case, the *GhRca* genes were codon optimised for wheat with the aim of increasing transcript expression. No conclusion can be made about protein targeting and transit peptide specificity in the wheat transgenic plants, but given the two

approaches used it is unlikely that the transit peptides chosen would account for the absence of cotton Rca.

The addition of extra amino acids to the mature Rca peptide was considered when designing the constructs, specifically regarding the cleavage site when using the WtRSSU-TP. One consideration was whether the amino acids 'RMQ' from the WtRSSU-TP should be included and, if so, whether they would be cleaved from the mature peptide along with the transit peptide. This is important as additional amino acids may impact upon the activity of the Rca protein in the plant. Justification for keeping the 'RMQ' sequence is based upon the fact they are in the same exon as the rest of the WtRSSU-TP and so may be required (Primavesi *et al.*, 2008). Chloroplast transit peptide sequences are the most diverse of the organelle targeting signal peptides (Li & Teng, 2013). Therefore, due to the difficulties in predicting the correct cleavage sites, the RMQ amino acids were also included in the constructs used in this study. Incomplete structures of Rca are available for higher plant Rca, including for creosote bush (*Larrea tridentata*) C-domain (residues 250–351 out of 379 total; Henderson *et al.* (2011)) and tobacco (*Nicotiana tabacum*) AAA + domain (residues 68–360 out of 383 total, i.e. missing the N-terminus; Stotz *et al.* (2011). Henderson *et al.* (2011) found that the N domain was proteolytically cleaved during initial crystallization trials, suggesting that it is flexibly attached. In CbbX, the Rca of red algae, the N-terminal residues 1- 7 are likely to be flexible, as they were only structured in only one CbbX molecule (Mueller-Cajar *et al.*, 2011). In addition, N-terminal truncation of Rca has been shown to decrease enzymatic activity (Esau *et al.*, 1996, Stotz *et al.*, 2011, van de Loo & Salvucci, 1996).

Various alternative promoters for the expression of the cotton Rca gene in wheat were considered. A heat shock promoter (the barley *Hvhspl7* gene promoter) was discounted due to the high temperature required for its initiation (Freeman *et al.*, 2011), and the consequent effects on plant metabolism and the accurate measurement of photosynthesis. The Rca promoter from *Brachypodium distachyon* was initially selected for expression as this (being closely related to wheat) would give the most appropriate spatial expression. However, investigations by colleagues at Rothamsted Research indicated that the proposed Rca promoter was non-functional.

Constitutive promoters direct expression in virtually all tissues and are independent of the majority of environmental or developmental factors, and so it was decided that this was the most appropriate option. Therefore, the *Rca* cotton genes were expressed under both a Rice *actin-1* (McElroy *et al.*, 1990) and a Maize *ubiquitin-1* promoter (Christensen *et al.*, 1992). As the constructs containing these promoters had both previously been used successfully in other wheat transformation experiments, they were both tested. These promoters have been shown to confer several advantages, including high amounts of protein production, ubiquitous expression throughout the plant and during all stages of development. Importantly, although the Maize *ubiquitin-1* promoter is considered constitutive, studies to characterise its specificity in detail have shown that position effects, developmental stage (Rooke *et al.*, 2000) and stress (Stoger *et al.*, 1999) may affect its activity in transgenic wheat lines (Jones, 2005). In the GUS labelled promoter lines, expression with either the *ubiquitin-1* or *actin-1* promoters was detected throughout development, and therefore both promoters were expected to drive constitutive expression of the transgene in wheat leaves.

GhRca- α and GhRca- β differ in both their length and in how they are regulated in the plant. The longer, redox-regulated GhRca- α and the shorter GhRca- β isoform differ at the N termini in 4 of 14 residues, and by the 39 amino acid C-terminal extension of GhRca- α (Salvucci *et al.*, 2003). The GhRca- α and GhRca- β isoforms have similar affinities for ATP and only minor differences in thermotolerance, with GhRca- β being inhibited by temperatures about 2°C lower than GhRca- α . The ATPase specific activity of the GhRca- β isoform was lower, but differences in Rubisco activation specific activities were less accentuated. Therefore, wheat transgenic plants expressing either of the cotton *Rca* isoforms were predicted to show similar responses to temperature regarding Rubisco activation state.

Other transformation efforts can be considered to better understand what could have been expected in these plants. It might not be expected that the GhRca- α and GhRca- β wheat plants should perform hugely differently, especially as the native *Rca* from wheat, including the redox-regulated isoform, is still present. The cotton *Rca* has been shown to interact and reactivate the wheat Rubisco but the efficiency of this interspecies interaction could be lower, and therefore, like in the transgenic *Arabidopsis* expressing *Rca* from Antarctic hairgrass (*Deschampsia antarctica*; Salvucci *et al.* (2006)), competition with the

wheat Rca may restrict any improvement in the thermal tolerance of photosynthesis. There is no clear indication that any of the amino acid residues known to confer differences in thermal tolerance (Kurek *et al.*, 2007) are relevant to the differences seen between the cotton and wheat sequences, but the high degree of primary sequence homology would indicate that conserved residues play similar roles in both species.

The amount of protein being expressed has been seen to impact upon the responses observed in other transgenic plants so this also requires consideration (Kim & Portis, 2005). Other potential impacts of expressing GhRca include the light regulation of photosynthesis. Carmo-Silva *et al.* (2013) showed that light induction of CO₂ assimilation after transition from low to high irradiance was much more rapid in Arabidopsis transformants expressing only the (ADP-insensitive) β Rca, compared with plants containing ADP-sensitive Rca forms.

Some controversy exists concerning the potential impacts of increasing Rubisco activation state at high temperatures. It has been argued that decreasing Rubisco activation state under heat stress conditions could actually act as a protective mechanism for photosynthesis (Sharkey, 2005). Photorespiration increases with temperature, as a consequence of altered solubility of CO₂ and O₂ and decreased S_{C/O} (Keys, 1999), and therefore it is possible that increasing Rubisco activation at high temperatures may-contrary to our initial expectations- have a negative impact on photosynthetic efficiency. Even if expression of the protein had been found, it is possible that this may had no impact upon thermal tolerance as the activity of other enzymes would eventually become limiting at higher temperatures. Resource allocation within the plant could also have limited production of the GhRca protein and so eliminated any positive impacts; there is argument that resource partitioning between enzymes is not optimal and a transformation like this could impact upon nitrogen budgets. However, the results with Arabidopsis (Kumar *et al.*, 2009) clearly demonstrate that maintaining Rubisco activity at moderately high temperatures in Arabidopsis is beneficial.

Further testing of these transgenic plants could yield lines with cotton Rca protein, but a higher throughput method to investigate protein expression is likely to be required. It is possible that rapid

degradation of the cotton Rca protein occurs in the transgenic lines and it would be interesting to investigate this further. However, it may be preferable, first of all, to repeat the transformations with a different vector backbone. An antibody specific to the GhRca proteins would show whether the cotton Rca protein was present in the transgenic plants, especially if the protein was being masked by changes in the expression of the native wheat Rca isoforms. However, this could be difficult due to the similarities between the wheat and cotton Rca proteins. Further research regarding the residues influencing the thermal tolerance of Rca is required. Transient expression experiments with Green Fluorescent Protein (GFP) or GUS tagged proteins associated with promoters and the wheat or cotton transit peptides would provide proof (or otherwise) of promoter or transit peptide function in wheat. Over-expression of wheat Rca in wheat plants would help answer questions about the regulation of Rca and whether the tight regulation of these proteins may be impacting upon the expression of the *GhRca* transgenes. Additionally, the amount of other photosynthetic enzymes should also be investigated as rice plants over expressing maize or barley Rca had slightly increased activation states and faster light activation yet decreased photosynthetic assimilation, due to a down-regulation of the amount of leaf Rubisco (Fukayama *et al.*, 2012).

4. Characterisation and regulation of Rubisco activase in wheat

Wheat Rubisco activase (Rca) gene analysis as published in: Carmo-Silva E., Scales J.C., Madgwick P.J. & Parry M.A.J. (2014) Optimizing Rubisco and its regulation for greater resource use efficiency. *Plant, Cell & Environment*. DOI: 10.1111/pce.12425

Gene sequences have been submitted by Scales J.C. to EMBL (<http://www.ebi.ac.uk/ena/>) and are publicly available under the accession numbers LM992844 (*TaRca1-β*), LM992845 (*TaRca2-β*) and LM992846 (*TaRca2-α*).

Virus-induced gene silencing experiment was completed in conjunction with a masters project student, Will Pelton, from Imperial College, Elizabeth Carmo-Silva and the VIGS group at Rothamsted.

4.1 Introduction

Improved understanding of the regulation of Rca will inform efforts to improve the regulation of Rubisco, with the ultimate aim of increasing carboxylation and crop yield. The number of Rca isoforms and their gene structure has been shown to differ between species. For example, *Nicotiana tabacum* only has only a short isoform of Rca, whilst *Spinacia oleracea* and *Arabidopsis* have both a longer and a shorter isoform (Salvucci *et al.* (1987); see Introduction). Western blot analysis of protein extracts from *Triticum aestivum* L. (wheat) leaf tissue detected two Rca bands, corresponding to a longer (α) 46 kDa TaRca, and a shorter (β) 42 kDa TaRca in (Salvucci *et al.*, 1987). The longer TaRca α isoform appears to represent only about 12.5% of the total Rca pool in this species (Law & Crafts-Brandner, 2001). Understanding the structure and regulation of *TaRca* genes and gene expression will assist with further research into understanding the regulation of Rubisco activity in wheat. Analysis of the available wheat genome sequence allowed identification of the *TaRca* genes and their splicing pattern. The diurnal accumulation of TaRca protein through the light-dark cycle in wheat was also investigated here.

Virus-induced gene silencing (VIGS) was used to silence genes encoding individual *TaRca* isoforms to provide initial information to begin characterising their regulation. VIGS exploits the fact that infection by many RNA viruses activates a conserved, RNA-based, antiviral defence response known as RNA-

interference (RNAi). This process is mediated by small RNAs in a sequence specific manner. By inserting a fragment of a plant gene into a cloned virus genome, transcripts of the gene expressed by the plant become targets for degradation; thus causing the gene of interest to be significantly down-regulated or knocked down (reviewed by Lee *et al.* (2012)). This knockdown approach of genes of interest allows phenotypes resulting from gene silencing to be observed in relatively short time scales (as little as four weeks).

For VIGS in wheat a binary Barley Stripe Mosaic Virus (BSMV) system can be used to first deliver the virus vector into leaves of an intermediate plant host, *Nicotiana benthamiana* (Yuan *et al.*, 2011).

Nicotiana benthamiana leaves are infiltrated with *Agrobacterium tumefaciens* transformed with the viral vector modified to silence the gene of interest; this infected leaf tissue can then be used to rub inoculate susceptible wheat plants. The BSMV has a tripartite genome made up of α , β and γ RNAs (Jackson *et al.*, 2009); the γ plasmid can be modified to contain the plant gene fragment needed to induce target gene silencing (Yuan *et al.*, 2011). In the host plant cell, the long double-stranded RNAs (dsRNAs) formed during viral replication are recognised by host Dicer-like enzymes (DCLs). DCLs cleave the dsRNAs into 21- 22 nucleotide short- interfering RNAs (siRNAs; Hamilton *et al.* (2002)). One strand of each siRNA is incorporated into host RNA-induced silencing complexes (RISC). RISC mediates the endonucleolytic cleavage of single-stranded RNAs with sequences complementary to the incorporated siRNA strand (reviewed by Hannon (2002)). As some of the siRNAs will be produced from the plant gene fragment of interest which is inserted in the BSMV genome, they will guide RISC to complementary plant mRNAs, resulting in silencing of the target plant gene.

In this VIGS experiment five constructs were generated to silence the two wheat *Rca* genes: two to silence *TaRca1- β* , one to silence *TaRca2* (preventing expression of both α and β isoforms) and two to silence *TaRca2- α* (only silencing the α isoform of *TaRca2*). The expression of the respective genes and the amount of total TaRca was evaluated in the BSMV:VIGS plants by comparison with control plants, inoculated with a construct containing a fragment of the GFP gene.

4.2 Materials and methods

4.2.1 Plant material and growth conditions

Triticum aestivum L. (cv. Cadenza) was grown in the glasshouse (16 hour day/ 8 hour night, 20°C/ 18°C) for measurement of TaRca protein amounts through the light/dark cycle. Plants were grown until approximately 30 cm high (~6 weeks old) with fully developed leaves. Plants were grown in trays and then individually transplanted into 12.5 cm pots. Two days prior to beginning sampling plants were moved to a controlled environment growth chamber on same light/temperature cycle as the glasshouse to ensure plants were in a completely stable environment.

For VIGS, plant growth and inoculation was carried out as in Lee *et al.* (2014). Plants were grown in a controlled environment chamber at 23°C, 60% RH and with a 16 hour photoperiod (of approximately 180 $\mu\text{mol m}^{-2} \text{s}^{-1}$ light). *Nicotiana benthamiana* was grown from seed in John Innes Levington F2+S compost, and *Triticum aestivum* L. (cv. Bob White) was germinated on moist sand until a radicle could clearly be seen and were then transplanted into Rothamsted Prescription Mix compost (see Chapter 3 for components).

4.2.2 Characterising wheat Rubisco activase genes

The Arabidopsis *Rca* sequence was BLAST searched against the *Brachypodium distachyon* genome (Phytosome; DOE Joint Genome Institute, Walnut Creek, USA; modelcrop.org.) to identify the *Rca* genes and their intron/exon structure. The sequences, including exons and introns, were used in turn to search the wheat genome database (cv. Chinese Spring; URGI, Unité de Recherche Génomique Info, Versailles, France; The International Wheat Genome Sequencing Consortium 2014). The genomic sequences identified from URGI were aligned using Geneious 7.1.5 (Biomatters, San Francisco, USA). The corresponding genes were sequenced from genomic DNA extracted from wheat (cv. Cadenza), using a QIAprep Spin Miniprep Kit (Qiagen, Manchester, UK). The genes were amplified using Phusion proofreading Taq (New England BioLabs Inc., Hitchin, UK) and cloned into pGEM-T easy vectors according to the manufacturer's instructions (Promega, Southampton, UK), prior to sequencing by Eurofins (Cambridge, UK). The PCR conditions for the TaRca primers (Table 4.1) were 98°C for 30 s

followed by 40 cycles of, 98°C for 10 s, 65°C for 50 s and 72°C for 20 s, and a final extension step at 72°C for 5 min.

Table 4.1. Primers used to amplify *TaRca* genes for sequencing.

	Primer sequences
<i>TaRca1-β</i>	
F- Rca1F	AAT CAT ATG GCG GCC AAA AAG GAA CTT GAC G
R- Rca1R	TTT GGA TCC TAC TTG CCG TAG AAG GCG C
<i>TaRca2- α/β</i>	
F- Rca2F	AAT CAT ATG GCA GCG GAA AAC CTC GAC GAG
R- Rca2longR	GAT GGA TCC TTA AAA GGT GTA AAG GCA GC

4.2.3 Diurnal Rubisco activase protein cycle

To enable measurement of the amount of Rca protein in wheat over the light/dark cycle, three leaf discs (1- 1.5 cm² leaf tissue) were harvested from three plants at 31 individual time points across 2.5 days and frozen in liquid nitrogen (Table 4.2). For the protein extractions, frozen leaf samples were homogenised in 0.5 mL extraction buffer (50 mM Tricine-NaOH, pH 8.0, 10 mM EDTA and 1% (w/v) PVP-40) in an ice cold homogeniser. The sample was then centrifuged for 3 min at 14, 000 x g at 4°C and the supernatant collected. Total soluble protein concentration was determined by the Bradford method (Bradford, 1976). Sample volumes corresponding to 1.5 µg TSP were separated by electrophoresis on 48-well 8% E-PAGE gels and western blotted as in Chapter 3, using the E-Base and iBlot Invitrogen systems (Invitrogen, Life Technologies, Paisley, UK).

Table 4.2. Sample collection times for measuring diurnal Rca protein amounts. Samples were collected at each time point for 2.5 days (with the last samples being collected at 10.50 on the third morning).

Sample collection time-point	
04:20	
04:50	Lights on
05:05	
05:20	
05:50	
06:35	
07:50	
10:50	
13:50	
16:50	
19:50	
20:50	Lights off
21:50	

4.2.4 Virus-induced gene silencing of Rubisco activase in wheat

To identify Rca silencing fragments the software program Si-Fi (<http://labtools.ipk-gatersleben.de/>) was used (by Kostya Kanyuka, VIGS group, Rothamsted Research) to predict the most efficient regions in each wheat Rca sequence for siRNA production, and to check that non-target genes were unlikely to be silenced. Using this information, sequences were selected for use in silencing constructs and primers were designed (Table 4.3) to amplify these fragments: BSMV:Rca1 β -1 (108 base pairs (bp)), BSMV:Rca1 β -2 (129bp), BSMV:Rca2 (190bp), BSMV:Rca2 α -1 (117bp) and BSMV:Rca2 α -2 (150bp). The VIGS vector used was the BSMV-VIGS system described by Yuan *et al.* (2011), comprising three T-DNA binary plasmids, pCaBS- α , pCaBS- β , and pCa- γ LIC.

Table 4.3. Primers used for amplification of *TaRca* gene fragments for VIGS construct preparation. Constructs were designed for silencing of: *TaRca1* (BSMV: Rca1 β -1 and BSMV: Rca1 β -2), both the *TaRca2- α* and *TaRca2- β* isoforms (BSMV: Rca2), and the *TaRca2- α* isoform only (BSMV: Rca2 α -1 and BSMV: Rca2 α -2)

<i>TaRca</i> silencing fragment	Primer sequences
BSMV:Rca1β-1	
F	AAC CAC CAC CAC CGT GCC AAA AAG GAA CTT GAC GAG
R	AAG GAA GTT TAA GGA GTC CAC GAT ACC TTT CC
BSMV:Rca1β-2	
F	AAC CAC CAC CAC CGT CGA TCG GTG GAA GGG TCT C
R	AAG GAA GTT TAA CCC TGG CTG ATG TAC TCG TA
BSMV:Rca2	
F	AAC CAC CAC CAC CGT AAG GAG GAG AAC CCT CGT GTG
R	AAG GAA GTT TAA GAC GAT CTT GAC GAC GGA CTC
BSMV:Rca2α-1	
F	AAC CAC CAC CAC CGT GCA CAG CAA GGT ACT TTG CCT GT
R	AAG GAA GTT TAA TTA AAA GGT GTA AAG GCA GCT SCC G
BSMV:Rca2α-2	
F	AAC CAC CAC CAC CGT GGT TCC TTC TAC GGT AAA GG
R	AAG GAA GTT TAA TTA AAA GGT GTA AAG GCA GCT S

To obtain *TaRca* cDNA sequences for the VIGS constructs, a TRIzol total RNA extraction protocol, adapted from the manufacturer's instructions (Invitrogen, Life Technologies, Paisley, UK) was used to extract RNA from wheat (cv. Cadenza). First-strand cDNA synthesis using oligo(dT)₂₀ was completed using SuperScript®III First-Strand Synthesis System for RT-PCR (Invitrogen, Life Technologies, Paisley, UK). Fragments for use in VIGS were amplified from the cDNA library using Phusion DNA polymerase (New England BioLabs Inc., Hitchin, UK). PCR conditions were 98°C for 30 s followed by 40 cycles of, 98°C for 10 s, 70°C for 10 s and 72°C for 10 s, and a final extension step at 72°C for 5 min.

The pCa- γ bLIC plasmid contains a ligation independent cloning site to allow insertion of sequences designed to induce silencing. The plasmid was digested with *ApaI* and both the PCR fragments and plasmid were treated with T4 DNA polymerase (NEB, Hitchin, UK) to produce complementary sticky ends. The PCR fragments and plasmids were then incubated together at 65°C for 2 min followed by 15 min at 22°C to allow them to anneal their complementary sticky ends. JM109 competent cells (Promega, Southampton, UK) were transformed with the ligated plasmid using the manufacturer's standard protocol. The cells were then plated on Lysogeny Broth (LB)- Lennox (10 g L⁻¹ tryptone, 5 g L⁻¹ yeast extract, 10 g L⁻¹ NaCl and 15 g L⁻¹ Agar) containing 50 μ g mL⁻¹ kanamycin. Plasmid DNA purification was completed using the QIAprep® Spin Miniprep Kit protocol (Qiagen, Manchester, UK).

For transformation of *Agrobacterium tumefaciens* cells by electroporation, a MicroPulser™ (Bio-Rad, Hercules, USA) was used following an adapted Bio-Rad protocol. Electro competent GV3103 cells (20 µL) were mixed with 2 µL of the γ plasmid DNA containing the silencing fragment (100 ng µL⁻¹), and pulsed for ~5 s at ~2 kV. The cells were then plated onto LB- Lennox agar plates containing 50 µg mL⁻¹ kanamycin (to select for the virus containing plasmid), and 25 µg mL⁻¹ gentamycin (to select for strain GV3101 containing the Ti (tumour inducing) helper plasmid pMP90, where the machinery necessary for T-DNA transfer resides). The plates were incubated for 2- 3 days at 28°C. BSMV plasmid-transformed *Agrobacterium* were prepared for inoculation into *N. benthamiana* by inoculating single colonies from the LB- Lennox plates into liquid LB, containing 50 µg mL⁻¹ of kanamycin. These were incubated for 22 hr at 28°C with shaking, and then centrifuged (2,400 x g for 15 min at 4°C) and re-suspended in inoculation buffer (10 mM MES, pH 5.6, 10 mM MgCl₂ and 100 µM acetosyringone) to an optical density at 600 nm of 1.5.

Suspensions of the α , β and γ (all prepared as described for the γ plasmid above) BSMV plasmids were then mixed together in a 1:1:1 ratio and infiltrated into the abaxial side of 3- 4 week old *N. benthamiana* plants with a 1 mL needleless syringe. Three to four days post-infiltration, once virus symptoms were visible on *N. benthamiana* infected leaves, the infiltrated leaves were harvested, and ground in 10 mM potassium phosphate buffer (pH 6.8) containing 1% celite. This homogenate was used to mechanically inoculate the first leaf of 11 day old wheat plants (by applying the homogenate onto wheat leaves dusted with caborundum and rubbing gently using a finger-tip). BSMV:asGFP, a construct containing a fragment of the GFP gene, was used as a control virus treatment. After 14 days samples were harvested for both qRT-PCR and western blotting. A 10 cm length of leaf tissue was harvested from the fourth leaf. Samples were collected 5- 7 hr into the light period to ensure maximal TaRca protein expression.

To investigate gene expression in the *TaRca* silenced plants RNA extractions for qRT-PCR were completed using the hot phenol method and cDNA was synthesised (see Chapter 3 for details). Three primer pairs were used for qRT-PCR (Table 4.4) of the *TaRca* genes, each pair specific to an isoform sequence. Eukaryotic Translation Initiation Factor (*eIF4E*) and Tonoplast Intrinsic Protein (*TIP*) were

used as reference genes. Between 8- 11 biological replicates were collected for each VIGS treatment with three technical replicates of each sample.

Table 4.4. qRT-PCR primer pairs for measuring *TaRca* gene expression in wheat plants inoculated with VIGS constructs.

Primer pairs	Primer sequences
TIP	
F- prTYW399_TIP41L_L_359	TGC AGC AAA ATG GAA ATT CA
R- prTYW400_TIP41L_R_475	TGC GTA GCA TCT TGG TTC AG
eIF4E	
F- eIF4E-1F	TGG CAA GCA GTG GAA GGA GT
R- eIF4E-1R	TCA CGG GAT CAA ACG GTG TAG
<i>TaRca1-β</i>	
F	GGG TCG GCG AGA TCG GCG T
R	CCA GCA TGT GGC CGT ACT CCA TG
<i>TaRca2-α</i>	
F	CCT TCT ACG GTA AAG GGG CAC AG
R	TGT AAA GGC AGC TCC CGT CGT
<i>TaRca2-β</i>	
F	CCA TAC ACA CCC ACC ATC TCT TGC
R	TGT AAA GGC AGC TCC CGT CGT

Analysis of the TaRca protein in the silenced plants was completed. For the protein extractions, frozen leaf samples were homogenised in 1.2 mL extraction buffer (50 mM Tricine-NaOH, pH 8.0, 10 mM EDTA and 1% (w/v) PVP-40) in an ice-cold homogeniser. The sample was then centrifuged for 3 min at 14,000 x g at 4°C and the supernatant collected. To 52 µL of the sample supernatant, 8 µL Novex Reducing Agent and 2 µL E-PAGE Loading Buffer were added before incubating at 95°C for 3 min. The total soluble protein (TSP) amount in each sample was measured using Bradford reagent (Bradford, 1976) and denatured samples were then diluted based upon TSP to a concentration of 0.75 mg mL⁻¹ with Novex reducing agent and E-PAGE loading buffer (Invitrogen, Life Technologies, Paisley, UK).

Sample volumes corresponding to 0.75 µg TSP were run on 48-well 8% E-Page gels (Life Technologies, Paisley, UK) using the E-Base Invitrogen system and western blotted using the Invitrogen iBlot system (Chapter 3). Each gel was repeated twice, once for coomassie staining and once for western blotting. The membranes and gels were photographed using a G:BOX system (Syngene, Gurgaon, India) and images analysed using Image Studio Lite Software (LI-COR, Lincoln, USA) and SigmaPlot 12.5 software (Systat Software Inc., San Jose, USA).

4.3 Results

4.3.1 Wheat Rubisco activase gene structure

The wheat genome is allohexaploid, containing three copies of each *TaRca* gene representing ancestrally distinct homologous genomes, A, B, and D. With use of bioinformatics homologous regions encoding for *TaRca* were identified on three different chromosomes, 4AL, 4BS and 4DS. The exon/intron structure of the tandem *TaRca* genes, *TaRca1* and *TaRca2*, is shown in Figure 4.1.

TaRca1-β is 1306 bp long contains two exons, and is predicted by ChloroP (Emanuelsson *et al.*, 1999) to have a chloroplast transit peptide (TP) of 48 amino acids, resulting in a mature polypeptide of 42.7 kDa. The intron occurs within the TP such that the mature protein (TaRca1-β) is encoded solely by exon 2. There is no evidence of alternative splicing of this gene and therefore it can be considered as encoding the short TaRca-β isoform. The longer *TaRca2* gene can produce both an α and β isoform through alternative splicing. *TaRca2* has up to six exons; the mature protein coding sequence starts in exon 2 and alternative splicing at the end of exon 5 results in either a stop codon (TaRca2-β) or when spliced five bases before this point, an extended intron with read-through allowing translation of exon 6 (TaRca2-α). The TaRca2-α isoform is 37 amino acid residues longer than TaRca2-β (Figure 4.1). *TaRca2* is predicted to have a transit peptide of 47 amino acids, giving a TaRca2-β isoform of 42.2 kDa, and a TaRca2-α isoform of 46 kDa. The two β isoforms cannot be separated visually, but are distinguishable from the longer α isoform on western blots.

Coding sequence for the mature forms of *TaRca1-β*, *TaRca2-β* and *TaRca2-α* from the B genome [the most highly expressed homologues, as indicated by expressed sequence tags (EST) data; Alison Huttly, personal communication] was cloned from *Triticum aestivum* (cv. Cadenza) and sequenced. The wheat *TaRca* nucleotide sequences from cloning have been submitted to EMBL (<http://www.ebi.ac.uk/ena/>) and are publicly available under the accession numbers LM992844 (*TaRca1-β*), LM992845 (*TaRca2-β*) and LM992846 (*TaRca2-α*).

The two *TaRca* genes share 83% identity in nucleotide sequence and encode TaRca-β proteins that are 88% identical in their amino acid sequences (Figure 4.2). Both coding sequences are identical to those

identified within the published Chinese Spring wheat genome sequences (URGI; IWGSC, 2014, The International Wheat Genome Sequencing Consortium). Comparison of the three wheat genomes showed a high homology (97- 98%) between the nucleotide sequences encoding mature TaRca protein (Table 4.5). Most of these nucleotide differences are silent and the resulting amino acid sequences are 99% identical, with a maximum of four amino acids differing between the isoforms encoded by the three wheat genomes Carmo-Silva, Scales *et al.* (2014).

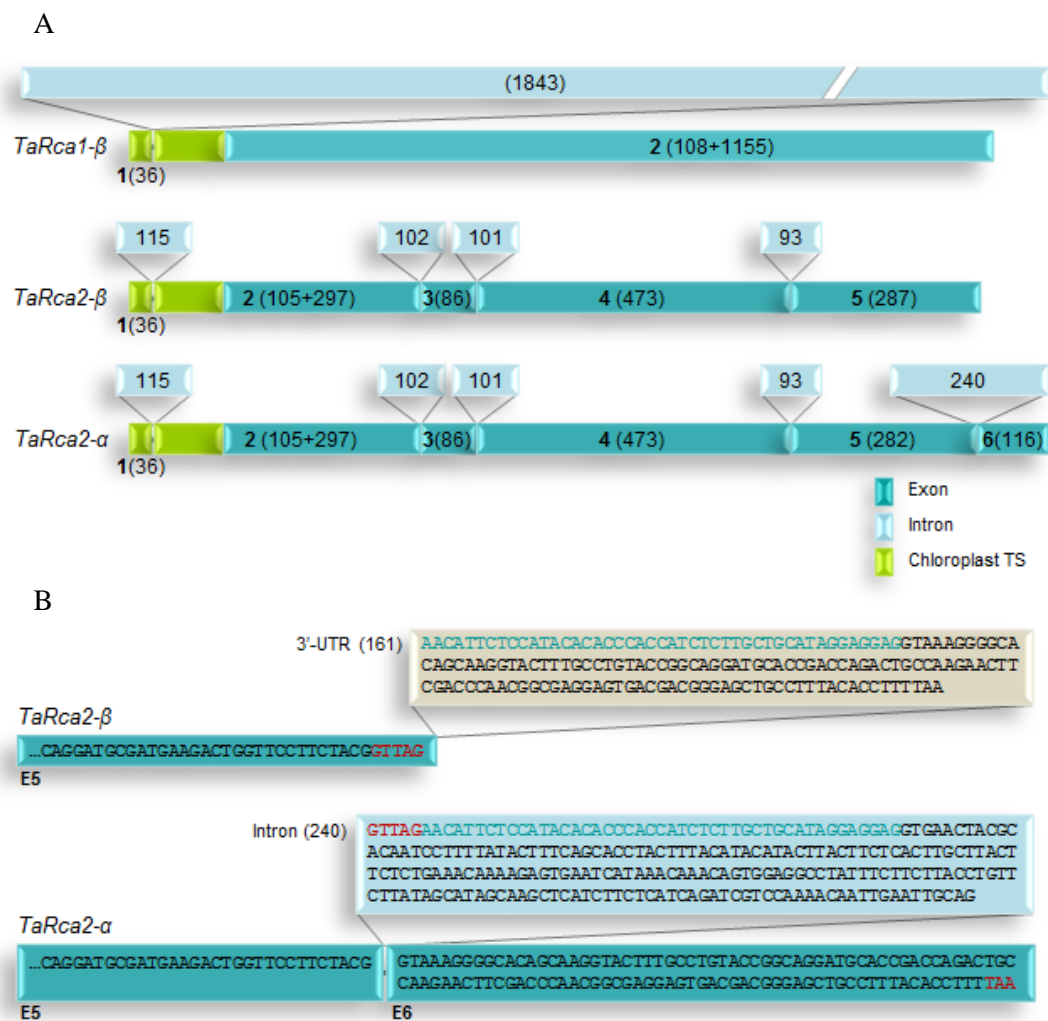


Figure 4.1. A representative schematic of the *TaRca* isoform gene sequences (*TaRca1* and *TaRca2*), and the splice variants of *TaRca2*.

The intron/ exon structure of the two *TaRca* genes is illustrated (A). Indicated are the predicted chloroplast transit peptide (green), the introns (pale blue) and exons (dark blue). The splicing at the end of exon 5 (E5) of *TaRca2* (B) shows the bases (red) and intron (pale blue) spliced out to result in the *TaRca2-α* isoform rather than the *TaRca2-β* isoform. Exon numbers are shown, with the corresponding number of nucleotides in brackets.

A

TaRca1-β	AAKKELDEGKQTNADRWKGLAYDISDDQQDITSGKGI VDSL FQAPMGDGT	50
TaRca2-β/α	AAEN-LDEKRNT--DKWKGLAYDISDDQQDITRGKGI VDSL FQAPTGDGT	50
TaRca1-β	HEAILSSYEYISQGLRKYDFDNTMDGLYIAPAFMDKLI VHLAKNFMTLPN	100
TaRca2-β/α	HEAVLSSYEYVVSQGLKKYDFDNTMGGFYIAPAFMDKLVVHLSKNFMTLPN	100
TaRca1-β	IKVPLILGIWGGKGQKSFQCELVFAKMGINPIMMSAGELESGNAGEPAK	150
TaRca2-β/α	IKIPLILGIWGGKGQKSFQCELVFAKMGINPIMMSAGELESGNAGEPAK	150
TaRca1-β	LIRQRYREAADIINKGKMCCLFINDLDAGAGRMGGTTQYTVNNQMVNATL	200
TaRca2-β/α	LIRQRYREAADMIIKKGKMCCLFINDLDAGAGRMGGTTQYTVNNQMVNATL	200
TaRca1-β	MNIADAPTNVQLPGMYNKEENPRVPIIVTGNDFSTLYAPLIRDGRMEKFY	250
TaRca2-β/α	MNIADAPTNVQLPGMYNKEENPRVPIIVTGNDFSTLYAPLIRDGRMEKFY	250
TaRca1-β	WAPTREDRIGVCKGIFRTDNVPEAVVRLVDTFPGQSIDFFGALRARVYD	300
TaRca2-β/α	WAPTRDDRIGVCKGIFQTDNVSDSVVKIVDTFPGQSIDFFGALRARVYD	300
TaRca1-β	DEVKRWVGEIGVENISKRLVNSREGPPTFDQPKMTIEKLM EYGHMLVQEQ	350
TaRca2-β/α	DEVKRWVITSTGIENIGKRLVNSRDGPVTFEQPKMTVEKLL EYGHMLVQEQ	350
TaRca1-β	ENVKRVQLADKYLSEAAALGQANDDAMKTGAFYGK-----	400
TaRca2-β	DNVKRVQLADTYMSQAALGDANQDAMKTGSFYG-----	400
TaRca2-α	DNVKRVQLADTYMSQAALGDANQDAMKTGSFYGKGAQQGTL PVPAGCTDQ	400
TaRca1-β	-----	418
TaRca2-β	-----	418
TaRca2-α	TAKNFDPTARSDDGSCLYTF	418

B



Figure 4.2. Predicted amino acid sequence and the structural protein regions of TaRca1 and TaRca2. Differences between the two amino acid sequences are highlighted in grey (A). The protein regions (B) are highlighted with coloured lines which correspond to the protein structure: N-terminus (green), AAA+ region (yellow), Rubisco recognition domain (blue), C-terminus (orange), C-terminal extension (red).

Table 4.5. Comparison of the mature coding sequence of *TaRca* genes and resulting proteins.

Gene	<i>TaRca1-β</i>	<i>TaRca2-β</i>	<i>TaRca1-α</i>
Total number of nucleotides	1155	1143	1254
Nucleotide differences			
Genomes A & B	26	15	17
Genomes B & D	29	16	17
Genomes A & D	19	12	13
Protein	TaRca1-β	TaRca2-β	TaRca1-α
Total number of amino acids	384	380	417
Amino acid differences			
Genomes A & B	4	2	2
Genomes B & D	4	3	3
Genomes A & D	0	1	1

4.3.2 Diurnal Rubisco activase protein amount

The relative amounts of Rca protein in young fully-expanded wheat leaves were consistent through the majority of the light phase. A decline was evident from the samples taken 1 hour before the lights were switched off, and continuing on into the dark period. The amount of Rca was already near maximal in the samples taken 30 min before the lights were switched on (Figure 4.3).

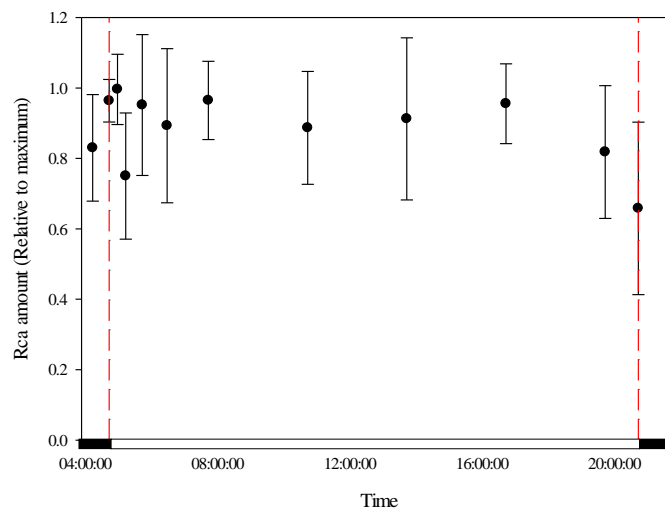


Figure 4.3. The relative amounts of Rca protein in wheat (cv. Cadenza) leaves collected at regular intervals during the light-dark diurnal cycle.

Samples were collected across 2.5 days and protein amount calculations were based on the western blot mean band density at each time point. Values are means \pm SEM of 5-9 biological replicates.

4.3.3 Virus-induced gene silencing of Rubisco activase in wheat

TaRca genes were independently silenced using VIGS. To maximise the chances of silencing the target *TaRca* genes, different length sequences were tested to silence the same genes (indicated on Figure 4.4). These included two partly overlapping constructs attempting to silence *TaRca1- β* (BSMV:Rca1 β -1 and BSMV:Rca1 β -2), two overlapping constructs to silence the *TaRca2- α* isoform (BSMV:Rca2 α -1 and BSMV:Rca2 α -2) and a single construct to silence both the *TaRca2- α* and β isoforms (BSMV:Rca2). The choices for silencing sequences were limited as the two *TaRca* wheat genes show high homology and the two *TaRca2* isoforms only differ in the C-terminal extension sequence, present in *TaRca2- α* but not *TaRca2- β* .

<i>TaRca1-β</i>	ATGGCTTCTGCTTTCTCTCCACCGTTGGAGCTCCGGCGTCGACCCCGACCACCTTCTCTCGGGAA	65
<i>TaRca2-α/β</i>	ATGGCTGCTGCTTTCTCTCCACCGTCGGTGCCCGGCTTCTACGCCGACCAACTTCTCTCGGGAA	65
<i>TaRca1-β</i>	GAAGGTGAAGAAGCAGG---CCGGTGCCTTGAAGTACTACCATGG--TG-GCAACAAGATCAACA	130
<i>TaRca2-α/β</i>	GAAGCTCAAGAAGCAGGTGACCTCGGCCGTGA---ACTACCATGGCAAGAGCTCCAAGGCCAACA	130
<i>TaRca1-β</i>	ATAGGGTGTTCAGGGCCATGGCGCCAAAAGGAAGTGTGACGAGGGCAAGCAGACCGATGCGGAT	195
<i>TaRca2-α/β</i>	G-----GTTACAGTTCATGGCAGCGGAAA---ACATCGACGAG---AAGAGGA---ACACAGAC	195
<i>TaRca1-β</i>	CGGTGGAAGGGTCTCGCTTACGACATCTCCGATGACCAGCAGGACATCACGAGGGGGAAAGGCAT	260
<i>TaRca2-α/β</i>	AAGTGGAAAGGGTCTTGCCTACGATATCTCCGACGACCAGCAGGACATCACGAGGGAAAGGCAT	260
<i>TaRca1-β</i>	CGTGGACTCCCTGTTCCAGGCCCCCATGGGCGACGGCACCCACGAGGCCATCTGAGCTCCTACG	325
<i>TaRca2-α/β</i>	CGTGGACTCCCTCTTCCAGGCGCCACGGGCGACGGCACCCACGAGGCCGTCCTCAGCTCCTACG	325
<i>TaRca1-β</i>	AGTACATCAGCCAGGGCTGCGCAAGTACGACTTCGACAACACCATGGACGGGCTGTACATCGCC	390
<i>TaRca2-α/β</i>	AGTACGTCAGCCAGGGACTCAAGAAGTACGACTTCGACAACACCATGGGAGGCTTCTACATCGCT	390
<i>TaRca1-β</i>	CCGGCGTTCATGGACAAGTTCATCGTCCACTCGCCAAGAACTTCATGACACTCCCAACATCAA	455
<i>TaRca2-α/β</i>	CCTGCTTTCATGGACAAGCTTGTGTGCCATCTCTCCAAGAACTTCATGACCTGCCAACATCAA	455
<i>TaRca1-β</i>	GGTCCCTCTCATCTTGGGTATCTGGGGAGGCAAGGGACAGGGCAAGTCGTTCCAGTGCAGCTGG	520
<i>TaRca2-α/β</i>	GATCCCACTCATCTTGGGTATCTGGGGAGGCAAGGGTCAAGGAAAATCCTTCCAGTGTGAGCTTG	520
<i>TaRca1-β</i>	TGTTCCGCAAGATGGGCATCAACCCCATCATGATGAGCGCCGAGAGCTGGAGAGCGGCAACGCC	585
<i>TaRca2-α/β</i>	TCTTCGCAAGATGGGCATCAACCCAAATCATGATGAGTGCCGAGAGCTGGAGAGTGGCAACGCC	585
<i>TaRca1-β</i>	GGCGAGCCGCCAAGCTGATCCGGCAGAGGTACCGCGAGGCTGCCGACATATCAAGAAGGGCAA	650
<i>TaRca2-α/β</i>	GGAGAGCCAGCCAAGCTCATCAGGCAGCGGTACCGTGAGGCTGCAGACATGATCAAGAAGGGTAA	650
<i>TaRca1-β</i>	GATGTGCTGCCTCTTCATCAACGACCTGGACGCCGGCGGGGGCGGATGGGCGGGACGACGAGT	715
<i>TaRca2-α/β</i>	GATGTGCTGCCTCTTCATCAACGATCTTGACGCCGGTGCGGGTTCGGATGGGCGGGACCACAGT	715
<i>TaRca1-β</i>	ACACGGTGAACAACCAGATGGTGAACGCCACCCTGATGAACATCGCGGACGCGCCACCAACGTG	780
<i>TaRca2-α/β</i>	ACACCGTGAACAACCAGATGGTGAACGCCACCCTCATGAACATCGCCGATGCCCCACCAACGTG	780
<i>TaRca1-β</i>	CAGCTCCCAGGATGTACAACAAGGAGGAGAACCACGCGTGCCCATCATCGTCACCGGCAACGA	845
<i>TaRca2-α/β</i>	CAGCTCCCAGGATGTACAACAAGGAGGAGAACCCTCGTGTGCCATCGTCGTCACCTGGTAACGA	845
<i>TaRca1-β</i>	CTTCTCGACGCTGTACGCCCCCTCATCCGGGACGGCCGATGGAGAAGTTCTACTGGGCGCCCA	910
<i>TaRca2-α/β</i>	TTTCTCAAGTGTACGCCCTCTCATCCGTGATGGTCTGATGGAGAAGTTCTACTGGGCTCCCA	910
<i>TaRca1-β</i>	CCCGGAGGACCGCATCGGCGTGTGCAAGGGCATCTTCCGACCGACAACGTCGCCGACGAGGCC	975
<i>TaRca2-α/β</i>	CCCGGAGGACCGCATCGGCGTGTGCAAGGGCATCTTCCGACCGACAATGTCAGCGACGAGTCC	975
<i>TaRca1-β</i>	GTGGTGAGGCTGGTGGACACCTTCCCGGGCAGTCCATCGACTTCTTCGGGCGCGCTGCGGGGCGG	1040
<i>TaRca2-α/β</i>	GTCGTCAAGATCGTCGACACCTTCCAGGACAATCCATCGACTTTTTCGGTGCTCTGCGTGTCTCG	1040
<i>TaRca1-β</i>	GGTGTACGACGACGAGGTGCGCAAGTGGGTCCGGCAGATCGGCGTCGAGAACATCTCCAAGCGGC	1105
<i>TaRca2-α/β</i>	GGTGTACGACGACGAGGTGCGCAAGTGGGTGACCTCTACCGGTATCGAGAACATTTGGCAAGAGC	1105
<i>TaRca1-β</i>	TCGTCAACTCCAGGGAGGGCCGCCGACGTTTCGACCAGCCCAAGATGACCATCGAGAAGCTCATG	1170
<i>TaRca2-α/β</i>	TTGTGAACTCGCGGGACGGACCAAGTACCTTTGAGCAGCCAAGATGACAGTCGAGAAGCTGCTA	1170
<i>TaRca1-β</i>	GAGTACGGCCACATGCTGGTCCAGGAGCAGGAGAAGCTGAAGCGCGTGCAGCTGCCGACAAGTA	1235
<i>TaRca2-α/β</i>	GAGTACGGCCACATGCTGGTCCAGGAGCAGGACAATGTCAAGCGGTGTGCAGCTTGTGACACCTA	1235
<i>TaRca1-β</i>	CCTCAGCGAGGCGGCGCTCGGCCAAGCCAACGACGACGCATGGCGACCGGCGCCTTCTACGGCA	1300
<i>TaRca2-α/β</i>	CATGAGCCAGGACGCTCTGGGTGATGCTAACCCAGGATGCATGAAGACTGGTTTCTTCTACGGTT	1300

BSMV:Rca1β-1
BSMV:Rca1β-2

BSMV:Rca1β-1
BSMV:Rca1β-2

BSMV:Rca1β-2

BSMV:Rca1β-1

BSMV:Rca1β-2

BSMV:Rca2β

BSMV:Rca2β

BSMV:Rca2β

BSMV:Rca2β

BSMV:Rca2α-2



Figure 4.4. Sequence of *TaRca* genes with the five BSMV:Rca construct sequences indicated by coloured lines. BSMV:Rca1β-1 and BSMV:Rca1β-2, and BSMV:Rca2α-1 and BSMV:Rca2α-2 contain overlapping sections of sequence. The second construct in each pair is longer to increase the likelihood of silencing. Differences between the *TaRca* gene sequences are highlighted in grey.

Primers specific to the *TaRca* genes and isoforms were used to determine gene expression levels in plants inoculated with each of the silencing constructs (Figure 4.5). This was achieved by targeting primers to amplify a region in the 3' untranslated region (3'-UTR) of *TaRca2-β*, i.e. after the splicing event, and in the C-terminal extension of *TaRca2-α*. Plants inoculated with BSMV:Rca1β-1 and BSMV:Rca1β-2 accumulated low levels of mRNA transcript across all the isoforms. Despite the silencing sequence being specific to the *TaRca1* gene, a reduction in the *TaRca2* gene transcripts was observed. The BSMV:Rca2 construct plants accumulated low levels of *TaRca2-α* and *TaRca β* mRNA, whereas *TaRca1-β* expression was comparable to that of the control BSMV:asGFP construct plants. The BSMV:Rca2α-1 and BSMV:Rca2α-2 constructs plants had reduced amounts of both *TaRca2-α* and *TaRca2-β* transcripts. In both the BSMV:Rca2α-1 and BSMV:Rca2α-2 constructs the level of *TaRca1-β* expression is comparable to that of the control.

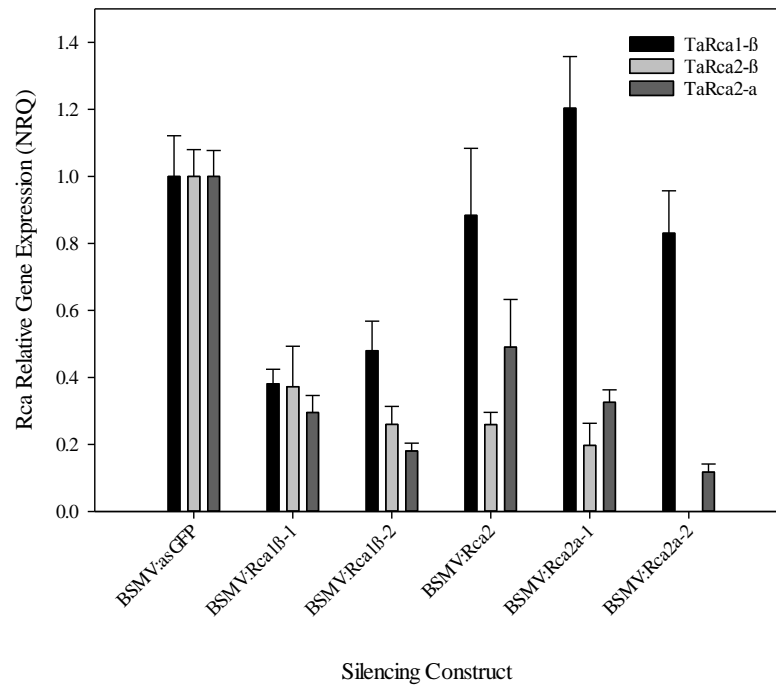


Figure 4.5. The relative gene expression levels (NRQ) of the three *TaRca* isoforms in wheat leaf tissue samples inoculated with BSMV:Rca silencing constructs. Calculations of transcript expression are shown relative to that of the individual gene expression in the control BSMV:asGFP samples. All the data were normalised using *eIF4E*. Data for *TaRca2-β* for BSMV:Rca2α-2 is not available. Values are means \pm SEM.

The western blot analysis (Figure 4.6A) revealed differing degrees of silencing when the relative amounts of TaRca protein were compared between the constructs. Plants infected with BSMV:Rca2 had the lowest amount of Rca protein (a 95% decrease compared to the BSMV:asGFP control). BSMV:Rca1β-1 and BSMV:Rca1β-2 showed a 60 and 74% decrease, respectively, and the BSMV:Rca2α-1 and BSMV:Rca2α-2 constructs a 36 and 52% decrease. The amount of Rubisco in the leaf samples was not significantly affected by the different BSMV:Rca silencing constructs (Figure 4.6B).

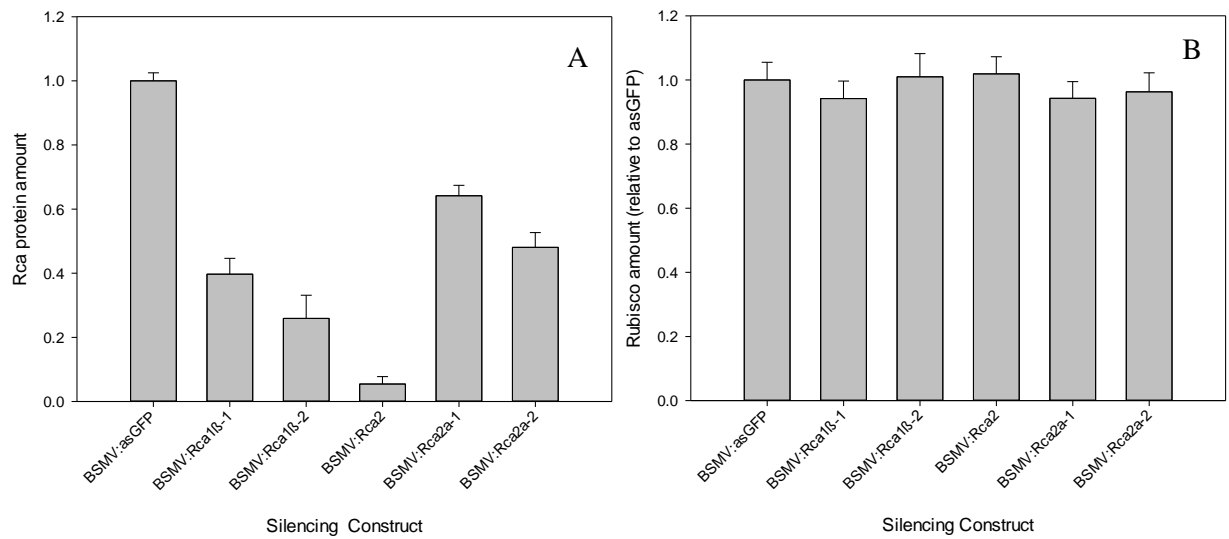


Figure 4.6. The relative protein amounts of Rca (A) and Rubisco (B) in wheat leaves of plants inoculated with Rca silencing constructs compared to the control (BSMV:asGFP). Calculations were based on the density of each western blot or stained SDS-Page gel band. Standard calibration curves were generated with dilution series from an BSMV:asGFP sample for each gel. Values are means \pm standard errors of the mean of 8- 11 biological replicates.

4.4 Discussion

The genes encoding Rca have previously been sequenced in other species including *Nicotiana tabacum* (Wang *et al.*, 1992), *Gossypium hirsutum* (Salvucci *et al.*, 2003) and *Arabidopsis* (Werneke *et al.*, 1989). The structure of the *TaRca* genes is similar to that of other related Poaceae species (i.e. *Oryza sativa* and *Brachypodium distachyon*). Information on the wheat gene structure (this chapter, Carmo-Silva, Scales *et al.* (2014)) provides a base for further research investigating wheat Rca properties and scope for improvement.

The diurnal protein amount pattern provides further evidence that there is a daily cycle regulating the amount of Rca protein in the plant, with this amount remaining stable through the light period and decreasing into the dark period. This information can be used to inform experiments investigating Rca, and it has been used here to indicate when to collect leaf samples to ensure Rca amounts are maximal (early in the light period). This also corroborates research in other plant species. Previous research investigating the abundance of *Rca* mRNA in apple plantlets (*Malus domestica* McIntosh 'Wijcik') also

showed a circadian cycle with a peak in protein amount 2 hours into the light period (Watillon *et al.*, 1993). Diurnal Rca cycles have also been reported in tobacco (Klein & Salvucci, 1995), Arabidopsis (Liu *et al.*, 1996), tomato (Martino-Catt & Ort, 1992) and cotton (Deridder & Salvucci, 2007). In barley, as in wheat, two genes are present; *RcaA* encodes alternatively spliced short and long isoforms, *RcaB* encodes a short form; and the three *Rca* mRNAs are differentially expressed both developmentally and diurnally (Rundle & Zielinski, 1991). Transcripts from the *RcaA* gene were found to be the predominant *Rca* mRNA in barley leaves with *RcaB* mRNA being 20- 100-fold less abundant than the *RcaA* transcripts. It would be of interest to complete further work to investigate the expression cycles of the different *Rca* transcripts in wheat and the interaction between mRNA transcripts and protein amounts and whether this changes upon exposure to stressful conditions.

Silencing the different *TaRca* isoforms using VIGS represents an early contribution towards increasing the understanding of *TaRca* gene expression regulation. The speed and ease of silencing and data collection was appealing. Rca isoforms have been effectively silenced with use of VIGS here in wheat, and in a previous study in rice. Ding *et al.* (2006) saw *Rca* mRNA levels decreased to 6% compared to the control plants when they used a VIGS construct targeted to the single *Rca* gene in rice.

The VIGS results here suggest that the constructs containing longer target sequences, BSMV:*Rca1β-2* and BSMV:*Rca2α-2*, induced stronger silencing in terms of the transcript and protein amounts. Previous research has shown that silencing sequences of lengths less than 120 bp produce lower levels of silencing (Scofield *et al.*, 2005), and the data here support this.

It is interesting that no impact was seen in this VIGS study on Rubisco protein amount. Studies in rice in which Rca is overexpressed lead to a decrease in the amount of Rubisco, and decreased photosynthetic rates (Fukayama *et al.*, 2012). This would suggest an association between the expression levels of these proteins; however this was not evidenced here when *TaRca* amounts were decreased by VIGS.

The combined results shown here suggest that co-regulation may occur both at the level of the *TaRca* mRNA transcript and *TaRca* protein. The qRT-PCR results showed that a decrease in *TaRca1* expression may also result in regulation of *TaRca2* expression. Based on the SiFi prediction programme results it is

unlikely that this response is due to non-target gene silencing and therefore this may suggest that a form of co-regulation of gene expression occurs in the plant. The differences between the gene sequences themselves, with SNPs spaced fairly evenly along the gene sequence, would also suggest any VIGS construct here would not silence both genes. A minimum of 21 consecutive identical bases between two genes would be needed to even theoretically result in the production of siRNAs that target both *TaRca1* and *TaRca2* (as dsRNA are cleaved into 21-22 base siRNAs). Silencing of the *TaRca2* gene did not have a significant effect on *TaRca1* expression. Inoculation with the BSMV:Rca2 α -1 and BSMV:Rca2 α -1 constructs lowered both *TaRca2*- α and *TaRca2*- β expression. Again, the latter is unlikely to be due to non-target silencing as the BSMV:Rca2 α construct sequences are specific to the C-terminal extension of the α -isoform, suggesting that expression of both the *TaRca2*- α and *TaRca2*- β isoforms is also co-regulated.

The amount of TaRca2- α protein in the plant is approximately 12.5% of the total TaRca protein amount (Law & Crafts-Brandner, 2001). It could therefore be predicted that the BSMV:Rca2 α constructs would reduce the total TaRca protein amount by up to 12.5%. The reduction in protein amount with the BSMV:Rca2 α -1 and BSMV:Rca2 α -2 constructs was considerably greater than 11%, which suggests that a reduction in the amount of the β isoform (TaRca1- β and/or TaRca2- β) in the plant also occurred. It would be beneficial in future studies to assess the protein amounts of the α and β isoforms independently to monitor their contribution to the total TaRca protein pool. With the BSMV:Rca2 construct the relative TaRca protein amount was decreased to only 5% of the controls, and the qRT-PCR results showed relatively low expression levels of both *TaRca2* isoforms, but not a great decrease in the expression of *TaRca1*- β . This may suggest that the majority of the β isoform is produced from transcripts derived from *TaRca2*, however this would have to be further studied and confirmed. In general, in both bacteria and eukaryotes, the cellular concentrations of proteins correlate with the abundance of their corresponding mRNAs, but not strongly. Discrepancies can be seen between transcript abundance and protein amount, and cross-species studies indicate that only approximately 40% of the variation in protein concentration can be explained by the mRNA abundance (Vogel & Marcotte, 2012).

Studies in wheat have shown that in response to heat stress *TaRca* transcript levels decrease, despite increased synthesis of the protein, indicating translational regulation (Law & Crafts-Brandner, 2001). In contrast, a study on the impact of heat stress on Rca in cotton showed that steady-state *Rca* mRNA levels measured at the beginning of the photoperiod were similar in control and heat-stressed tissue, in contrast with Rubisco small subunit transcript levels, which were reduced 75% by heat stress (Law *et al.*, 2001). *Rca* transcript abundance was correlated with *de novo* synthesis of Rca protein during heat stress, suggesting Rca synthesis in cotton is controlled at the level of transcript accumulation. In *Arabidopsis* *Rca* mRNA accumulation appears to be coordinated with transcriptional activity (Pilgrim & McClung, 1993). Nuclear transcription appears to be controlled by specific regions of the *Rca* promoter, which have been shown in reporter gene studies to be sufficient to confer a circadian pattern of expression (Liu *et al.*, 1996). These studies highlight the complexity of Rca regulation in different plant species.

The BSMV virus is a natural virus of some monocots; in natural infections it can cause severe stress to plants and this is similar in the laboratory plants. Research into Rca protein levels in response to stress indicates post-translational degradation; *Pinus halepensis* exposed to high levels of ozone or drought stress produced a marked decrease in Rca protein (Pelloux *et al.*, 2001). The BSMV:asGFP infected control and silenced plants showed similar virus symptoms indicating that the effects seen here are not due primarily to a stress response due to *TaRca* silencing; however these symptoms do make the study of photosynthesis difficult. The silencing fragments used in this study could be used for further research using interfering RNA (RNAi) constructs. The advantages of RNAi are that it offers constitutive silencing and there is no additional stress response or viral symptoms. Alternatively, novel mutagenic techniques could be used to specifically silence the *Rca* genes. The CRISPR-Cas system has recently proved to be very promising; studies have shown specific and predictable mutagenesis of rice and wheat genes (Shan *et al.*, 2013). The production of a wheat plant with all *Rca* isoforms silenced would be interesting, but would require plants to be grown under high CO₂. Clearly, many questions on the regulation of Rca and the mechanism of interaction with Rubisco remain. Further research into the functional differences and significance of the diverse Rca isoforms is warranted and will provide valuable information for improving the efficiency and climate resilience of photosynthesis.

5. Non-radioactive assay for measuring Rubisco and Rubisco activase activity

Chapter as published in:

Scales J C, Parry M A J, Salvucci M E (2014) A non-radioactive method for measuring Rubisco activase activity in the presence of variable ATP: ADP ratios, including modifications for measuring the activity and activation state of Rubisco, *Photosynthesis Research* 119, 3, 355-365

5.1 Introduction

To determine the effects of naturally occurring variation or artificially introduced modifications of Rubisco on carboxylation activity or the interaction with the catalytic chaperone, Rubisco activase (Rca), it is important to have a reliable method for measuring Rubisco and Rca activity. Ideally, the assay should be amenable to high-throughput measurement of activity in plant tissue and with purified proteins. Given the central role of Rca in controlling the activation state of Rubisco, it is also desirable that the assay can measure Rca activity in response to variable ratios of ADP: ATP. The ratio of these adenine nucleotides is the major physiological factor affecting Rca activity (Carmo-Silva & Salvucci, 2013, Robinson & Portis, 1989a).

The activities of Rubisco and Rca are commonly measured by determining the rate of incorporation of $^{14}\text{CO}_2$ into acid-stable compounds using a short, timed assay (Lorimer *et al.*, 1977). However, ^{14}C is a hazardous material that requires safety precautions in its handling. This feature limits the use of the ^{14}C -based assay to individuals with specialised training in the safe handling of radioactive material and liquid scintillation cocktail. Even with the proper training, the costs associated with a license to purchase, use and dispose of radioactive material, and to purchase and maintain a liquid scintillation counter can be prohibitive.

Photometric assays, either continuous (Sharkey *et al.* 1991) or two-stage using enzyme cycling (Sulpice *et al.*, 2007), offer alternative methods for measuring Rubisco activity. Rca activity can be measured by its ability to increase the activity of Rubisco and a continuous photometric assay for Rubisco has been

adapted for use in measuring Rca activity (Esau *et al.*, 1996, Lan *et al.*, 1992). However, these assays employ 3-PGA kinase for the conversion of 3-PGA and ATP to 1,3-bisPGA. This enzyme exhibits a low affinity for ATP and a very high affinity for inhibition by ADP (Pacold & Anderson, 1975). These properties preclude assay of Rca activity at variable ratios of ADP: ATP. This limitation is a drawback in the study of Rca because the sensitivity of Rca activity to inhibition by ADP is a major regulatory process controlling the activation state of Rubisco in response to irradiance, and probably other environmental factors (Carmo-Silva & Salvucci, 2013).

A novel method for measuring Rubisco and Rca activity is described here. Instead of coupling 3-PGA formation to NADH oxidation via 3-PGA kinase, 2,3-bisPGAdependent phosphoglycerate mutase (dPGM) was used to convert 3-PGA to 2-PGA (Figure 5.1). Enolase was then used to convert 2-PGA to PEP. For measurement of Rca activity in the presence of variable ratios of ADP:ATP, the formation of PEP was coupled to NADH oxidation via PEP carboxylase and malic dehydrogenase. A modification of the basic method is described for the routine assay of Rubisco activity and Rubisco activation state. This modification replaces the PEP carboxylase–malate dehydrogenase link with pyruvate kinase and lactate dehydrogenase, two relatively inexpensive linking enzymes. By dividing the reaction into two-stages, both the standard and the modified assays can be automated for high-throughput processing.

5.2 Materials and methods

5.2.1 Materials

Biochemical reagents of the highest purity available were purchased from Sigma–Aldrich (St. Louis, MO, USA). Ribulose 1,5-bisphosphate was synthesized by isomerization and phosphorylation of ribose 5-phosphate (Jordan & Ogren, 1984). Rubisco was purified from tobacco or Arabidopsis leaves as described previously and converted to the ER form (Carmo-Silva *et al.*, 2011). Recombinant tobacco and Arabidopsis Rca was expressed in *Escherichia coli* and purified as described previously (Barta *et al.*, 2011a, van de Loo & Salvucci, 1996).

5.2.2 Plant material and growth conditions

The conditions used for growth of *Arabidopsis* (Heynh. wild-type, cv. Columbia), and the transgenic line rwt43 (Zhang et al. 2002) were described previously (Carmo-Silva & Salvucci, 2013). *Camelina* (*Camelina sativa* (L.) Crantz cv. Robinson) and tobacco (*Nicotiana tabacum* L. cv. Petit Havana) plants, including transgenic tobacco plants that express a His-tagged Rubisco (Rumeau *et al.*, 2004), were grown under the conditions described in Carmo-Silva *et al.* (2012). Measurements were conducted on fully expanded leaves of 4- 5 week old plants of *Arabidopsis* and *Camelina*, and 5- 6 week old plants of tobacco.

5.2.3 Isolation and expression of cDNAs and protein for dPGM and PEP carboxylase

A cDNA clone for 2,3bisPGA-dependent phosphoglycerate mutase (dPGM) was isolated from *Escherichia coli* (Fraser *et al.*, 1999) and cloned into the pET23a (Novagen, Madison, WI, USA). Nucleotides that encode for a C-terminal Streptactin (S-Tag) were added to the cDNA clone by PCR using a modified reverse primer. The modified primer encoded for the eight amino acid S-Tag (W-S-H-P-Q-F-EK) that was linked to the authentic C-terminus by two amino acids; Ser-Ala. Recombinant dPGM protein containing the S-Tag (dPGM-ST) was expressed in *E. coli* BL21Star™(DE3)pLysS as described by van de Loo & Salvucci (1996). Frozen cell pellets containing dPGM-ST were thawed in 0.1 M potassium phosphate, pH 8.0, containing 75 mM NaCl, (buffer A) and 10 mM 2-mercaptoethanol, 1 mM phenylmethylsulfonyl fluoride and 10 µM leupeptin and sonicated for 3 min at 4°C. Following centrifugation for 20 min at 26,000 x g, protein in the extract was precipitated with 80% ammonium sulphate, collected by centrifugation and suspended in buffer A. Following desalting on a Sephadex G-25 column, the dPGM-ST was purified by passage over a 20 mL column of Strep-tactin Sepharose (IBA GmbH, Goettingen, Germany) that had been equilibrated in buffer A. After washing with 10 column volumes of buffer A, dPGM-ST was eluted with 5 mM desthiobiotin in buffer A. The purified dPGM-ST was precipitated with ammonium sulphate and desalted on a Sephadex G-25 column, equilibrated with 60 mM Tris-HCl, pH 7.9. Fractions containing protein were pooled and stored at -80°C.

For the initial development of the assay, PEP carboxylase was purified from maize leaves by a procedure described for Rubisco (Carmo-Silva *et al.*, 2011). The protein peak corresponding to PEP carboxylase eluted from the ion-exchange column just prior to that of Rubisco. A commercially available PEP carboxylase (Sigma–Aldrich #C1744) from a microbial source was also used in the assay.

5.2.4 Measurement of Rubisco activase activity using purified proteins

Rca activity was measured as the ability to restore activity to the inactive Rubisco–RuBP (ER) complex (Salvucci *et al.*, 1985). Rubisco activity was measured in reactions containing 100 mM Tricine–NaOH, pH 8.0, 10 mM MgCl₂, 10 mM NaHCO₃, 5 mM DTT, 5 % (w/v) PEG-3350, 1 mM NADH, 0.48 U enolase, 0.75 U dPGM-ST, 0.2 mM 2,3-bisPGA, 2 mM RuBP, 10 mM glucose-6-phosphate, 0.75 U PEP carboxylase, 1 U malic dehydrogenase and 5 mM ATP, plus ADP at various ratios, and recombinant Rca and Rubisco at the concentrations indicated in the text. For assays using the commercially available microbial PEP carboxylase, the microbial PEP carboxylase (1 U) was substituted for the maize enzyme and glucose-6-phosphate and PEG-3350 were omitted from the mix. To avoid underestimating activity and to eliminate long lags in product conversion, the specific activities of the linking enzymes were more than ten-fold higher than the maximum activity of Rubisco at the highest concentration used. When tested using sub-saturating and saturating concentrations of 3-PGA, the activities of the linking enzymes catalysed NADH oxidation at rates that were several-fold higher than the maximum rate of Rubisco activity.

Rubisco assays were conducted at 30°C in 96-well plates in a total volume of 0.1 or 0.2 mL. Rca was added to reactions containing all of the components except Rubisco. After 30 s, reactions were initiated with Rubisco in the ER form and the decrease in absorbance at 340 nm, linked to the stoichiometric production of 3-PGA, was measured continuously using a Synergy HT (Bio-Tek, Denkendorf, Germany) plate reader. To determine the activity of the fully carbamylated ECM form, reactions were first incubated for 3 min without RuBP. When incubated without RuBP, the ER form rapidly carbamylated in the presence of Rca and ATP (Robinson, 1988).

5.2.5 Measurement of Rubisco activation state

For measurement of Rubisco activation, leaf discs (0.5 cm²) were excised from the plants and floated on a solution of 25 mM MES-NaOH, pH 5.5, contained within a water-jacketed beaker. The solution was flushed with humidified air (380 $\mu\text{L L}^{-1}$ CO₂ in 21% O₂, balance N₂) under the conditions of irradiance and temperature indicated in the text. After each treatment, leaf discs were quickly frozen in liquid nitrogen and stored at -80°C. Samples consisting of one or two frozen leaf discs, (0.5–1 cm²), were extracted in Ten Broeck glass homogenisers with 1 mL cm⁻² of 100 mM Tricine-NaOH, pH 8.0, 5 mM MgCl₂, 1 mM EDTA, 5 % PVP-40, 6 % PEG-4000, 5 mM DTT, 1 mM phenylmethylsulfonyl fluoride and 10 μM leupeptin. Assays were conducted at 30°C either immediately after extraction or after centrifugation for 20 s at 10, 000 x g. To measure initial Rubisco activity, 0.02 mL of leaf extract was added to assay mix in clear 96-well plates to a final volume of 0.2 mL. The assay mix contained 100 mM Tricine-NaOH, pH 8.0, 10 mM MgCl₂, 10 mM NaHCO₃, 20 mM KCl, 5 mM DTT, 1 mM NADH, 1.85 U pyruvate kinase, 2.33 U lactate dehydrogenase, 0.96 U enolase, 0.75 U dPGM, 0.2 mM 2,3-bisPGA, 2 mM ADP and 0.5 mM RuBP. To measure total activity, leaf extracts were incubated in the assay mix without RuBP to fully carbamylate Rubisco (Carmo-Silva & Salvucci, 2013). The rate of decrease in absorbance at 340 nm during the first 1- 2 min of the assay was measured using a Synergy HT (Bio-Tek, Denkendorf, Germany) plate reader immediately after addition of the leaf extract to the assay mix containing 1 mM RuBP (initial), or after 3 min incubation in the assay mix prior to addition of RuBP (total). For some experiments, assays were conducted in microcuvettes and the absorbance at 340 nm was monitored using a UV-Vis spectrophotometer (Varian, Cary Bio100). For these reactions, the total assay volume was 0.4 mL and the leaf extract volume was 0.04 mL.

5.2.6 Two-stage assay for Rubisco activity using purified proteins

A two-stage assay was also used to assay Rca activity. The first stage assay contained 100 mM Tricine-NaOH, pH 8.0, 10 mM MgCl₂, 10 mM NaHCO₃, 2 mM DTT, 5 mM ATP, 5 mM RuBP, 5 % PEG-3350, and 0.1 mg mL⁻¹ tobacco Rca in a total volume of 50 μL . Reactions were initiated with 1 mg mL⁻¹ tobacco Rubisco. At set time points, 0.01 mL aliquots were transferred to microtubes containing 0.03 mL of 100 mM Tricine-NaOH, pH 8.0 at 95°C to stop the reactions. To determine the amount of 3-PGA

formed during the first stage, 15 μL aliquots of the quenched samples were added to 185 μL of 100 mM Tricine-NaOH, pH 8.0, 10 mM MgCl_2 , 10 mM NaHCO_3 , 5 mM DTT, 1 mM NADH, 0.96 U enolase, 0.75 U dPGM, 0.2 mM 2,3-bis-PGA, 1.85 U pyruvate kinase, 2.33 U lactate dehydrogenase and 2 mM ADP. The change in absorbance at 340 nm was measured as described above using a plate reader.

5.2.7 Data analysis

The carboxylase activity of Rubisco, expressed as $1 \text{ mol CO}_2 \text{ incorporated min}^{-1} \text{ mg}^{-1} \text{ protein}$ or converted to $\text{kcat (s}^{-1}\text{)}$, i.e., turnover number, was determined from the stoichiometric production of two molecules of 3-PGA per molecule of CO_2 fixed. The rate of 3-PGA production was determined continuously from the decrease in absorbance at 340 nm due to the oxidation of NADH and converted to Rubisco specific activity. To determine the fraction of sites activated, the specific activity was divided by the specific activity of the fully carbamylated Rubisco, i.e., $\text{ECM} = 100\%$ of the sites carbamylated.

RCA affects both the rate and the final extent of Rubisco activation (van de Loo & Salvucci, 1996).

Consequently, for experiments comparing different Rca or Rubisco, Rca activity was based on the final steady-state specific activity of Rubisco and then converted to the fraction of Rubisco sites activated after interacting with Rca. To determine the effect of Rca and Rubisco concentrations on the rate of Rubisco activation, the fraction of Rubisco sites activated min^{-1} was determined from a linear regression of the progress curve at each concentration of Rca and Rubisco. Adjusting the rate for the amounts of Rca and Rubisco made it possible to calculate the specific activity of Rca as $\text{mol Rubisco sites activated min}^{-1} \text{ mol}^{-1}$ Rca protomer. All assays were conducted in at least triplicate and the results are the mean \pm SE.

Statistical comparisons between different treatments were made using analysis of variance (ANOVA) followed by the Holm-Sidak method for multiple pairwise comparisons (for more than two treatments). P-values lower than 0.05 were considered statistically significant.

5.2.8 Miscellaneous

Protein concentration in leaf extracts was determined by the method of Bradford (1976). The same method was used to determine the concentration of Rca protein. Rubisco protein was determined based on the extinction coefficient at 280 nm (Paulsen & Lane, 1966).

5.3 Results

5.3.1 Considerations in developing the assay

The most important consideration in developing a continuous assay for Rca was the requirement for analysing the main regulatory property of the enzyme, i.e., the response of activity to variable ADP: ATP. To satisfy this criterion, a method was developed for coupling 3-PGA formation to pyridine nucleotide oxidation that was independent of adenine nucleotides. The method involved converting 3-PGA to PEP using dPGM and enolase and then coupling PEP production to the oxidation of NADH using PEP carboxylase and malic dehydrogenase (Figure 5.1A).

For the first step, 2,3-bisPGA-dPGM was selected over the cofactor-independent PGM because of its higher specific activity and lower affinity for 2-PGA (Fraser *et al.*, 1999). To our knowledge, dPGM is not commercially available but the cDNA that encodes for the protein can be isolated from and expressed in *E. coli*. By using a pET expression system similar to the one described previously (Fraser *et al.*, 1999), and including a C-terminal S-tag to facilitate purification, copious amounts of soluble dPGMST protein could be isolated in recombinant form. The additional eight amino acids of the S-tag plus a two amino acid linker did not interfere with expression or activity.

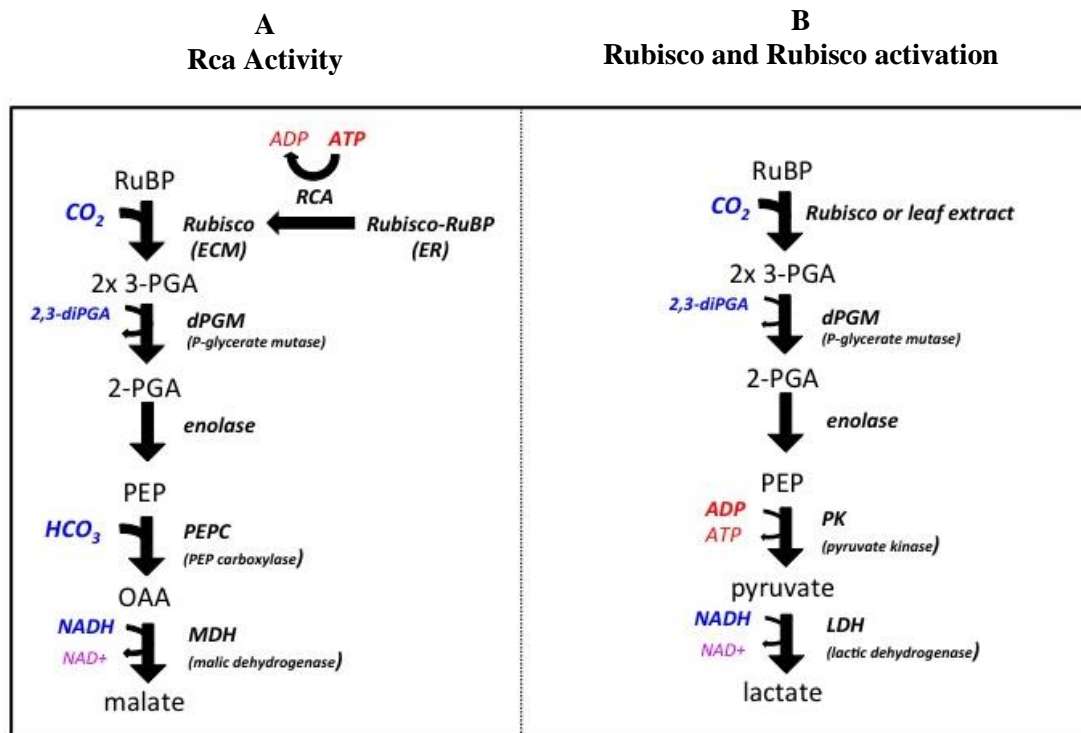


Figure 5.1. Reaction schemes for measuring the activities of Rca and Rubisco in continuous assays. The two diagrams show alternative pathways for coupling 3-PGA formation to NADH oxidation. Pathway for measuring Rca activity. The coupling of 3-PGA formation to NADH oxidation is independent of adenine nucleotides, allowing measurement of Rca activity at variable ratios of ADP: ATP (A). Pathway for measuring Rubisco and Rubisco activation. The coupling of 3-PGA formation to NADH oxidation requires ADP (B).

Conversion of 3-PGA via dPGM and enolase produces PEP that was then linked to NADH oxidation using PEP carboxylase and malate dehydrogenase. Formation of PEP can also be linked to NADH oxidation via pyruvate kinase and lactate dehydrogenase. However, this link cannot be used for continuous measurement of Rca activity because the pyruvate kinase reaction requires ADP, an inhibitor of Rca (see below). For the initial experiments using PEP carboxylase, the enzyme was purified from maize leaves. Active maize PEP carboxylase with an N-terminal affinity tag has been expressed in recombinant form (Dong *et al.*, 1997). Thus, the recombinant maize enzyme could be used as a ready source of PEP carboxylase for the Rca assay. In addition, a relatively inexpensive microbial PEP carboxylase is available commercially. This enzyme exhibited very low activity in the standard assay due to precipitation of the protein by PEG. By removing PEG from the assay mix, the commercially available microbial PEP carboxylase was a suitable substitute for maize PEP carboxylase in the Rca assay.

In preliminary experiments, the oxidation of NADH in the coupled system using maize PEP carboxylase was slow when the concentration of 3-PGA was low, even though the activities of the coupling enzymes

were in excess based on their specific activities at saturating substrate concentrations. Addition of the PEP carboxylase activator, glucose-6-phosphate, to the assay greatly increased the rates, indicating that the assay system required this effector to overcome the low affinity of maize PEP carboxylase for PEP (Coombs *et al.*, 1973). In contrast, the activity of the microbial PEP carboxylase was unaffected by glucose-6-phosphate, catalysing the linked reaction at adequate rates for the assay of Rubisco.

5.3.2 Validation of the assay

Effect of Rubisco and Rubisco activase concentration on Rubisco activase activity

Rca activity can be measured by its ability to increase the activity of uncarbamylated Rubisco containing tightly bound RuBP, commonly referred to as the ER form of the enzyme. This form of Rubisco is inactive and slow to activate, in contrast to the active ECM form that is fully carbamylated and contains bound Mg^{2+} . As shown in Figure 5.2, the dPGM-based assay developed here was suitable for measuring the activity of Rubisco, as evidenced by the marked differences in the rate of NADH oxidation between the ER and ECM forms of Rubisco. Similarly, the increased rate of NADH oxidation from the conversion of the inactive ER to the active ECM form of Rubisco was apparent when ER was added to reactions containing ATP and Rca. The raw data show that with Rca, Rubisco activity increases progressively during the time course, indicating that the proportion of Rubisco in the active form increases with time. To demonstrate the versatility of the assay, the dependence of Rca and Rubisco concentrations on activation of the inactive ER complex by Rca was examined (Figure 5.3 and 5.4). As shown previously using the timed, two-stage ^{14}C assay (Robinson, 1988), the rate of activation of Rubisco, measured as the fraction of Rubisco sites activated per min, increased with increasing concentrations of Rca. However, the specific activity of Rca, i.e., mol Rubisco sites activated $min^{-1} mol^{-1}$ Rca protomer, decreased with increasing Rca concentration (Figure 5.3). These results indicate that, at the concentrations of Rubisco and Rca protein used here, the rate of Rubisco activation per mol of Rca protein decreased with increasing ratios of Rca to Rubisco. In contrast, at a constant concentration of Rca, the specific activity of Rca increased with increasing amounts of ER (Figure 5.4).

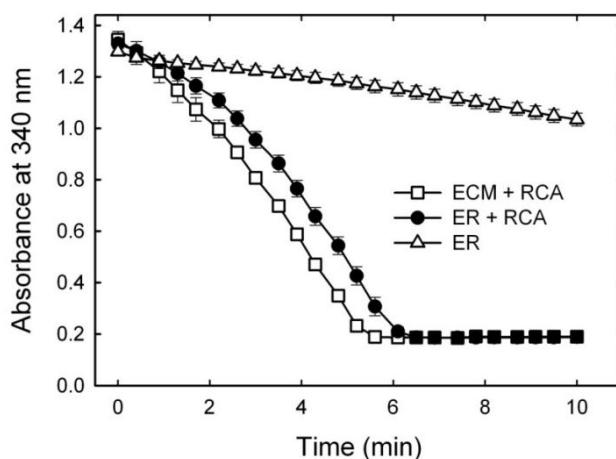


Figure 5.2. Continuous measurement of Rubisco activity demonstrating the conversion of Rubisco from the inactive ER to the active ECM form by Rca.

The data shows the time course of the decrease in A_{340} in assays linking RuBP-dependent 3-PGA formation to NADH oxidation (see Figure 5.1A). Reactions contained either 0.1 mg mL^{-1} Rubisco in the fully carbamylated ECM form plus 0.1 mg mL^{-1} Rca (white squares), 0.1 mg mL^{-1} Rubisco in the ER form (white triangles) or 0.1 mg mL^{-1} Rubisco in the ER form plus 0.1 mg mL^{-1} Rca (black circles). All reactions were conducted at 30°C and contained 5 mM ATP.

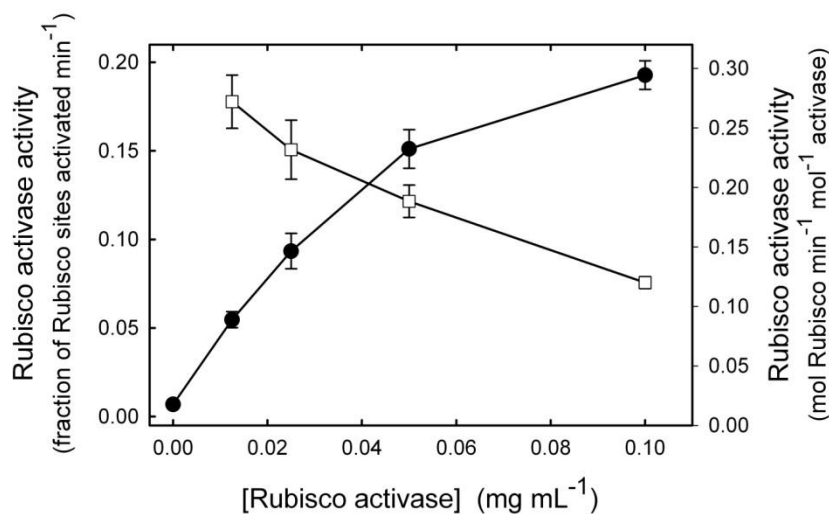


Figure 5.3. Effect of Rca concentration on Rca activity.

Tobacco Rubisco in the ER form was incubated with the indicated concentrations of tobacco Rca at 30°C in the presence of 5 mM ATP. Rubisco activity was measured continuously as described in Figure 5.2 and the fraction of sites activated was determined at each time point. From a linear regression of the progress curve, Rca activity was determined at each concentration of Rca as the fraction of Rubisco sites activated min^{-1} (black circle). The specific activity of Rca, $\text{mol Rubisco sites activated min}^{-1} \text{ mol}^{-1}$ Rca protomer (white squares), was calculated using these rates and the amounts of Rubisco and Rca protein in the assays.

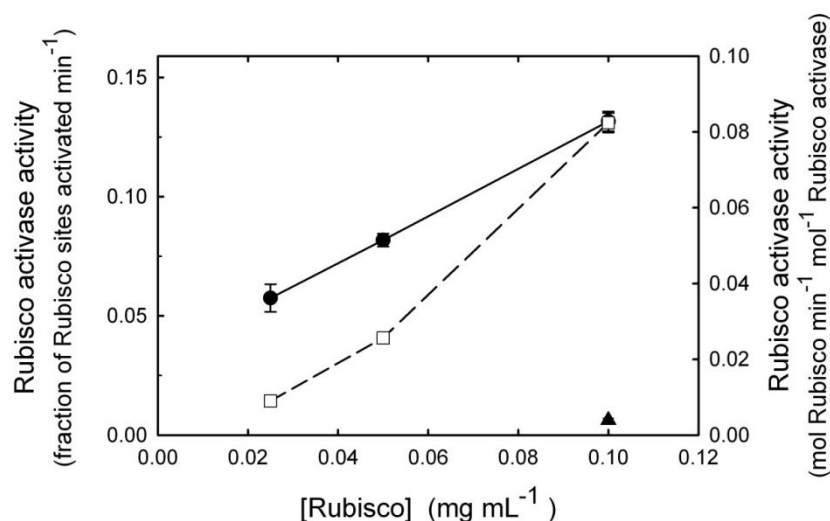


Figure 5.4. Effect of Rubisco concentration on Rca activity.

Rca at 0.1 mg mL^{-1} was incubated with the indicated concentrations of Rubisco in the ER form and Rubisco activity was measured at 30°C in the presence of 5 mM ATP. Rubisco activity was measured continuously as described in Figure 5.2 and the fraction of sites activated was determined at each time point. From a linear regression of the progress curve, Rca activity was determined for each concentration of Rubisco as the fraction of Rubisco sites activated min^{-1} (black circle). The rate of spontaneous activation of the ER form in the absence of Rca is indicated by the closed triangle. The specific activity of Rca, $\text{mol Rubisco sites activated min}^{-1} \text{ mol}^{-1}$ Rca protomer (white squares), was calculated by adjusting the rate for the amounts of Rubisco and Rca in the assays.

Effect of ADP/ATP on Rubisco activase activity

To further validate the continuous assay system (Figure 5.1A) the effect of ADP: ATP ratio on Rca activity was investigated (Figure 5.5). As shown previously, Rca activity decreased as the ratio of ADP:ATP increased. At a ratio of 0.5, the activity of ER in the presence of Rca and ATP was not statistically different from the activity determined without Rca, indicating that tobacco Rca was completely inactive. With physiological ratios of 0.33 ADP: ATP (Stitt *et al.*, 1982, Zhang & Portis, 1999) the rate of Rubisco activation by Rca was reduced by 46% compared to the rate with no ADP.

In a separate set of experiments, the effect of ADP on Rca activity was compared for the β isoforms of Rca from tobacco and Arabidopsis (Table 5.1). Previous studies using the ^{14}C Rubisco assay have shown that the β Rca from Arabidopsis is much less inhibited by ADP than the enzyme from tobacco (Carmo-Silva & Salvucci, 2013). Measurements using the continuous assay confirmed these findings; at 0.33 ADP:ATP the Arabidopsis β Rca was inhibited by 25% compared with 65% inhibition of the tobacco enzyme.

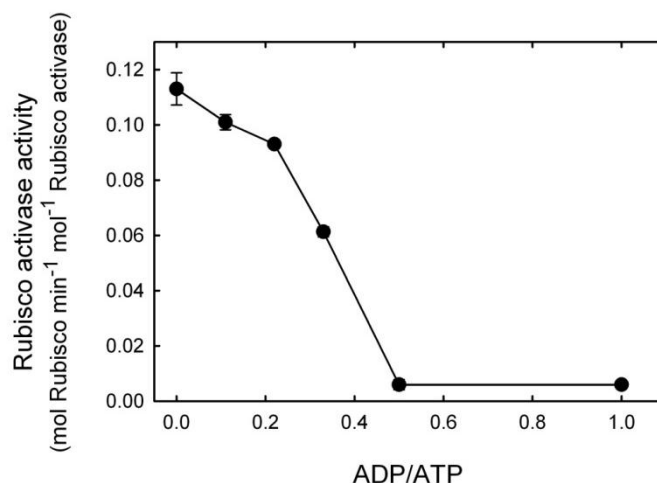


Figure 5.5. Effect of ADP:ATP ratio on the activity of Rca.

Rubisco at 0.1 mg mL^{-1} was incubated in the ER form with 0.1 mg mL^{-1} Rca at 30°C in the presence of 5 mM ADP:ATP. Rubisco activity was measured continuously as described in Figure 5.2 and the fraction of sites activated was determined at each time point. From a linear regression of the progress curve, Rca activity was determined at each ratio of ADP:ATP as the fraction of Rubisco sites activated min^{-1} and converted to Rca specific activity, $\text{mol Rubisco sites activated min}^{-1} \text{ mol}^{-1}$ Rca protomer (black circle), by adjusting the rate for the amounts of Rubisco and Rca protein in the assays.

Table 5.1. Differences in the sensitivity of β -isoform Rca to inhibition by ADP.

Recombinant Rca from tobacco and Arabidopsis were incubated at 0.1 mg mL^{-1} with 0.075 mg mL^{-1} of the ER forms of tobacco and Arabidopsis Rubisco, respectively, in the presence of either 5 mM ATP or 5 mM ATP plus ADP at a ratio of 0.33 ADP:ATP. Rubisco activity was measured continuously using the assay shown in Figure 5.1A. Maximum rates were determined and used to calculate k_{cat} . The values in parentheses indicate the fraction of Rubisco sites that were activated. The turnover rates of the ER forms in the absence of Rca were 0.08 and 0.2 s^{-1} for tobacco and Arabidopsis Rubisco, respectively.

Plant species	Rubisco activity (k_{cat})	
	ADP/ATP	
	0	0.33
tobacco	1.73 ± 0.05 (100)	0.53 ± 0.05 (0.35)
Arabidopsis	2.96 ± 0.06 (0.95)	2.21 ± 0.06 (0.71)

Measuring activation of polyhistidine-modified Rubisco by Rubisco activase

In another test of the assay, the continuous assay for Rca activity was used to determine if the addition of six histidine residues to the C-terminus of the large subunit of Rubisco (Rumeau *et al.*, 2004) affected Rubisco activity or activation of Rubisco by Rca (Figure 5.6). Measurement of the specific activities of the ECM form of wild-type and modified Rubisco, 0.83 ± 0.03 and 0.78 ± 0.01 U mg⁻¹ protein, respectively, indicated that the poly-His addition did not significantly affect the maximal carboxylase activity. Similarly, the activity of the ER forms of both of these enzymes remained below 20% of the maximum when incubated with high CO₂ and Mg²⁺ in the presence of 0.5 and 2 mM RuBP. The low activity of the His-modified Rubisco indicated that the stability of the ER complex was unaffected by the modification. Finally, the extent of activation of the ER form of the polyhistidine-modified Rubisco by various amounts of tobacco Rca was similar to wild-type Rubisco at both 0.5 and 2 mM RuBP. These results indicate that the effectiveness of Rca in converting Rubisco from the inactive ER form to the active ECM form was not compromised by extending the C-terminus of the large subunit of Rubisco by six histidine residues.

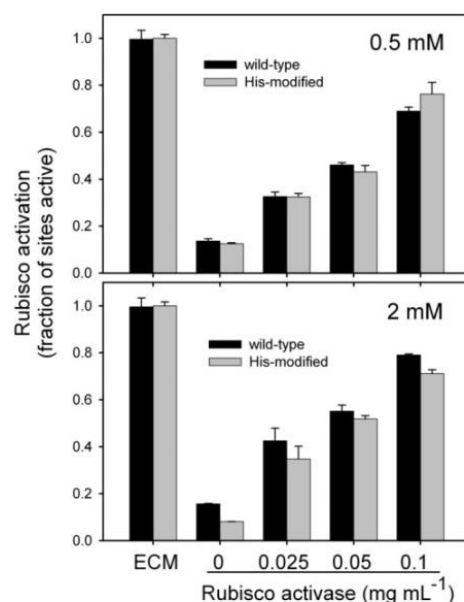


Figure 5.6. Activation of wild-type (black) and His-tagged modified Rubisco (grey) by Rca. Tobacco Rubisco at 0.1 mg mL^{-1} was incubated in the ER form with the indicated amounts of tobacco Rca at 30°C in the presence of 5 mM ATP or converted to ECM form by incubation with CO_2 and Mg^{2+} . Assays were completed with either 0.5 mM or 2 mM RuBP . Rubisco activity was measured continuously as described in Figure 5.2 and the fraction of sites activated was determined by comparing the steady-state activity with the activity of the fully carbamylated enzyme (ECM).

5.3.3 Modification of the standard assay for measuring Rubisco activity and activation state

The activation state of Rubisco in leaves can be determined by measuring the activity of Rubisco in rapidly prepared leaf extracts, i.e., initial activity, and comparing this activity to the activity of the fully carbamylated enzyme, i.e. total activity (Perchorowicz *et al.*, 1981). To measure Rubisco activation, the standard assay described above (Figure 5.1A) or a modified version (Figure 5.1B) can be used as a stand-alone assay for either purified Rubisco or Rubisco in leaf extracts (Figure 5.1B). The modified version still uses dPGM-ST and enolase to convert 3-PGA to PEP, but couples PEP formation to NADH oxidation via pyruvate kinase and lactate dehydrogenase. The pyruvate kinase lactate dehydrogenase link requires ADP, a potent inhibitor of Rca, but not Rubisco. Thus, these linking enzymes, while suitable for measuring Rubisco activity *per se*, cannot be used for measuring the effects of Rca on Rubisco activity in a continuous assay. The main advantage of the modified assay for measuring Rubisco is that the two linking enzymes are commercially available and inexpensive.

To demonstrate the usefulness of the assay for measuring Rubisco activation, the effect of irradiance on the activation state of Rubisco was determined in wild-type and transgenic Arabidopsis using the modified assay (Figure 5.1B). As shown in Table 5.2, the results demonstrated that the assay was capable of measuring light-dependent changes in Rubisco activation that occur in wild-type plants. The measurements also confirmed that (1) deactivation of Rubisco in response to low light was minimal in the *rwt43* transformant, a transgenic Arabidopsis that expresses only the ADP-insensitive β isoform of Rca (Carmo-Silva & Salvucci, 2013) and (2) the rates of Rubisco activity in crude leaf extracts of wild-type and transgenic plants were similar to those determined with a ^{14}C -based Rubisco assay (Salvucci *et al.*, 2006). In a separate set of experiments, the non-radioactive assay was used to detect the decrease in Rubisco activation state that occurred in camelina plants subjected to heat stress (Table 5.3). These results confirmed previous findings obtained using the ^{14}C -based assay (Carmo-Silva & Salvucci, 2012).

Table 5.2. Effect of irradiance on the activation state of Rubisco in wild-type Arabidopsis and the transgenic line, rwt43. Leaf discs were exposed to the indicated irradiance for 120 min prior to sampling. Letters indicate activation states that are statistically different at the $P < 0.001$ level.

Arabidopsis line	Rubisco activity			
	Irradiance	Initial	Total	Activation
	($\mu\text{E m}^{-2} \text{s}^{-1}$)	($\mu\text{mol min}^{-1} \text{mg}^{-1}$)		(%)
wild-type	1200	0.40 ± 0.03	0.46 ± 0.08	86 ± 3^a
	75	0.35 ± 0.03	0.59 ± 0.02	60 ± 4^b
	25	0.13 ± 0.01	0.59 ± 0.03	23 ± 2^c
rwt43	1200	0.42 ± 0.08	0.45 ± 0.07	91 ± 4^a
	75	0.45 ± 0.04	0.53 ± 0.04	85 ± 4^a
	25	0.47 ± 0.03	0.55 ± 0.04	87 ± 3^a

Table 5.3. Effect of temperature on the activation state of Rubisco in camelina. Letters indicate activation states that are statistically different at the $P < 0.001$ level.

Temperature	Rubisco activity		
	Initial	Total	Activation
	($\mu\text{mol min}^{-1} \text{mg}^{-1} \text{protein}$)		(%)
23	0.34 ± 0.005	0.40 ± 0.003	84 ± 0.5^a
42	0.18 ± 0.01	0.32 ± 0.01	55 ± 1^b

5.3.4 Adapting assay to a two-stage method for high-throughput analysis

While continuous assays can be automated for high-throughput analysis, it is often more convenient to conduct two-stage, timed assays and then allow product conversion in the second stage to run to completion (Gibon *et al.*, 2004). Either the standard or modified assay described above could be used as a two-stage assay. To demonstrate this fact, Rca activity was measured in two-stages using a timed assay to determine the suitability of the dPGM linked reaction sequence for automation. In the first stage, Rubisco in the ER form was incubated with RuBP, ATP and Rca before heating at 95°C. The 3-PGA produced during the first stage was then determined by adding an aliquot of the reaction to a second stage assay that converted 3-PGA to lactic acid (Figure 5.1B). The data showed that it was possible to measure activation of the ER form of Rubisco by Rca using this two-stage assay with a single time point (Table 5. 4).

Table 5.4. Effect of Rca on the activation of Rubisco, measured in a two-stage assay.

Rubisco activity was determined by measuring the amount of 3-PGA formed after 5 min in reactions containing 1 mg mL⁻¹ of Rubisco in the presence and absence of 0.1 mg mL⁻¹ Rca. The activity of the ECM form of Rubisco was measured by incubating the Rubisco with 10 mM MgCl₂ and NaHCO₃ in the absence of RuBP for 10 min prior to assay.

Rubisco form	Rca (mg mL ⁻¹)	Rubisco activation (fraction of sites active)
ER	0	0.12 ± 0.01
ER	0.1	0.71 ± 0.03
ECM	0.1	1.00 ± 0.06

5.4 Discussion

5.4.1 The interaction of Rubisco and Rubisco activase

The physical interaction between Rca and Rubisco has long been enigmatic, presumably because of the transient nature of the binary complex. Rubisco and Rca do not form a stable binary complex that would facilitate a thorough characterisation of the molecular details of the interaction (Blayney *et al.*, 2011, Portis *et al.*, 2008). However, the consequence of the interaction can easily be detected by measuring the effect of Rca on Rubisco activity (Salvucci *et al.*, 1985). In the presence of ATP, Rca increases the activity of inhibited forms of Rubisco, i.e., forms produced by the tight binding of certain sugar-phosphates (Portis, 2003), including the unproductive binding of the substrate, RuBP, to uncarbamylated enzyme. Wang and Portis (1992) showed that the increases in Rubisco activity that resulted from the productive interaction of ER with Rca were associated with more rapid dissociation of inhibitory sugar-phosphates. These data indicate that “activation of Rubisco” by Rca involves altering the positions of specific domains around the Rubisco active site to allow bound sugar-phosphates to dissociate more rapidly. Although the precise nature of the interaction between Rca and Rubisco is unknown, specific residues of both Rubisco and Rca that are involved in the interaction have been identified (Larson *et al.*, 1997, Li *et al.*, 2005, Ott *et al.*, 2000, Portis *et al.*, 2008). The positions of these residues suggest some possibilities for how Rca remodels the conformation of Rubisco (Henderson *et al.*, 2011, Stotz *et al.*, 2011, Wachter *et al.*, 2013)

5.4.2 Significance of measuring Rubisco activase activity at variable ADP: ATP

The effect of Rca on Rubisco activity has been investigated most often using purified proteins in a simple, timed assay that measures the incorporation of radioactive carbon from CO₂ into acid-stable products. A high-throughput version of this assay was even used to screen for Rca variants with increased thermotolerance (Kurek *et al.*, 2007). However, the logistical issues associated with using radioactive material provide motivation for developing a versatile, non-radioactive assay that could be used for

measuring Rubisco and Rca activity. With modifications, the basic assay could also be used as an inexpensive method for measuring the activation state of Rubisco.

Unlike other photometric assays (Sharkey *et al.*, 1991, Sulpice *et al.*, 2007), the continuous assay described here could be used to measure the activity of Rca in the presence of variable ratios of ADP:ATP. This feature is an important consideration since the ratio of ADP:ATP is a major factor regulating the activity of Rca in plants (Robinson & Portis, 1989a) and influencing the rate of photosynthetic induction (Carmo-Silva & Salvucci, 2013). This fact was demonstrated in studies using *Arabidopsis* plants that express forms of Rca that differ in their sensitivity to ADP. These plants exhibit marked differences in the response of Rubisco activation to irradiance (Carmo-Silva & Salvucci, 2013, Zhang *et al.*, 2002). As a result, plants whose Rca was less sensitive to inhibition by ADP exhibited faster rates of photosynthetic induction during transitions from low to high irradiance because Rubisco was already highly active under low irradiance in these plants (Carmo-Silva & Salvucci, 2013); see also Table 5.1). This finding indicates that manipulating the regulatory properties of Rca might provide a strategy for increasing the rate of photosynthesis in variable light environments.

The assay described here should provide a useful tool for evaluating the interaction between Rubisco and Rca, including variants of both proteins. To demonstrate this application, the activation of a His-tagged Rubisco by Rca was measured to test the hypothesis that Rca alters the conformation of Rubisco via a pore threading mechanism involving movement of the C-terminus of the Rubisco large subunit by Rca (Mueller-Cajar *et al.*, 2011, Stotz *et al.*, 2011). While the data did not conclusively support or reject the hypothesis, they show that the interaction of Rca with Rubisco is unaffected by extending the C-terminus of the large subunit of Rubisco by six histidine residues.

5.4.3 Measuring Rubisco activity and Rubisco activation state

Due to the investment associated with producing the dPGM-ST used in the Rca assay, it was desirable to use the central portion of the assay, the conversion of 3-PGA to PEP, to measure Rubisco activation in leaf extracts. These assays demonstrated the influence of both irradiance and temperature on the activation state of Rubisco in leaves, verifying that the amount of active Rubisco changes in response to

these environmental factors. The high sensitivity of ^{14}C -based assays for Rubisco allow for very short reaction times, i.e. 30- 60 s (Lorimer *et al.*, 1977). Short reaction times minimize the problem with “fall-over”; the slow, progressive decrease in catalytic activity caused by either the presence of inhibitory compounds in the RuBP preparation (Kane *et al.*, 1998) or the production of catalytic misfire products at the active site (Edmondson *et al.*, 1990). It should be noted that fall-over does not occur in assays containing active Rca, because Rca reverses the tight-binding of the inhibitory sugar-phosphates (Robinson & Portis, 1989b). However, a fall-over type decline occurred during the later time points (i.e., after 5- 10 min) in assays of Rubisco that did not contain Rca (data not shown). For this reason, we recommend determining Rubisco activity and Rubisco activation during the initial 1- 2 min when the activity decline is negligible (Robinson & Portis, 1989b).

5.4.4 Summary

The continuous photometric assay described here for measuring the activities of Rubisco and Rca is flexible and easily adaptable to a variety of experimental situations, including for use with purified proteins and leaf extracts. All but one of the linking enzymes is commercially available and the dPGM-ST can be produced in *E. coli* and isolated by affinity chromatography. The assays can be conducted in microplates and the changes in absorbance detected using a plate reader. The basic assay for Rca activity described in Figure 5.1A could be prepared as a master mix containing all of the components except Rubisco, Rca and RuBP. The master mix was stable when stored either frozen at -80°C or lyophilized at 4°C . By dividing the assay into two-stages, the assay can be used in a high-through put or robotic system. While the assay described here provides a reliable measurement of the carboxylase activity of Rubisco, the simultaneous assay of carboxylase and oxygenase activity using $^{14}\text{CO}_2$ and ^3H -RuBP developed by (Jordan & Ogren, 1981) is still the most accurate method for determining the substrate specificity of Rubisco. With a growing interest in Rubisco regulation, the assay described here provides a timely alternative to radioactive assays for measuring Rubisco and Rca activity.

6. General Discussion

Wheat is a staple crop providing 20% of the calories consumed globally (Reynolds *et al.*, 2011).

However, wheat yields are under threat, in particular due to rising global temperatures, and increasingly variable weather conditions (Asseng *et al.*, 2014). Strategies to increase the resilience of wheat yields to heat stress are required, as well as meeting the challenge to increase yields to support the growing global population (Ray *et al.*, 2013).

The effective survival of some wheat cultivars in hotter, drier environments has been argued as being largely due to heat escape, due to variations in the timing of growth stages, and not tolerance as such (Semenov *et al.*, 2014). These escape strategies may involve altering the date, duration or the diurnal pattern of specific developmental stages. Improved water availability through more efficient root systems and architectures may additionally provide some protection against excessive temperatures, by enabling leaf cooling through transpiration. The argument that natural selection has already maximized photosynthesis and that further gains will not be achieved has been raised (Leister, 2012). However, natural selection has maximised fitness for survival, rather than maximal agriculturally beneficial yield (i.e. high quality and quantity) in past and possibly present, but certainly not future, environments. Moreover, natural selection will have taken place in environments radically different to those of agricultural systems which are often nutrient rich, irrigated and protected from pests. Physiological models that can accurately predict crop growth will become an increasingly indispensable tool, as they can help breeders to anticipate traits which may prove useful in the future (Stratonovitch & Semenov, 2015).

Photosynthesis is particularly sensitive to elevated temperatures and Rca has been shown to be associated with heat inhibition of photosynthesis. Rca plays a central role in photosynthesis, maintaining the activity of the carboxylating enzyme, Rubisco. Rca is heat labile and when temperatures rise it is unable to maintain the activation state of Rubisco, therefore carbon assimilation is reduced (Salvucci & Crafts-Brandner, 2004a). This decrease in the supply of fixed carbon ultimately results in a decrease in biomass

production and therefore yield. Evidence suggests that improving Rca thermal tolerance (Kumar *et al.*, 2009, Kurek *et al.*, 2007, Scafaro *et al.*, 2012) would increase the productivity and yield of crop plants. Two approaches were taken here to improve the thermal tolerance of Rca in wheat: investigation of the intraspecies variation in the response of photosynthesis to high temperature, and a transgenic approach to engineer Rca thermal tolerance into wheat.

Limited variation in the response of photosynthesis to the temperature treatment was measured between different wheat cultivars. This was found to be associated with yield, with higher yielding cultivars tending to have higher photosynthetic rates and Rubisco activation states after an elevated temperature treatment, and additionally, more Rubisco. However, beneficial traits were not necessarily correlated in the chosen group of wheat cultivars from the 'ERYCC' panel.

One possible limitation to this study was the modest number of cultivars screened and the fact that the majority were elite lines of UK origin which would have missed adaptive traits that could have emerged in more diverse climates. Investigating the thermal tolerance of a more diverse panel of cultivars, a screen which included crop growth at higher temperature, together with the monitoring of development and productivity throughout the growth season, may have had greater success in identifying differences in thermal tolerance. The Temperature and Free-Air CO₂ Enrichment experiments being conducted at the Soybean FACE facility in Illinois, and the CIMMYT High Temperature Wheat Yield Trial (HTWYT), at El Batán, in which wheat is bred to better withstand high temperatures, are critical to research investigating crop yield improvement under elevated temperatures. For example, in the HTWYT, Lillemo *et al.* (2005) identified a subset of genotypes that showed stable, and high yield across both heat-stressed and temperate environments. A significant problem facing wheat breeders is that of identifying novel allelic sources, particularly when looking at complex multi-genic traits, such as that of temperature tolerance (Kumar *et al.*, 2013). Due to the difficulty in successfully identifying genes involved in complex traits, one benefit of the present study is that, by investigating one protein already known to be involved in thermal tolerance, subsequent breeding approaches would be relatively straightforward. The latest genomic resources combined with ecophysiological research will assist in increasing the

understanding of genotype-environment interactions and identifying novel genomic resources for thermal tolerance.

Marker-assisted selection is routinely used in plant breeding to target traits such as pest resistance, in which a single known gene confers a trait. Forward genetics approaches are being applied to more complex traits to search for genetic markers for traits of interest. Such studies involve assessing individuals which differ in genotype for phenotypes of interest. Phenotypic differences are then linked back to the underlying causative loci via various approaches, including QTL mapping (Korte & Farlow, 2013). To identify QTLs, doubled haploid sets, bi-parental recombinant inbred lines, and genetically characterised accessions for population genetics, have all been used. Despite the difficulty in identifying QTLs for complex traits in wheat (such as yield or thermal tolerance) this has been achieved. For example, Huang *et al.* (2003) used advanced-backcross QTL analysis to identify QTLs for yield in a population derived from a cross between a German winter wheat variety (Prinz) and a synthetic wheat line developed by CIMMYT (W-7984). Favourable QTL alleles could be transferred into an elite wheat variety for improvement of yield.

Genome-Wide Association Studies (GWAS) are a complementary tool to QTL mapping in which the association between phenotypes of interest (which have been scored across a large number of individuals) and genotype markers, is evaluated (reviewed by Korte & Farlow (2013)). In GWAS populations are often genotyped once but are scored for the occurrence of multiple traits. GWAS may provide a valuable tool for future research into thermal tolerance in wheat. Although pioneered in human genetics, GWAS has been successfully applied to crop plants, for example: a study in rice identified 32 new loci associated with flowering time and ten for grain-related traits (Huang *et al.*, 2012); in Barley 32 morphological and 10 agronomical traits were identified in a collection of 615 barley cultivars (Wang *et al.*, 2012); and in wheat, loci for grain yield and yield components were identified in spring wheat (Sukumaran *et al.*, 2014) and winter wheat (Neumann *et al.*, 2011). However, since wheat has a large, polyploid genome it is difficult to assign markers flagged by GWAS to individual genomes (reviewed by Sukumaran & Yu (2014)), and large numbers of individuals are required, necessitating high-throughput phenotyping methods.

Phenotyping populations is recognised as being the most time consuming and challenging part of establishing the link between genotype and phenotype (reviewed by Furbank *et al.* (2011)), and undoubtedly this limited the number of cultivars which could be investigated here. The development of effective, field-based, high-throughput phenotyping platforms, together with improvements in the management and interpretation of data will help to increase the speed and accuracy of crop genetic improvement (reviewed by Araus & Cairns (2014)). Furthermore, data collection in two or three environments (which may include different representative sites or experimentation over several seasons) is required to assess for consistent expression of the trait of interest, and emphasises the need for suitable screening methods.

Ultimately, the outcome of combining heat tolerance traits in breeding programmes is unpredictable in terms of the overall impact on crop productivity and especially over a range of environments. Crosses between parents with different, but potentially complementary, physiological traits increases the likelihood of cumulative gene action (Reynolds *et al.*, 2009). Qin *et al.* (2008) completed an analysis of genes expressed in heat tolerant and heat intolerant wheat cultivars, indicating that many apparently unrelated genes showed altered expression in response to heat stress. Wider breeding strategies to improve thermal tolerance in wheat need to focus on identifying genetic markers (as described above) to increase the likelihood of successful allelic combinations for improved thermal tolerance. Once established, integration of key traits conferring thermal tolerance into modelling algorithms will further inform the breeding of wheat cultivars which are resilient to a range of possible future climates. Work such as that by Yin and Struik (2010) suggests that to address challenges involving complex genotype–phenotype relationships, crop-based systems research should draw on existing modelling and, at the same time, should parameterize and make use of biochemistry and genomics. Crop systems biology aims to bring the information from functional genomics to the crop level, to better understand the intra- and interplant competition of the whole crop and its response to environmental conditions.

Exploration of larger panels of more varied wheat cultivars than used here (and grown at elevated temperatures throughout the growing season) may help to elucidate the role that Rca thermal tolerance plays in conferring tolerance to different wheat cultivars. The use of appropriate germplasm is extremely

important when investigating variation in any trait; germplasm collections, collections of breeding lines, landraces, or samples from natural populations are likely to be a source of useful genetic diversity (Zhu *et al.*, 2008a). The possibility of finding beneficial traits in historic cultivars, and the role wild relatives may play in supplying novel traits, should not be discounted. Research to screen wild wheat (*Aegilops* species) for tolerance to heat stress at the reproductive stage indicates that there is genetic variability available which may be of benefit (Pradhan *et al.*, 2012). Ideally, germplasm used in physiological breeding experiments should include cultivars which are generally adapted to the target environment and which have a broad genetic background and variability in the trait under investigation (Zhu *et al.*, 2008a). Differences in height, maturity, adaptation and disease susceptibility are all potentially confounding factors to the study of a specific trait, and may increase experimental error.

The results on the natural variation in Rca thermal tolerance in wheat shown here, illustrates the complexity of breeding thermal tolerance into wheat and further justifies the approach of genetic modification for the introduction of a more thermally tolerant Rca into wheat. Genetic modification carries its own additional challenges and issues beyond the scientific implementation. In particular, public perception and changing legislation will significantly impact upon the potential future application of these technologies, and must be considered when determining appropriate research strategies.

It was hypothesised that the expression of a more thermally stable form of Rca, in combination with the native less thermally stable forms of Rca in wheat (Carmo-Silva & Salvucci, 2011), would broaden the temperature response of Rubisco activation and photosynthesis. If so, it would be informative to determine whether there was a trade-off between sustaining photosynthesis at elevated temperature (using thermally tolerant combinations of Rca) and potentially increased photorespiratory activity.

The oxygenase activity of Rubisco initiates photorespiration, which competes with photosynthetic carbon assimilation, producing CO₂, while consuming ATP and NADPH, thus reducing the photosynthetic efficiency. Without a CO₂ concentrating mechanism (Edwards *et al.*, 2004) the losses due to photorespiration associated with the maintenance of Rubisco activity at elevated temperatures could be significant. Despite this potentially negative impact on plant efficiency, studies in *Arabidopsis* clearly

showed that increased productivity accompanied the improved thermal tolerance of Rca (Kurek *et al.*, 2007).

Cotton Rca has been shown to be more thermally tolerant than that from cooler season species (Carmo-Silva & Salvucci, 2011). Since cotton Rca was shown to activate wheat Rubisco, it was an appropriate choice for use in the experiments reported here. The available information regarding cotton Rca isoforms and catalytic activity additionally made it an attractive protein for further investigation in the context of expression in wheat. The species specificity of the interaction between Rubisco and Rca (Wang & Portis, 1992) may limit alternative cross-species combinations in transgenic approaches such as this.

Additionally, expressing Rca from a dicot in a monocot may have associated problems due to protein sequence differences. In the phylogenetic tree for Rca generated by Lawson *et al.* (2014), the Rca sequences from dicots and monocots can indeed be seen to group separately. It would be valuable to discover whether these differences- as well as the competition between wheat and cotton Rca in the plant- had an impact on productivity.

The challenges encountered here in the development of transgenic plants illustrate the difficulties of such speculative experimentation. In GM crop development, a substantial amount of effort is required to identify the best promoters, construct combinations, and to select the highest performing lines (in addition to safety and environmental impact testing) making GM a long-term and expensive process. In terms of the actual number of GM crops being successfully grown and sold globally, there are relatively few individual crops, emphasising the challenges associated with this technology. GM soya bean, maize, cotton and canola crops account for nearly all GM crop species grown, which equated to about 12% of the 1.5 billion ha of arable land worldwide in 2012 (Nature, 2013). It is estimated that GM crops have increased agricultural production by more than US\$98 billion and saved 473 million kilograms of pesticides from being sprayed over the last twenty years (Gilbert, 2013), showing the rewards of successful GM crop production to be substantial.

Difficulties identifying the cotton Rca protein in the transgenic lines may have been due to a variety of factors, including impaired translation and the possibility of rapid post-translational protein degradation

and/or modification. The amount of protein found in plant tissues at any instant reflects a balance between protein synthesis and protein degradation (Doran, 2006). Post-translational modification is an important mechanism for regulation of protein function and longevity; it can involve reversible or irreversible chemical alterations of a protein after its translation, and will frequently impact upon protein function via changes in the protein structure and dynamics. More than 200 different types of post-translational modifications have been identified (Jensen, 2006), from small chemical modifications (e.g. phosphorylation and acetylation), to the addition of complete proteins (e.g. ubiquitylation). The VIGS experiment (Chapter 4) indicates that the regulation of Rca in wheat may be complex, and this regulation may also be instrumental in the difficulties encountered in expressing cotton Rca in wheat.

Further transgenic work, investigating the expression of other thermally tolerant forms of Rca in wheat, would help to answer questions on the impacts of Rca on wheat Rubisco activity and grain yield at moderately high temperatures. Attempts to express the *GhRca* genes in a different vector backbone may also produce better results. Identifying amino acid residues accounting for interspecies diversity may lead either to the selection of Rca with beneficial properties, or to the improvement of wheat Rca through more directed gene editing approaches. A wider scale bioinformatics analysis of *Rca* gene sequences from different species may identify further residues involved in thermal tolerance, and *E. coli* protein expression experiments could be devised to permit these modifications to be tested.

Replication to confirm the results of the VIGS experiment, and further research into the regulation of the wheat Rca isoforms, both in terms of mRNA and protein expression, will help to inform future wheat Rca research. Investigating the *in vitro* thermal tolerance of purified wheat Rca isoforms would also be a valuable addition. Identification of the genes and isoforms which are most highly expressed and whether the pattern of expression changes in response to elevated temperature, will facilitate efforts to improving Rca thermal tolerance in wheat.

The impact of heat stress on wheat yields, and the importance of photosynthesis to biomass production, makes the thermal tolerance of photosynthesis, and in particular of Rca, a critical target for improving yield resilience to climate change. As methods for phenotyping improve, and the costs of molecular tools

decline, it is expected that it will be possible to examine wider panels of germplasm for traits such as Rca thermal tolerance, and that the use of genomic analysis will provide a clearer genetic basis for heat adaptive traits. Where research on Rca and Rubisco is considered, it is expected that methods such as the non-radioactive assay described here will greatly assist in high- throughput screens to look for variation or to assess the activity of these enzymes. Transgenic approaches potentially provide a highly rewarding route to crop improvement, and research to improve understanding of the regulation of the genes of interest will help to ensure successful crop engineering.

7. Conclusions

Variation was observed between ten elite wheat cultivars in their photosynthetic response to high temperatures

In field grown material, wheat cultivars which differed in their photosynthetic and Rubisco activity at an elevated temperature of 35°C were identified. Greater tolerance to the high temperature treatment was demonstrated in the higher yielding cultivar group, which maintained higher photosynthetic rates and Rubisco activation states. Leaves which contained more Rubisco, were also associated with higher yielding cultivars. Of the high yielding wheat cultivars, Battalion, Gatsby and Rialto all showed positive traits, having small changes in Rubisco activation state and no significant decrease in photosynthesis with the temperature treatment. However, the complexity of the physiological traits associated with yield potential and tolerance to elevated temperature was highlighted, with low yielding cultivars Robigus and Bacanora actually showing the smallest decrease in Rubisco activation state with the temperature treatment and therefore potentially more thermally tolerant Rca. Traits identified in the different wheat cultivars could be used in breeding programmes to improve the thermal tolerance of wheat to heat stress.

Cotton Rca protein was absent from genetically modified wheat

Genes encoding the Rca α and β isoforms from cotton were introduced into wheat using biolistic transformation, to test the hypothesis that addition of these proteins would broaden the range of temperatures at which wheat could photosynthesise. Cotton Rca genes were expressed but the protein was not detected in the wheat transgenic lines tested using western blots and IEF. Further work to investigate the impact of the cotton Rca transgene in these plants and to look further at other possibilities for introducing more thermally tolerant Rca into wheat would be beneficial.

Three Rca isoforms encoded by two genes, for which expression is co-regulated, were identified in wheat

The gene sequence of the wheat Rca α and β isoforms was determined (Carmo-Silva *et al.*, 2014). Two tandem genes (*TaRca1* and *TaRca2*) were identified on chromosomes 4A, 4B and 4D of wheat. *TaRca1* encodes the shorter β isoform of Rca and *TaRca2* can be alternatively spliced to produce the longer redox

regulated α isoform, or the shorter β isoform. Silencing of the different Rca isoforms in wheat was completed with use of Virus-Induced Gene Silencing (VIGS). The VIGS experiment indicates that the expression of the two wheat genes and isoforms is co-regulated; when the expression of one isoform was silenced an impact was also seen in the expression levels of the others.

A non-radioactive assay for measuring Rubisco and Rubisco activase activity was devised and characterised

A novel non-radioactive assay (Scales *et al.*, 2014), applicable to both leaf extracts and to purified proteins, was developed for use in Rubisco and Rca research. This has been successfully adopted by other research groups investigating Rca and Rubisco, e.g. Kuriata *et al.* (2014), and can be used to increase throughput of samples as well as being suitable for use in labs for which radioactive based assays are not feasible.

8. References

- Ainsworth E.A. & Long S.P. (2004) What have we learned from 15 years of free-air CO₂ enrichment (FACE)? A meta-analytic review of the responses of photosynthesis, canopy properties and plant production to rising CO₂. *New Phytologist*, **165**, 351-372.
- Ainsworth E.A. & Ort D.R. (2010) How Do We Improve Crop Production in a Warming World? *Plant Physiology*, **154**, 526-530.
- Aisawi K.A.B., Reynolds M.P., Singh R.P. & Foulkes M.J. (2015) The Physiological Basis of the Genetic Progress in Yield Potential of CIMMYT Spring Wheat Cultivars from 1966 to 2009. *Crop Science*, **55**, 1749-1764.
- Amani I., Fischer R.A. & Reynolds M.P. (1996) Canopy temperature depression association with yield of irrigated spring wheat cultivars in a hot climate. *Journal of Agronomy and Crop Science*, **176**, 119-129.
- Andralojc J., Madgwick P., Keys A., Parry M. & Gutteridge S. (2006) *Properties of CA1P phosphatase and its role in rubisco regulation*. Paper presented at the Society for Experimental Biology Annual Main Meeting: Comparative Biochemistry and Physiology A-Molecular & Integrative Physiology.
- Andralojc P.J., Madgwick P.J., Tao Y., Keys A., Ward J.L., Beale M.H., Loveland J.E., Jackson P.J., Willis A., C., Gutteridge S. & Parry M.A.J. (2012) 2-Carboxy-D-arabinitol 1-phosphate (CA1P) phosphatase: evidence for a wider role in plant Rubisco regulation. *Biochemical Journal*, **442**, 733-742.
- Andrews T.J., Hudson G.S., Mate C.J., Voncaemmerer S., Evans J.R. & Arvidsson Y.B.C. (1995) Rubisco - the consequences of altering its expression and activation in transgenic plants. *Journal of Experimental Botany*, **46**, 1293-1300.
- Araus J.L. & Cairns J.E. (2014) Field high-throughput phenotyping: the new crop breeding frontier. *Trends in Plant Science*, **19**, 52-61.
- Asseng S., Ewert F., Martre P., Rötter R.P., Lobell D.B., Cammarano D., Kimball B.A., Ottman M.J., Wall G.W. & White J.W. (2014) Rising temperatures reduce global wheat production. *Nature Climate Change*, **3**, 827- 832.
- Austin R.B., Bingham J., Blackwell R.D., Evans L.T., Ford M.A., Morgan C.L. & Taylor M. (1980) Genetic improvements in winter wheat yields since 1900 and associated physiological changes. *The Journal of Agricultural Science*, **94**, 675-689.
- Ayala-Ochoa A., Vargas-Suarez M., Loza-Tavera H., Leon P., Jimenez-Garcia L.F. & Sanchez-de-Jimenez E. (2004) In maize, two distinct ribulose 1, 5-bisphosphate carboxylase/oxygenase activase transcripts have different day/night patterns of expression. *Biochimie*, **86**, 439-449.
- Barta C., Carmo-Silva A.E. & Salvucci M.E. (2011a) Purification of Rubisco activase from leaves or after expression in *Escherichia coli*. (ed R. Carpentier), pp. 363-374. Humana Press, New York, Photosynthesis Research Protocols. Methods in Molecular Biology.
- Barta C., Carmo-Silva A.E. & Salvucci M.E. (2011b) Rubisco activase activity assays. In: *Photosynthesis Research Protocols* (ed R. Carpentier), pp. 375-382. Humana Press, New York, Photosynthesis Research Protocols. Methods in Molecular Biology.
- Berry J. & Bjorkman O. (1980) Photosynthetic Response and Adaptation to Temperature in Higher-Plants. *Annual Review of Plant Physiology and Plant Molecular Biology*, **31**, 491-543.
- Beuf L., Kurano N. & Miyachi S. (1999) Rubisco activase transcript (*rca*) abundance increases when the marine unicellular green alga *Chlorococcum littorale* is grown under high-CO₂ stress. *Plant Molecular Biology*, **41**, 627-635.
- Bhalla P.L. (2006) Genetic engineering of wheat – current challenges and opportunities. *Trends in Biotechnology*, **24**, 305-311.
- Blayney M.J., Whitney S.M. & Beck J.L. (2011) NanoESI mass spectrometry of Rubisco and Rubisco activase structures and their interactions with nucleotides and sugar phosphates. *Journal of the American Society for Mass Spectrometry*, **22**, 1588-1601.

- Blum A. (1990) Variation among wheat cultivars in the response of leaf gas exchange to light. *The Journal of Agricultural Science*, **115**, 305-311.
- Blum A. (1998) Improving wheat grain filling under stress by stem reserve mobilisation. *Euphytica*, **100**, 77-83.
- Bradford M.M. (1976) A rapid and sensitive method for the quantitation of microgram quantities of protein utilizing the principle of protein-dye binding. *Analytical Biochemistry*, **72**, 248-254.
- Brisson N., Gate P., Gouache D., Charmet G., Oury F.-X. & Huard F. (2010) Why are wheat yields stagnating in Europe? A comprehensive data analysis for France. *Field Crops Research*, **119**, 201-212.
- Brooks A., Portis A.R. & Sharkey T.D. (1988) Effects of irradiance and methyl viologen treatment on ATP, ADP, and activation of ribulose biphosphate carboxylase in spinach leaves. *Plant Physiology*, **88**, 850-853.
- Carmo-Silva A.E., Andralojc J., Scales J.C., Driever S.M., Lawson T., Raines C.A. & Parry M.A.J. (2015) Photosynthesis and yield in field-grown wheat. *In Preparation*.
- Carmo-Silva A.E., Barta C. & Salvucci M.E. (2011) Isolation of ribulose-1, 5-bisphosphate carboxylase/oxygenase from leaves. In: *Photosynthesis Research Protocols*, pp. 339-347.
- Carmo-Silva A.E., Gore M.A., Andrade-Sanchez P., French A.N., Hunsaker D.J. & Salvucci M.E. (2012) Decreased CO₂ availability and inactivation of Rubisco limit photosynthesis in cotton plants under heat and drought stress in the field. *Environmental and Experimental Botany*, **83**, 1-11.
- Carmo-Silva A.E. & Salvucci M.E. (2011) The activity of Rubisco's molecular chaperone, Rubisco activase, in leaf extracts. *Photosynthesis Research*, **108**, 143-155.
- Carmo-Silva A.E. & Salvucci M.E. (2012) The temperature response of CO₂ assimilation, photochemical activities and Rubisco activation in *Camelina sativa*, a potential bioenergy crop with limited capacity for acclimation to heat stress. *Planta*, **236**, 1433-1445.
- Carmo-Silva A.E. & Salvucci M.E. (2013) The regulatory properties of Rubisco activase differ among species and affect photosynthetic induction during light transitions. *Plant Physiology*, **161**, 1645-1655.
- Carmo-Silva E., Scales J.C., Madgwick P.J. & Parry M.A.J. (2014) Optimizing Rubisco and its regulation for greater resource use efficiency. *Plant, Cell & Environment*.
- Cen Y.P. & Sage R.F. (2005) The regulation of rubisco activity in response to variation in temperature and atmospheric CO₂ partial pressure in sweet potato. *Plant Physiology*, **139**, 979-990.
- Chaves M.M., Flexas J. & Pinheiro C. (2009) Photosynthesis under drought and salt stress: regulation mechanisms from whole plant to cell. *Annals of Botany*, **103**, 551.
- Chaves M.M., Pereira J.S., Maroco J., Rodrigues M.L., Ricardo C.P.P., Osorio M.L., Carvalho I., Faria T. & Pinheiro C. (2002) How plants cope with water stress in the field. Photosynthesis and growth. *Annals of Botany*, **89**, 907-916.
- Chen Z. & Spreitzer R.J. (1992) How various factors influence the CO₂/O₂ specificity of ribulose-1, 5-bisphosphate carboxylase/oxygenase. *Photosynthesis Research*, **31**, 157-164.
- Christensen A.H., Sharrock R.A. & Quail P.H. (1992) Maize polyubiquitin genes: structure, thermal perturbation of expression and transcript splicing, and promoter activity following transfer to protoplasts by electroporation. *Plant Molecular Biology*, **18**, 675-689.
- Chytky C., Hucl P. & Gray G. (2011) Leaf photosynthetic properties and biomass accumulation of selected western Canadian spring wheat cultivars. *Canadian Journal of Plant Science*, **91**, 305-314.
- Clarke S., Sylvester-Bradley R., Foulkes J., Ginsburg D., Gaju O., Werner P., Jack P., Flatman E. & Smith-Reeve L. (2012) *Adapting Wheat to Global Warming Or 'ERYCC': Earliness and Resilience for Yield in a Changing Climate*. HGCA.
- Coombs J., Baldry C.W. & Bucke C. (1973) The C-4 pathway in *Pennisetum purpureum*. *Planta*, **110**, 95-107.
- Cossani C.M. & Reynolds M.P. (2012) Physiological traits for improving heat tolerance in wheat. *Plant Physiology*, **160**, 1710-1718.
- Cousins A.B., Ghannoum O., Von Caemmerer S. & Badger M.R. (2010) Simultaneous determination of Rubisco carboxylase and oxygenase kinetic parameters in *Triticum aestivum* and *Zea mays* using membrane inlet mass spectrometry. *Plant, Cell & Environment*, **33**, 444-452.

- Crafts-Brandner S.J. & Law R.D. (2000) Effect of heat stress on the inhibition and recovery of the ribulose-1,5-bisphosphate carboxylase/oxygenase activation state. *Planta*, **212**, 67-74.
- Crafts-Brandner S.J. & Salvucci M.E. (2000) Rubisco activase constrains the photosynthetic potential of leaves at high temperature and CO₂. *Proceedings of the National Academy of Sciences*, **97**, 13430-13435.
- Crafts-Brandner S.J. & Salvucci M.E. (2002) Sensitivity of photosynthesis in a C4 plant, maize, to heat stress. *Plant Physiology*, **129**, 1773-1780.
- Crafts-Brandner S.J., van de Loo F.J. & Salvucci M.E. (1997) The two forms of ribulose-1,5-bisphosphate carboxylase/oxygenase activase differ in sensitivity to elevated temperature. *Plant Physiology*, **114**, 439-444.
- Deridder B. & Salvucci M. (2007) Modulation of Rubisco activase gene expression during heat stress in cotton (*Gossypium hirsutum* L.) involves post-transcriptional mechanisms. *Plant Science*, **172**, 246-254.
- DeRidder B.P., Shybut M.E., Dyle M.C., Kremling K.A.G. & Shapiro M.B. (2012) Changes at the 3'-untranslated region stabilize Rubisco activase transcript levels during heat stress in Arabidopsis. *Planta*, **236**, 463-476.
- Dias A.S. & Lidon F.C. (2009) Evaluation of grain filling rate and duration in bread and durum wheat, under heat stress after anthesis. *Journal of Agronomy and Crop Science*, **195**, 137-147.
- Ding X.S., Schneider W.L., Chaluvadi S.R., Mian M.A.R. & Nelson R.S. (2006) Characterization of a Brome mosaic virus strain and its use as a vector for gene silencing in monocotyledonous hosts. *Molecular Plant-Microbe Interactions*, **19**, 1229-1239.
- Dong L.-Y., Hata S. & Izui K. (1997) High-level expression of maize C4-type phosphoenolpyruvate carboxylase in *Escherichia coli* and its rapid purification. *Bioscience, Biotechnology, and Biochemistry*, **61**, 545-546.
- Doran P.M. (2006) Foreign protein degradation and instability in plants and plant tissue cultures. *Trends in Biotechnology*, **24**, 426-432.
- Driever S.M., Lawson T., Andralojc P.J., Raines C.A. & Parry M.A.J. (2014) Natural variation in photosynthetic capacity, growth, and yield in 64 field-grown wheat genotypes. *Journal of Experimental Botany*, doi: 10.1093/jxb/eru1253
- Eckardt N.A. & Portis A.R. (1997) Heat denaturation profiles of Ribulose-1,5-bisphosphate carboxylase/oxygenase (Rubisco) and Rubisco activase and the inability of Rubisco activase to restore activity of heat-denatured Rubisco. *Plant Physiology*, **113**, 243-248.
- Eckardt N.A., Snyder G.W., Portis A.R. & Ogren W.L. (1997) Growth and photosynthesis under high and low irradiance of *Arabidopsis thaliana* antisense mutants with reduced Ribulose-1,5-bisphosphate carboxylase/oxygenase activase content. *Plant Physiology*, **113**, 575-586.
- Edmondson D.L., Badger M.R. & Andrews T.J. (1990) Slow inactivation of Ribulose bisphosphate carboxylase during catalysis is caused by accumulation of a slow, tight-binding inhibitor at the catalytic site. *Plant Physiology*, **93**, 1390-1397.
- Edwards G.E., Franceschi V.R. & Voznesenskaya E.V. (2004) Single-cell C4 photosynthesis versus the dual-cell (Kranz) paradigm. *Annual Review of Plant Biology*, **55**, 173-196.
- Ellis R.J. (1979) The most abundant protein in the world. *Trends in Biochemical Sciences*, **4**, 241-244.
- Emanuelsson O., Nielsen H. & Von Heijne G. (1999) ChloroP, a neural network-based method for predicting chloroplast transit peptides and their cleavage sites. *Protein Science*, **8**, 978-984.
- Ennahli S. & Earl H.J. (2005) Physiological limitations to photosynthetic carbon assimilation in cotton under water stress. *Crop Science*, **45**, 2374-2382.
- Esau B.D., Snyder G.W. & Portis A.R. (1996) Differential effects of N- and C-terminal deletions on the two activities of Rubisco activase. *Archives of Biochemistry and Biophysics*, **326**, 100-105.
- Evans J.R. & Austin R.B. (1986) The specific activity of ribulose-1,5-bisphosphate carboxylase in relation to genotype in wheat. *Planta*, **167**, 344-350.
- Evenson R.E. & Gollin D. (2003) Assessing the impact of the Green Revolution, 1960 to 2000. *Science*, **300**, 758-762.
- FAO (2015), <http://faostat3.fao.org/home/E>.
- Farquhar G.D., Caemmerer S.V. & Berry J.A. (1980) A biochemical-model of photosynthetic CO₂ assimilation in leaves of C3 species. *Planta*, **149**, 78-90.

- Feller U., Crafts-Brandner S.J. & Salvucci M.E. (1998) Moderately high temperatures inhibit Ribulose-1,5-bisphosphate carboxylase/oxygenase (Rubisco) activase-mediated activation of Rubisco. *Plant Physiology*, **116**, 539-546.
- Ferris R., Ellis R.H., Wheeler T.R. & Hadley P. (1998) Effect of high temperature stress at anthesis on grain yield and biomass of field-grown crops of wheat. *Annals of Botany*, **82**, 631-639.
- Fire A. (1999) RNA-triggered gene silencing. *Trends in Genetics*, **15**, 358-363.
- Fischer R.A., Bidinger F., Syme J.R. & Wall P.C. (1981) Leaf photosynthesis, leaf permeability, crop growth, and yield of short spring wheat genotypes under irrigation. *Crop Science*, **21**, 367-373.
- Foulkes M.J., Snape J.W., Shearman V.J., Reynolds M.P., Gaju O. & Sylvester-Bradley R. (2007) Genetic progress in yield potential in wheat: recent advances and future prospects. *Journal of Agricultural Science*, **145**, 17.
- Fraser H.I., Kvaratskhelia M. & White M.F. (1999) The two analogous phosphoglycerate mutases of *Escherichia coli*. *Febs Letters*, **455**, 344-348.
- Freeman J., Sparks C.A., West J., Shewry P.R. & Jones H.D. (2011) Temporal and spatial control of transgene expression using a heat-inducible promoter in transgenic wheat. *Plant Biotechnology Journal*, **9**, 788-796.
- Fukayama H., Ueguchi C., Nishikawa K., Katoh N., Ishikawa C., Masumoto C., Hatanaka T. & Misoo S. (2012) Overexpression of Rubisco Activase Decreases the Photosynthetic CO₂ Assimilation Rate by Reducing Rubisco Content in Rice Leaves. *Plant and Cell Physiology*, **53**, 976-986.
- Furbank R.T. & Tester M. (2011) Phenomics—technologies to relieve the phenotyping bottleneck. *Trends in Plant Science*, **16**, 635-644.
- Galmes J., Flexas J., Keys A.J., Cifre J., Mitchell R.A.C., Madgwick P.J., Haslam R.P., Medrano H. & Parry M.A.J. (2005) Rubisco specificity factor tends to be larger in plant species from drier habitats and in species with persistent leaves. *Plant Cell and Environment*, **28**, 571-579.
- Galmes J., Ribas-Carbo M., Medrano H. & Flexas J. (2011) Rubisco activity in Mediterranean species is regulated by the chloroplastic CO₂ concentration under water stress. *Journal of Experimental Botany*, **62**, 653-665.
- Gasteiger E., Hoogland C., Gattiker A., Wilkins M.R., Appel R.D. & Bairoch A. (2005) Protein identification and analysis tools on the ExpASY server. In: *The Proteomics Protocols Handbook*, pp. 571-607. Springer.
- Gerland P., Raftery A.E., Ševčíková H., Li N., Gu D., Spoorenberg T., Alkema L., Fosdick B.K., Chunn J. & Lalic N. (2014) World population stabilization unlikely this century. *Science*, **346**, 234-237.
- Gibon Y., Blaesing O.E., Hannemann J., Carillo P., Höhne M., Hendriks J.H.M., Palacios N., Cross J., Selbig J. & Stitt M. (2004) A robot-based platform to measure multiple enzyme activities in Arabidopsis using a set of cycling assays: comparison of changes of enzyme activities and transcript levels during diurnal cycles and in prolonged darkness. *The Plant Cell Online*, **16**, 3304-3325.
- Gilbert N. (2013) A hard look at GM crops. *Nature*, **497**, 24-26.
- Gill B.S., Appels R., Botha-Oberholster A.M., Buell C.R., Bennetzen J.L., Chalhoub B., Chumley F., Dvořák J., Iwanaga M. & Keller B. (2004) A workshop report on wheat genome sequencing. *Genetics*, **168**, 1087.
- Gooding M.J., Ellis R.H., Shewry P.R. & Schofield J.D. (2003) Effects of restricted water availability and increased temperature on the grain filling, drying and quality of winter wheat. *Journal of Cereal Science*, **37**, 295-309.
- Gutteridge S., Parry M.A.J., Burton S., Keys A.J., Mudd A., Feeney J., Servaites J.C. & Pierce J. (1986) A nocturnal inhibitor of carboxylation in leaves. *Nature*, **324**, 274-276.
- Hamilton A., Voinnet O., Chappell L. & Baulcombe D. (2002) Two classes of short interfering RNA in RNA silencing. *The EMBO Journal*, **21**, 4671-4679.
- Hannon G.J. (2002) RNA interference. *Nature*, **418**, 244-251.
- He Z.L., von Caemmerer S., Hudson G.S., Price G.D., Badger M.R. & Andrews T.J. (1997) Ribulose-1,5-bisphosphate carboxylase/oxygenase activase deficiency delays senescence of ribulose-1,5-bisphosphate carboxylase/oxygenase but progressively impairs its catalysis during tobacco leaf development. *Plant Physiology*, **115**, 1569-1580.

- Hede A.R., Skovmand B., Reynolds M.P., Crossa J., Vilhelmsen A.L. & Stølen O. (1999) Evaluating genetic diversity for heat tolerance traits in Mexican wheat landraces. *Genetic Resources and Crop Evolution*, **46**, 37-45.
- Henderson J.N., Kuriata A.M., Fromme R., Salvucci M.E. & Wachter R.M. (2011) Atomic resolution X-ray structure of the substrate recognition domain of higher plant Ribulose-bisphosphate Carboxylase/Oxygenase (Rubisco) Activase. *Journal of Biological Chemistry*, **286**, 35683-35688.
- Hendrickson L., Sharwood R., Ludwig M., Whitney S.M., Badger M.R. & Von Caemmerer S. (2008) The effects of Rubisco activase on C4 photosynthesis and metabolism at high temperature. *Journal of Experimental Botany*, **59**, 1789-1798.
- Heo J.Y. & Holbrook G.P. (1999) Regulation of 2-carboxy-D-arabinitol 1-phosphate phosphatase: activation by glutathione and interaction with thiol reagents. *Biochemical Journal*, **338**, 409-416.
- HGCA (2008) *The wheat growth guide*.
- Huang X., Zhao Y., Wei X., Li C., Wang A., Zhao Q., Li W., Guo Y., Deng L. & Zhu C. (2012) Genome-wide association study of flowering time and grain yield traits in a worldwide collection of rice germplasm. *Nature Genetics*, **44**, 32-39.
- Huang X.Q., Cöster H., Ganai M.W. & Röder M.S. (2003) Advanced backcross QTL analysis for the identification of quantitative trait loci alleles from wild relatives of wheat (*Triticum aestivum* L.). *Theoretical and Applied Genetics*, **106**, 1379-1389.
- Hudson G.S., Evans J.R., Voncaemmerer S., Arvidsson Y.B.C. & Andrews T.J. (1992) Reduction of ribulose-1,5-bisphosphate carboxylase oxygenase content by antisense RNA reduces photosynthesis in transgenic tobacco plants. *Plant Physiology*, **98**, 294-302.
- IPCC (2013) Working Group I Contribution to the IPCC Fifth Assessment Report on Climate Change 2013: The Physical Science Basis, Summary for Policy Makers.
- Jackson A.O., Lim H.-S., Bragg J., Ganesan U. & Lee M.Y. (2009) Hordeivirus replication, movement, and pathogenesis. *Annual Review of Phytopathology*, **47**, 385-422.
- Jensen O.N. (2006) Interpreting the protein language using proteomics. *Nature Reviews Molecular Cell Biology*, **7**, 391-403.
- Jiang C.Z., Quick W.P., Alred R., Kliebenstein D. & Rodermeil S.R. (1994) Antisense RNA inhibition of Rubisco activase expression. *Plant Journal*, **5**, 787-798.
- Jiang Y., Wang J., Tao X. & Zhang Y. (2013) Characterization and expression of Rubisco activase genes in *Ipomoea batatas*. *Molecular Biology Reports*, **40**, 6309-6321.
- Jones H.D. (2005) Wheat transformation: current technology and applications to grain development and composition. *Journal of Cereal Science*, **41**, 137-147.
- Jordan D.B. & Ogren W.L. (1981) A sensitive assay procedure for simultaneous determination of ribulose-1, 5-bisphosphate carboxylase and oxygenase activities. *Plant Physiology*, **67**, 237-245.
- Jordan D.B. & Ogren W.L. (1984) The CO₂/O₂ specificity of ribulose 1, 5-bisphosphate carboxylase/oxygenase. *Planta*, **161**, 308-313.
- Joshi J., Mueller-Cajar O., Tsai Y.-C.C., Hartl F.U. & Hayer-Hartl M. (2015) Role of small subunit in mediating assembly of red-type form I rubisco. *Journal of Biological Chemistry*, **290**, 1066-1074.
- Kane H.J., Wilkin J.-M., Portis A.R. & Andrews T.J. (1998) Potent inhibition of ribulose-bisphosphate carboxylase by an oxidized impurity in ribulose-1, 5-bisphosphate. *Plant Physiology*, **117**, 1059-1069.
- Keys A.J. (1999) Biochemistry of photorespiration and the consequences for plant performance. In: *Plant Carbohydrate Biochemistry*, pp. 147-161. BIOS Scientific Oxford, UK.
- Khan S., Andralojc P.J., Lea P.J. & Parry M.A.J. (1999) 2'-Carboxy-D-arabinitol 1-phosphate protects ribulose 1,5-bisphosphate carboxylase/oxygenase against proteolytic breakdown. *European Journal of Biochemistry*, **266**, 840-847.
- Kim K. & Portis A.R. (2005) Temperature dependence of photosynthesis in Arabidopsis plants with modifications in Rubisco Activase and membrane fluidity. *Plant and Cell Physiology*, **46**, 522-530.
- Kim K. & Portis A.R. (2006) Kinetic analysis of the slow inactivation of Rubisco during catalysis: effects of temperature, O₂ and Mg⁺⁺. *Photosynthesis Research*, **87**, 195-204.
- Klein R.R. & Salvucci M.E. (1995) Rubisco, rubisco activase and ribulose-5-phosphate kinase gene expression and polypeptide accumulation in a tobacco mutant defective in chloroplast protein synthesis. *Photosynthesis Research*, **43**, 213-223.

- Kohli A., González-Melendi P., Abranches R., Capell T., Stoger E. & Christou P. (2006) The quest to understand the basis and mechanisms that control expression of introduced transgenes in crop plants. *Plant Signaling & Behavior*, **1**, 185-195.
- Kooter J.M., Matzke M.A. & Meyer P. (1999) Listening to the silent genes: transgene silencing, gene regulation and pathogen control. *Trends in Plant Science*, **4**, 340-347.
- Korte A. & Farlow A. (2013) The advantages and limitations of trait analysis with GWAS: a review. *Plant Methods*, **9**, 29.
- Kozak M. (1984) Compilation and analysis of sequences upstream from the translational start site in eukaryotic mRNAs. *Nucleic Acids Research*, **12**, 857-872.
- Ku S.-B. & Edwards G.E. (1978) Oxygen inhibition of photosynthesis. *Planta*, **140**, 1-6.
- Kumar A., Li C. & Portis A.R. (2009) *Arabidopsis thaliana* expressing a thermostable chimeric Rubisco activase exhibits enhanced growth and higher rates of photosynthesis at moderately high temperatures. *Photosynthesis Research*, **100**, 143-153.
- Kumar S., Kumari P., Kumar U., Grover M., Singh A.K., Singh R. & Sengar R.S. (2013) Molecular approaches for designing heat tolerant wheat. *Journal of Plant Biochemistry and Biotechnology*, **22**, 359-371.
- Kumar U., Joshi A.K., Kumari M., Paliwal R., Kumar S. & Röder M.S. (2010) Identification of QTLs for stay green trait in wheat (*Triticum aestivum* L.) in the 'Chirya 3' × 'Sonalika' population. *Euphytica*, **174**, 437-445.
- Kurek I., Chang T.K., Bertain S.M., Madrigal A., Liu L., Lassner M.W. & Zhu G. (2007) Enhanced thermostability of Arabidopsis Rubisco Activase improves photosynthesis and growth rates under moderate heat stress. *The Plant Cell Online*, **19**, 3230-3241.
- Kuriata A.M., Chakraborty M., Henderson J.N., Hazra S., Serban A.J., Pham T.V.T., Levitus M. & Wachter R.M. (2014) ATP and Magnesium Promote Cotton Short-Form Ribulose-1, 5-bisphosphate Carboxylase/Oxygenase (Rubisco) Activase Hexamer Formation at Low Micromolar Concentrations. *Biochemistry*, **53**, 7232-7246.
- Laemmli U.K. (1970) Cleavage of structural proteins during the assembly of the head of bacteriophage T4. *Nature*, **227**, 680-685.
- Lan Y., Woodrow I.E. & Mott K.A. (1992) Light-dependent changes in ribulose bisphosphate carboxylase activase activity in leaves. *Plant Physiology*, **99**, 304-309.
- Larson E.M., O'Brien C.M., Zhu G., Spreitzer R.J. & Portis A.R. (1997) Specificity for activase is changed by a Pro-89 to Arg substitution in the large subunit of ribulose-1, 5-bisphosphate carboxylase/oxygenase. *Journal of Biological Chemistry*, **272**, 17033-17037.
- Lauerer M., Saftic D., Quick W.P., Labate C., Fichtner K., Schulze E.D., Rodermel S.R., Bogorad L. & Stitt M. (1993) Decreased ribulose-1, 5-bisphosphate carboxylase-oxygenase in transgenic tobacco transformed with "antisense" rbcS. *Planta*, **190**, 332-345.
- Law R.D. & Crafts-Brandner S.J. (2001) High temperature stress increases the expression of wheat leaf ribulose-1,5-bisphosphate carboxylase/oxygenase activase protein. *Archives of Biochemistry and Biophysics*, **386**, 261-267.
- Law R.D., Crafts-Brandner S.J. & Salvucci M.E. (2001) Heat stress induces the synthesis of a new form of ribulose-1,5-bisphosphate carboxylase/oxygenase activase in cotton leaves. *Planta*, **214**, 117-125.
- Lawlor D.W. (2002) Limitation to photosynthesis in water-stressed leaves: Stomata vs. metabolism and the role of ATP. *Annals of Botany*, **89**, 871-885.
- Lawson T., Davey P.A., Yates S.A., Bechtold U., Baeshen M., Baeshen N., Mutwakil M.Z., Sabir J., Baker N.R. & Mullineaux P.M. (2014) C3 photosynthesis in the desert plant *Rhazya stricta* is fully functional at high temperatures and light intensities. *New Phytologist*, **201**, 862-873.
- Lazar G. & Goodman H.M. (2000) The Arabidopsis splicing factor SR1 is regulated by alternative splicing. *Plant Molecular Biology*, **42**, 571-581.
- Le Quere C., Raupach M.R., Canadell J.G., Marland G., Bopp L., Ciais P., Conway T.J., Doney S.C., Feely R.A., Foster P., Friedlingstein P., Gurney K., Houghton R.A., House J.I., Huntingford C., Levy P.E., Lomas M.R., Majkut J., Metzl N., Ometto J.P., Peters G.P., Prentice I.C., Randerson J.T., Running S.W., Sarmiento J.L., Schuster U., Sitch S., Takahashi T., Viovy N., van der Werf G.R. & Woodward F.I. (2009) Trends in the sources and sinks of carbon dioxide. *Nature Geoscience*, **2**, 831-836.

- Lee W.-S., Hammond-Kosack K.E. & Kanyuka K. (2012) Barley stripe mosaic virus-mediated tools for investigating gene function in cereal plants and their pathogens: virus-induced gene silencing, host-mediated gene silencing, and virus-mediated overexpression of heterologous protein. *Plant Physiology*, **160**, 582-590.
- Lee W.-S., Rudd J.J., Hammond-Kosack K.E. & Kanyuka K. (2014) Mycosphaerella graminicola LysM effector-mediated stealth pathogenesis subverts recognition through both CERK1 and CEBiP homologues in wheat. *Molecular Plant-Microbe Interactions*, **27**, 236-243.
- Leister D. (2012) How can the light reactions of photosynthesis be improved in plants? *Frontiers in Plant Science*, **3**, doi: 10.3389/fpls.2012.00199.
- Li C., Salvucci M.E. & Portis A.R. (2005) Two residues of Rubisco activase involved in recognition of the Rubisco substrate. *Journal of Biological Chemistry*, **280**, 24864-24869.
- Li H.-m. & Teng Y.-S. (2013) Transit peptide design and plastid import regulation. *Trends in Plant Science*, **18**, 360-366.
- Li H. & Chiu C.C. (2010) Protein transport into chloroplasts. *Annual Review of Plant Biology*, **61**, 157-180.
- Li L.A., Gibson J.L. & Tabita F.R. (1993) The Rubisco Activase (Rca) Gene Is Located Downstream from Rbcs in Anabaena Sp Strain Ca and Is Detected in Other Anabaena/Nostoc Strains. *Plant Molecular Biology*, **21**, 753-764.
- Lillemo M., Van Ginkel M., Trethowan R.M., Hernandez E. & Crossa J. (2005) Differential adaptation of CIMMYT bread wheat to global high temperature environments. *Crop Science*, **45**, 2443-2453.
- Liu C.M., Young A.L., Starling-Windhof A., Bracher A., Saschenbrecker S., Rao B.V., Rao K.V., Berninghausen O., Mielke T., Hartl F.U., Beckmann R. & Hayer-Hartl M. (2010) Coupled chaperone action in folding and assembly of hexadecameric Rubisco. *Nature*, **463**, 197-U181.
- Liu M., Qi H., Zhang Z.P., Song Z.W., Kou T.J., Zhang W.J. & Yu J.L. (2012) Response of photosynthesis and chlorophyll fluorescence to drought stress in two maize cultivars. *African Journal of Agricultural Research*, **34**, 4751-4760.
- Liu Z.R., Taub C.C. & McClung C.R. (1996) Identification of an *Arabidopsis thaliana* ribulose-1,5-bisphosphate carboxylase oxygenase activase (RCA) minimal promoter regulated by light and the circadian clock. *Plant Physiology*, **112**, 43-51.
- Lobell D.B. & Field C.B. (2007) Global scale climate - crop yield relationships and the impacts of recent warming. *Environmental Research Letters*, **2**, DOI: 10.1088/1748-9326/1082/1081/014002
- Lobell D.B., Ortiz-Monasterio J.I., Asner G.P., Matson P.A., Naylor R.L. & Falcon W.P. (2005) Analysis of wheat yield and climatic trends in Mexico. *Field Crops Research*, **94**, 250-256.
- Long S.P., Ainsworth E.A., Leakey A.D.B., Nösberger J. & Ort D.R. (2006a) Food for thought: lower-than-expected crop yield stimulation with rising CO₂ concentrations. *Science*, **312**, 1918-1921.
- Long S.P. & Ort D.R. (2010) More than taking the heat: crops and global change. *Current Opinion in Plant Biology*, **13**, 241-248.
- Long S.P., Zhu X.-G., Naidu S.L. & Ort D.R. (2006b) Can improvement in photosynthesis increase crop yields? *Plant, Cell and Environment*, **29**, 315-330.
- Lorimer G.H., Badger M.R. & Andrews T.J. (1977) D-Ribulose-1, 5-bisphosphate carboxylase-oxygenase: improved methods for the activation and assay of catalytic activities. *Analytical Biochemistry*, **78**, 66-75.
- Lu C.-M. & Zhang J.-H. (2000) Heat-induced multiple effects on PSII in wheat plants. *Journal of Plant Physiology*, **156**, 259-265.
- Majumdar S., Ghosh S., Glick B.R. & Dumbroff E.B. (1991) Activities of chlorophyllase, phosphoenolpyruvate carboxylase and ribulose-1,5-bisphosphate carboxylase in the primary leaves of soybean during senescence and drought. *Physiologia Plantarum*, **81**, 473-480.
- Martinez- Barajas E., Molina- Galan J. & Sanchez de Jimenez E.S. (1997) Regulation of Rubisco activity during grain-fill in maize: Possible role of Rubisco activase. *Journal of Agricultural Science*, **128**, 155-161.
- Martino-Catt S. & Ort D.R. (1992) Low temperature interrupts circadian regulation of transcriptional activity in chilling-sensitive plants. *Proceedings of the National Academy of Sciences*, **89**, 3731-3735.
- Mate C.J., Hudson G.S., Von Caemmerer S., Evans J.R. & Andrews T.J. (1993) Reduction of ribulose-bisphosphate carboxylase activase levels in tobacco (*Nicotiana tabacum*) by antisense RNA

- reduces ribulose-bisphosphate carboxylase carbamylation and impairs photosynthesis. *Plant Physiology*, **102**, 1119-1128.
- Mate C.J., von Caemmerer S., Evans J.R., Hudson G.S. & Andrews T.J. (1996) The relationship between CO₂-assimilation rate, Rubisco carbamylation and Rubisco activase content in activase-deficient transgenic tobacco suggests a simple model of activase action. *Planta*, **198**, 604-613.
- Matzke A.J.M. & Matzke M.A. (1998) Position effects and epigenetic silencing of plant transgenes. *Current Opinion in Plant Biology*, **1**, 142-148.
- Maxwell K. & Johnson G.N. (2000) Chlorophyll fluorescence—a practical guide. *Journal of Experimental Botany*, **51**, 659-668.
- McElroy D., Zhang W., Cao J. & Wu R. (1990) Isolation of an efficient actin promoter for use in rice transformation. *The Plant Cell Online*, **2**, 163-171.
- Meza T.J., Kamfjord D., Håkelien A.-M., Evans I., Godager L.H., Mandal A., Jakobsen K.S. & Aalen R.B. (2001) The frequency of silencing in *Arabidopsis thaliana* varies highly between progeny of siblings and can be influenced by environmental factors. *Transgenic Research*, **10**, 53-67.
- Monteith J.L. & Moss C.J. (1977) Climate and the efficiency of crop production in Britain [and discussion]. *Philosophical Transactions of the Royal Society of London. B, Biological Sciences*, **281**, 277-294.
- Mueller-Cajar O., Stotz M., Wendler P., Hartl F.U., Bracher A. & Hayer-Hartl M. (2011) Structure and function of the AAA+ protein CbbX, a red-type Rubisco activase. *Nature*, **479**, 194-199.
- Mueller-Cajar O. & Whitney S.M. (2008) Directing the evolution of Rubisco and Rubisco activase: first impressions of a new tool for photosynthesis research. *Photosynthesis Research*, **98**, 667-675.
- Mullan D.J. & Reynolds M.P. (2010) Quantifying genetic effects of ground cover on soil water evaporation using digital imaging. *Functional Plant Biology*, **37**, 703-712.
- Murchie E.H., Pinto M. & Horton P. (2009) Agriculture and the new challenges for photosynthesis research. *New Phytologist*, **181**, 532-552.
- Nature (2013) GM crops: A story in numbers. *Nature News*, pp. 22–23.
- Neumann K., Kobiljski B., Denčić S., Varshney R.K. & Börner A. (2011) Genome-wide association mapping: a case study in bread wheat (*Triticum aestivum* L.). *Molecular Breeding*, **27**, 37-58.
- Ober E.S., Werner P., Flatman E., Angus W.J., Jack P., Smith-Reeve L. & Tapsell C. (2014) Genotypic differences in deep water extraction associated with drought tolerance in wheat. *Functional Plant Biology*, **41**, 1078-1086.
- Ortiz R., Sayre K.D., Govaerts B., Gupta R., Subbarao G.V., Ban T., Hodson D., Dixon J.M., Ortiz-Monasterio J.I. & Reynolds M. (2008) Climate change: can wheat beat the heat? *Agriculture, Ecosystems & Environment*, **126**, 46-58.
- Ott C.M., Smith B.D., Portis A.R. & Spreitzer R.J. (2000) Activase Region on Chloroplast Ribulose-1, 5-bisphosphate Carboxylase/Oxygenase : Non-conservative substitution in the large subunit alters species specificity of protein interaction. *Journal of Biological Chemistry*, **275**, 26241-26244.
- Pacold I. & Anderson L.E. (1975) Chloroplast and Cytoplasmic Enzymes VI. Pea Leaf 3-Phosphoglycerate Kinases. *Plant Physiology*, **55**, 168-171.
- Parikh M.R., Greene D.N., Woods K.K. & Matsumura I. (2006) Directed evolution of RuBisCO hypermorphs through genetic selection in engineered E.coli. *Protein Engineering Design & Selection*, **19**, 113-119.
- Parry M.A.J., Andralojc P.J., Khan S., Lea P.J. & Keys A.J. (2002) Rubisco activity: Effects of drought stress. *Annals of Botany*, **89**, 833-839.
- Parry M.A.J., Andralojc P.J., Mitchell R.A.C., Madgwick P.J. & Keys A.J. (2003) Manipulation of Rubisco: the amount, activity, function and regulation. *Journal of Experimental Botany*, **54**, 1321-1333.
- Parry M.A.J., Andralojc P.J., Parmar S., Keys A.J., Habash D., Paul M.J., Alred R., Quick W.P. & Servaites J.C. (1997) Regulation of Rubisco by inhibitors in the light. *Plant, Cell & Environment*, **20**, 528-534.
- Parry M.A.J., Andralojc P.J., Scales J.C., Salvucci M.E., Carmo-Silva A.E., Alonso H. & Whitney S.M. (2013) Rubisco activity and regulation as targets for crop improvement. *Journal of Experimental Botany*, **64**, 717-730.
- Parry M.A.J., Keys A.J., Madgwick P.J., Carmo-Silva A.E. & Andralojc P.J. (2008) Rubisco regulation: a role for inhibitors. *Journal of Experimental Botany*, **59**, 1569-1580.

- Parry M.A.J., Madgwick P.J., Carvalho J.F.C. & Andralojc P.J. (2006) *Prospects for increasing photosynthesis by overcoming the limitations of Rubisco*. Paper presented at the International workshop on increasing wheat yield potential.
- Parry M.A.J., Madgwick P.J., Carvalho J.F.C. & Andralojc P.J. (2007) Prospects for increasing photosynthesis by overcoming the limitations of Rubisco. *Journal of Agricultural Science*, **145**, 31-43.
- Parry M.A.J., Reynolds M., Salvucci M.E., Raines C., Andralojc P.J., Zhu X.G., Price G.D., Condon A.G. & Furbank R.T. (2011) Raising yield potential of wheat. II. Increasing photosynthetic capacity and efficiency. *Journal of Experimental Botany*, **62**, 453-467.
- Paulsen J.M. & Lane M.D. (1966) Spinach Ribulose Diphosphate Carboxylase. I. Purification and Properties of the Enzyme. *Biochemistry*, **5**, 2350-2357.
- Pearce F. (2006) Catalytic by-product formation and ligand binding by ribulose biphosphate carboxylases from different phylogenies. *Biochem. J*, **399**, 525-534.
- Pelloux J., Jolivet Y., Fontaine V., Banvoy J. & Dizengremel P. (2001) Changes in Rubisco and Rubisco activase gene expression and polypeptide content in *Pinus halepensis* M. subjected to ozone and drought. *Plant, Cell & Environment*, **24**, 123-131.
- Perchorowicz J.T., Raynes D.A. & Jensen R.G. (1981) Light limitation of photosynthesis and activation of ribulose biphosphate carboxylase in wheat seedlings. *Proceedings of the National Academy of Sciences*, **78**, 2985-2989.
- Pilgrim M.L. & McClung C.R. (1993) Differential involvement of the circadian clock in the expression of genes required for ribulose-1, 5-biphosphate carboxylase/oxygenase synthesis, assembly, and activation in *Arabidopsis thaliana*. *Plant Physiology*, **103**, 553-564.
- Ploegh H.L. (1995) One-Dimensional Isoelectric Focusing of Proteins in Slab Gels. *Current Protocols in Protein Science*, DOI: 10.1002/0471140864.
- Poorter H., Niinemets Ü., Poorter L., Wright I.J. & Villar R. (2009) Causes and consequences of variation in leaf mass per area (LMA): a meta-analysis. *New Phytologist*, **182**, 565-588.
- Porter J.R. & Gawith M. (1999) Temperatures and the growth and development of wheat: a review. *European Journal of Agronomy*, **10**, 23-36.
- Portis A.R. (2003) Rubisco activase - Rubisco's catalytic chaperone. *Photosynthesis Research*, **75**, 11-27.
- Portis A.R., Li C.S., Wang D.F. & Salvucci M.E. (2008) Regulation of Rubisco activase and its interaction with Rubisco. *Journal of Experimental Botany*, **59**, 1597-1604.
- Portis A.R. & Parry M.A.J. (2007) Discoveries in Rubisco (Ribulose 1,5-biphosphate carboxylase/oxygenase): a historical perspective. *Photosynthesis Research*, **94**, 121-143.
- Portis A.R., Salvucci M.E. & Ogren W.L. (1986) Activation of Ribulose biphosphate carboxylase/oxygenase at physiological CO₂ and ribulosebiphosphate concentrations by Rubisco activase. *Plant Physiology*, **82**, 967-971.
- Pradhan G.P., Prasad P.V.V., Fritz A.K., Kirkham M.B. & Gill B.S. (2012) High temperature tolerance in species and its potential transfer to wheat. *Crop Science*, **52**, 292-304.
- Primavesi L.F., Wu H., Mudd E.A., Day A. & Jones H.D. (2008) Visualisation of plastids in endosperm, pollen and roots of transgenic wheat expressing modified GFP fused to transit peptides from wheat SSU RubisCO, rice FtsZ and maize ferredoxin III proteins. *Transgenic Research*, **17**, 529-543.
- Qian J. & Rodermel S.R. (1993) Ribulose-1, 5-biphosphate carboxylase/oxygenase activase cDNAs from *Nicotiana tabacum*. *Plant Physiology*, **102**, 683-684.
- Qin D., Wu H., Peng H., Yao Y., Ni Z., Li Z., Zhou C. & Sun Q. (2008) Heat stress-responsive transcriptome analysis in heat susceptible and tolerant wheat (*Triticum aestivum* L.) by using Wheat Genome Array. *BMC Genomics*, **9**, doi:10.1186/1471-2164-1189-1432.
- Raines C.A. (2003) The Calvin cycle revisited. *Photosynthesis Research*, **75**, 1-10.
- Raines C.A. (2006) Transgenic approaches to manipulate the environmental responses of the C3 carbon fixation cycle. *Plant, Cell and Environment*, **29**, 331-339.
- Raines C.A. (2010) Increasing Photosynthetic Carbon Assimilation in C3 Plants to Improve Crop Yield: Current and Future Strategies. *Plant Physiology*, **155**, 36-42.
- Raines C.A. (2011) Increasing photosynthetic carbon assimilation in C3 plants to improve crop yield: current and future strategies. *Plant Physiology*, **155**, 36-42.

- Ramakers C., Ruijter J.M., Deprez R.H.L. & Moorman A.F.M. (2003) Assumption-free analysis of quantitative real-time polymerase chain reaction (PCR) data. *Neuroscience Letters*, **339**, 62-66.
- Raven J.A. (2013) Rubisco: still the most abundant protein of Earth? *New Phytologist*, **198**, 1-3.
- Ray D.K., Mueller N.D., West P.C. & Foley J.A. (2013) Yield trends are insufficient to double global crop production by 2050. *PLoS One*, **8**, doi:10.1371/journal.pone.0066428.
- Ray D.K., Ramankutty N., Mueller N.D., West P.C. & Foley J.A. (2012) Recent patterns of crop yield growth and stagnation. *Nature Communications*, **3**, 1293.
- Rees D., Sayre K.D., Acevedo E., Nava Sanchez T., Lu Z., Zeiger E. & Limon A. (1993) *Canopy temperatures of wheat: Relationship with yield and potential as a technique for early generation selection*. CIMMYT. Series: CIMMYT Wheat Special Report (WPSR).
- Reynolds M., Bonnett D., Chapman S.C., Furbank R.T., Manes Y., Mather D.E. & Parry M.A.J. (2011) Raising yield potential of wheat. I. Overview of a consortium approach and breeding strategies. *Journal of Experimental Botany*, **62**, 439-452.
- Reynolds M., Manes Y., Izanloo A. & Langridge P. (2009) Phenotyping approaches for physiological breeding and gene discovery in wheat. *Annals of Applied Biology*, **155**, 309-320.
- Reynolds M.P., Gutiérrez-Rodríguez M. & Larqué-Saavedra A. (2000a) Photosynthesis of wheat in a warm, irrigated environment: I: Genetic diversity and crop productivity. *Field Crops Research*, **66**, 37-50.
- Reynolds M.P., Nagarajan S., Razzaque M.A. & Ageeb O.A.A. (2001) Heat tolerance. *Application of Physiology in Wheat Breeding*, 124-135.
- Reynolds M.P., Van Ginkel M. & Ribaut J.M. (2000b) Avenues for genetic modification of radiation use efficiency in wheat. *Journal of Experimental Botany*, **51**, 459-473.
- Rieu I. & Powers S.J. (2009) Real-time quantitative RT-PCR: design, calculations, and statistics. *The Plant Cell Online*, **21**, 1031-1033.
- Ristic Z., Bukovnik U. & Prasad P.V. (2007) Correlation between heat stability of thylakoid membranes and loss of chlorophyll in winter wheat under heat stress. *Crop Science*, **47**, 2067-2073.
- Ristic Z., Momcilovic I., Bukovnik U., Prasad P.V.V., Fu J.M., DeRidder B.P., Elthon T.E. & Mladenov N. (2009) Rubisco activase and wheat productivity under heat-stress conditions. *Journal of Experimental Botany*, **60**, 4003-4014.
- Robinson S.P. (1988) Release of the nocturnal inhibitor, carboxyarabinitol-1-phosphate, from ribulose biphosphate carboxylase/oxygenase by rubisco activase. *Febs Letters*, **233**, 413-416.
- Robinson S.P. & Portis A.R. (1989a) Adenosine triphosphate hydrolysis by purified Rubisco activase. *Archives of Biochemistry and Biophysics*, **268**, 93-99.
- Robinson S.P. & Portis A.R. (1989b) Ribulose-1, 5-bisphosphate carboxylase/oxygenase activase protein prevents the in vitro decline in activity of ribulose-1, 5-bisphosphate carboxylase/oxygenase. *Plant Physiology*, **90**, 968.
- Roesler K.R. & Ogren W.L. (1990) Primary Structure of *Chlamydomonas reinhardtii* Ribulose 1,5-Bisphosphate Carboxylase Oxygenase Activase and Evidence for a Single Polypeptide. *Plant Physiology*, **94**, 1837-1841.
- Rokka A., Zhang L.X. & Aro E.M. (2001) Rubisco activase: an enzyme with a temperature-dependent dual function? *Plant Journal*, **25**, 463-471.
- Rooke L., Byrne D. & Salgueiro S. (2000) Marker gene expression driven by the maize ubiquitin promoter in transgenic wheat. *Annals of Applied Biology*, **136**, 167-172.
- Rumeau D., Bécuwe-Linka N., Beyly A., Carrier P., Cuiné S., Genty B., Medgyesy P., Horvath E. & Peltier G. (2004) Increased zinc content in transplastomic tobacco plants expressing a polyhistidine-tagged Rubisco large subunit. *Plant Biotechnology Journal*, **2**, 389-399.
- Rundle S.J. & Zielinski R.E. (1991) Alterations in barley ribulose-1,5-bisphosphate carboxylase oxygenase activase gene-expression during development and in response to illumination. *Journal of Biological Chemistry*, **266**, 14802-14807.
- Ryan J., Andralojc P., Willis A., Gutteridge S. & Parry M. (1998) Cloning and Sequencing of a *Phaseolus vulgaris* cDNA (Accession No. AF041068) Encoding Rubisco Activase. *Plant Physiology*, **116**, 1192.
- Saadalla M.M., Quick J.S. & Shanahan J.F. (1990) Heat tolerance in winter wheat: II. Membrane thermostability and field performance. *Crop Science*, **30**, 1248-1251.

- Sadras V.O., Lawson C. & Montoro A. (2012) Photosynthetic traits in Australian wheat varieties released between 1958 and 2007. *Field Crops Research*, **134**, 19-29.
- Sage R.F. & Kubien D.S. (2007) The temperature response of C3 and C4 photosynthesis. *Plant Cell and Environment*, **30**, 1086-1106.
- Sage R.F., Way D.A. & Kubien D.S. (2008) Rubisco, Rubisco activase, and global climate change. *Journal of Experimental Botany*, **59**, 1581-1595.
- Salvucci M.E. (2008) Association of Rubisco activase with chaperonin-60 beta: a possible mechanism for protecting photosynthesis during heat stress. *Journal of Experimental Botany*, **59**, 1923-1933.
- Salvucci M.E. & Anderson J.C. (1987) Factors affecting the activation state and the level of total activity of ribulose biphosphate carboxylase in tobacco protoplasts. *Plant Physiology*, **85**, 66-71.
- Salvucci M.E. & Crafts-Brandner S.J. (2004a) Inhibition of photosynthesis by heat stress: the activation state of Rubisco as a limiting factor in photosynthesis. *Physiologia Plantarum*, **120**, 179-186.
- Salvucci M.E. & Crafts-Brandner S.J. (2004b) Mechanism for deactivation of Rubisco under moderate heat stress. *Physiologia Plantarum*, **122**, 513-519.
- Salvucci M.E. & Crafts-Brandner S.J. (2004c) Relationship between the heat tolerance of photosynthesis and the thermal stability of rubisco activase in plants from contrasting thermal environments. *Plant Physiology*, **134**, 1460-1470.
- Salvucci M.E., DeRidder B.P. & Portis A.R. (2006) Effect of activase level and isoform on the thermotolerance of photosynthesis in Arabidopsis. *Journal of Experimental Botany*, **57**, 3793-3799.
- Salvucci M.E., Osteryoung K.W., Crafts-Brandner S.J. & Vierling E. (2001) Exceptional sensitivity of rubisco activase to thermal denaturation in vitro and in vivo. *Plant Physiology*, **127**, 1053-1064.
- Salvucci M.E., Portis A.R. & Ogren W.L. (1985) A Soluble Chloroplast Protein Catalyzes Ribulosebiphosphate Carboxylase Oxygenase Activation *In vivo*. *Photosynthesis Research*, **7**, 193-201.
- Salvucci M.E., van de Loo F.J. & Stecher D. (2003) Two isoforms of Rubisco activase in cotton, the products of separate genes not alternative splicing. *Planta*, **216**, 736-744.
- Salvucci M.E., Werneke J.M., Ogren W.L. & Portis A.R. (1987) Purification and species distribution of Rubisco activase. *Plant Physiology*, **84**, 930-936.
- Sanford J.C., Smith F.D. & Russell J.A. (1993) [36] Optimizing the biolistic process for different biological applications. *Methods in Enzymology*, **217**, 483-509.
- Sasanuma T. (2001) Characterization of the *rbcS* multigene family in wheat: subfamily classification, determination of chromosomal location and evolutionary analysis. *Molecular Genetics and Genomics*, **265**, 161-171.
- Savir Y., Noor E., Milo R. & Tlustý T. (2010) Cross-species analysis traces adaptation of Rubisco toward optimality in a low-dimensional landscape. *Proceedings of the National Academy of Sciences*, **107**, 3475-3480.
- Scafaro A.P., Haynes P.A. & Atwell B.J. (2010) Physiological and molecular changes in *Oryza meridionalis* Ng., a heat-tolerant species of wild rice. *Journal of Experimental Botany*, **61**, 191-202.
- Scafaro A.P., Yamori W., Carmo-Silva A.E., Salvucci M.E., Von Caemmerer S. & Atwell B.J. (2012) Rubisco activity is associated with photosynthetic thermotolerance in a wild rice (*Oryza meridionalis*). *Physiologia Plantarum*, **146**, 99-109.
- Scales J.C., Parry M.A.J. & Salvucci M.E. (2014) A non-radioactive method for measuring Rubisco activase activity in the presence of variable ATP: ADP ratios, including modifications for measuring the activity and activation state of Rubisco. *Photosynthesis Research*, **119**, 355-365.
- Schrader S.M., Kane H.J., Sharkey T.D. & von Caemmerer S. (2006) High temperature enhances inhibitor production but reduces fallover in tobacco Rubisco. *Functional Plant Biology*, **33**, 921-929.
- Schrader S.M., Wise R.R., Wacholtz W.F., Ort D.R. & Sharkey T.D. (2004) Thylakoid membrane responses to moderately high leaf temperature in Pima cotton. *Plant, Cell & Environment*, **27**, 725-735.
- Scofield S.R., Huang L., Brandt A.S. & Gill B.S. (2005) Development of a virus-induced gene-silencing system for hexaploid wheat and its use in functional analysis of the Lr21-mediated leaf rust resistance pathway. *Plant Physiology*, **138**, 2165-2173.

- Semenov M.A. & Shewry P.R. (2011) Modelling predicts that heat stress, not drought, will increase vulnerability of wheat in Europe. *Scientific Reports*, **1**, doi:10.1038/srep00066
- Semenov M.A., Stratonovitch P., Alghabari F. & Gooding M.J. (2014) Adapting wheat in Europe for climate change. *Journal of Cereal Science*, **59**, 245-256.
- Shan Q., Wang Y., Li J., Zhang Y., Chen K., Liang Z., Zhang K., Liu J., Xi J.J. & Qiu J.-L. (2013) Targeted genome modification of crop plants using a CRISPR-Cas system. *Nature Biotechnology*, **31**, 686-688.
- Shanahan J.F., Edwards I.B., Quick J.S. & Fenwick J.R. (1990) Membrane thermostability and heat tolerance of spring wheat. *Crop Science*, **30**, 247-251.
- Sharkey T.D. (2005) Effects of moderate heat stress on photosynthesis: importance of thylakoid reactions, rubisco deactivation, reactive oxygen species, and thermotolerance provided by isoprene. *Plant Cell and Environment*, **28**, 269-277.
- Sharkey T.D., Badger M.R., von Caemmerer S. & Andrews T.J. (2001) Increased heat sensitivity of photosynthesis in tobacco plants with reduced Rubisco activase. *Photosynthesis Research*, **67**, 147-156.
- Sharkey T.D., Savitch L.V. & Butz N.D. (1991) Photometric method for routine determination of kcat and carbamylation of rubisco. *Photosynthesis Research*, **28**, 41-48.
- Shearman V.J., Sylvester-Bradley R., Scott R.K. & Foulkes M.J. (2005) Physiological processes associated with wheat yield progress in the UK. *Crop Science*, **45**, 175-185.
- Shen J.B., Orozco E.M. & Ogren W.L. (1991) Expression of the 2 Isoforms of Spinach Ribulose 1,5-Bisphosphate Carboxylase Activase and Essentiality of the Conserved Lysine in the Consensus Nucleotide-Binding Domain. *Journal of Biological Chemistry*, **266**, 8963-8968.
- Shinmachi F., Buchner P., Stroud J.L., Parmar S., Zhao F.-J., McGrath S.P. & Hawkesford M.J. (2010) Influence of sulfur deficiency on the expression of specific sulfate transporters and the distribution of sulfur, selenium, and molybdenum in wheat. *Plant Physiology*, **153**, 327-336.
- Sparks C.A. & Jones H.D. (2009) Biolistics transformation of wheat. In: *Transgenic Wheat, Barley and Oats*, pp. 71-92. Springer.
- Spreitzer R.J. & Salvucci M.E. (2002) Rubisco: Structure, regulatory interactions, and possibilities for a better enzyme. *Annual Review of Plant Biology*, **53**, 449-475.
- Stitt M., Lilley R.M. & Heldt H.W. (1982) Adenine nucleotide levels in the cytosol, chloroplasts, and mitochondria of wheat leaf protoplasts. *Plant Physiology*, **70**, 971-977.
- Stoger E., Williams S., Keen D. & Christou P. (1998) Molecular characteristics of transgenic wheat and the effect on transgene expression. *Transgenic Research*, **7**, 463-471.
- Stoger E., Williams S., Keen D. & Christou P. (1999) Constitutive versus seed specific expression in transgenic wheat: temporal and spatial control. *Transgenic Research*, **8**, 73-82.
- Stotz M., Mueller-Cajar O., Ciniawsky S., Wendler P., Hartl F.U., Bracher A. & Hayer-Hartl M. (2011) Structure of green-type Rubisco activase from tobacco. *Nature Structural & Molecular Biology*, **18**, 1366-1370.
- Stratonovitch P. & Semenov M.A. (2015) Heat tolerance around flowering in wheat identified as a key trait for increased yield potential in Europe under climate change. *Journal of Experimental Botany*, doi: 10.1093/jxb/erv1070
- Sukumaran S., Dreisigacker S., Lopes M., Chavez P. & Reynolds M.P. (2014) Genome-wide association study for grain yield and related traits in an elite spring wheat population grown in temperate irrigated environments. *Theoretical and Applied Genetics*, **128**, 353-363.
- Sukumaran S. & Yu J. (2014) Association mapping of genetic resources: Achievements and future perspectives. In: *Genomics of Plant Genetic Resources*, pp. 207-235. Springer.
- Sulpice R., Tschöep H., Von Korff M., Büssis D., Usadel B., Höhne M., Witucka-Wall H., Altmann T., Stitt M. & Gibon Y. (2007) Description and applications of a rapid and sensitive non-radioactive microplate-based assay for maximum and initial activity of D-ribulose-1,5-bisphosphate carboxylase/oxygenase. *Plant, Cell & Environment*, **30**, 1163-1175.
- Tcherkez G.G.B. (2006) From the Cover: Despite slow catalysis and confused substrate specificity, all ribulose bisphosphate carboxylases may be nearly perfectly optimized. *Proceedings of the National Academy of Sciences*, **103**, 7246-7251.
- Tewolde H., Fernandez C.J. & Erickson C.A. (2006) Wheat Cultivars Adapted to Post-Heading High Temperature Stress. *Journal of Agronomy and Crop Science*, **192**, 111-120.

- Tilman D., Balzer C., Hill J. & Befort B.L. (2011) Global food demand and the sustainable intensification of agriculture. *Proceedings of the National Academy of Sciences*, **108**, 20260-20264.
- To K.Y., Suen D.F. & Chen S.C.G. (1999) Molecular characterization of ribulose-1,5-bisphosphate carboxylase/oxygenase activase in rice leaves. *Planta*, **209**, 66-76.
- Tuomi J.M., Voorbraak F., Jones D.L. & Ruijter J.M. (2010) Bias in the *C_q* value observed with hydrolysis probe based quantitative PCR can be corrected with the estimated PCR efficiency value. *Methods*, **50**, 313-322.
- van de Loo F.J. & Salvucci M.E. (1996) Activation of ribulose-1, 5-bisphosphate carboxylase/oxygenase (Rubisco) involves Rubisco activase Trp16. *Biochemistry*, **35**, 8143-8148.
- Van Deynze A. & Stoffel K. (2006) High-throughput DNA extraction from seeds. *Seed Science and Technology*, **34**, 741-745.
- Vara Prasad P.V. & Djanaguiraman M. (2014) Response of floret fertility and individual grain weight of wheat to high temperature stress: sensitive stages and thresholds for temperature and duration. *Functional Plant Biology*, **41**, 1261-1269.
- Vargas-Suarez M. (2004) Rubisco activase chaperone activity is regulated by a post-translational mechanism in maize leaves. *Journal of Experimental Botany*, **55**, 2533-2539.
- Verma D. & Daniell H. (2007) Chloroplast vector systems for biotechnology applications. *Plant Physiology*, **145**, 1129.
- Verwoerd T.C., Dekker B.M. & Hoekema A. (1989) A small-scale procedure for the rapid isolation of plant RNAs. *Nucleic Acids Research*, **17**, 2362.
- Vijayalakshmi K., Fritz A.K., Paulsen G.M., Bai G., Pandravada S. & Gill B.S. (2010) Modeling and mapping QTL for senescence-related traits in winter wheat under high temperature. *Molecular Breeding*, **26**, 163-175.
- Vogel C. & Marcotte E.M. (2012) Insights into the regulation of protein abundance from proteomic and transcriptomic analyses. *Nature Reviews Genetics*, **13**, 227-232.
- von Caemmerer S., Hendrickson L., Quinn V., Vella N., Millgate A.G. & Furbank R.T. (2005) Reductions of Rubisco activase by antisense RNA in the C₄ plant *Flaveria bidentis* reduces Rubisco carbamylation and leaf photosynthesis. *Plant Physiology*, **137**, 747-755.
- Vu J.C.V., Gesch R.W., Allen L.H., Boote K.J. & Bowes G. (1999) CO₂ enrichment delays a rapid, drought-induced decrease in Rubisco small subunit transcript abundance. *Journal of Plant Physiology*, **155**, 139-142.
- Wachter R.M., Salvucci M.E., Carmo-Silva A.E., Barta C., Genkov T. & Spreitzer R.J. (2013) Activation of interspecies-hybrid Rubisco enzymes to assess different models for the Rubisco–Rubisco activase interaction. *Photosynthesis Research*, **117**, 557-566.
- Wang D., Li X.-F., Zhou Z.-J., Feng X.-P., Yang W.-J. & Jiang D.-A. (2010) Two Rubisco activase isoforms may play different roles in photosynthetic heat acclimation in the rice plant. *Physiologia Plantarum*, **139**, 55-67.
- Wang D., Xie S.Z., Yang J. & Wang Q.F. (2014) Molecular characteristics and expression patterns of Rubisco activase, novel alternative splicing variants in a heterophyllous aquatic plant, *Sagittaria graminea*. *Photosynthetica*, **52**, 83-95.
- Wang M., Jiang N., Jia T., Leach L., Cockram J., Waugh R., Ramsay L., Thomas B. & Luo Z. (2012) Genome-wide association mapping of agronomic and morphologic traits in highly structured populations of barley cultivars. *Theoretical and Applied Genetics*, **124**, 233-246.
- Wang Z.Y. & Portis A.R. (1992) Dissociation of ribulose-1, 5-bisphosphate bound to ribulose-1, 5-bisphosphate carboxylase/oxygenase and its enhancement by ribulose-1, 5-bisphosphate carboxylase/oxygenase activase-mediated hydrolysis of ATP. *Plant Physiology*, **99**, 1348-1353.
- Wang Z.Y., Snyder G.W., Esau B.D., Portis A.R. & Ogren W.L. (1992) Species-dependent variation in the interaction of substrate-bound ribulose-1,5-bisphosphate carboxylase oxygenase (Rubisco) and Rubisco activase. *Plant Physiology*, **100**, 1858-1862.
- Wardlaw I.F. & Wrigley C.W. (1994) Heat tolerance in temperate cereals: an overview. *Functional Plant Biology*, **21**, 695-703.
- Watanabe N., Evans J.R. & Chow W.S. (1994) Changes in the photosynthetic properties of Australian wheat cultivars over the last century. *Functional Plant Biology*, **21**, 169-183.
- Watillon B., Kettmann R., Boxus P. & Burny A. (1993) Developmental and circadian pattern of Rubisco activase messenger-RNA accumulation in apple plants. *Plant Molecular Biology*, **23**, 501-509.

- Weis E. (1981) Reversible Heat-Inactivation of the Calvin Cycle - a Possible Mechanism of the Temperature Regulation of Photosynthesis. *Planta*, **151**, 33-39.
- Werneke J.M., Chatfield J.M. & Ogren W.L. (1989) Alternative mRNA splicing generates the two ribulosebiphosphate carboxylase/oxygenase activase polypeptides in spinach and Arabidopsis. *The Plant Cell Online*, **1**, 815-825.
- Werneke J.M., Zielinski R.E. & Ogren W.L. (1988) Structure and expression of spinach leaf cDNA encoding ribulosebiphosphate carboxylase/oxygenase activase. *Proceedings of the National Academy of Sciences*, **85**, 787-791.
- Weston D.J., Bauerle W.L., Swire-Clark G.A., Moore B.D. & Baird W.M.V. (2007) Characterization of Rubisco activase from thermally contrasting genotypes of *Acer rubrum* (Aceraceae). *American Journal of Botany*, **94**, 926-934.
- Whitney S.M., Baldett P., Hudson G.S. & Andrews T.J. (2001) Form I Rubiscos from non-green algae are expressed abundantly but not assembled in tobacco chloroplasts. *Plant Journal*, **26**, 535-547.
- Whitney S.M., Kane H.J., Houtz R.L. & Sharwood R.E. (2009) Rubisco Oligomers Composed of Linked Small and Large Subunits Assemble in Tobacco Plastids and Have Higher Affinities for CO₂ and O₂. *Plant Physiology*, **149**, 1887-1895.
- Whitney S.M., Sharwood R.E., Orr D., White S.J., Alonso H. & Galmés J. (2011) Isoleucine 309 acts as a C4 catalytic switch that increases ribulose-1, 5-bisphosphate carboxylase/oxygenase (rubisco) carboxylation rate in *Flaveria*. *Proceedings of the National Academy of Sciences*, **108**, 14688-14693.
- WHO (2003) Diet, nutrition and the prevention of chronic diseases. *WHO technical report series*, 1-60.
- Wingler A., Lea P.J., Quick W.P. & Leegood R.C. (2000) Photorespiration: metabolic pathways and their role in stress protection. *Philosophical Transactions of the Royal Society of London. Series B: Biological Sciences*, **355**, 1517-1529.
- Wullschlegel S.D. (1993) Biochemical limitations to carbon assimilation in C3 plants—a retrospective analysis of the A/Ci curves from 109 species. *Journal of Experimental Botany*, **44**, 907-920.
- Xu K., He B., Zhou S., Li Y. & Zhang Y. (2010) Cloning and characterization of the Rubisco activase gene from *Ipomoea batatas* (L.) Lam. *Molecular Biology Reports*, **37**, 661-668.
- Xu W., Rosenow D.T. & Nguyen H.T. (2000) Stay green trait in grain sorghum: relationship between visual rating and leaf chlorophyll concentration. *Plant Breeding*, **119**, 365-367.
- Yin X. & Struik P.C. (2010) Modelling the crop: from system dynamics to systems biology. *Journal of Experimental Botany*, **61**, 2171-2183.
- Yin Z., Meng F., Song H., Wang X., Xu X. & Yu D. (2010) Expression quantitative trait loci analysis of two genes encoding rubisco activase in soybean. *Plant Physiology*, **152**, 1625-1637.
- Yin Z., Zhang Z., Deng D., Chao M., Gao Q., Wang Y., Yang Z., Bian Y., Hao D. & Xu C. (2014) Characterization of Rubisco Activase Genes in Maize: An α -Isoform Gene Functions alongside a β -Isoform Gene. *Plant Physiology*, **164**, 2096-2106.
- Yuan C., Li C., Yan L., Jackson A.O., Liu Z., Han C., Yu J. & Li D. (2011) A high throughput barley stripe mosaic virus vector for virus induced gene silencing in monocots and dicots. *PLoS One*, **6**, doi:10.1371/journal.pone.0026468.
- Zadoks J.C., Chang T.T. & Konzak C.F. (1974) A decimal code for the growth stages of cereals. *Weed Research*, **14**, 415-421.
- Zhang N., Kallis R.P., Ewy R.G. & Portis A.R. (2002) Light modulation of Rubisco in Arabidopsis requires a capacity for redox regulation of the larger Rubisco activase isoform. *Proceedings of the National Academy of Sciences of the United States of America*, **99**, 3330-3334.
- Zhang N. & Portis A.R. (1999) Mechanism of light regulation of Rubisco: A specific role for the larger Rubisco activase isoform involving reductive activation by thioredoxin-f. *Proceedings of the National Academy of Sciences of the United States of America*, **96**, 9438-9443.
- Zhu C., Gore M., Buckler E.S. & Yu J. (2008a) Status and prospects of association mapping in plants. *The Plant Genome*, **1**, 5-20.
- Zhu X.-G., Long S.P. & Ort D.R. (2008b) What is the maximum efficiency with which photosynthesis can convert solar energy into biomass? *Current Opinion in Biotechnology*, **19**, 153-159.
- Zhu X.-G., Long S.P. & Ort D.R. (2010) Improving Photosynthetic Efficiency for Greater Yield. *Annual Review of Plant Biology*, **61**, 235-261.

Zhu X.G., Portis A.R. & Long S.P. (2004) Would transformation of C3 crop plants with foreign Rubisco increase productivity? A computational analysis extrapolating from kinetic properties to canopy photosynthesis. *Plant Cell and Environment*, **27**, 155-165.